



School of Life Sciences

**The Effects of Endocannabinoids and Phytocannabinoids
on Bronchial Epithelial Permeability**

Valerie CM Shang, MPharm

Thesis submitted to the University of Nottingham for the degree of

Doctor of Philosophy

October 2015

Table of Contents

Table of Contents	i
List of Abbreviations	x
Abstract.....	xvi
1. General Introduction.....	1
1.1 The Human Respiratory System.....	3
1.2 Anatomy of the Bronchial (Airway) Epithelium.....	5
1.2.1 Ciliated Epithelial Cells	6
1.2.2 Goblet Cells	6
1.2.3 Clara Cells.....	7
1.2.4 Basal Cells	8
1.2.5 Neuroepithelial Bodies (NEBs).....	8
1.2.6 Immune Cells	9
1.3 Roles of the Airway Epithelium.....	13
1.3.1 Barrier Function - The Airway Epithelial Tight Junction Protein Complex.....	13
1.4 Inflammatory Diseases Associated to Impaired Airway Epithelial Permeability.....	16
1.4.1 Asthma	17
1.4.2 COPD	20
1.4.3 Asthma-COPD Overlap Syndrome (ACOS).....	23
1.5 The Mechanism of Airway Inflammation in Asthma and COPD	25
1.6 Current Pharmacological Treatments for Airway Inflammation	27
1.7 Cellular Signalling Pathways Involved in Modulation of Bronchial Epithelial Permeability	30
1.7.1 Mitogen Activated Protein Kinases (MAPKs) Cascades	30
1.7.2 RhoA Signalling.....	35
1.8 Cannabinoids as the Potential Therapeutic Area for Asthma and COPD ...	40
1.9 History of Cannabis for Respiratory Disorders	41
1.10 Evidence on the Effects of Cannabinoids in Regulating Inflammatory Responses	43
1.11 Cannabinoids and Airway Inflammation.....	45
1.11.1 Endogenous Cannabinoids (or Endocannabinoids)	45

1.11.2	Phytocannabinoids.....	51
1.12	Sites of Action of the Cannabinoids	54
1.12.1	The Classical Cannabinoid Receptors (CB ₁ and CB ₂ receptor)	54
1.12.2	Putative Cannabinoid Receptors.....	55
1.12.3	Peroxisome Proliferator-Activated Receptors (PPARs).....	57
1.12.4	Transient Receptor Potential Channels (TRP channels).....	58
1.13	Aims of the Study	60
2	Materials, General Methods and Protocol Development	61
2.1	Materials	61
2.1.1	Materials Used for Cell Culture	61
2.1.2	Materials Used in TEER Experiments	62
2.1.3	Materials Used in FITC-Dextran Permeability Studies.....	63
2.1.4	Materials Used for Dot Blotting and Western Blotting.....	64
2.1.5	List of Primary and Secondary Antibodies Used in Dot Blotting and Western Blotting.....	66
2.1.6	Materials Used in Radioligand-Binding Studies	68
2.1.7	Materials Used in Cytotoxicity Studies.....	68
2.1.8	Materials Used in Bronchial Contractility Studies.....	69
2.2	<i>In Vitro</i> Models for the Investigation of Human Airway Epithelial Permeability.....	70
2.2.1	Primary Human Bronchial Epithelial Cells.....	70
2.2.2	Calu-3 Bronchial (or Airway) Epithelial Cell Line	71
2.3	<i>In Vitro</i> Permeability Enhancement Agents	73
2.3.1	Synthetic Compound	73
2.3.2	Biological Agents.....	73
2.4	Calu-3 Cell Culture.....	77
2.4.1	Cell Culture Maintenance.....	77
2.4.2	Quantification of Cell Viability.....	78
2.4.3	Cells Cryopreservation	78
2.4.4	Cell Revival from Frozen	78
2.5	Evaluation of Bronchial Epithelial Tight Junction Integrity using Transepithelial Electrical Resistance (TEER)	79
2.5.1	TEER Measurement with STX2 Electrodes.....	79
2.5.2	Development of TEER Measurement for Calu-3 Cells when Cultured at ALI	81
2.5.3	Resistance/TEER Calculations.....	84

2.5.4	Modifications to the TEER Measurement Protocol (Method Development).....	85
2.6	FITC-Dextran (FD) Permeability Studies	87
2.6.1	Method for the Assessment of FD Permeability	89
2.6.2	Establishing an FD4-concentration Calibration Curve	90
2.6.3	P_{app} Calculations.....	92
2.7	Quantification of Mucin (of MUC5AC Subtype) Expression Post Treatment	93
2.7.1	Sample Preparation	93
2.7.2	Optimisation of MUC5AC Quantification Protocol with Dot Blotting (Method Development).....	93
2.7.3	Modifications to the Dot Blotting Protocol.....	96
2.8	Radioligand-Binding Studies	98
2.8.1	Preparation of Membranes	98
2.8.2	Radioligand-binding Assay.....	98
2.9	Investigating Cannabinoid Receptor Expression and Signalling Pathways underlying TEER changes with Western Blotting	99
2.9.1	Western Blotting Protocol.....	99
2.10	Cytotoxicity Studies	100
2.10.1	Resazurin Assay.....	100
2.10.2	MTT Assay	101
2.11	Bronchial Contractility Studies	104
2.11.1	Tissue Preparation.....	104
2.11.2	Organ Bath Experiments.....	105
2.12	Statistical Analysis	107
3.	The Effects of Endocannabinoids on Human Bronchial Epithelial Permeability.....	109
3.1	Introduction	109
3.1.1	Aims	111
3.2	Materials and Methods	112
3.2.1	Materials	112
3.2.2	Methods.....	112
3.2.3	Statistical Analysis.....	117
3.3	Results	118
3.3.1	Pilot Experiments.....	118
3.3.2	Optimisation of TEER Measurement Protocol	119

3.3.3	The Impact of Disrupted Bronchial Epithelial Barrier on TEER Measurement by EDTA.....	120
3.3.4	Alterations in Bronchial Epithelial Cell Permeability following Basolateral Application of the Endocannabinoids or TNF α	121
3.3.5	Interaction of Endocannabinoids with the Cytokine, TNF α	123
3.3.6	Cannabinoid Receptor Antagonists Did Not Alter Anandamide-induced Increased Permeability	125
3.3.7	Inhibitors of Enzymes FAAH, and Combined COX and LOX Inhibition Prevents Anandamide-Induced Increased Permeability	126
3.3.8	MUC5AC Protein Expression following Treatment with Anandamide and the Cytokine, TNF α	130
3.4	Discussion.....	132
3.5	Conclusion.....	143
4.	Mechanisms of Anandamide-induced Increases in Human Bronchial Epithelial Permeability	146
4.1	Introduction	146
4.1.1	Aims	148
4.2	Materials and Methods	149
4.2.1	Materials.....	149
4.2.2	Methods.....	149
4.2.3	Statistical Analysis	152
4.3	Results	153
4.3.1	Anandamide Decreases Expression of Tight Junction Proteins, Occludin and ZO-1.....	153
4.3.2	Inhibition of ERK Activation Prevents Increased Epithelial Permeability due to Anandamide or TNF α	156
4.3.3	Inhibition of ERK Activation Prevented Decreased Expression of the Tight Junction Protein, Occludin in Anandamide-Treated Cells	161
4.3.4	Inhibition of p38 MAPK Activation also Prevents Anandamide- and TNF α -Induced Increased in Cell Permeability and Occludin Expression.....	166
4.4	Discussion.....	171
4.5	Conclusion.....	176
5.	The Effects of Phytocannabinoids on Human Bronchial Epithelial Permeability	178
5.1	Introduction	178
5.1.1	Aims	180
5.2	Materials and Methods	181
5.2.1	Materials.....	181

5.2.2	General Methods	181
5.2.3	Statistical Analysis	186
5.3	Results	187
5.3.1	Phytocannabinoids Did Not Directly Affect Bronchial Epithelial Permeability	187
5.3.2	Phytocannabinoids Reversed Cytokine-Induced Increases in Bronchial Epithelial Permeability	188
5.3.3	THC Prevents Calu-3 Epithelial Permeability in the Presence of Other Pro-inflammatory Mediators	190
5.3.4	Effect of THC on P_{app} (Epithelial Permeability) in $TNF\alpha$ -treated Calu-3 Cells	192
5.3.5	The Effect of Cannabinoid Receptor Antagonism on THC-mediated Reversal of $TNF\alpha$ -induced Increase in Permeability	194
5.3.6	The Effect of Competitive Antagonism with Cannabinoids Receptors Antagonists on CBD Action	196
5.3.7	Investigation of Cannabinoid Receptor Expression in Calu-3 Cells	198
5.3.8	Cannabinoid Receptor Agonists Reverse $TNF\alpha$ -induced Increases in Bronchial Epithelial Permeability	203
5.3.9	THC Decreases Mucin (MUC5AC) Protein Expression	205
5.3.10	THC Concentrations Up to 30 μM Do Not Affect Calu-3 Cell Viability	207
5.3.11	The Effect of Repeated THC Treatment on Bronchial Epithelial Permeability	209
5.3.12	Effect of Long-term Exposure to a Cannabinoid Receptor Agonist on Calu-3 cell Permeability	211
5.3.13	Repeated THC (30 μM) Treatment Does Not Alter Proliferation Rate in Calu-3 Epithelial Cells	212
5.3.14	THC Does Not Reverse Carbachol-induced Bronchoconstriction in Porcine Tissue	214
5.4	Discussion	216
5.5	Conclusion	227
6.	The Mechanism Involved in THC-Mediated Response on the Bronchial Epithelial Tight Junction	231
6.1	Introduction	231
6.1.1	Aims	233
6.2	Materials and Methods	234
6.2.1	Materials	234
6.2.2	Methods	234
6.2.3	Statistical Analysis	237

6.3	Results	238
6.3.1	THC Prevents Reduced Tight Junction Proteins, Occludin and ZO-1 Expression Induced by TNF α	238
6.3.2	THC Increases ERK1/2 MAPK Phosphorylation	241
6.3.3	Selective Inhibition of ROCK Prevents TNF α Effect on Epithelial Permeability and Tight Junction Proteins Expression.....	244
6.3.4	Effect of THC on MYPT1 phosphorylation.....	248
6.3.5	The Role of CB ₁ and CB ₂ Receptors Activation in the Regulation of MYPT1 Signalling	250
6.4	Discussion.....	253
6.5	Conclusion	264
7.	General Discussion.....	267
7.1	The Proposed Hypothesis	267
7.2	The Key Questions	270
7.3	Summary of Findings and Future Investigations.....	271
	Appendix	283
	References	315

Publications and Presentations

Publications

SHANG, V., KENDALL, D. A & ROBERTS, R. E. The Role of the Endogenous Cannabinoid Anandamide on Human Airway Epithelial Cell Permeability (2013). <http://www.pa2online.org/abstract/abstract.jsp?abid=31245>. *Proceeding abstract for Pharmacology 2013*.

SHANG, V., KENDALL, D. A & ROBERTS, R. E. Δ^9 -Tetrahydrocannabinol (THC) reverses increased airway epithelium permeability during inflammation (2013). <http://www.physoc.org/proceedings/abstract/Proc%20Physiol%20Soc%2030PC26>. *Proceeding abstract for the Epithelia and Smooth Muscle Interactions in Health and Disease meeting*.

Presentations

Pharmacology 2013 - The Role of the Endogenous Cannabinoid Anandamide on Human Airway Epithelial Cell Permeability. Poster presentation. London, UK. December 2013.

Epithelia and Smooth Muscle Interactions in Health and Disease Meeting - Δ^9 -Tetrahydrocannabinol (THC) Reverses Increased Airway Epithelium Permeability during Inflammation. Poster presentation. Dublin, Ireland. December 2013.

The 24th Annual International Cannabinoid Research Society (ICRS) Symposium on the Cannabinoids - The Effects of Cannabinoids on Human Bronchial Epithelial Cell Permeability. Poster presentation. Baveno, Italy, June/July 2014.

Acknowledgements

First and foremost, my deepest gratitude to my primary supervisor, Dr Richard Roberts for his endless support and encouragement during my time as a postgraduate student at the University. It has been a privilege learning and working under the guidance of a talented scientist like Richard.

My sincere appreciation to my secondary supervisor, Professor David Kendall for his expert opinions and the support he had provided towards the ‘discoveries’ I have made in my studies.

I would also like to thank Dr Saoirse O’Sullivan and her group for their help especially during the initial stages of my study. Many thanks to Dr Steve Alexander for his advice on cannabinoids-related subjects, generosity in sharing some of the cannabinoid reagents and help to expand my network in the cannabinoids research group. My sincere thanks to Dr Cynthia Bousquillon for her advice and experimental tips in conducting my studies. Special thanks to Dr Roger Knaggs who have encouraged me to enrol a career in scientific research and for being such a supportive professional mentor.

My heartiest appreciation to Paul Millns, Dr Michael Garle and Liaque Latif for their technical and administrative support; Dave Hunt and Helen Gawronska for their help, encouragement and friendship.

I would like to express my sincere appreciation towards the School of Life Sciences, University of Nottingham for the opportunity to fulfil my ambition in pursuing for a doctorate degree and for their generous sponsorship in this project.

Special thanks to my close friend, Carolyn who has been always there for me. To my dear friend, Aneesa, thank you for those late nights/early mornings entertainment exchanging Grant Snider's comics during the times that were supposed to be spent for writing. *Ribuan terima kasih* to all my Malaysian friends for their support and friendship especially Judd, Rizal, Pui San, Vik, Lin, Susan and Midah. Home doesn't feel too far away with all of you around. To all my friends in particular Esther, Kar Lai, Matt, Fawaz, Mouhammad Saleem, Entadhar, Ayoub, Mouhammed Alsaqati, Junaid, Hussain, Hammad, Samia, Nahed, Wafa, Tammy, Alaa, Rick and Omar - thanks for all the help around the lab and friendship.

To my dearest fiancé, Wen Hua Liew - thank you for listening to all my ramblings and undying support from halfway across the world. To my beloved mommy, Rose Chin, thank you for being such a great model in life and supportive in everything I do. My brothers, Victor and Valentin who are absolutely clueless of my pursuits - thanks anyway for regularly checking up on me and the banter on WhatsApp. To my little nephew, Edward whom I most adore, thank you for keeping your auntie sane.

Lastly, a special dedication to my daddy and *popo* (grandmother) who are no longer in this world - their love and guidance had fuelled my determination to succeed since my earlier days.

List of Abbreviations

$^{\circ}\text{C}$	Temperature degrees in celcius
Δ	Delta
Ω	Resistance unit in Ohm
μM	Micromolar
μl	Microlitre
2-AG	2-arachidonoylglycerol
5-HT	5-hydroxytryptamine
ACEA	Arachidonyl-2'-chloroethylamide
ACOS	Asthma-Chronic Obstructive Pulmonary Disease Syndrome
ALI	Air-liquid interface
AMPK	Adenosine monophosphate protein kinase
ANOVA	Analysis of variance
ATCC	American Type Culture Collection
B.C.	Before Christ
BSA	Bovine serum albumin
Ca^{2+}	Calcium ion
cAMP	Cyclic adenosine monophosphate
CB_1	Cannabinoid receptor 1
CB_2	Cannabinoid receptor 2
CBD	Cannabidiol
CD	Controlled drug
CHO	Chinese hamster ovary cells
cm	Centimetre
COPD	Chronic Obstructive Pulmonary Disease
COX	Cyclooxygenase

DABCO	1,4-diazobicyclo-[2,2,2]-octane
DAG	Diacylglycerol
DAGL	Diacylglycerol lipase enzyme
DAPI	4',6-diamidino-2-phenylindole dihydrochloride
Derp	<i>Dermatophagoides pteronyssinus</i> (allergen groups 1-9)
DMEM	Dulbecco's Modified Eagle's Medium
DMSO	Dimethyl sulfoxide
dpm	Disintegration per minute
ECS	Endocannabinoid system
EDTA	Ethylenediaminetetraacetic acid
EGTA	Ethyleneglycoltetraacetic acid
ERK1/2	Extracellular signal-regulated kinases 1 and 2
EtOH	Ethanol
EVOM2	Epithelial voltohmmeter version 2
FAAH	Fatty acid amide hydrolase
FBS	Fetal bovine serum
FD4	Fluorescein isothiocyanate dextran of 4 kilodalton
FITC	Fluorescein isothiocyanate
GAPDH	Glutaraldehyde 3-phosphate dehydrogenase
GAPs	GTPase-activating proteins
GEF-H1	Guanine nucleotide exchange factor-H1
GEFs	Guanine-nucleotide-exchange factors
GINA	Global initiative for asthma
GM-CSF	Granulocyte macrophage colony stimulating factor
GPCR	G-protein coupled receptor
GTP	Guanosine triphosphate
HEK293	Human embryonic kidney-293 cells

HEPES	4-(2-hydroxyethyl)-1-piperazineethanesulfonic acid
HPETE	5-hydroperoxyeicosatetraenoic acid
IC ₅₀	Half maximal (50%) inhibitory concentration
IFN γ	Interferon- γ
IgE	Immunoglobulin E
IgG	Immunoglobulin G
IL	Interleukin
IP ₃	Inositol triphosphate
IQGAP1	Ras GTPase-activating-like protein IQGAP1
IR	Infrared
kDa	kiloDalton
JAM	Junctional adhesion molecule
JNK	c-Jun N-terminal kinases
K _i	Inhibitory constant
LLI	Liquid-liquid interface
LOX	Lipoxygenase
LPS	Lipopolysaccharide
mAb	Monoclonal antibody
MAGL	Monoacylglycerol lipase enzyme
MAPKs	Mitogen-activated protein kinases
MAPKK	Mitogen-activated protein kinases kinase
MDa	Mega dalton
MDCK	Madin-Darby canine kidney epithelial cells
MEK	MAP/ERK1/2 kinases
ml	millimetre
MLC	Myosin light chain
MLCK	Myosin light chain kinase

MLKs	Mixed lineage kinases
mM	Millimolar
MMP-9	Matrix metalloproteinase-9 enzyme
MP	Myosin phosphatase
mRNA	Messenger ribonucleic acid
MTT	3-[4,5-dimethylthiazol-2-yl]-2,5 diphenyl tetrazolium bromide
MUC5AC	Mucin 5AC subtype
MW	Molecular weight
MYPT	Myosin phosphatase target subunit
<i>n</i>	Number of experiments
nAChR	Nicotinic acetylcholine receptor
NANC	Non-adrenergic non-cholinergic nerves
NAPE	N-arachidonoylphosphatidylethanolamine
NAPE-PLD	N-arachidonoylphosphatidylethanolamine phospholipase D
NEBs	Neuroendocrine bodies
NDGA	Nordihydroguaiaretic acid
NF- κ B	Nuclear factor kappa-B
ng/ml	Nanograms per millimetre
nm	Wavelength in nanometre
nM	Nanomolar
NSAIDs	Non-steroidal anti-inflammatory drugs
OEA	N-oleoylethanolamine
OD	Optical density
<i>P</i> -value	Probability value
PAA	Palmitoylethanolamine-preferring acid amidase
<i>P</i> _{app}	Apparent permeability coefficient
PBS	Phosphate buffered solution

PEA	N-palmitoylethanolamine
PG	Prostaglandin
PGE2	Prostaglandin E2
PIP2	Phosphatidylinositol 4,5-biphosphate
PKA	Protein kinase A
PLC	Phospholipase C
PPAR	Peroxisome proliferation-activated receptor
PRK2	Protein kinase C-related kinase 2
R _{Blank}	Transepithelila resistance of blank Transwell [®]
ROCK	Rho-associated protein kinase
R _{Total}	Total transepithelial resistance of cells and filter
R _{True cells}	True transepithelial resistance of cells
SA _{Filter}	Surface area of filter in Transwell [®]
siRNA	Small interfering RNA
SD	Standard deviation
SDS-PAGE	Sodium dodecyl sulphate polyacrylamide gel
Sec	Seconds
SEM	Standard error of mean
TBST	Tris-buffered saline and tween 20
TEER	Transepithelial electrical resistance
TGF _β	Transforming growth factor beta
Th2	T-helper 2 cells
Thr	Threonine
THC	Δ ⁹ -tetrahydrocannabinol
TLR4	Toll-like receptor 4
TNFα	Tumour necrosis factor-α
TRP	Transient receptor potential channel

TRPA	Transient receptor potential channel ankyrin subtype
TRPC	Transient receptor potential channel canonical subtype
TRPM	Transient receptor potential channel melastatin subtype
TRPMP	Transient receptor potential channel mucopilin subtype
TRPP	Transient receptor potential channel polycystin subtype
TRPV	Transient receptor potential channel vanilloid subtype
UK	United Kingdom
US	United States of America
V	Unit for voltage in volts
v/v	Volume in millilitres per unit volume in millilitres
w/v	Weight in milligrams per unit volume in millilitres
WHO	World Health Organisation
ZO	Zona occludens
ZONAB	Zona occludens-1 associated nucleic acid binding protein

Abstract

Injury to the bronchial epithelium in respiratory diseases such as asthma and COPD results in the loss of barrier function and an elevated sensitivity to environmental insults. An increased release of the endogenous cannabinoid, anandamide in response to inhalation of allergen in asthmatic patients has been reported. In contrast, previous clinical trial findings suggest anti-inflammatory and broncho-relaxant properties of the phytocannabinoid, Δ^9 -tetrahydrocannabinol (THC). The aim of this study was, therefore, to determine the effects of endocannabinoids and phytocannabinoids on bronchial epithelial cell permeability and to investigate the mechanisms involved.

Calu-3 human bronchial epithelial cells were cultured at air-liquid interface to allow development of tight junctions. Changes in transepithelial electrical resistance (TEER), a reflection of epithelial permeability, were measured at various time points post-treatment.

The endogenous cannabinoid anandamide produced a significant reduction in TEER, which was unaffected by cannabinoid receptor antagonists, but attenuated by URB597, an inhibitor of fatty acid amide hydrolase, and by a combination of cyclooxygenase and lipoxygenase blockade. Subsequent immunoblotting data revealed that the expression of tight junction proteins, occludin and ZO-1, were also reduced by anandamide. Inhibition of ERK activation by MEK1/2 inhibitors, PD98059 and U0126, prevented the anandamide-induced reduction in TEER and prevented the reduction in occludin expression. Thus, ERK activation is likely to mediate these effects by altering the expression of tight junction proteins.

Treatment with THC prevented TNF α -induced decrease in TEER and increased in paracellular permeability. CB₁ and CB₂ receptor-like immunoreactivity was found in

Calu-3 cells. Subsequent pharmacological blockade of either cannabinoid receptor inhibited the THC effect. In comparison, stimulation of both or either CB₁ or CB₂ receptors displayed similar effect to that of THC. Western immunoblotting also revealed reproducible decreases in occludin and ZO-1 expression in TNF α -treated cells, whereas cells pre-incubated with THC alone or in combination with TNF α did not alter expression levels. Phosphorylation of myosin-phosphatase target protein at threonine 696 residue by TNF α was attenuated in the presence of THC, indicating the involvement of RhoA/ROCK cascade. Selective stimulation of either cannabinoid receptor in TNF α -treated cells suggests THC-induced inhibitory effect on RhoA/ROCK signalling was mediated through CB₂ receptor, and not CB₁.

In summary, these data suggest that the reduction in transepithelial resistance by anandamide, indicative of increased epithelial permeability, is caused by its metabolites rather than anandamide itself. Inhibition of anandamide degradation might provide a novel approach to treat airway inflammation. Conversely, THC reverses the reduction in transepithelial resistance caused by TNF α , through an effect at CB₁ and CB₂ receptors. Hence, THC, or perhaps other cannabinoid receptor ligands may have potential therapeutic roles in inflammation-induced changes in airway epithelial cell permeability, such as asthma and COPD.

1. General Introduction

Airway inflammatory diseases, such as asthma and Chronic Obstructive Pulmonary Diseases (COPD), show overlapping pathological features of heightened immune response within the airway structures. A prevalence study conducted by the World Health Organisation (WHO) revealed a growing population of asthmatics of approximately 235 million to date, in which patients were affected due to various environmental factors or genetically inherited the condition (WHO, 2015a). In comparison, the estimated number of COPD patients worldwide was 65 million (WHO, 2015b). However, this figure was thought to be an underestimation as the process in determining the accurate prevalence was challenged by the confusion in distinguishing COPD from other similar conditions at diagnosis stage – including chronic asthma, emphysema, and chronic bronchitis.

Furthermore, the latest epidemiological data shows that COPD is globally the third leading disease resulting in death in the world (WHO, 2014). Asthma is in fact, more responsible for one of the major causes for emergency admissions and hospitalisation. The mortality rates caused by asthma was significantly lower compared to COPD as asthma does not involve a gradual deterioration over time, provided that symptoms are adequately controlled. The quality-of-life in patients with asthma and or COPD is generally reduced owing to the chronic nature of these conditions. There are currently no cures for asthma and COPD thus drug interventions aim only to decelerate the deterioration in pulmonary function. Oral and inhaled corticosteroids are amongst the currently available treatments that reportedly provide the best efficacy in symptomatic control and improve lung function due to their anti-inflammatory properties (Barnes et al., 1998). However,

observations from clinical trials have shown ongoing infiltration of immune cells in the airway structures despite the use of corticosteroids (Sont et al., 1999, Nuijsink et al., 2007). Histological study in endobronchial biopsy samples of moderate to severe asthmatics revealed that treatment with corticosteroids even at high doses exerts little or no effect in rectifying airway remodelling, including epithelial denudation (Pepe et al., 2005). The loss of barrier function in damaged airway epithelium contributes to progression of the conditions as it continually allows the intrusion of pro-inflammatory mediators into the systemic environment. Increasingly, asthma and COPD are now recognised as epithelial disorders, in addition to their inflammatory feature.

The demand for such new therapeutic aims encourages research into drugs that correct both the epithelial structure and inflammatory activity within the airways. The approach in studying the effects of cannabinoids on human airway epithelium in this project is considered a novel yet historical one. Traditionally, the *marijuana* plant was smoked or orally consumed to treat coughs and asthma, which scientists now thought were the effects of phytocannabinoids. Modern experimental studies have also suggested the potential of cannabinoids, either endogenously released or plant-derived in the treatment of airway inflammation, such as asthma. In contrast, endocannabinoids were shown to exhibit pro-inflammatory effects during the acute phase of airway inflammation (Calignano et al., 2000). Although yet to be proven in the respiratory system, studies in human intestinal epithelial models have shown promising insights of cannabinoids in regulating the barrier property of the epithelium. Hence this chapter introduces the various backgrounds involved in this project, justifying cannabinoids as a potential new therapeutic target to treat airway inflammation.

1.1 The Human Respiratory System

The main function of the lungs is to ensure the gaseous exchange of oxygen from the atmosphere into the bloodstream during inhalation, which is then transported to various parts of the body. The exhalation process, on the other hand, involves the removal of carbon dioxide from the body, produced mainly as a waste product during energy production.

The respiratory system allows air to enter through nasal passages or mouth which passes through nasopharynx (i.e. the throat) and subsequently into the trachea (refer *Figure 1-1*). Air is then conducted to the lungs through the left and right bronchi. Within the lungs, the air enters into highly branched and narrower airways, the bronchioles. Air conductance then terminates at the clustered ends of the bronchioles, at thin air sacs known as the alveoli, to allow oxygen to be diffused from air into the bloodstream whilst expelling carbon dioxide into the air for exhalation.

Thus, the continuum of conducting airways within the lungs must remain open to ensure efficient air movement in and out of the respiratory system. The larger airways, such as trachea, main (primary) bronchi are encircled with tough cartilages rings that widen and lengthen during breathing reflexes (refer *Figure 1-1*). In comparison, smaller conducting airways including lobar (secondary) and segmental (tertiary) bronchi as well as bronchioles, consist of softer cartilages with smooth muscles walls that are sensitive to chemical and physical stimuli to constrict and dilate. The underlying smooth muscle (i.e. submucosal) compartment of the smaller bronchi and bronchioles is densely innervated by the parasympathetic nervous system that can be stimulated by chemical and physical stimuli to convey signals for the bronchioles to contract or dilate. Within the cavities of the conducting airways,

lies the epithelial layer that lines the luminal surfaces to separate the submucosal compartment from the environment.

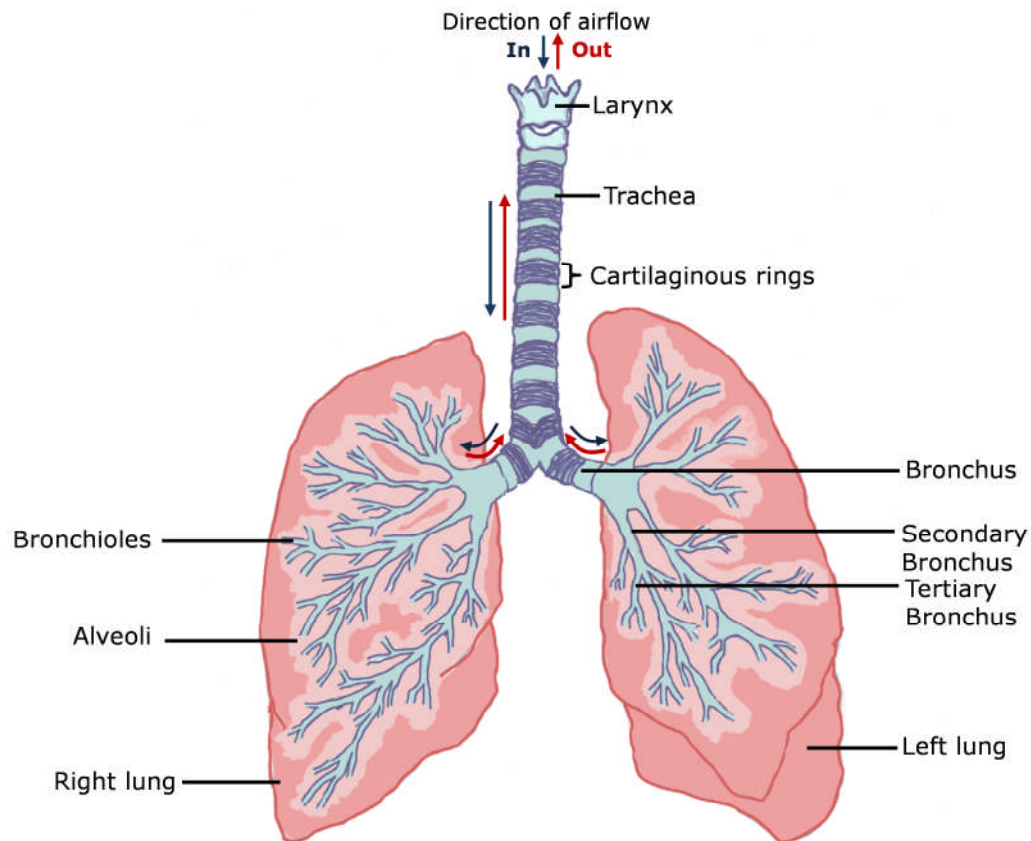


Figure 1-1 Diagram of a human respiratory structure. It is noted that the conducting airway begins from the trachea to the alveolar region. Arrows in blue showed the direction of airflow during inhalation, whereas the red represents direction of airflow during exhalation.

1.2 Anatomy of the Bronchial (Airway) Epithelium

The epithelial cells that are found on the surfaces of the bronchi consist of ciliated columnar cells, mucous-secreting goblet cells, surfactant-producing Clara cells and basal cells (refer *Figure 1-2*).

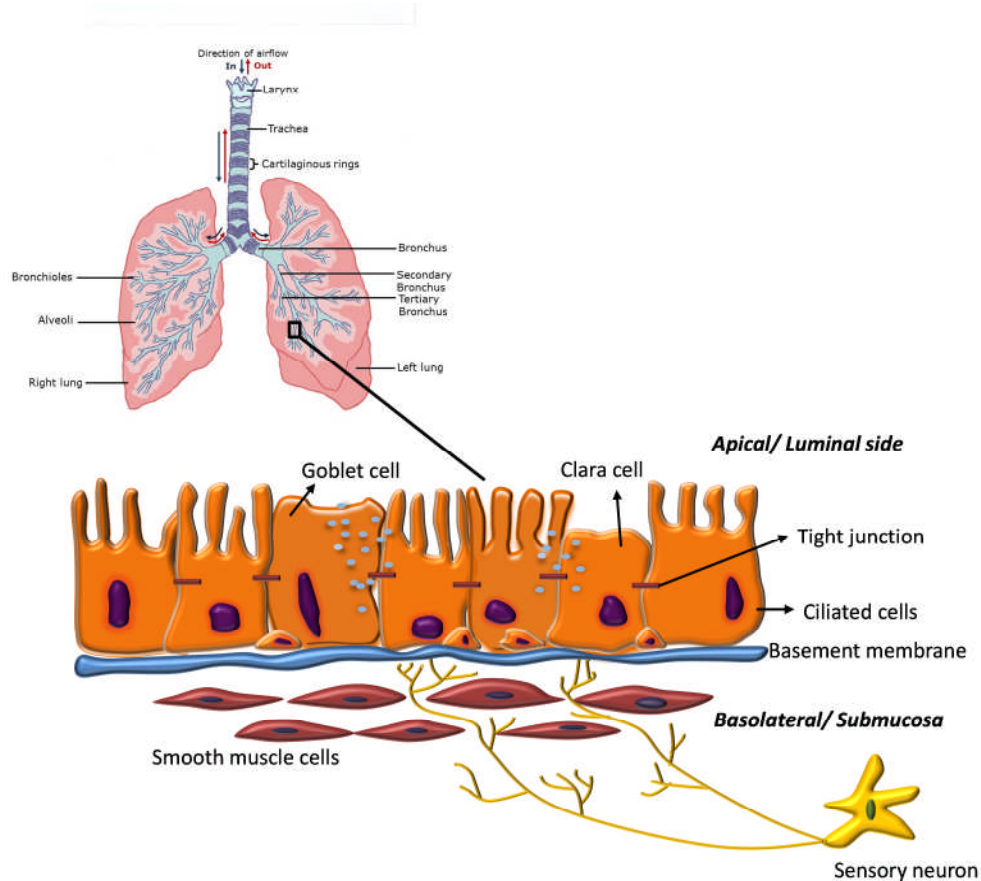


Figure 1-2 The bronchial epithelium structure is exposed to two different interfaces. First, the top part which faces the environment is known as the apical or luminal side. Second, the basolateral side faces the submucosal compartment which contains the sensory neurons, immune cells and smooth muscle cells. The bronchial epithelium consists of various types of cells including ciliated columnar cells, mucus-secreting goblet cells and surfactant-producing Clara cells that are fastened together by tight junctions. Basal cells are expressed beneath these larger cells and are attached firmly onto the basement membrane.

1.2.1 Ciliated Epithelial Cells

Earlier histological investigation revealed that more than half of the epithelial cells in the larger and smaller conducting airways are ciliated cells (Spina, 1998). These cells appear in rectangular shape and also often known as the ‘ciliated columnar cells’. Owing to their shape and the hair-like protrusion at the tip, ciliated epithelial cells expel trapped particles in the mucus through brushing motion towards the upper respiratory tract so that they can be expectorated or swallowed. ‘Tidying’ of the airway surface by such a mechanism is known as ‘mucociliary clearance’. It is reported that these cells are differentiated from the goblet, Clara or basal cells (Jain et al., 2010).

1.2.2 Goblet Cells

Goblet cells are distributed throughout the airway epithelial structure, although reports have claimed that they are more abundantly distributed in the tracheal and bronchial regions, than bronchioles (Rogers, 2004). In normal conditions, goblet cells produce regulated amount of mucus that provides hydration on the luminal surfaces of conducting airways whilst acting as a chemical defence to entrap aeroallergens, such as pollens, bacteria and viruses. Goblet cells also respond acutely upon exposure to harmful substances and physical stimuli, such as cough, by temporarily increasing the release of mucins to protect the epithelium. However, normal regulation of mucus secretion is lost in pathogenic states, such as asthma and COPD. Mucosal biopsy sections of patients with mild to moderate asthma and COPD (Ordonez et al., 2001, Saetta et al., 2000) revealed increased proliferation and enlargement of goblet cells. This subsequently leads to overproduction of mucus, which clogs the conducting airways.

The earliest study in the 1980's using electron microscopy revealed secretory membrane-bound granules within the goblet cells that contain heavily glycosylated glycoproteins called mucins (Lumsden et al., 1984). Thus, mucus is only formed when several mucins glycoproteins are excreted from the Goblet cells to produce chains of oligomeric structures. A single goblet cell is known to produce several types of mucins that differ in pH, depending on the moiety expressed, which ultimately affects the viscoelasticity of mucus (Thornton et al., 2008). Highly sulphated mucins confer for mucus with higher pH values and thicker consistency, whereas the presence sialic acid produces mucus that is less viscous.

1.2.3 Clara Cells

It has been claimed that Clara cells are exclusively distributed in the bronchus and bronchioles [review article by (Knight and Holgate, 2003)]. Like Goblet cells, surfactants produced by the Clara cells function to provide a chemical coat that protect the epithelium whilst maintaining the structural integrity of the lung. The secretion from Clara cells were also known to contain metabolising enzymes, such as cytochrome P450 oxidase and anti-proteases [review by (Hukkanen et al., 2002)] that are believe to also play a chemo-protective role in digesting foreign materials. In addition, studies have demonstrated the plasticity property of Clara cells as a progenitor cells during tissue injury, enabling themselves to differentiate either into goblet or terminally, as ciliated columnar epithelial cells (Hong et al., 2001).

1.2.4 Basal Cells

In contrast to other epithelial cell types, the sizes of basal cells are relatively small thus attaching themselves firmly onto the basement membrane. The distribution of basal cells is concentrated mostly along the larger conducting airways such as the trachea and bronchi, rather than that of the smaller conducting airways (Evans et al., 2001). It is postulated that the number of basal cells found in conducting airways is correlated to the likelihood for cell detachment as these cells act as primary progenitor cells that aid in epithelial cell renewal (Rock et al., 2009). Reports revealed that basal cells can differentiate into ciliated, goblet or Clara cells (Hong et al., 2004, Walters et al., 2013).

1.2.5 Neuroepithelial Bodies (NEBs)

Electron microscopy investigations revealed NEBs that are granule-containing cells that appeared like a group of cells clustering together, forming a triangular shape (Adriaensen et al., 2003). Like basal cells, NEBs are relatively small in size and found attached firmly onto the basement membrane. It is noted that NEBs are also referred to as Kulchitsky cells, neuroendocrine-like cells and Feyrter cells. As their names suggest, NEBs release various neuropeptides to stimulate the pulmonary nerves that are innervated the airways (Adriaensen et al., 2006). Separate studies suggest NEBs derived from the human airway epithelium secrete serotonin (5-hydroxytryptophan), calcitonin, substance P and calcitonin gene-related peptide (CGRP) (Reynolds et al., 2000, Hong et al., 2001, Fu et al., 2002). Integration of the neuropeptide release with the afferent nerve terminals and possibly stretch fibres in NEBs is thought to have a significant role in recognising hypoxia by enhancing the release of 5-hydroxytryptamine (5-HT) and inhibiting the oxygen-sensitive

potassium channels to alter subsequent cardiovascular and respiratory activities (Kemp et al., 2003). In addition to their secretory function, studies have suggested a role of NEBs as progenitor cells during epithelial wound healing (Reynolds et al., 2000, Peake et al., 2000).

1.2.6 Immune Cells

i. Mast Cells

Mast cells are known to mediate allergy responses hence mainly involved in extrinsic (allergic) asthma, although studies have suggested that mast cells also mediate airway inflammation in intrinsic (non-allergic) asthma or COPD patients with asthmatic symptoms (refer *section 1.4*). In a study conducted by Paul Ehrlich, mast cells were distinguished as cells with secretory granules that when activated by allergens, resulted in the release of these granulated contents [review by (Beaven, 2009)]. Such phenomenon, which is known as degranulation, is referred to as the secretion of biological compounds from the granules which consist mainly of histamine, leukotrienes and heparin. It has been now established that the release of histamine occurs during the early phase of an extrinsic asthmatic event, causing bronchoconstriction, which obstruct the airflow within the conducting airways. Histological examination of the bronchial biopsy samples from asthmatic patients demonstrated increased mast cells infiltration from the epithelium into the smooth muscle compartment in their degranulated form (Carroll et al., 2002). Mast cells are also reportedly to be involved in the production of pro-inflammatory cytokines, IL-4, IL-5, IL-6 and tumour necrosis factor- α (TNF α) [review by (Bischoff, 2007)]. The release of these cytokines is linked to the broncho-hyperresponsiveness response as the airway epithelium layer is disrupted.

ii. Eosinophils

Following their development and maturation in the bone marrow, eosinophils are transported in the blood to the sites of inflammation. Histological investigation revealed enhanced infiltration of eosinophils within the bronchial epithelium is commonly found patients with asthma and COPD (Rutgers et al., 2000, Berry et al., 2007). Studies revealed an increased in eosinophilic count in the sputum and bronchoalveolar lavage fluid of patients with asthma and COPD (Louis et al., 2000, Singh et al., 2014). The investigators of these experiments have also commented that the number of eosinophils detected is directly linked to the severity of the disease. Recruitment of eosinophils to the epithelium was reportedly to be driven by cytokines released by the Th2 cells, mainly IL-4, IL-5 and IL-13 during the early phase responses in asthmatic symptoms (Akbari et al., 2006, Vijayanand et al., 2007). Presence of the eosinophils was thought to be one of the contributing factors for airway remodelling during airway inflammation by inducing fibrosis within the subepithelial layer (Minshall et al., 1997) as well as epithelial thinning (Benayoun et al., 2003).

iii. Neutrophils

Neutrophils are the most abundant type of immune cells that circulate in the bloodstream thus has an important role in mediating the innate immune response. Evidence suggests that neutrophils are actively recruited to the site of inflammation following the release of TNF α mainly by macrophages and Th2 cells as demonstrated in rodent airway inflammatory model (Lukacs et al., 1995). Further study then revealed that a proportion of humans with asthmatic symptoms also showed significant increase in sputum neutrophil levels, which was accompanied by

elevated levels of circulating chemokines for neutrophils within the serum including TNF α and IL-6 (Wood et al., 2012). This indicates that the inflammatory response is exclusively localised within the airway structures, but also affected systemically. It was also demonstrated that asthmatic patients showing such inflammatory characteristics generally exhibit accelerated deterioration in lung function and poorer prognosis (Donaldson et al., 2005).

iv. Macrophages

Macrophages are pathogen-engulfing cells that protect the normal functions of the airway as part of the innate immune response. These cells are frequently expressed in the alveolar region, although a study has demonstrated that they were also observed within the bronchial region in patients with asthma (Vignola et al., 1999, Saha et al., 2009). Bronchoalveolar lavage samples from asthmatic subjects showed an increased macrophage count (John et al., 1998). Within the same study, isolation of the macrophages detected within the alveoli revealed that pro-inflammatory cytokines, such as granulocyte-macrophage colony-stimulating factor (GM-CSF), TNF α , IL-1 β and interferon- γ (IFN γ) are released from these cells.

v. Pulmonary Dendritic Cells

Dendritic cells found within the intact human airway epithelium are immune cells that participate in activating Th2-mediated responses when stimulated following an increased exposure to noxious stimuli from the environment. This subsequently activates Th2 cells to secrete pro-inflammatory cytokines and propagate the inflammatory reaction that stimulates eosinophils and mast cells activities. Previous histological observation have reported increased recruitment of dendritic cells onto

the airway epithelium of asthmatic patients who had not received corticosteroid treatment to reduce airway inflammation (Moller et al., 1996). Previous study in rodents exposed to the aeroallergen ovalbumin, indicated an increase in paracellular movement of dendritic cells, which led to disruption airway epithelium barrier function (Vermaelen and Pauwels, 2003).

1.3 Roles of the Airway Epithelium

1.3.1 Barrier Function - The Airway Epithelial Tight Junction

Protein Complex

Based on the illustration in *Figure 1-3*, tight junctions comprise the main barrier function as they are found on the apex of the epithelial cells layer. At the molecular level, bronchial tight junctions are constructed of complex protein networks between intracellular plaque zona occludens (ZO) 1-3, occludin, claudin and junctional adhesion molecules (Harhaj and Antonetti, 2004, Fanning et al., 1998).

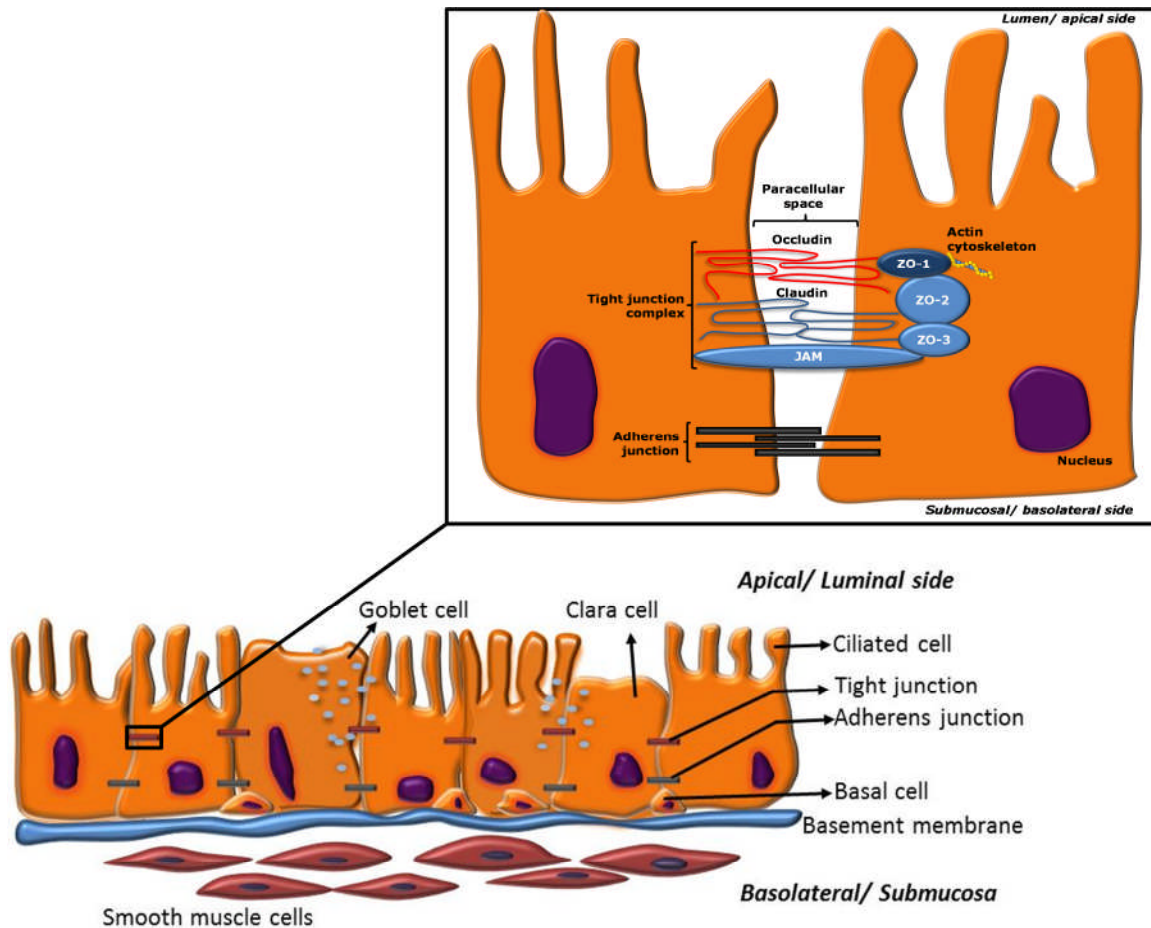


Figure 1-3 A diagram of the bronchial epithelium layer which includes ciliated columnar cells, Goblet cells, Clara cells and basal cells. These cells are attached onto the basement membrane which acts as an anchor and maintains intercellular adhesion. The focused view shows various isoforms of zona occluden (ZO) as scaffolding proteins which are situated intracellularly. Other protein components include occludin, claudin and junctional adhesion molecule (JAM), are membrane-spanning proteins that form a complex network with respective ZO isoforms to maintain the barrier function of the epithelial layer. Collectively, these intercellular junctional complexes are known as ‘tight junction’. Situated under the tight junction protein complex is the adherens junction that enhances cell-to-cell contact and provide additional support to maintain the integrity of the epithelium structure.

The loss of the structural integrity of the tight junctions, such as seen in asthma, increases the permeability to pro-inflammatory mediators and cytokines leading to bronchoconstriction due to excessive stimulation of the afferent nerves (Bousquet et al., 2000). Such phenomenon is also known as bronchial hyper-responsiveness, whereby the sensitivity of the airways to broncho-constricting stimuli is heightened. Histological observations have also revealed that the development of tissue oedema within the bronchial wall of asthmatic patients is due to leaky epithelial tight junctions, that allows bulk flow of plasma into the lumen (Holgate, 2007).

Understanding of tight junction disruption in diseased state was not well-established until the late 1990's, when Wan *et al* revealed a significant reduction in ZO-1 staining in bronchial epithelial cells samples from asthmatic patients (Wan et al., 1999). In their study, formation of broken tight junction rings was observed in immunofluorescent images of the human bronchial epithelial cell line, 16HBE14o- even after four hours of exposure to cysteine proteinase allergen Derp1. Following the authors' claim of the novel therapeutic approach to asthma, subsequent investigations using primary human bronchial epithelial cells (HBEC) (Heijink et al., 2010) and other cell line models, Calu-3 (Vinhas et al., 2011, Petecchia et al., 2012) and BEAS-2B (Chang et al., 2010) grown in air-liquid interface have produced consistent findings when triggered by cytokines or aeroallergens. In addition, these publications reported reduction in transepithelial electrical resistance (TEER) measurement in inflammatory states owing to disruption of the epithelial cell monolayer and, indirectly, indicate leaky epithelial tight junctions such as those seen in asthma.

Mechanisms of tight junction breakdown caused by pro-inflammatory mediators have been proposed. First, cytokine such as TNF α , was found to activate the protein-

activated receptor (PAR) in the normal human bronchial epithelial cells, which subsequently promoted the production of extracellular matrix digestive enzymes, the matrix metalloproteinases (MMP) that leads to epithelial tight junction disruption (Hozumi et al., 2001, Hardyman et al., 2013). However, the molecular mechanism of MMP in cleaving the tight junction proteins structure is yet to be investigated. Second, the presence of cytokine, like TNF α was linked to activation of the RhoA cascade that mechanically damaged the tight junction structure due to the exaggerated contraction of the actomyosin skeleton (Soong et al., 2011). Further detail of the involvement of RhoA in TNF α -induced tight junction disruption is discussed in *section 1.7.2*. Lastly, TNF α was shown to induce bronchial epithelial cell apoptosis (Bucchieri et al., 2002) hence was postulated to lead to tight junction disruption due to the loss of intercellular structural support.

1.4 Inflammatory Diseases Associated to Impaired Airway Epithelial Permeability

Airway inflammatory diseases that are associated with the loss of the epithelium barrier function include asthma, chronic obstructive diseases (COPD), cystic fibrosis, allergic rhinitis, infective pulmonary diseases and lung carcinoma. The present study focuses on asthma and COPD only as these two conditions demonstrate similarities in their site of inflammation, pathogenesis and the mechanism of airway (i.e. bronchial) epithelium disruption.

1.4.1 Asthma

Earlier literature described asthma as a condition featuring wide variation in intrapulmonary airflow over a brief period of time (Scadding, 1983). This definition solely describes the disease based on its physiological feature, mainly due to the fact that wheezing is an exclusive feature in asthmatics. As understanding in asthma continues to accumulate, there is a general consensus that in addition to its symptoms, the central definition of asthma should also acknowledge long-term inflammatory response that occurs on the airway structures. According to the latest Global Initiative for Asthma (GINA) report, a complete description for asthma should entail its pathological characteristics in addition to its clinical features:

“a heterogeneous disease, usually characterized by chronic airway inflammation. It is defined by the history of respiratory symptoms such as wheeze, shortness of breath, chest tightness, and cough that vary over time and in intensity, together with variable expiratory airflow limitation” (GINA, 2014).

However, the British Thoracic Society advises that such a definition should not be used as a gold standard in making a diagnosis (BTS, 2014). In fact, they suggest advanced clinical assessments to detect signs of asthma which are mainly evident in the smaller bronchial region, albeit involving invasive techniques. They include sampling of the epithelium and its secretion through bronchial biopsy or bronchoalveolar lavage for evidence of inflammation by quantifying the number of immune cells recruited and their associated release of cytokines. In addition, inhalation challenges to allergens at titrated doses, such as histamine and methacholine, allow clinicians to estimate the severity of the condition based on the concentration of allergen needed to stimulate bronchoconstriction. The tendency for

the bronchial airway to constrict following exposure to aeroallergen is known as, bronchial hyperresponsiveness [review by (Holgate and Polosa, 2006).

The diagnosis of asthma is separated into two main categories:

i. Allergic (extrinsic) asthma

Asthmatic patients of this category are allergic to various environmental insults which normally include mould, plant pollens, alcohol, etc. It is regarded as an immediate type I hypersensitivity reaction as the acute allergic response which then leads to the production of immunoglobulin E (IgE). Previous studies have reported that the IgE antibody, which is synthesised by B-lymphocyte cells, binds to the high-affinity IgE receptors expressed on the surface of mast cells and basophils [review by (Stone et al., 2010)]. Allergens then attach onto the bound IgE conformation to induce the release of pro-inflammatory mediators such as histamine, cytokines and leukotrienes from these immune cells. Such reaction then leads to bronchoconstriction and mucus secretion, whilst further recruits other lymphocytes to the site of inflammation.

As the condition progresses, T-lymphocytes are activated to enhance the production of other cytokines, mainly tumour necrosis factor- α (TNF $_{\alpha}$) and interleukin-1 β (IL-1 β) (Holgate and Polosa, 2006). Studies have claimed that the mechanism of airway inflammation involves an orchestrated response to various types of inflammatory cells supported by the findings of increased numbers of eosinophils, neutrophils, macrophages and T-lymphocyte cells in endobronchial and transbronchial biopsy tissue samples of patients with severe asthma (Balzar et al., 2005, Bartemes and Kita, 2012). The inflammatory reaction occurs

predominantly on the bronchial epithelium, as epithelial lining is damaged and causes epithelial cells to shed. The loss of the epithelial barrier exposes afferent nerves directly to the environment, hence increasing the risk for bronchial hyperresponsiveness, as allergens can directly stimulate these nerves.

Allergic asthma also includes other non-IgE related responses such as hypersensitivity reactions to aspirin (Szczeklik and Stevenson, 2003), non-steroidal anti-inflammatory drugs (NSAIDs) (Mitchell and Warner, 1999) and occupational asthma, due to repeated exposure to harmful substances like ethylene diamine, asbestos and hardwood dusts. Bronchoalveolar lavage fluid of patients with aspirin allergy revealed elevated level of cysteinyl-leukotriene due to the overexpression of leukotriene C4 synthase enzyme, which are likely to be released from eosinophils and mast cells (Cowburn et al., 1998). The mechanism of airway inflammation caused by industrial substances varies depending on the chemicals involved, the route and intensity of exposure as well as genetic susceptibility. An article which reviewed a wide range of organic and inorganic chemicals suggested that inflammation may be triggered by the increased in leukotriene, cytokines and abnormal secretions of growth factors (Maestrelli et al., 2009).

ii. *Non-allergic (intrinsic) asthma*

In contrast to allergic asthma, non-allergic asthmatic attacks are induced by emotional stress, anxiety, dry air and exercise. Patients usually show a later onset in life, hence mainly affects adults. Interestingly, traces of IgE were detected in these patients despite showing negative responses to allergic skin-prick testing (Taskapan et al., 2008). This suggests that IgE-mediated responses are vital for

the pathogenesis asthma regardless of its type. Furthermore, sputum samples from non-allergic asthmatics revealed increases in eosinophilic recruitment, which is also a prominent feature of bronchial inflammation in allergic asthma (Pavord et al., 2012). High eosinophilic counts found from the surface of bronchial structure were also thought to have contributed to the epithelial damage seen in asthmatic patients. Hence, this elucidates the similarity in the symptoms presented in both types of asthma as the loss of epithelial barrier accounts for bronchial hyperresponsiveness and airway inflammation.

1.4.2 COPD

COPD causes progressive decline in lung function despite the use of pharmacological treatments. Ultimately, this leads to respiratory failure hence the mortality rate in COPD is higher compared to patients diagnosed with asthma alone. It is a preventable disease that is predominantly a result of a long-term history of smoking.

As a general guideline to aid diagnosis, GINA defines COPD as:

“a condition that is preventable and treatable, characterised by persistent airflow limitation that is usually progressive and associated with chronic inflammatory responses in the airways and in the lungs to noxious particles and gases. Exacerbation and comorbidities contribute to the overall severity in individual patients” (GINA, 2015).

The term COPD is clinically used when patients present more than one symptoms of the following conditions:-

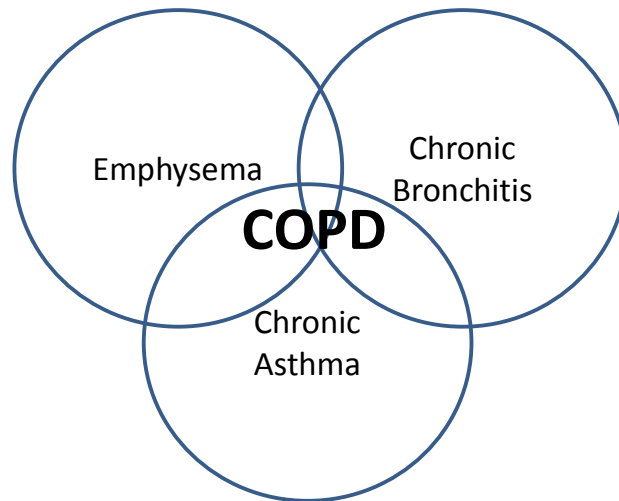


Figure 1-4 The Venn diagram illustrates that COPD is a combination of long-term, irreversible conditions which include chronic asthma, emphysema and chronic bronchitis.

Individual features of the conditions listed in *Figure 1-4* are discussed as below;

i. Chronic asthma

A condition due to the presence of chronic bronchial inflammation in COPD patients. In contrast to asthma, chronic asthma shown in COPD has a later onset, due to inflammation within the bronchial structure in patients with long history of smoking habit. The mechanism of airway inflammation in COPD patients with chronic asthma is similar to that of intrinsic asthmatics. Further details of chronic asthma associated with COPD are discussed in *section 1.4.3*.

ii. Emphysema

A disease that involves enhanced air sac distention within the alveoli that result in the loss elasticity of the alveolar wall or loss in elasticity. The mechanism underlying such structural destruction is predominantly due to the inflammatory response that takes place following the exposure of cigarette smoke as the key

irritant. Toxicology investigation revealed that cigarette smoke contains a range of toxic substances that increases both the level of oxidative stress, the expression of the cytokine, TNF α , and proteolytic enzymes, mainly elastases that damage the alveolar epithelial cell layer (Rahman et al., 1996, Nadel, 2000, Churg et al., 2002). As the alveoli walls are disrupted and become fibrotic, this impairs the oxygen-carbon dioxide transfer. At the same time, lungs would also be hyperinflated, owing to the decreasing number of functional alveoli that could assist the elastic recoil of the diaphragm and rib cages during exhalation. The loss of such spring mechanism provided by the alveoli results in shortness of breath and cough as patients struggle to inhale and exhale normally. This eventually leads to hypoxaemia as the lungs persistently failed to deliver the required oxygen concentration during respiration, which is the key reason for extrapulmonary comorbidities associated to COPD (Kent et al., 2011).

iii. Chronic bronchitis

The presence of chronic bronchitis in COPD is confirmed when patients clinically present with ongoing cough and increased sputum production for at least three months within the two years of an unestablished diagnosis for productive chronic cough (GINA, 2015). In contrast to asthma, patients with chronic bronchitis do not show signs of bronchial hyperresponsiveness and airway obstruction, despite inflammation within the bronchial structure in chronic bronchitis is also known to be mediated by eosinophils (Barnes et al., 2006). It is speculated that there are variable mechanisms of bronchial inflammation involved in the pathogenesis of asthma and chronic bronchitis,

although the difference in their associated inflammatory pathways is still yet to be further explored [review by (Kim and Criner, 2015)].

1.4.3 Asthma-COPD Overlap Syndrome (ACOS)

ACOS are classified as a combination of chronic obstructive airway diseases that shows clinical features of intrinsic and or extrinsic asthma associated with COPD - mainly wheezing, increased sputum production, cough and breathlessness. GINA defines ACOS as:

“a condition characterized by persistent airflow limitation with several features usually associated with asthma and several features usually associated with COPD. ACOS is therefore identified by the features that it shares with both asthma and COPD” (GINA, 2015).

Bronchial surfaces of patients with ACOS show overlapping feature in the histological changes as that seen in asthmatics, with the presence of bronchial epithelial injury. It is noted that the surface epithelium topology of patients with COPD alone tends to thicken due to fibrosis. An *in vitro* study using primary human bronchial epithelial cells also revealed that the presence of cigarette smoke is biased towards triggering abnormal changes to epithelial cell differentiation, reducing the number of ciliated cells, whilst inducing goblet and Clara cells hyperplasia (Schamberger et al., 2015). Although airway epithelial denudation is an exclusive feature of asthma, the study conducted by Schamberger *et al* postulated that the epithelial barrier function in COPD is similarly decompensated as Transepithelial Electrical Resistance (TEER) measurements are decreased following

the exposure of cigarette smoke extract to the cells. Such findings thus imply that experimentally-induced airway epithelial leakiness in an *in vitro* model is also applicable to represent disrupted bronchial epithelial cell layer found in ACOS.

1.5 The Mechanism of Airway Inflammation in Asthma and COPD

In asthmatics or COPD patients showing signs of asthma, the site of inflammation occurs particularly within the smaller conducting airways, thus causing the bronchioles to constrict, especially during acute asthma attacks. Bronchoconstriction limits the amount of airflow in and out of the lungs as the opening of the bronchiole lumen tightens. Such phenomenon is clinically presented as wheezing, as patients struggle to breathe. Bronchoconstriction, which is a symptom of airway inflammation, is initiated when a surge of pro-inflammatory insults is released to stimulate the parasympathetic nerve endings. This subsequently promotes acetylcholine to activate bronchial M3-muscarinic receptors, resulting in bronchoconstriction and excessive production of mucus that obstructs the airflow between the lung and atmosphere. The involvement of other types of sensory nerve and receptors in mediating bronchoconstriction, such as the non-adrenergic non-cholinergic (NANC) nerves and tachykinin NK2 receptors have also been indicated in previous literature [review by (Joos et al., 2000)].

Narrowing of the airway passages or bronchoconstriction can be manifested via several mechanisms, depending on the type of stimuli (Busse et al., 1995). For example, environmental exposure to allergens activates Th2-type lymphocytes, macrophages and mast cells which promote the expression of various cytokines, such as TNF α , IL-1 β , IL-4 which facilitate the synthesis of IgE (see *section 1.2.6*). On the other hand, a study demonstrated that in aspirin-intolerant patients, suppression of prostaglandin E₂ (PGE₂) induced an excessive production of cysteinyl leukotrienes following the inhibition of cyclooxygenase-1 (COX-1) (Wang et al., 2007). This is also true for those who are intolerant to non-steroid anti-inflammatory drugs

(NSAIDs) as they inhibit the metabolism of arachidonic acid (Stevenson and Szczeklik, 2006), also through the COX pathway.

However, there is increasing evidence that claims that airway epithelial injury was the first step to occur following heightened inflammatory activity, irrespective of the type of triggering factors involved [review by (Holgate, 2007)]. Histological studies revealed that the airway epithelium of patients with asthmatic symptoms consistently demonstrated physical damage that worsened with increasing severity (Xiao et al., 2011). It is thought that airway inflammatory diseases is initiated from the impaired epithelial function which subsequently allows the invasion of immune cells into the smooth muscle layer that release various cytokines and chemokines. Within the same study, it was hypothesised that chronic exposure to these inflammatory markers or immune cells then leads to a recurring injury or healing cycle that causes structural alteration within the epithelial layer itself. Morphometric investigations of biopsy and post-mortem airway samples consistently displayed thickening of the smooth muscle layer, goblet cell metaplasia as well as epithelial damage (McKay and Hogg, 2002, Grainge et al., 2011), also collectively known as airway remodelling

Thus, this suggests the necessity to preserve the airway epithelium structure to maintain normal airway tone. Understanding of the interrelationship between airway inflammation and its structural remodelling in influencing the severity or progression of asthma has since, gradually emerged as a novel therapeutic target.

1.6 Current Pharmacological Treatments for Airway Inflammation

β_2 -adrenoceptor agonists, such as salbutamol and terbutaline are short-acting bronchodilators that are prescribed to provide symptomatic relief of asthma. On the other hand, salmeterol and formoterol are long-acting β_2 -adrenoceptor agonists have slower onset of action but provide a longer therapeutic effect, as their molecules are highly lipophilic to aid in retaining the binding interaction between the drug molecule and the receptor (Szczuka et al., 2009). The β_2 -adrenoceptor agonists act by stimulating the receptors expressed on the airway smooth muscle. It is noted that the β_2 -adrenoceptors belongs to the group of G protein-coupled receptors (GPCRs) that are coupled positively to the G_s protein, adenylyl cyclase. Hence, subsequent activation of the β_2 -adrenoceptor enhances the level of intracellular second messenger, cyclic adenosine monophosphate (cAMP). The mechanism of bronchorelaxation induced by β_2 -adrenoceptor agonists remained debatable although it is generally accepted that they acted by reducing cytosolic Ca^{2+} concentration as the release of Ca^{2+} from the intracellular stores is inhibited (Wray et al., 2005). Alternatively, cAMP was postulated to stimulate the protein kinase A (PKA) cascade which eventually leads to deactivation of the myosin light chain kinase, hence resulting in bronchorelaxation. Nevertheless, evidence revealed that long-term use of β_2 -adrenoceptor agonists induced desensitisation of the β_2 -adrenoceptor rendering the drug ineffective (Taylor et al., 2000).

The muscarinic receptor antagonist, ipratropium may be used in patients who are intolerant of β_2 -adrenoceptor agonist treatment. It acts by inhibiting the stimulation of parasympathetic-mediated effects which takes place as a result of the binding of acetylcholine to the muscarinic receptors. Muscarinic receptors are coupled to the G_q

protein. Hence, binding of the muscarinic receptor antagonist prevents activation of the phospholipase C (PLC) that usually hydrolyses phosphatidylinositol 4,5-biphosphate (PIP₂) to inositol triphosphate (IP₃) and diacyl glycerol (DAG). This subsequently inhibits the release of Ca²⁺ from the calcium stores, prevents airway smooth muscle contractility that is normally mediated by acetylcholine. The role of Ca²⁺ in mediating airway smooth muscle contractility was established when data from a pre-clinical study suggested that the calcium channel blockers, nifedepine or diltiazem reduced the intracellular Ca²⁺ concentration had proven to prevent both exercise-induced bronchoconstriction and allergic asthma (Twiss et al., 2002). Tiotropium bromide was later developed to provide a longer-lasting symptomatic relief, more commonly prescribed as a bronchodilator for patients with COPD. Although the muscarinic antagonists have been shown to decrease the recruitment of immune cells, mainly neutrophils in mouse models, such phenomenon was not observed in human (Wollin and Pieper, 2010).

Corticosteroids, which have been a mainstay in the asthma treatment ladder, act by suppressing inflammatory responses, whereas leukotriene receptor antagonists and mast cell stabilisers are commonly prescribed as add-on therapies if inadequate response is achieved (Bateman et al., 2008). Although these drugs have proved to be effective in reducing airway inflammation, clinical evidence suggests that lung function continues to decline as airway remodelling persists (Sont et al., 1999, Diamant et al., 2009). Newer drugs treatment strategies have employed the use of monoclonal antibody (mAb) inhibitors that directly target pro-inflammatory mediators, such as IL-5 (Leckie et al., 2000). However, neither mAb nor recombinant human IL-12, which promotes the favourable Th2-type lymphocyte response (Bryan

et al., 2000), were able to improve bronchial hyper-responsiveness in their respective double-blind, randomised clinical trials.

Hence, recent studies (Roth et al., 2012, Barker et al., 2013) have gradually shifted their focus towards restructuring the damaged epithelium as it forms the first point-of-contact for noxious stimuli. It is thought that the epithelium interprets gene-environment interactions and that the apical columnar cells undergo apoptosis in asthma (Davies et al., 2003). In contrast to the thickening of the epithelial lining that is seen in chronic obstructive pulmonary disease (COPD), epithelial desquamation is an exclusive characteristic of asthma (Montefort et al., 1993). This has, therefore, made the bronchial epithelial cell layer an interesting target in the search for future asthma therapies.

1.7 Cellular Signalling Pathways Involved in Modulation of Bronchial Epithelial Permeability

1.7.1 Mitogen Activated Protein Kinases (MAPKs) Cascades

MAP kinases are a group of serine/threonine protein kinases, involved in the regulation of intracellular molecular cascades to mediate fundamental cellular responses such as gene expression, proliferation, differentiation, apoptosis, differentiation and mitosis. Four different groups of MAP kinases were identified so far. They include the classical extracellular signal-regulated kinases 1 and 2 (ERK1/2), p38, c-Jun N-terminal kinases (JNKs) and ERK5.

Evidence from the past decade or so, revealed that MAP kinases have an additional role in modulating epithelial tight junction barrier function, mainly by ERK1/2 and p38 [review by (Gonzalez-Mariscal et al., 2008, Doerfel and Huber, 2012)]. JNKs have also been associated to the regulation of epithelial permeability, though was covered to a lesser extent than ERK1/2 and p38 in the literature. Reports suggest that JNKs were predominantly involved in regulating gene transcription and proliferation instead [review by (Davies and Tournier, 2012)]. ERK5, which was shown to regulate cell differentiation and proliferation [review by (Drew et al., 2012)], has never been linked to its involvement in influencing epithelial paracellular permeability. *Figure 1-5* illustrates the respective intracellular cascades of the MAP kinases.

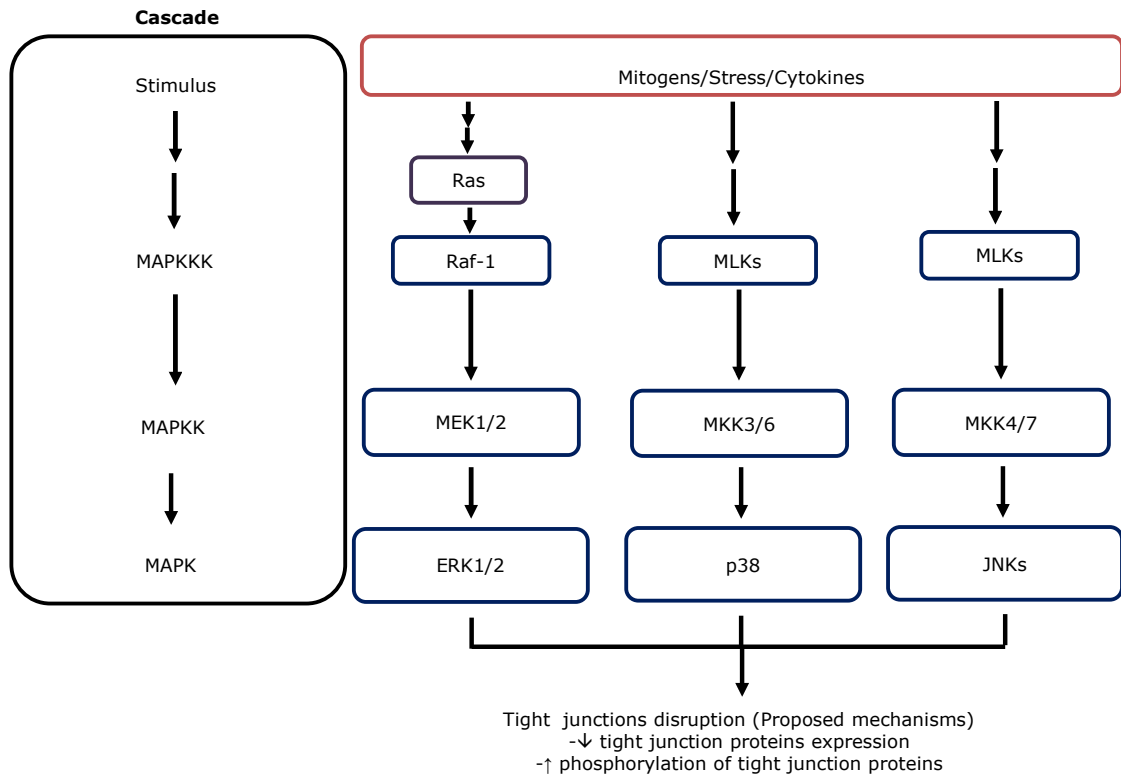


Figure 1-5 Schematic diagram of the proposed MAPKs signalling cascade that leads to the disruption of tight junctions. [Adapted from (Gonzalez-Mariscal et al., 2008)]. Intracellular signal transduction is conducted through the activation of respective mitogen-activated protein kinases (MAPKs) at a cascade of the main three kinases consisting MAPK kinase kinase (MAPKKK), MAPK kinase (MAPKK or MEK) and MAPK.

The hypothesis for MAPK involvement in the disruption of tight junction signalling pathways was initially proposed by Li *et al* who reported abnormal distribution of ZO-1, claudin and occludin in an immortalised rodent salivary gland epithelial cell model, Pa-4 transfected with oncogenic Raf-1 (Li and Mrsny, 2000). Within the cellular cytoplasmic region, the downstream effector for Ras, Raf-1 sequentially stimulates one of the mitogen-activated protein kinases kinase (MAPKK or MEK)

through phosphorylation of its serine/threonine residues (refer *Figure 1-5*). Sequentially, phosphorylation of the MAPK, extracellular signal-regulated kinases 1 and 2 (ERK1/2) activates various downstream proteins that may occur both within the cytoplasmic and nuclear regions of the cell.

The MAPKK that acts through the ERK1/2 pathway is also known as MEK1/2. Subsequent phosphorylation of ERK1/2 then poses detrimental effects to the expression of various tight junction proteins (Petcchia et al., 2012) (*Figure 1-5*). It has been postulated that the underlying mechanism could involve regulation of gene transcription to downregulate tight junction proteins expression that takes place in the nucleus or phosphorylation of tight junction proteins that could occur in either in cytoplasm or nucleus [review by (Gonzalez-Mariscal et al., 2008)]. However, studies have yet to prove such compartmental phenomenon.

Recent studies carried out to examine the effects of cigarette smoke (Petcchia et al., 2009) and cytokines (Petcchia et al., 2012) in bronchial epithelial cell lines, BEAS-2B and Calu-3 respectively, generated similar outcomes in which results from Western blots revealed that cells that were exposed to noxious stimuli showed increased total and phosphorylated ERK1/2 whilst concurrent immunohistochemistry studies revealed reduced expression of tight junction proteins, occludin and ZO-1. Unfortunately, evidence for the role of stimulated ERK1/2 pathway produce increased bronchial epithelial cell permeability is limited as the majority of the related studies were published by the same group of investigators. Hence, this has posed a challenge to the reproducibility of their findings or determining whether other MAPK pathways, such as p38 and Jnk may also be involved.

Besides ERK1/2, the phosphorylation of the MAPK p38 has also been found to disrupt epithelial tight junction structure in several *in vitro* epithelial models including, the MDCK cell line derived from the kidney epithelium (Gonzalez et al., 2009), primary nasal epithelium cells (Koizumi et al., 2008) and Caco-2 intestinal epithelial cells (Wang et al., 2008) following exposure to stimuli, such as hydrogen peroxide, TNF α , IFN γ and IL-1 β . Stimulation of the p38 pathway begins with the stimulation of the MAPKKK, mixed-lineage kinases (MLKs) which subsequently phosphorylate MAPKKs, MKK3 and MKK6 (refer *Figure 1-5*). The MAPK p38 in its phosphorylated form then activate various transcription factors within the cytoplasm or nucleus, leading to changes in gene expression. In the context of the present study, p38 downregulates gene transcription for tight junction proteins, hence caused an increase in epithelial paracellular permeability. Such hypothesis was proven in a study using the gastric GES-1 epithelial cell line; whereby disruption of the epithelial layer due to reduced expression of tight junction proteins, occludin and ZO-1, caused by an NSAID, clopidogrel was reversible in the presence of a selective p38 inhibitor, SB203580 (Wu et al., 2013)

The intracellular signalling of JNKs activation is similar to that of p38; whereby the MAPKKK, MLKs are involved to activate MAPKKs specific to the JNKs pathway, such as MKK4 and MKK7 (refer *Figure 1-5*). Activation of MKK4/7 leads to phosphorylation of JNK which then transmits signals to downregulate or interfere with the gene expression of tight junction proteins [review by (Doerfel and Huber, 2012)]. A study has shown that exposure of the Caco-2 intestinal epithelial cells to IL-1 β resulted in increase in epithelial permeability that was accompanied by decreases in tight junction proteins, claudin, ZO-1 and occludin expression (Youmba et al., 2012). Interestingly, the authors reported that besides the JNK inhibitor II, these

effects were also prevented by MEK1 inhibitor, U0126 and NF- κ B inhibitor, caffeic acid phenethyl ester (CAPE). Thus, the results suggest that there was a crosstalk between the conventional JNK and MEK1 pathway, which consequently altered gene expression of tight junction proteins through NF- κ B signalling. Activation of JNK by MEK1 was also recently reported. The expression of a novel junctional regulator of MEKK1 and JNK, MarvelD3 in Caco-2 intestinal epithelial cells was found to inhibit JNK phosphorylation that preserved normal epithelial barrier function. Indeed, depletion of MarvelD3 expression with siRNA caused JNK pathway activation that disrupted the epithelial tight junction structure (Steed et al., 2014). Investigation on the interaction between these MAP kinases in the regulation of tight junction proteins and gene expression is an interesting area of study that is still at its infancy stages. Future studies are therefore needed to further our understanding both in the molecular signalling involved in conditions with damaged epithelia, and the exploration of tight junction proteins as potential therapeutic targets of MAP kinases.

1.7.2 RhoA Signalling

Another commonly suggested pathway linked structurally and functionally to the tight junction is the Rho cascade (refer *Figure 1-6*) [reviews by (Matter and Balda, 2014)]. Besides maintaining cell-cell adhesion through the regulation of the tight junction structure, Rho is also known to mediate cell contractility, proliferation, motility and gene expression. The Rho signalling pathway can be activated by various extracellular stimuli, which may include pro-inflammatory cytokines, hormones and growth factors, to promote activation of the Rho-associated small GTPases.

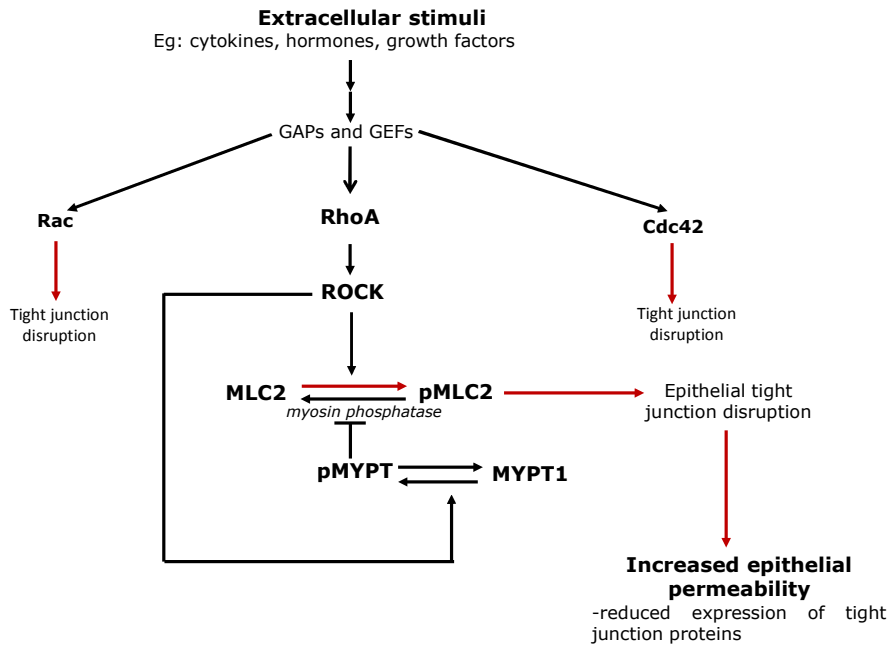


Figure 1-6 Schematic diagram of the proposed RhoA pathway in the regulation of epithelial tight junction functions. Following the exposure to external stimuli, the regulatory proteins including guanine-nucleotide-exchange factors (GEFs) and GTPase-activating proteins (GAPs) are stimulated which catalyses the activation of a wide range of Rho GTPases including RhoA, Rac and Cdc42. However, studies have demonstrated that RhoA plays the most significant role in epithelial tight junction modulation. (Bruewer et al., 2004, Jou et al., 1998). Subsequently, the Rho-associated protein kinase (ROCK) enzyme is activated. ROCK-induced epithelial tight junction disruption can take place either through phosphorylation of the regulatory myosin light chain 2 (MLC2) or inhibition of the enzyme myosin phosphatase activity through myosin phosphatase target subunit (MYPT) phosphorylation, which leads to accumulation of activated, phosphorylated MLC2 form. It is thought that activation of the ROCK cascade would eventually result in the downregulation of tight junction proteins expression, including occludin and ZO-1.

The Rho cascade is initiated upon exposure to extracellular stimuli (including cytokines, hormones or growth factors) that stimulate small GTPases of Rho including RhoA-C, Rac and Cdc42. It is noted that these RhoGTPases act as molecular switches within the α -subunit of the G-protein, cycling between inactive GDP-bound and active GTP-bound conformations. Such reaction is catalysed by the guanine-nucleotide-exchange factors (GEFs) and GTPase-activating proteins (GAPs). Genetically modified Madin-Darby canine kidney (MDCK) epithelial cells expressing constitutively activated conformations of RhoA, Rac and Cdc42 were shown to disrupt tight junction structures, yet the active RhoA mutants were reported to induce the most dramatic effect (Jou et al., 1998, Bruewer et al., 2004). In a similar approach, earlier studies demonstrated that selective inhibition of RhoA following the exposure with C3 transferase, a *Clostridium botulinum*-derived toxin, prevented the assembly of epithelial tight junction proteins (Nusrat et al., 1995, Takaishi et al., 1997). Other RhoGTPases, including Rac and Cdc42, as previously mentioned, caused damage to the epithelial tight junction to a lesser extent compared to RhoA (Bruewer et al., 2004). In addition, Rac and Cdc42 modulate downstream effectors, such as MAPK ERK1/2 and protein kinase C (PKC) that are not specific to the Rho cascade [review by (Matter and Balda, 2014)], thus complicate the investigation on RhoGTPases activity. RhoA on the other hand, only affects ROCK [review by (Quiros and Nusrat, 2014)]; hence RhoA/ROCK pathway remained as the focus in the present study.

A study in the 16HBEo- bronchial epithelial cells showed increased paracellular permeability following infection with the pathogenic protein, *Staphylococcus aureus* protein A was attenuated by the ROCK inhibitor, Y27632 (Soong et al., 2011). This suggests that stimulation of ROCK enzyme following RhoA activation can lead to

disruption of the epithelial barrier function. Previously, it was understood that phosphorylation of MLC2 following ROCK activation causes contraction of the actomyosin structure. Nevertheless, there is increasing evidence that suggests such phenomenon can also lead to epithelial tight junction disassembly owing to the increased mechanical stress exerted on the actomyosin belt. This hypothesis was proven in a recent investigation using primary rat alveolar epithelial cells in which stimulation with a potent serine/threonine protein phosphatase inhibitor, calyculin A, enhances the activity of RhoA/ROCK/MLC2 cascade that resulted in an increased actinmyosin stretch and redistribution of F-actin fibres from the membrane when examined with immunofluorescence staining of the F-actin fibres (DiPaolo and Margulies, 2012). The alternative mechanism for MLC2-mediated epithelial tight junction disruption through MYPT1 was also demonstrated in a treatment with a potent adenosine monophosphate protein kinase (AMPK) agonist in MDCK epithelial cells which induced disruption of the actinmyosin structure that was linked to the activation of MYPT1/MLC2 pathway (Miranda et al., 2010).

Nevertheless, evidences revealed that phosphorylation of MLC2 could take place through several pathways, besides the ROCK pathway. Studies in intestinal epithelial cell lines, Caco-2 and T84 cells have demonstrated that the exposure to TNF α and IFN γ (Fischer et al., 2013) or the PKC activator, phorbol 12-myristate 13-acetate (PMA) (Turner et al., 1999), were shown promote MLC2 phosphorylation through the MAPK p38 and PKC pathways respectively. In comparison, MYPT1 is specifically mediated through the ROCK [review by (Matter and Balda, 2014)]; i.e. the level of MYPT1 phosphorylation thus, directly reflects on ROCK activity. Interestingly, commercially available kits for ROCK activity assay was designed

based on the basis of such molecular mechanism within the RhoA/ROCK pathway (Cell Biolabs, 2015, Merck Millipore, 2015).

Current evidence on the effect of RhoA/ROCK cascade activation is limited within the regulation of functional expression of tight junction proteins (Matter and Balda, 2003). Studies have yet to investigate the role of RhoA/ROCK activation in the modulation of junctional proteins-associated gene expression. To date, it is only hypothesised that signalling through the RhoA pathway results is dependent on the activities of key transcriptional factors, ZO-1 associated nucleic acid binding protein (ZONAB) and guanine nucleotide exchange factor-H1 (GEF-H1) (Terry et al., 2010). ZONAB, is a multifunctional transcription factor that is believed to influence paracellular permeability through its regulation on cellular proliferation and cytoskeleton arrangements. Previous study demonstrated that the cytokine $\text{TNF}\alpha$ inhibits ZONAB activity through stimulation of RalA, a small GTPase of the Ras superfamily which was shown to disrupt the actin cytoskeletal structure (Sugihara et al., 2002). In addition, the tight junction-associated GTPase, GEF-H1 is known to regulate the arrangement of microtubules and actin cytoskeleton by interacting with following stimulation of the RhoA pathway. A study using MDCK epithelial cells revealed that GEF-H1 is activated by $\text{TNF}\alpha$ as a result of RhoA/ROCK/MLC activation which resulted enhanced paracellular permeability and disrupted actin cytoskeleton arrangements (Kakiashvili et al., 2009). Although the study of the gene interaction involved in RhoGTPase signalling is deemed interesting, the present study has focused on the role of ROCK activation on the functional expression of epithelial tight junction proteins.

1.8 Cannabinoids as the Potential Therapeutic Area for Asthma and COPD

Scientific advances made in the understanding of pathogenesis of airway inflammatory diseases, such as asthma and COPD, have led to the improvement in the pharmacological management of these conditions; mainly in terms of efficacy and safety of the drugs. Nonetheless, the exploration into a new therapeutic target is still ongoing as airway inflammatory conditions are thought to be manifested from damaged airway epithelium. Corticosteroids (as discussed in *section 1.6*), which are currently deemed as the most effective pharmacological treatment of asthma, failed to restore normal airway epithelium structure and function. Monoclonal antibodies that was then emerged as an alternative to the treatment of airway inflammatory diseases are either restricted by the clinical guidelines; i.e. use in severe asthmatics only [review by (Humbert et al., 2014)], or disappointing outcomes reported in clinical trials which demonstrated their clinical inefficacy and serious adverse effects (Holgate et al., 2011, Busse et al., 2013).

Thus, the present study took a novel, yet historical approach in investigating for a new therapeutic field using cannabinoids. Although known for its potential for misuse, the Cannabis plant, which contains phytocannabinoids, has previously demonstrated its medicinal usefulness in treating asthma and coughs (see *section 1.9*). Furthermore, vast scientific evidences are now available to aid the physiological and pharmacological investigations for this project. The present study therefore aims to optimise cannabinoids as a new area of target for airway inflammatory diseases, with a specific focus on their effects on the bronchial epithelium.

1.9 History of Cannabis for Respiratory Disorders

The use of cannabis for the treatment of airway inflammation began centuries ago although its exact chronology remains a debate until the present day. It was documented in the Indian *Materia Medica* that the sticky resin exuded from the leaves and flowers on the female cannabis plant was prescribed by the traditional Ayurvedic practitioners, between the period of 2000-1000 B.C. to treat asthma and whooping cough (Nandakarni, 1976).

In the early 19th century, W.B. O'Shaughnessy, a physician at the Medical College of Calcutta, introduced cannabis to the West after convincing himself of its clinical efficacy and safety profile. Cannabis was then frequently recommended to treat pain and neurological disorders. Smoking of cannabis or 'Indian cigarettes' was also popular and acknowledged to be effective against chronic bronchitis and asthma. Claims were also made that cannabis was therapeutically more superior than the opiates as it does not lead to addiction or drug dependency (Mikuriya, 1969). Manufacture of patented cannabis-containing medicines soon ensued especially in the US due to increasing demand, despite little being known about its mode of action. Among the bestselling commercially available products used for respiratory-related ailments were the Smith Brothers' of Edinburgh cough drops and tinctures, produced in the beginning of 20th century.

However, cannabis was officially banned in the UK in 1968 following reports of anti-social behaviour and aggression when misused. Consequently, this has imposed the restriction to the access of cannabis or its psychoactive ingredient, Δ^9 -tetrahydrocannabinol (THC) for medicinal purposes. Phytocannabinoids-containing products are currently categorised as a Schedule 1 Controlled Drug (CD), or CD

License Prescription-Only Medicine which defines it as a drug that has no therapeutic benefit and a license is required for their production, possession and supply. On the contrary, Sativex, which was developed by GW Pharmaceuticals, is the only phytocannabinoid-containing product that has proven to have medicinal value in treating spasticity in multiple sclerosis. Prescription for such treatment is still unlicensed in the UK and dispensing of Sativex sublingual sprays is tightly controlled due to its susceptibility for substance abuse.

1.10 Evidence on the Effects of Cannabinoids in Regulating Inflammatory Responses

The isolation and characterisation of the two main constituents from the cannabis plant, THC and cannabidiol (CBD) which began in the 1960s (Gaoni and Mechoulam, 1964, Mechoulam and Shvo, 1963) had led to the discovery of a specific set of receptors known as the cannabinoids CB₁ and CB₂ receptors that can be stimulated by these phytocannabinoids. Evidence suggests that activation of the CB₁ and CB₂ receptors by these phytocannabinoids yield anti-inflammatory effects in various systems mainly by suppressing the release of pro-inflammatory cytokines (Klein et al., 2000, Vuolo et al., 2015) or interfering with the intracellular pro-inflammatory signalling such as the arachidonic acid metabolism pathway (Anggadiredja et al., 2004). Subsequent research then identified that the phytocannabinoids also have a role in mediating inflammatory responses through other non-cannabinoid receptors which will be discussed in further detail in *section 1.12.2* to *section 1.12.4*. Despite their stark differences in chemical structures, endogenously secreted compounds, anandamide and 2-arachidonoylglycerol (2-AG), identified in the early 1990's, displayed cannabimimetic effects as they also bind and activate the cannabinoid receptors like the phytocannabinoids (compare structures in *Figure 1-7* and *Figure 1-9*). Hence, these compounds are termed endocannabinoids (Devane et al., 1992, Mechoulam et al., 1995). Studies have demonstrated that the release of endocannabinoid expression is commonly upregulated as a negative feedback in inflamed conditions such as inflammatory bowel diseases (Massa et al., 2004) and inflammatory pain (Okine et al., 2012). This was necessary to promote CB₁ and CB₂ receptor stimulation in reversing the inflammation. However, the presence of degrading enzymes at the sites of inflammation reduces the chemical

stability of the endogenous cannabinoids. Studies have demonstrated that the products of anandamide and 2-AG catabolism serve as pro-inflammatory mediators instead [review article by (Di Marzo et al., 2005)]. Details of such phenomenon will be discussed in greater depth in *section 1.11.1*.

Thus, this study aimed to elucidate the role of both endogenous cannabinoids and phytocannabinoids in regulating airway epithelial barrier function during inflammatory state.

1.11 Cannabinoids and Airway Inflammation

1.11.1 Endogenous Cannabinoids (or Endocannabinoids)

Anandamide, the first endocannabinoid to be described, was isolated from porcine brain (Devane et al., 1992) using nuclear magnetic resonance spectroscopy and mass spectrometry. A few years later, another successful attempt was made by Mechoulam *et al* in screening for peripheral production of the second endocannabinoid, 2-arachidonylglycerol (2-AG) from canine gut (Mechoulam et al., 1995). Latter ligands that were discovered are mainly analogues of anandamide and 2-AG, which include the orphan endocannabinoids *N*-palmitoylethanolamine (PEA) and *N*-oleoyl ethanolamine (OEA) (Pertwee, 2005).

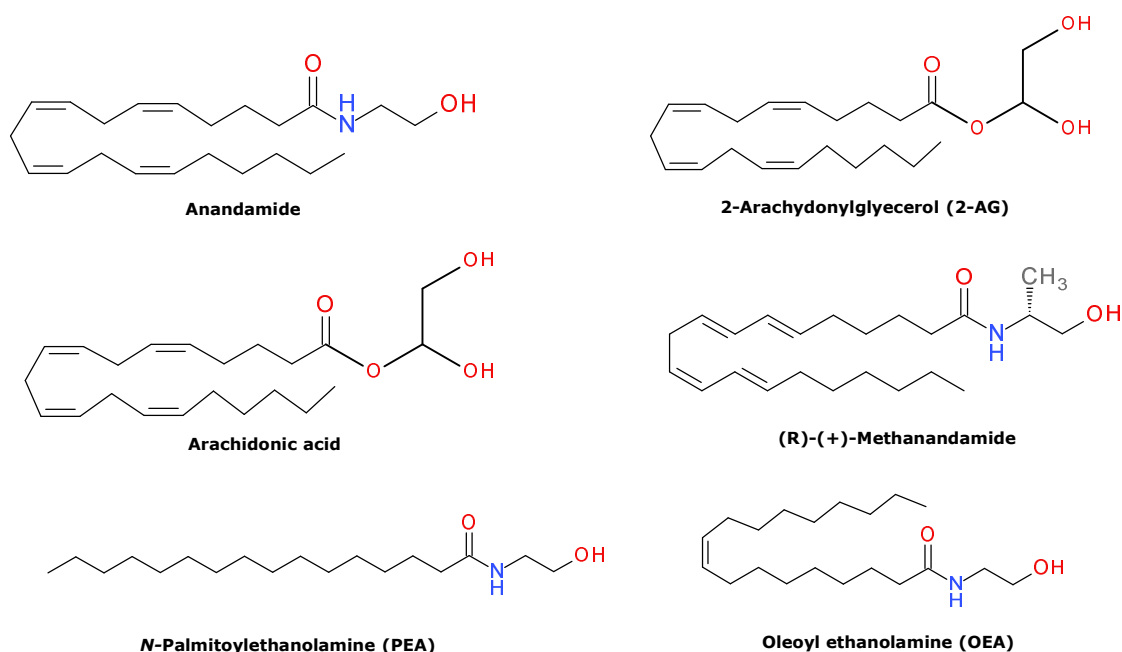


Figure 1-7 Chemical structures of various endocannabinoids. Note the structural resemblance of the endocannabinoids with arachidonic acid that carry the long-chain polyunsaturated fatty acid tail, hence categorising endocannabinoids as *eicosanoids*.

Endocannabinoids are members of the eicosanoid group of compounds containing the basic ‘hairpin-like’ structure of arachidonic acid (*Figure 1-7*), as well as the presence of a long polyunsaturated hydrocarbon chain (Howlett, 2005). These ligands are known to stimulate a family of G-protein coupled receptor (GPCR), the cannabinoid receptors (CB₁ and CB₂) which may be expressed at respective sites of action. In addition, current evidence has shown that the two archetypal endocannabinoids, anandamide and 2-AG share similar biosynthetic and metabolic pathways with those of the eicosanoids (Di Marzo et al., 2005).

Several proposals have been made to elucidate the mechanisms involved in the synthesis of anandamide (*Figure 1-8*) (Liu et al., 2008) which are thought to be dependent on various pathological factors and biosynthetic site. Currently, it is generally accepted that anandamide is generated from the precursor, *N*-arachidonoylphosphatidylethanolamine (NAPE), catalysed by the selective enzyme, phospholipase D (NAPE-PLD). 2-AG, on the other hand, is derived from arachidonate-containing lysophosphatidic acid which is then hydrolysed by phospholipase C to diacylglycerol (Sugiura, 2007). This is then converted to 2-arachidonylglycerol as a result of the diacylglycerol lipase (DAGL) enzymes. While 2-AG is mainly removed by monoacylglycerol lipase (MAGL), anandamide is degraded mainly by fatty acid amide hydrolase (FAAH), and to a lesser extent palmitoylethanolamine-preferring acid amidase (PAA), lipoxygenases as well as cytochrome P450 (Di Marzo et al., 2005). Endocannabinoids are also metabolised by cyclooxygenase-2 enzyme to form the pro-inflammatory, prostaglandin ethanolamines (Yu et al., 1997, Kozak et al., 2000). Collectively, this pinpoints potential roles of endocannabinoids in the regulation of inflammatory diseases.

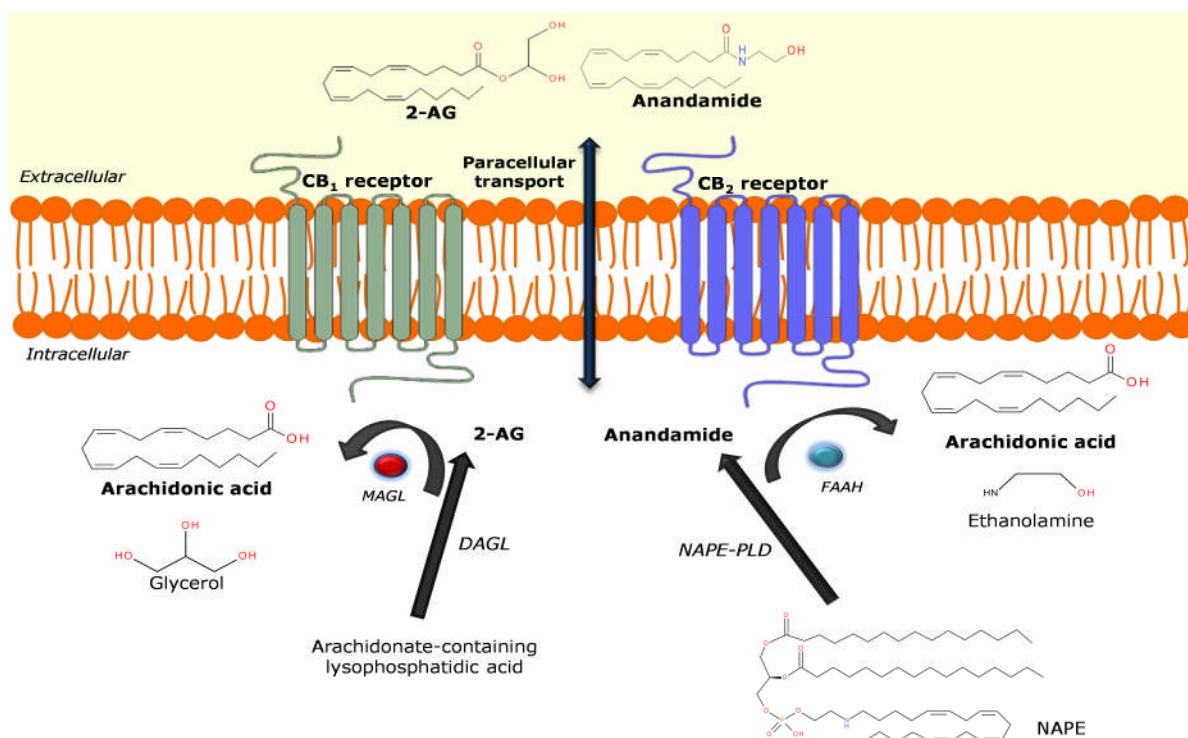


Figure 1-8 Illustration of the main biosynthesis and metabolism pathways for anandamide and 2-arachidonylglycerol (2-AG). Anandamide is formed from N-arachidonoylphosphatidylethanolamine (NAPE) in the presence of the enzyme NAPE phospholipase D (NAPE-PLD) and metabolised by fatty acid amide hydrolase (FAAH) into arachidonic acid and ethanolamine. In comparison, the biosynthesis of 2-AG is catalysed by the enzyme diacylglycerol lipase (DAGL) from its precursor, arachidonate-containing lysophosphatidic acid. 2-AG is also broken down to arachidonic acid by its selective enzyme, monoacylglycerol lipase (MAGL). The transport mechanisms of anandamide and 2-AG through cell membranes remain controversial while it is generally accepted that they are transported paracellularly through the cell membrane due to the hydrophobicity of their chemical structures.

In the past decade, the endocannabinoid system has been associated with the regulation of airway inflammation, such as asthma. Studies in humans have demonstrated that the release of anandamide is up-regulated in response to an inhaled allergen (Zoerner et al., 2011). The source for anandamide within the airway is still unknown, though it is hypothesised that heightened release of presynaptic acetylcholine in asthma may have stimulated postsynaptic nicotinic acetylcholine receptor (nAChR) to induce anandamide release, whilst establishing contraction of the airway smooth muscle. Evidence of increased anandamide production following stimulation of nAChR was previously observed in primary rat cortical neurone cells (Stella and Piomelli, 2001). It is then speculated that increased availability of the endocannabinoid during active inflammatory state is a natural response to maintain normal airway tone, or prevent acetylcholine-induced bronchoconstriction. Such effect, which is known as retrograde signalling, may be achieved as anandamide binds to the presynaptic cannabinoid receptors that are possibly expressed on peripheral afferent sensory neurones.

On the other hand, 2-arachidonoylglycerol (2-AG), is thought to be potentially involved in promoting eosinophilic migration (Lunn et al., 2006). At present, the expression of both cannabinoid receptors within the airway structure is still yet to be discovered, although claims were made that they can be found on the immune cells instead (Giannini et al., 2008, Zoerner et al., 2011).

Previous *in vivo* studies involving pre-treatment with inhaled anandamide in guinea pigs showed it to partially prevent bronchospasm following exposure to leukotriene-D4 aerosols, whereas intravenous administration of anandamide failed to provide a similar outcome (Stengel et al., 2007). It was hypothesised that inhalation of anandamide yielded a higher airway tissue concentration than that delivered

intravenously as anandamide is rapidly catabolised by FAAH enzyme to arachidonic acid. Studies have shown that anandamide induced cough (Jia et al., 2002) and bronchoconstriction (Tucker et al., 2001) in guinea pigs which responses remained unaltered by either CB₁ receptor antagonist, SR141716A or CB₂ receptor antagonist, SR144528. Interestingly, pharmacological blockade of the anandamide effect within the airway with CB₂ receptor antagonists. Experiments conducted by Giannini *et al* had later shown that the potent, non-selective cannabinoid receptor agonist CP 55,940 successfully inhibited asthma-like reactions, which indicated that anandamide could potentially act on cannabinoid receptors found in the airways (Giannini et al., 2008). The study of anandamide-mediated effect within the airway has never been investigated in CB₁ and CB₂ knockout animal models, although this may provide further insight into the possibility for the involvement of cannabinoid receptors activation by anandamide. On the other hand, a recent small-scale preclinical study also detected anandamide at picomolar concentrations in bronchoalveolar lavage (BAL) fluid of patients with allergic asthma, and when exposed to grass pollen or house dust mites, the concentration was elevated up to four-fold (Zoerner et al., 2011). It is also reported that the apparent increase in anandamide level was accompanied by a rise in the expression of cytokines and eosinophils. These results are consistent with earlier findings by Calignano *et al* which reported asthma-like responses due to elevated anandamide synthesis from its precursor, NAPE through a Ca²⁺-dependent activity in airway smooth muscle (Calignano et al., 2000). Hence, these studies suggest strong correlation of anandamide to the airway inflammation regulation. Nonetheless, whether anandamide secretion is a cause or consequence of allergic asthma and the involvement of cannabinoids receptors remain a puzzle.

Other endocannabinoid-like ligands, such as the orphan endocannabinoids PEA and OEA have never been studied to link their effects to airway inflammatory diseases. Unlike anandamide and 2-AG, these compounds have little or no activity at CB₁ and CB₂ receptors but demonstrated to modulate inflammatory responses through binding to deorphanised G-coupled receptor such as GPR55 and other receptors known to be activated by cannabinoid ligands including TRP channels and PPARs (refer *section 1.12.2* to *section 1.12.4*). These compounds are long chain fatty acid molecules which are speculated to interact with anandamide and 2-AG. Binding studies have demonstrated that the presence of PEA and OEA was thought to have an ‘entourage effect’ to enhance anandamide or 2-AG activity at the CB₁ and CB₂ receptors (Ben-Shabat et al., 1998).

1.11.2 Phytocannabinoids

Cannabinoid ligands derived from the *marijuana* plant (*Cannabis sativa*) contain the psychotropic constituent Δ^9 -tetrahydrocannabinol (THC) that binds readily to both CB₁ and CB₂ receptors in the low nanomolar range, and the non-psychotropic CBD that has a much lower affinity for the cannabinoid receptors (*Figure 1-9*) (Pertwee et al., 2010, Izzo et al., 2001).

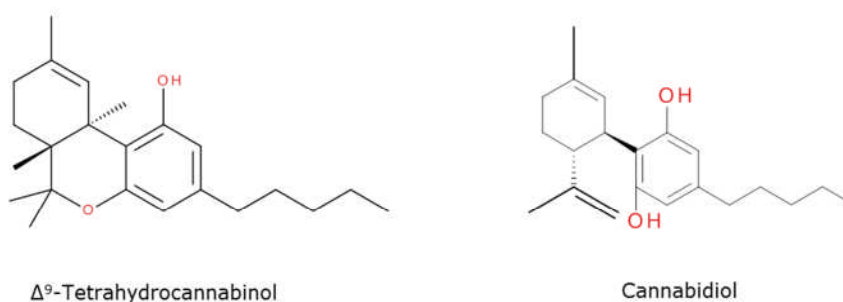


Figure 1-9 Chemical structures of the phytocannabinoids, Δ^9 -tetrahydrocannabinol (THC) and cannabidiol (CBD). Unlike endocannabinoids, the plant-derived cannabinoids consist of variable hydrocarbon side chains attached to the aromatic rings that still capable to bind to the CB₁ and CB₂ receptors as partial agonists.

The medicinal value of phytocannabinoids for respiratory disorders was first published by Vachon *et al* in the early 1970 when the researchers recruited healthy participants to smoke *marijuana* containing high (84 μ g) or low (32 μ g) doses of THC (Vachon et al., 1973). Results revealed that subjects who received *marijuana* experienced bronchodilatation followed by an increase in flow rate irrespective of the dose given. The pharmacological effect of THC was later reinvestigated in asthmatic patients in a randomised, double-blind clinical study conducted by Tashkin and colleagues (Tashkin et al., 1977). In this experiment, those subjects that were assigned single dose treatment of aerosolised 5 mg or 20 mg THC experienced

greater bronchodilator effects than the group that was given the non-selective β -adrenoceptor agonist, isoproterenol after an hour of drug administration. Predictably, it was reported that subjects who inhaled the higher dose of THC were more prone to experiencing undesirable effects such as tachycardia, chest discomfort or cough. These data may suggest the potential action of THC in providing symptomatic relief from asthma despite the reports of adverse effects. However, there is no literature discussing or even considering its effect in reducing airway inflammation thus far. On the contrary, weekly oral consumption of THC capsules did not significantly result in bronchodilatation or improve pulmonary functions in asthmatic subjects compared to its placebo (Abboud and Sanders, 1976). Instead, paradoxical bronchospasms were reported which might have obscured the actual effects of THC. Results obtained from these two clinical studies thus hinted at the differing pharmacokinetics of THC when administered orally or through inhalation. Although the method of administration may not be a major area of study at this point, the role of THC in inflammation needs to be verified, assuming that the delivery of THC to airway epithelium is protected from any form of catabolism.

On the other hand, investigation on the effect of CBD in asthmatic patients or experimental models is still limited thus far, although CBD is widely known for its anti-inflammatory effects *in vivo* and *in vitro* [review article by (Pertwee, 2008)]. Earlier evidence demonstrated that the administration of the neurotransmitter glutamate at high concentrations induced oxidative stress in primary rodents cortical neuron cells that was attenuated by CBD (Hampson et al., 1998). *In vitro* application of CBD directly to the human primary peripheral blood mononuclear cultures was demonstrated to decrease the immune cells activity as the expression levels of cytokines, TNF α and IL-1 were reduced (Watzl et al., 1991). A recent study in

rodents showed intraperitoneal injection of CBD before the exposure of aeroallergen, ovalbumin caused a significant reduction of the serum level of various pro-inflammatory cytokines among which included $\text{TNF}\alpha$, IL-4, IL-5 and IL-13 (Vuolo et al., 2015). The potential target sites for such CBD action and its mechanism of action was not elucidated in their study, despite claims of the potential use of CBD in the treatment of allergic asthma.

Investigation by Alhamoruni *et al*, reported that increased intestinal epithelial cell permeability induced by cytokines was effectively reversed shortly after the introduction of one of the phytocannabinoids, THC or CBD (Alhamoruni et al., 2012). Such findings indicated the role of phytocannabinoids in safeguarding the epithelial barrier function, thus highlighted the therapeutic potential THC and CBD in treating conditions with disordered permeability in inflammatory bowel diseases such as that intended by the authors, and airway inflammation of which the bronchial epithelium is disrupted.

1.12 Sites of Action of the Cannabinoids

1.12.1 *The Classical Cannabinoid Receptors (CB₁ and CB₂ receptor)*

Isolation and characterisation of the first cannabinoid receptor, CB₁, was undertaken in the late 1980s with rat brain as a model (Devane et al., 1988), whereas the second cannabinoid receptor, CB₂, was initially discovered in myeloid cells through use of the polymerase chain reaction (PCR) (Munro et al., 1993). Both CB₁ and CB₂ receptors are members of the GPCR superfamily which possess distinct, yet overlapping binding profiles (Montero et al., 2005). This is because 42% of the CB₂ residues in the transmembrane domain are divergent from that of CB₁, but CB₂ displays 44% identity in the protein sequence (Munro et al., 1993) of the entire GPCR structure.

CB₁ receptors are predominantly present at the presynaptic terminals of central and peripheral neurons, where they are strategically positioned to influence the motor control, the induction of analgesia, memory and cognition by altering the release of excitatory and inhibitory neurotransmitters (Pertwee, 2010). However, studies have demonstrated that CB₁ receptors are also located peripherally in immune tissues (Samson et al., 2003, Jean-Gilles et al., 2015), where CB₂ receptors are commonly found. Further investigations then revealed that both or either CB₁ or CB₂ receptors were also widely distributed within the structures of various other systems such as the spleen (Marini et al., 2013), liver (Mallat et al., 2013), vasculatures of the heart (Randall et al., 2004) and gastrointestinal tract mainly the intestines and colon (Wright et al., 2005, Wright et al., 2008).

Recent studies (Patel et al., 2010, Pini et al., 2012) have attempted to link the role of cannabinoid receptors with asthma but so far, the expression of CB₁ or CB₂ receptors in any parts of the respiratory system is yet to be investigated. Instead, these authors hypothesised that cannabinoid receptors are expressed on the immune cells based on the fact stimulation of the cannabinoids suppressed airway inflammatory response.

Evidence for the role of cannabinoid receptors in mediating epithelial permeability thus far has only been reported by Alhamoruni *et al* (2012). The authors reported that the effect of the phytocannabinoids, THC and CBD in reversing the cytokines-induced epithelial permeability in Caco-2 intestinal cells were sensitive to the opposing effect of AM251, a CB₁ receptor antagonist. This signifies that the anti-inflammatory response by both phytocannabinoids is mediated through the CB₁ receptor.

1.12.2 Putative Cannabinoid Receptors

Evidence on the existence of an orphan receptor GPR55 emerged when scientists at major pharmaceutical firms, GlaxoSmithKline and AstraZeneca had patented their discovery that the newly characterised receptor was activated by various cannabinoid ligands, independent of CB₁ and CB₂ receptor stimulation (Brown and Wise, 2001, Drmota et al., 2004). Presence of the GPR55 receptor was later verified in a study reported reporting that a potent synthetic cannabinoid agonist CP55,940, the endogenous cannabinoids anandamide and 2-AG, as well as the phytocannabinoid THC displayed higher potency as agonists at this putative target site compared to that at CB₁ and CB₂ receptors (Ryberg et al., 2007). CBD on the other hand, was shown to antagonise the stimulation of GPR55 caused by the cannabinoid agonist,

CP55,940. The authors also revealed that GPR55-induced [³⁵S]GTPγS binding studies was unaffected despite the presence of G_{i/o} inhibitor, pertussis toxin. Instead, peptide studies demonstrated that anti-G_{α13} was shown to inhibit GTPγS binding, suggesting that unlike the CB₁ and CB₂ receptors, the GPR55 receptor is coupled through G_{α13} instead. Evidence for the functional roles of GPR55 is still currently limited owing to its rather recent discovery. An investigation in rodents revealed GPR55 expression in the mucosal segments throughout the gastrointestinal tract and was enhanced when stimulated with pro-inflammatory mediator, LPS (Lin et al., 2011). Thus these data suggest the likelihood that GPR55 may be expressed on the intestinal epithelium and its potential role in mediating intestinal epithelial permeability. GPR55 was also found to interact with the classical CB₁ and CB₂ receptors (Waldeck-Weiermair et al., 2008, Balenga et al., 2011) in regulating inflammatory responses, which further complicated the approach to understanding the specific role of GPR55 in disease states. Nonetheless, the involvement of GPR55 in mediating airway inflammation will be considered for future investigations within this project as the present study aimed to first establish the role of the basic CB₁ and CB₂ receptors.

The involvement of a different putative cannabinoid receptor includes GPR120, which is speculated to be the most likely one to participate in airway inflammation as its expression was detected on the membranes of surfactant-releasing Clara cells within the airway epithelial structures (Ichimura et al., 2009). However, ligands that were found to be activating GPR120 are not cannabinoid ligands, but are unsaturated long chain fatty acid compounds (of 14 to 22 carbon atoms in length) that resemble the chemical structures of endogenous cannabinoids or putative endocannabinoids like PEA and OEA.

1.12.3 Peroxisome Proliferator-Activated Receptors (PPARs)

PPARs belong to the nuclear receptor family that can modulate gene transcription when activated which subsequently influence the outcome in protein expression. Evidence suggests that both endogenous cannabinoids and phytocannabinoids are ligands for the various subtypes of PPARs, mainly PPAR α , PPAR β/δ and PPAR γ . The earliest evidence of the interaction between cannabinoid and PPARs was demonstrated when the metabolites form from the endocannabinoids, anandamide and 2-AG following lipoxygenase catabolism, 15-hydroxyeicosatetraenoic acid glyceryl ester, 15-HETE-G, caused an increase in PPAR α activity (Kozak et al., 2002b). A review on the data presented various independent studies revealing that PPAR α and PPAR β/δ preferentially bind to long chain saturated and unsaturated fatty acids including the putative endocannabinoids, PEA and OEA as these compounds do not affect the classical cannabinoid receptors (Pertwee et al., 2010). On the other hand, isolated rat arteries treated with the phytocannabinoid, THC was shown to cause vasorelaxation that was attenuated in the presence of a selective PPAR γ antagonist, GW9662 (O'Sullivan et al., 2006).

Interestingly, studies with human bronchial BEAS-2B epithelial cells and A549 alveolar epithelial cells demonstrated that only PPAR γ was expressed. PPAR γ activation by its agonist, thiazolidinedione was shown to confer an overall decline in cytokine release (Wang et al., 2001). However, studies in Caco-2 epithelial cells treated with THC and CBD showed no contribution of the PPARs in mediating the phytocannabinoid responses in reversing cytokine-induced increase in epithelial permeability (Alhamoruni et al., 2010).

Nevertheless, the PPARs, particularly of PPAR γ subtype could potentially play a significant role as an alternative target site for the cannabinoids to treat chronic airway inflammatory diseases.

1.12.4 Transient Receptor Potential Channels (TRP channels)

The TRP channels are a group of cationic channels that consist of six transmembrane subunit proteins which are arranged in such a way that a pore region exists to allow the influx of cations into the cells when activated. These voltage-gated channels are divided into six different subfamilies including ankyrin (TRPA), canonical (TRPC), melastatin (TRPM), mucolipin (TRPML), polycystin (TRPP) and vanilloid (TRPV). The type of stimuli to activate the TRP channels vary in each subfamily which could involve pressure, temperature, sound, light and tastes stimuli and various endogenous fatty ligands such as eicosanoids metabolites (Ramsey et al., 2006). A review by Pertwee et al (2010) revealed that the endogenous cannabinoids, phytocannabinoids and other synthetic cannabinoid ligands known to stimulate the classical cannabinoid receptors were proven to activate TRPA1, TRPM8, TRPV1, TRPV2 as well as TRPV4 in various separate studies.

Among these TRP channels that can be activated by the cannabinoids, all except TRPV2 is found to be expressed in the primary human airway epithelium and cell lines such as BEAS-2B and 16HBEo- cells [review by (Grace et al., 2014)]. However, evidence was available for TRPA1 and TRPM8 is still limited, hence only TRPV1 and TRPV4 will be discussed further.

It is postulated that the increased availability of pro-inflammatory mediators, such as the breakdown product of eicosanoids will generally heighten these TRP channels responses during inflammatory conditions, such as asthma and COPD. Such hypothesis is proven when the data from calcium imaging in a separate investigation which reported TRPV4 channels expressed in human embryonic kidney (HEK293) cells showed a surge of intracellular calcium signalling when stimulated with the endocannabinoids, anandamide or 2-AG and the endocannabinoids metabolite, arachidonic acid (Watanabe et al., 2003).

Immunohistochemistry investigation of bronchial biopsy samples of patients with severe asthma demonstrated upregulated TRPV1 expression on the bronchial epithelium and was thought to have a role in mediating bronchial tone and cough reflex (McGarvey et al., 2014). Primary bronchial epithelial cultures derived from COPD patients also had similar increase in mRNA expression of TRPV1 and TRPV4 channels (Baxter et al., 2014). A study in transfected human embryonic kidney-293 (HEK-293) cells demonstrated that anandamide is indeed a ligand for the TRPV1 channels (Movahed et al., 2005). Analysis of data obtained from several binding studies then revealed that anandamide binds to TRPV1 as an agonist, although at an affinity which is relatively lower compared to the typical TRPV1 agonist capsaicin (Pertwee et al., 2010). Interestingly, anandamide expression level is also increased in asthmatic patients (Zoerner et al., 2011), hence further suggesting that either anandamide or its metabolite, arachidonic acid, might activate TRPV1 channel, thus triggering an inflammatory response within the airway structures.

1.13 Aims of the Study

The main key question for the present study was to identify the effects of endocannabinoids, including anandamide and 2-AG, as well as the phytocannabinoids, such as THC and CBD on the human bronchial epithelial cell permeability. Furthermore, the effect of the cannabinoids on airway epithelial mucus secretion was investigated as mucus hypersecretion is also one of the key features of airway inflammation. An *in vitro* model using the Calu-3 bronchial epithelial cell line was employed in this study to address the question.

Subsequently, the mechanism and intracellular signalling pathways involved were determined to enable further understanding of how these compounds mediate their respective effects.

2 Materials, General Methods and Protocol

Development

2.1 Materials

2.1.1 Materials Used for Cell Culture

Compound/Reagent	Catalogue number	Source/Manufacturer
Calu-3 cells (used between passages 3 and 30)	ATCC [®] HTB-55 [™]	ATCC (Rockville, USA)
Dulbecco's modified Eagle's medium/nutrient mixture F12 Ham (DMEM F12 Ham)	D6421	Sigma-Aldrich (Poole, UK)
Fetal bovine serum (FBS)	F4135	
MEM Non-essential amino acids	M7145	
L-glutamine	59202	
10,000 units Penicillin/10 mg streptomycin per mL in 0.9% sodium chloride	P0781	
Phosphate-buffered saline (PBS)	D8537	
Trypsin/EDTA (x10) solution	59418C	
Trypan Blue Dye 0.4% solution	#1450021	Bio-Rad (Hercules, CA, USA)
Counting Slides	# 1450003	

Table 2-1 Reagents used in Calu-3 cell culture, maintenance and cryopreservation.

2.1.2 Materials Used in TEER Experiments

Compound/Reagent	Rationale for use	Catalogue number	Source/Manufacturer
2-arachidonoylglycerol (2-AG)	Endocannabinoid. Partial agonist of CB ₁ /CB ₂ R	#1298	Tocris Bioscience (Bristol, UK)
AM251	Most selective CB ₁ R antagonist	#1117	
Anandamide	Endocannabinoid. Partial agonist of CB ₁ /CB ₂ R	#1339	
Arachidonyl-2'-chloroethylamide (ACEA)	Most selective CB ₁ R agonist	#1319	
Arachidonic acid	Putative metabolite of anandamide metabolite	A8798	Sigma-Aldrich (Poole, UK)
Cannabidiol	Phytocannabinoid	#1570	Tocris Bioscience (Bristol, UK)
Dimethylsulfoxide (DMSO)	Amphiphilic vehicle	W387520	Sigma-Aldrich (Poole, UK)
EDTA	Chelating agent	E6758	
Ethanol (EtOH)	Vehicle for lipophilic compounds	459844	
HU-210	Highly potent CB ₁ /CB ₂ R agonist	#0966	
IL-1 β	Cytokine	I9401	Sigma-Aldrich (Poole, UK)
Indometacin	COX inhibitor	I7378	
JWH133	Most selective CB ₂ R agonist	#1343	Tocris Bioscience (Bristol, UK)
Nordihydroguaiaretic acid (NDGA)	LOX inhibitor	N5023	Sigma-Aldrich (Poole, UK)
PD98059	MEK1/2 inhibitor	P215	

R(+)-Methanandamide	Stable analog of anandamide	#1121	Tocris Bioscience (Bristol, UK)
SB203580	MAPK p38 inhibitor	S8307	Sigma-Aldrich (Poole, UK)
SR144528	Most selective CB ₂ R antagonist	192703-06-3	Cayman Chemical Europe, (Tallinn, Estonia)
THC	Phytocannabinoid.	#1990	Tocris Bioscience (Bristol, UK)
TNF α	Cytokine	T7539	Sigma-Aldrich (Poole, UK)
U0126	Highly selective MEK1/2 inhibitor	U0120	
URB597	Selective FAAH enzyme inhibitor	#4612	Tocris Bioscience (Bristol, UK)
Y27632	Selective ROCK inhibitor	#Y0503	Sigma-Aldrich (Poole, UK)

Table 2-2 List of chemicals used for TEER experiments. It is noted that the cannabinoid ligands and enzyme inhibitors were prepared to a standard stock concentration of 10mM in their respective vehicle (DMSO, EtOH or distilled water) before administration into the cells. Details on the concentrations used and the affinity of the drugs to their respective receptors will be further discussed in the following results chapters.

2.1.3 Materials Used in FITC-Dextran Permeability Studies

Compound/Reagent	Catalogue number	Source/Manufacturer
N-acetylcysteine (NAC)	A7250	Sigma Aldrich, Poole, UK
FITC-dextran (FD) of molecular weight 4 kDa (FD4)	FD4 SIGMA	

Table 2-3 Chemicals used in FITC-dextran Permeability Studies

2.1.4 Materials Used for Dot Blotting and Western Blotting

Reagent (Concentration)	Catalogue number	Source/Manufacturer
<i>Lysis buffer, pH 7.6, EDTA-free</i>		
β-glycerophosphate (10 mM)	G9422	Sigma Aldrich, Poole, UK
Ethylene glycol tetraacetic acid (EGTA) (1 mM)	E4378	
Protease inhibitor cocktail 1% (v/v)	P8340	
Sodium fluoride (1 mM)	S7920	
Triton X-100 (0.1% (v/v))	X100	
Tris (20 mM)	T4661	
<i>6 x Concentrated Laemmli solubilisation buffer</i>		
β-mercaptoethanol (5% (v/v))	M6250	Sigma Aldrich, Poole, UK
Bromophenol blue (0.01% (v/v))	B0126	
Glycerol (5% (v/v))	G2025	
Sodium dodecyl sulphate (SDS) (8.3 mM)	L3771	
Tris hydrochloride (62.5 mM)	T4661	
<i>10 x Electrophoresis buffer</i>		
Glycine (1.9 M)	L3771	Sigma Aldrich, Poole, UK
SDS (35 mM)	L3771	
Tris hydrochloride (0.19 M)	T4661	

<i>Transfer buffer</i>		
Glycine (1.9 M)	L3771	Sigma Aldrich, Poole, UK
Methanol (20% (v/v))	322415	
Tris hydrochloride (0.19 M)	T4661	
<i>Ponceau S buffer</i>		
Acetic acid (5% (w/v))	695092	Sigma Aldrich, Poole, UK
Ponceau S	P3504	
<i>Tris-Buffered Saline and Tween 20 (TBST), pH 7.6</i>		
Concentrated 1M hydrochloride acid (sufficient drops until pH 7.6)	38283	Sigma Aldrich, Poole, UK
Sodium chloride (125 mM)	38283	
Tris hydrochloride (25 mM)	T4661	
Tween 20 (0.1% (v/v))	P1379	
<i>Milk powder solution</i>		
Skimmed milk powder 5% (w/v) dissolved in TBST buffer		TBST reagents: Sigma Aldrich (Dorset, UK). Skimmed milk powder: Co-operative foods (Somerset, UK)

Western blotting procedures		
4–20% sodium dodecyl sulphate-polyacrylamide gel for electrophoresis	(SDS-PAGE) Mini-PROTEAN® TGX™	Bio-Rad (Hercules, USA)
Nitrocellulose membrane	LC2006	Thermo Scientific (Rockford, USA)

Table 2-4 List of materials and reagents used to prepare buffers necessary for dot blotting and Western blotting procedures.

2.1.5 List of Primary and Secondary Antibodies Used in Dot Blotting and Western Blotting

Target	Host	Dilution	Catalogue no.	Secondary antibody
MUC5AC	Mouse	1:1000	Abcam Ab3649	Goat anti-mouse IgG (Red) IRDye®680RD Conjugate (Licor 926-68070) Dilution 1: 10,000
Occludin	Rabbit	1:1000	Abcam Ab31721	Goat anti-rabbit IgG (Green) IRDye®800CW Conjugate (Licor 926-32211) Dilution 1: 10,000
ZO-1	Rabbit	1:1000	Zymed 40-2200	
GAPDH	Mouse	1: 10,000	Sigma Aldrich	Goat anti-mouse IgG

(As loading control)			SAB1405848	(Red) IRDye® 680RD Conjugate (Licor 926-68070) Dilution 1: 10,000
CB ₁ Receptor	Rabbit	1:1000	Cayman Chemical #10006590	Goat anti-rabbit IgG (Green) IRDye® 800CW
CB ₂ receptor	Rabbit	1:500	Enzo Life Sciences ADI-905-749-100	Conjugate (Licor 926-32211) Dilution 1: 10,000
Total MYPT1	Rabbit	1:1000	Cell Signaling Technology #2634	Goat anti-rabbit IgG (Red) IRDye® 680RD Conjugate (Licor 926-68071) Dilution at 1: 10,000
Phospho-MYPT (Thr696)	Rabbit	1:500	Cell Signaling Technology #5163	Goat anti-rabbit IgG (Green) IRDye® 800CW Conjugate (Licor 926-32211) Dilution at 1: 10,000
Total ERK1/2 MAPK	Rabbit	1:1000	Cell Signalling Technology #9102	Goat anti-rabbit IgG (Red) IRDye® 680RD Conjugate (Licor 926-68071) Dilution at 1: 10,000

Phospho- ERK1/2 MAPK	Mouse	1:1000	Cell Signalling Technology #9107	Goat anti-mouse IgG (Green) IRDye [®] 800CW Conjugate (Licor 926-32210) Dilution at 1: 10,000
----------------------------	-------	--------	--	--

Table 2-5 List of primary and secondary antibodies used in dot blotting and Western blotting experiments.

2.1.6 Materials Used in Radioligand-Binding Studies

Compound/Reagent	Catalogue number	Source/Manufacturer
[³ H]-CP 55,940	NET1051001MC	PerkinElmer (Bucks, UK)
Liquid scintillation cocktails		

Table 2-6 Reagents used in radioligand-binding studies.

2.1.7 Materials Used in Cytotoxicity Studies

Compound/Reagent	Catalogue number	Source/Manufacturer
Resazurin	R7017	Sigma Aldrich, Poole, UK
3-(4,5-dimethylthiazol-2-yl)-2,5-diphenyltetrazolium bromide (MTT)	M5655	

Table 2-7 Reagents used in resazurin and MTT assay.

2.1.8 Materials Used in Bronchial Contractility Studies

Reagent (Concentration)	Catalogue number	Source/Manufacturer
<i>Chemicals for Krebs-Henseleit buffer, pH 7.4, gassed for 15 minutes with 95% oxygen, 5% carbon dioxide</i>		
Calcium chloride (1.25 mM)	C1016	Sigma Aldrich, Poole, UK
Glucose (11 mM)	G0350500	
Magnesium sulfate (1.1 mM)	G0350500	
Potassium chloride (4.8 mM)	P9333	
Potassium dihydrogen orthophosphate (1.2 mM)	P5655	
Sodium chloride (118 mM)	S7653	
Sodium hydrogen carbonate (25 mM)	S6014	
<i>Chemicals for organ bath studies:</i>		
Carbachol	C4382	Sigma Aldrich, Poole, UK
EtOH	459844	
Ficoll® PM 70	F2878	
Potassium chloride	P9333	
THC	#1990	Tocris Bioscience Ltd (Bristol, UK)

Table 2-8 List of chemicals used for organ bath studies.

2.2 *In Vitro* Models for the Investigation of Human Airway Epithelial Permeability

2.2.1 *Primary Human Bronchial Epithelial Cells*

Primary human bronchial epithelial cells are obtained by isolating the cells from bronchial biopsy specimens from normal or diseased human donors. The use of primary airway epithelial cell culture is advantageous as it provides the closest biological response to that of an intact bronchial epithelium due to the absence of genetic alteration, compared to immortalised cell lines. However, a comparative study of various bronchial epithelial cell models revealed that these primary cells expressed variable TEER values, ranging from $100\Omega\cdot\text{cm}^2$ up to $600\Omega\cdot\text{cm}^2$ at day 21 of culture to full confluency and differentiation (Stewart et al., 2011). This potentially poses a challenge to evaluating the pharmacological effect of a drug owing to the inconsistent TEER despite when untreated. Primary bronchial epithelial cells are also viable for a low number of passages as a study has demonstrated that they can neither achieve confluency nor express tight junction proteins that constitute for the transepithelial resistance (Ehrhardt et al., 2006) (Ehrhardt et al., 2006). Furthermore, the need for ethical approval, specialist skills to perform bronchial biopsies and extra supplements such as antibiotics, growth hormones and amino acids or micronutrients mixes are subjected to significant costs implications.

2.2.2 Calu-3 Bronchial (or Airway) Epithelial Cell Line

The chosen *in vitro* model for this study is Calu-3 which is an immortalised bronchial epithelial cell line derived from lung adenocarcinoma tissue of a 25-year old patient (ATCC, catalogue #HTB-55). A typical Calu-3 cell culture protocol involves growing the cells on a filter support, known as Transwell®, which creates two separate, permeable layers - the basolateral and apical sides of the cell layer. Therefore, this offers the option to grow cells in either a submerged culture liquid-liquid interface (LLI) or at an air-liquid interface (ALI) in which cell culture medium is only present in the basolateral compartment. Such culture condition resembles the normal human bronchial epithelium in which the basolateral side represents the underlying smooth muscle compartment, whilst apical side mimics the luminal compartment that exposes top part of the epithelium to the environment.

The use of Calu-3 bronchial epithelial cell line at ALI was the preferred choice of study for several reasons. First, Calu-3 cells grown in ALI display a desirable morphology as cells differentiate into ciliated columnar cells and mucus-secreting goblet cells, whereas cells grown in LLI develop only the ciliated cell morphology (Grainger et al., 2006). This was thought to be due to a greater atmospheric exposure to oxygen in air-liquid interface cultures which promotes bronchial epithelial cell differentiation. Second, Calu-3 cells cultured in LLI produce higher TEER readings compared to air-liquid interface cultures, owing to a more defined tight junctions formation (Kreft et al., 2015). However, growing cells at the ALI is the preferred condition as it mimics the environmental conditions of physiological bronchial epithelia, and has been shown to yield reproducible TEER values of above $300 \Omega \cdot \text{cm}^2$ over an extended number of

passages compared to the primary human bronchial epithelial cells (Cooney et al., 2004, Stentebjerg-Andersen et al., 2011). Calu-3 cells were also the chosen model in this study owing to their ability to express tight junction proteins, such as occludin, ZO-1, claudin and JAM which provided another mean to reflect on the epithelial cell permeability.

The Calu-3 epithelial cell line has been commonly used to study the permeation potential of drugs within the respiratory tract (Forbes and Ehrhardt, 2005), and other investigations have also demonstrated the reliability of Calu-3 cells as an *in vitro* model for pharmacological studies (Winton et al., 1998, Vinhas et al., 2011). This is due to its ability to form confluent, polarised cell sheets in which physiological features change as a result of altered tight junction proteins expression or regulation of mucus secretion following treatments with drugs. More recent studies have shown Calu-3 cells also express receptors that are found on the native bronchial epithelium such as the cystic fibrosis transmembrane regulator (CFTR) (Zhang et al., 2010), and drug transporters including the ATP-binding cassette (ABC) transporters family (Kreft et al., 2015). These findings further support the ability of Calu-3 cells to respond effectively to various pharmacological treatments that are similar to the intact airway epithelium. Thus, the present study aimed to evaluate the expression of receptors that are known to bind cannabinoid ligands, such as the CB₁ and CB₂ receptors to further strengthen to choice of Calu-3 cell line as a model of study.

2.3 *In Vitro* Permeability Enhancement Agents

2.3.1 Synthetic Compound

i. Ethylenediaminetetraacetic acid (EDTA)

Studies have demonstrated that Ca^{2+} is the key cation to complete tight junction protein sealing as switching epithelial cells from a high to low calcium concentration in culture medium impaired tight junction function (Stuart et al., 1994, Wan et al., 2000). Predictably, the administration of a Ca^{2+} chelating agent EDTA sequesters these metal ions from both the medium and the epithelial cells. Such phenomenon was observed in Caco-2 intestinal and Calu-3 bronchial epithelial cells as EDTA caused prompt and reproducible increase in epithelial paracellular permeability and a significant fall in TEER measurement (Tomita et al., 1996, Kibangou et al., 2008, Petecchia et al., 2012). The lack of Ca^{2+} availability caused by EDTA was shown to prevent the assembly of the tight junction proteins, including occludin, E-cadherin, claudin and ZO-1 which depends on Ca^{2+} to maintain cell-cell adhesion [review by (Deli, 2009)]. Therefore, EDTA is commonly employed as a positive control to induce an increase in epithelial permeability.

2.3.2 Biological Agents

i. Cytokines

One of the most commonly used pro-inflammatory cytokines in epithelial permeability studies is tumour necrosis factor- α (TNF α). It is a biological product secreted mainly by the Th2 cells, macrophages and mast cells (refer *section 1.2.6*) as part of the innate immune response. TNF α also promotes further release

of its own and other cytokines such as IL-6 and IL-8 to exaggerate the existing inflammatory response (Cromwell et al., 1992). Furthermore, the presence of TNF α on the epithelial structure is thought to have a negative impact on epithelial barrier function. Previous TEER experiments demonstrated that TNF α caused a concentration-dependent increase in epithelial permeability using LLC-PK1 kidney epithelial cell line (Mullin et al., 1992). It was noted that TNF α is markedly increased in airway inflammation and its expression is thought to be one of the major causes of airway hyperresponsiveness in asthma (Choi et al., 2005) and COPD (Sun et al., 1998). Experiments conducted by Petecchia *et al* (2012) reported that exposure of Calu-3 cells to TNF α decreased its transepithelial resistance which was mediated by ERK1/2 phosphorylation. Hence, it can be speculated that *in vivo* TNF α that disrupts the epithelial tight junction expression, decreasing in cell-cell adhesion. Ultimately, this results in epithelial cell detachment and the exposure of sensory nerve endings directly to the environment.

Bronchial biopsy specimens obtained from asthmatics (Sousa et al., 1996) and sputum samples of COPD patients (Sapey et al., 2008) revealed a common increase in IL-1 β expression. The sites at which IL-1 β was detected from these studies suggest that IL-1 β could be present on the luminal side of the bronchial structure, and hence has a role in mediating the airway epithelium permeability during diseased states. The use of IL-1 β in epithelial permeability experiments is less extensively studied compared to TNF α . Nevertheless, one study has demonstrated that the cytokine induced an anticipated increased in Caco-2 intestinal epithelial cell permeability which was associated with modulation of gene transcription through activation of the NF- κ B cascade that was hypothesised

to subsequently decrease the translation of tight junction proteins (Al-Sadi et al., 2010).

Other pro-inflammatory cytokines that are frequently found in the airway epithelial structures of asthma and COPD patients include IL-4 and IL-13 (Broide et al., 1992, Lanone et al., 2002), or histamine which is particularly increased in allergic asthma responses (Laitinen et al., 1985). Combined application of IL-4 and IL-13 resulted in a significant increase in paracellular permeability and reduction in transepithelial resistance measured in 16HBEo- airway epithelial cells (Saatian et al., 2013). The effect of histamine caused a similar decrease in transepithelial resistance in the primary human bronchial epithelial cells that was accompanied by a decrease in the expression of the tight junction protein, E-cadherin (Zabner et al., 2003). Although it is interesting to screen the individual effect of these cytokines on the barrier function of airway epithelial cells, the use of one of the cytokines with pleiotropic function, such as TNF α and IL-1 β could be sufficient to represent the breadth of pro-inflammatory mediators known to be involved in airway inflammation.

ii. Lipopolysaccharide (LPS)

LPS is an endotoxin found on the outer membrane of the Gram-negative bacteria to protect the microorganism against heat, extreme pH and lipophilic antibiotics that can penetrate through normal cell membranes. Airway inflammation induced by LPS on the surface of the bronchial epithelial cells is foreseeable when asthmatic symptoms are exacerbated by the presence of pathogens that are introduced from the environment. Binding of LPS to its receptor, Toll-like receptor 4 (TLR4), was observed to cause a surge in cytokine release which

mainly consists of $\text{TNF}\alpha$ and $\text{IL-1}\beta$ (Chow et al., 1999). LPS was shown to modulate the barrier function of the rat trachea epithelium indicated by the increase in paracellular permeability to radioactive-labelled albumin, a mechanism which was mediated through the activation of myosin light chain (MLC) kinase (Eutamene et al., 2005).

2.4 Calu-3 Cell Culture

2.4.1 Cell Culture Maintenance

Calu-3 cells (used between passages 3 and 30) were cultured in DMEM F12 Ham, supplemented with 10% of fetal bovine serum (FBS), 1% non-essential amino acids, 1% L – glutamine and 1% penicillin/streptomycin. Upon achieving approximately 90% confluency by day 7 of seeding, existing media in T75 flasks (CoStar, Corning, UK) were aspirated and cells were washed with 5 ml PBS. Cells were harvested with 2 ml of trypsin/EDTA (x1) for 10-15 minutes then collected by centrifugation at 75 x g, for 5 minutes. Calu-3 cells were consistently sub-cultured in a 1:3 split ratio on a weekly basis into one T75 flask and seeded into two semi-permeable 12-Transwell® plates (CoStar, Corning, UK) at a density of 10^5 cells per well (see *Figure 2-2(a)*), quantified according to the protocol in *section 2.4.2*. Volumes of pre-warmed medium for the basolateral and apical compartments of Transwell® were 1.5 ml and 0.5 ml respectively.

Cells in Transwells were initially grown in LLI until day 5 to ensure adherence of cells onto the surface of the filter membrane and to allow ample time for the cells to become fully confluent. Medium from the apical layer was then aspirated to change the growth condition to ALI. They were routinely washed with 0.5 ml of PBS and replaced with 1.5 ml of fresh medium on the basolateral sides every 2 to 3 days. Calu-3 cells were left to grow in the incubator at 37°C with 5% carbon dioxide for up to day 21 to 28 (see *Figure 2-2(c)*).

2.4.2 Quantification of Cell Viability

Routine viability counts were carried out for every sub-cultured confluent T75 flask (relate to *section 2.4.1*). After a cell pellet was suspended in 1 ml of medium, 10 μ l of the cell suspension were mixed with an equal volume of 0.4% (v/v) trypan blue dye in a 500 μ l Eppendorf tube. 10 μ l of this cell mixture were pipetted carefully into a cell-counting chamber slide, and then inserted into an automated cytometer. Dilutions of the cell suspension were performed according to the numbers of live cells counted.

2.4.3 Cells Cryopreservation

Upon reaching about 90% confluency in a T75 flask, Calu-3 cells were trypsinised, as described previously in *section 2.4.1*. Following centrifugation, each cell pellet was suspended in 3 mL (1:3 split ratio) of freezing solution (containing 90% (v/v) fetal bovine serum and 10% (v/v) DMSO). The cell suspension was then pipetted into three separate cryogenic vials labelled with cell type, passage number, date of freezing and username. All cryogenic vials were stored into a designated freezing tub, i.e. Mr FrostyTM, for overnight freezing in the -80⁰C freezer, so that a gradual decrease in temperature at a rate of -1⁰C/minute could be achieved to ensure optimal cell preservation. These cryogenic vials were then deposited into racks submerged in liquid nitrogen for storage until needed.

2.4.4 Cell Revival from Frozen

Cryogenic vials containing frozen Calu-3 cells were removed from the liquid nitrogen tank. They were then rapidly warmed to 37⁰C for approximately 3 minutes

in a water bath, to ensure optimal cell viability during the thawing process. Thawed cell suspensions from each of the cryogenic vial were then transferred into a 30 mL universal flask containing 9 mL of pre-warmed 37°C medium. Cells were collected following centrifugation at 75 x g for 5 minutes to ensure most of traces of DMSO from the freezing solution were removed. After suspending each cell pellet with 1 mL of medium, they were then transferred into separate T75 flasks containing 19 mL of medium, labelled with cell type, passage number, date on which the cells were thawed and username. Calu-3 cells were placed in a 37°C incubator with 5% carbon dioxide to ensure cells attachment onto the surface of the flask. The medium in each flask was then replaced on the next day to keep traces of DMSO to a minimum, as its presence can interfere with normal cell growth. Finally, T75 flasks were returned into the incubator until the Calu-3 cells were confluent.

2.5 Evaluation of Bronchial Epithelial Tight Junction

Integrity using Transepithelial Electrical Resistance (TEER)

2.5.1 TEER Measurement with STX2 Electrodes

Inserts containing Calu-3 cells were washed with 0.5 mL PBS and 1.5 mL of basolateral medium was replaced. Next, 0.5 mL medium was added into the apical side of each Transwell®. This step is vital to ensure that the electrodes are fully submerged into the medium so that a complete circuit for TEER measurement can be established. Transwell® plates were then placed in the incubator for 30 minutes to allow cultures to equilibrate. Basal TEER readings were collected using STX2 electrodes (World Precision Instrument UK, Stevenage). Readings were then

generated on an EVOM² meter (World Precision Instrument UK, Stevenage) by directly dipping the shorter electrode into the insert (apical), with the longer one on the outer (basolateral) side of the Transwell[®]. A typical set up for the experiment is illustrated in *Figure 2-1*.

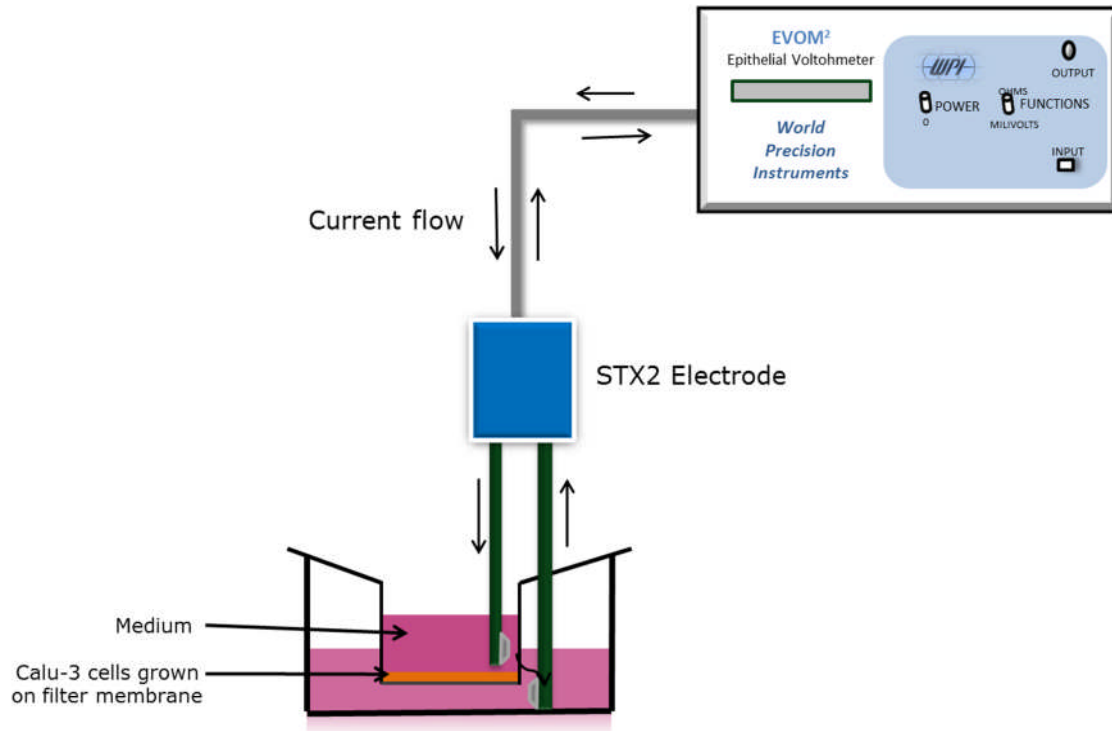
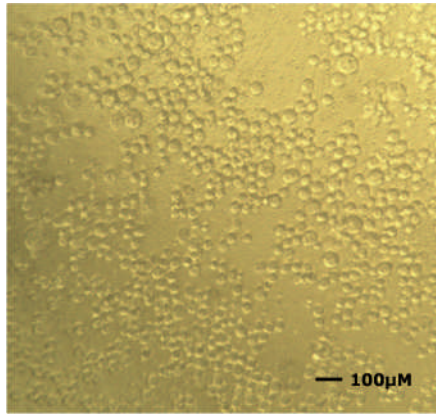


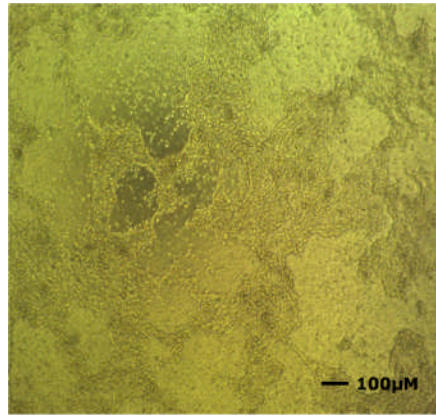
Figure 2-1 Set up for TEER measurement using STX2 electrodes which measures the resistance across the monolayer of Calu-3 cells grown between days 21 and 28. Following the addition of 0.5 mL medium on the apical compartment, STX2 electrodes were placed carefully into the Transwell[®], with the shorter electrode dipped into the medium of the apical side and longer electrode into the basolateral side. Current that was supplied by the EVOM² device travelled from the shorter electrode then across the Transwell[®] to the longer electrode to establish a complete circuit connection for resistance measurements. Readings were generated and displayed on the EVOM² device.

2.5.2 Development of TEER Measurement for Calu-3 Cells when Cultured at ALI

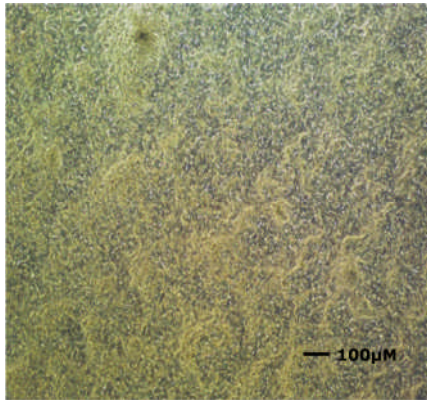
TEER readings of Calu-3 cells were measured on every other day (at passages 5-27), starting on day 5 (after seeding) when cells appeared confluent in each Transwell®. It has been previously reported that Calu-3 cells are slow to achieve full confluency because of their propensity to form isolated colonies (refer *Figure 2-2(b)*) (Stewart et al., 2011). Thereafter, TEER readings increased gradually up to Day 21, and then remained relatively constant until day 28 with values of 700-800 $\Omega\cdot\text{cm}^2$ (refer *Figure 2-3*) indicating that the cells were fully differentiated and had developed tight junctions generating substantial resistance across the cell layer (Zhu et al., 2010).



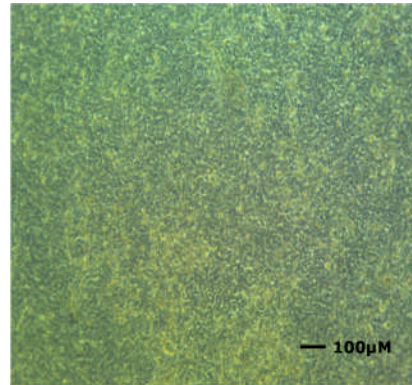
A. Day 0 (day of seeding)



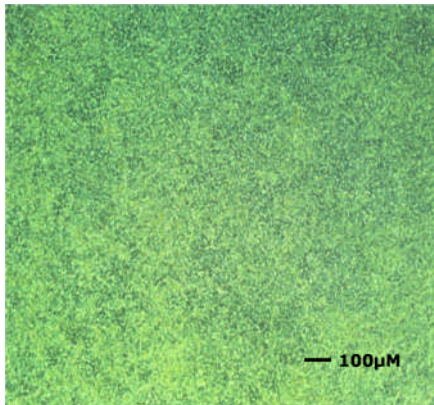
B. Day 3



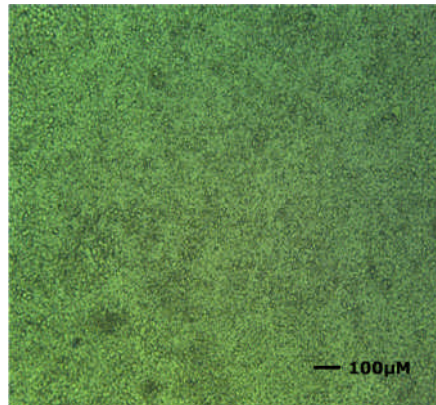
C. Day 5



D. Day 7



E. Day 14



F. Day 21

Figure 2-2 Phase contrast images of Calu-3 cells at different stages of growth at **A.** Day 0, which was the day of cell seeding into a Transwell®; **B.** Day 3 shows cells attaching onto the filter membrane in the Transwell®, forming distinct cell colonies; and **C. to F.** Day 5-21 display confluent layer of Calu-3 cells, maintained at ALI. Images were taken at 10x objective.

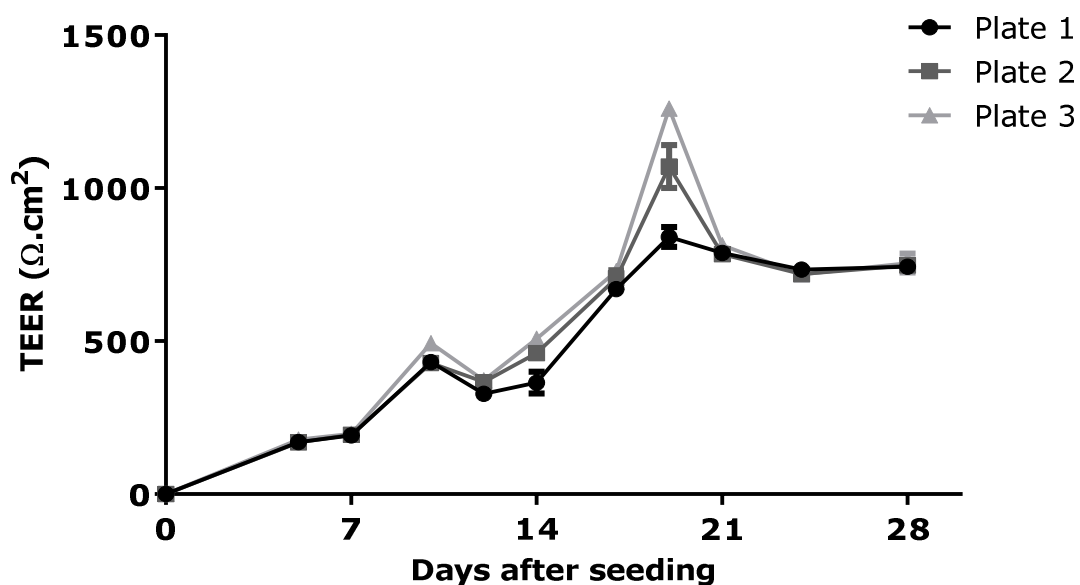


Figure 2-3 TEER development of Calu-3 cells grown at ALI. TEER readings were taken every 2 or 3 days over 28 days using STX2 electrode, connected to an EVOM² device. Results show TEER for Calu-3 cells cultured in three individual plates at passages 3-5, which also reflect the different n number of experiment. Error bars denote standard deviation of the TEER readings measured in triplicates; i.e. three separate Transwells of the same plate.

2.5.3 Resistance/TEER Calculations

TEER was calculated using the formula below:-

$$R_{\text{True cells}} = R_{\text{Total}} - R_{\text{Blank}}$$

The total resistance (R_{Total}) read on the EVOM² meter device comprises of the sum of intrinsic resistance generated by Transwell[®] inserts (R_{Blank}) and the resistance of the epithelial cell layer. Hence, subtracting R_{Blank} (which may range between 130-160 $\Omega \cdot \text{cm}^2$), provides a net value of resistance from cells alone ($R_{\text{True cells}}$).

$$\text{Therefore, TEER } (\Omega \cdot \text{cm}^2) = R_{\text{True cells}} \times SA_{\text{Filter}}$$

SA_{Filter} which stands for ‘surface area of the filter membrane’ expresses TEER as resistance generated by the cells per cm^2 .

Note: SA_{Filter} of Transwell[®] used in this experiment is 1.12 cm^2 .

2.5.4 Modifications to the TEER Measurement Protocol (Method Development)

Initial attempts to measure TEER involved administration of drugs, including EDTA (1 mM), anandamide (10 μ M) and TNF $_{\alpha}$ (10 ng/mL) onto the apical side of designated wells in Calu-3 cells cultured to day 21.

Anandamide was dissolved in 1.4 mL of pure ethanol to achieve a stock concentration of 10 mM. The desired concentration of 10 μ M was achieved by performing 1 in 1000 dilution of anandamide (10 mM) in pure ethanol into labelled universal flasks containing 2 mL of pre-warmed medium. Hence, this yields a final ethanol concentration of 0.1% (v/v). Only 500 μ L of the anandamide solution was administered into each apical side of designated Transwell[®].

Stock concentrations of EDTA and TNF $_{\alpha}$ were prepared to 1 M and 10 μ g/ml respectively with autoclaved water. Like anandamide, the treatment concentrations for both drugs were obtained by a dilution factor of 1:1000, with basolateral medium as vehicle.

Changes in TEER at allocated time points were then recorded. TEER readings were made at basal, 15 minutes, 30 minutes, 1 hour, 1.5 hours, 2 hours, 3 hours, 4 hours, 8 hours, 24 hours and 48 hours.

The unexpected, irregular control TEER recorded (see *Figure 3-1*) called for the need to re-evaluate the methods employed. Variable factors such as the type of interface employed throughout the experimental period and temperature variability were considered. Consequently, later TEER experiments were conducted on a heating block at a constant temperature of 37⁰C to reduce temperature fluctuations in

the environment after which Transwell[®] plates were transferred from the incubator to the cell culture hood for TEER measurements.

A one-time only optimisation experiment was done which compared TEER of the zero control and positive control (+ EDTA) groups. Results from this experiment (*Figure 3-2*) suggested three key changes for future TEER experiments;

- i. Transwell[®] plates should be placed on a 37⁰C hot plate during resistance measurements.
- ii. 500 µL of apical medium should only be added directly before readings were taken, and aspirated afterwards, rather than leaving the medium on for the duration of the experiment.
- iii. As a result of the possible effects of repeated addition and removal of apical medium, basolateral administration of drugs was preferred thereafter.

Subsequent TEER experiments also employed higher concentrations of cannabinoid receptor ligands which were anticipated to produce enhanced responses.

2.6 FITC-Dextran (FD) Permeability Studies

As a complementary approach to TEER measurements of tight junction integrity in Calu-3 epithelial cells, FD permeability assays were conducted. This method measures the amount of FD transported paracellularly through the filter, from the apical to basolateral side of the Transwell[®] (refer *Figure 2-4*). The physical movement of FD represents inhaled micro-allergens including pollen, mould spores, pathogens and house dust mites. These aeroallergens penetrate the lumen of bronchial structures (apical side), thereby provoking subsequent inflammatory responses in the smooth muscle layer (basolateral side) of sensitive asthmatic lungs.

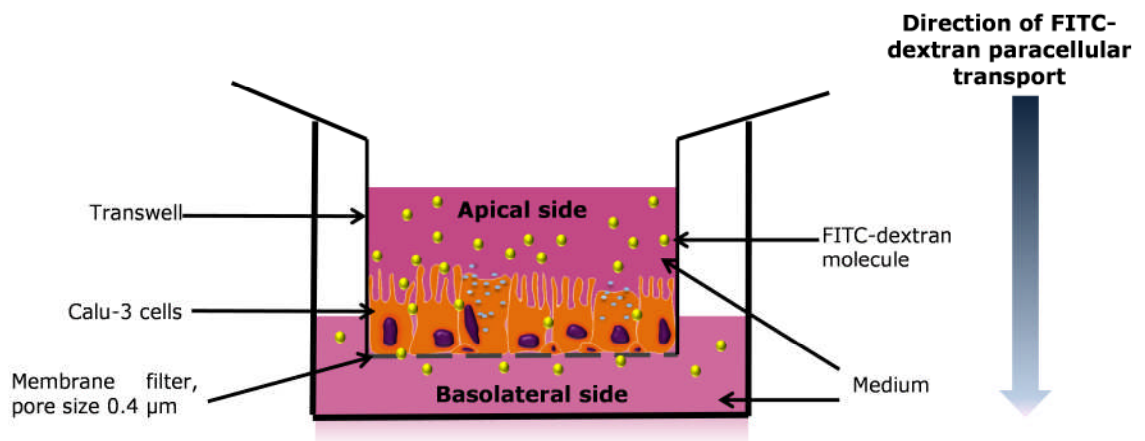


Figure 2-4 A typical set-up for FD permeability assay in a Transwell[®] using Calu-3 cells cultured at Day 21. Medium containing a known concentration of the fluorescent tracer, FITC-dextran, was added onto the apical side. The concentration of FITC-dextran leaking into the basolateral medium thus reflects epithelial permeability; I.e. a high concentration of FITC-dextran detected in the basolateral medium signifies an increased epithelial permeability.

The ability of the FD molecules to be transported across the filter membrane is then quantified and expressed as the apparent permeability coefficient (P_{app}). An increase in P_{app} , therefore, represents an enhanced epithelial permeability, which is likely due to tight junction disruption, and *vice versa*.

FD permeability assays commonly employed the Calu-3 cell line as an *in vitro* model to study the efficiency of drug delivery (Vllasaliu et al., 2011). This was due to Calu-3 cells having a close phenotypic and physiological resemblance to the human bronchial epithelial structure. Nevertheless, Calu-3 cells were initially reported to be a poor model for studying tight junction integrity, owing to their densely packed morphology which obstructs the paracellular route for compounds of larger molecular mass (Forbes and Ehrhardt, 2005). A study conducted by Vllasaliu and colleagues (2011) then revealed that, removal of the apical mucus layer of Calu-3 cells using N-acetylcysteine (NAC) significantly increased FD permeability (Vllasaliu et al., 2011). Results from their investigation reported the highest permeability with FD4, compared to the larger FITC-dextran molecules, such as FD20, FD40 and FD70, following the removal of apical mucus with NAC. Hence, the use of FD4 increases the sensitivity of this method for detecting changes in permeability without disrupting the bronchial epithelial cell layer.

TEER readings were also measured before and after the addition of NAC and drug treatments to confirm tight junction integrity at various stages of the experiment.

2.6.1 Method for the Assessment of FD Permeability

Following medium equilibration for 30 minutes at 37°C, basal TEER measurements of cells in each Transwells[®] were recorded (refer standard TEER protocol in *section 2.5.1 to section 2.5.4*). Calu-3 cells that exhibited TEER of 700-800 $\Omega\cdot\text{cm}^2$ at Day 21 were included in this experiment. This was to ensure consistency in studies and that differentiated cells cultured at ALI were confluent, with fully developed tight junctions. Next, designated cells were exposed to an hour incubation with either vehicle control (0.3% v/v) EtOH or THC (30 μM), followed by cytokine challenge; TNF α (10 ng/mL) or IL-1 β (1 ng/mL). Cells were then left at ALI in the incubator at 37°C, with 5% carbon dioxide, for 48 hours.

TEER readings were measured again after 48 hours of treatment. Medium on the apical side was then removed and replaced with either PBS (vehicle control for NAC) or 0.3% w/v N-acetyl cysteine (NAC), dissolved in warm (37°C) medium. Pre-incubation of the apical face of Calu-3 cells was necessary to remove the mucus layer. Cells were then placed in the incubator for 20 minutes, after which TEER readings were taken, and then medium containing NAC was aspirated. The apical side was then treated with 500 $\mu\text{g/ml}$ of FD4 solution dissolved in warm (37°C) medium and replaced into the incubator. Permeability of the FD molecules was estimated by sampling 100 μl of basolateral medium at basal (i.e. time zero), then every 30 minutes, for up to 3 hours. After sampling at each time point, Transwells[®] were transferred to another 12-well plate, containing fresh warmed basolateral medium with their appropriate drug treatments. Samples of basolateral medium were pipetted into a black 96-well plate, wrapped in aluminium foil between sampling times as FD molecules are photosensitive. Fluorescence intensity was quantified

using a FluoStarGalaxy[®] fluorometer, set at wavelengths 485 nm (excitation) and 520 nm (emission).

A calibration curve (see *Figure 2-5*) was established by quantifying the fluorescence intensity of a series of known FD4 concentrations as described below. Concentrations of FD4 at various time points of each treatment group were then interpolated from the calibration curve.

2.6.2 Establishing an FD4-concentration Calibration Curve

A standard curve is shown in *Figure 2-5*. A maximum FD4 concentration (500 µg/mL) was selected based on the study by (Vllasaliu et al., 2011). The stock FD4 solution was prepared by dissolving the fluorophore in culture medium. Further dilutions were prepared by performing serial 2-fold dilutions, to a minimum concentration of 0.49 µg/ml. The fluorescence intensities of these known concentrations were detected at 485 nm (excitation) and 520 nm (emission). Readings were then plotted, resulting in a linear calibration line, with a correlation coefficient (r^2) of 0.99.

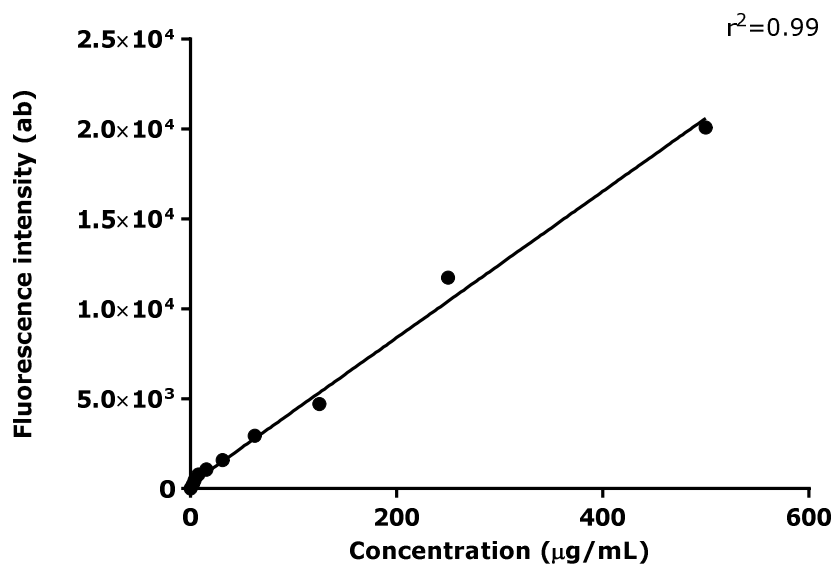


Figure 2-5 A linear calibration line for fluorescence intensities of known concentrations of fluorophore, FD4 to enable quantification of the amount of fluorophore transported into the basolateral side (of Transwell[®]) from their respective apical chambers. Each point represents the mean \pm SEM of fluorescence intensity (in arbitrary units), $n=6$.

2.6.3 P_{app} Calculations

The apparent permeability coefficient (P_{app}) was calculated according to the equation below:-

$$P_{app} = \frac{\left(\frac{\Delta Q}{\Delta t}\right)}{A \cdot C_0}$$

Where,

- P_{app} is the apparent permeability coefficient expressed in cm/sec.
- $\frac{\Delta Q}{\Delta t}$ stands for the change in FD4 concentration (ΔQ) over a fixed period of time (Δt).
- A represents the surface area of the filter membrane of which Calu-3 cells were cultured (1.12 cm² for 12 mm Transwell®).
- C_0 is the initial FD4 concentration administered onto the apical side of the Transwell (500 µg/mL).

2.7 Quantification of Mucin (of MUC5AC Subtype)

Expression Post Treatment

2.7.1 Sample Preparation

Calu-3 cells were cultured in 12-Transwell[®] plates at ALI for 21 days, as previously described in *section 2.5.1* to *section 2.5.4*. Samples were harvested on day 21, using the flat end of a 1 mL syringe plunger, after adding 200 μ L of ice-cold lysis buffer containing 1% v/v protease inhibitor cocktail into each Transwell[®]. The samples were then centrifuged at 6000 x g for 5 minutes at 4⁰C. 100 μ L of the supernatant from the samples were subsequently transferred into labelled 500 μ L Eppendorfs placed on ice. 20 μ L of 6 x concentrated solubilisation buffer were mixed into each Eppendorf and homogenised using a Vortex mixer. Samples were finally stored in a -20⁰C freezer until needed.

2.7.2 Optimisation of MUC5AC Quantification Protocol with Dot Blotting (Method Development)

Samples of the control and TNF α -treated groups (prepared according to *section 2.7.1*) were dotted using a 20 μ L pipette onto a 5 x 10 cm nitrocellulose membrane increasing concentration of; 2, 5, 10, 15 and 20 μ L (refer *Figure 2-6*). Note that sample concentrations were expressed in terms of volumes (in μ L) as Calu-3 cells were seeded at a fixed density of 100,000 cells per Transwells[®]. Samples of more than 5 μ L were gently applied onto the membrane in steps of 5 μ L, allowing drying of the dot between additions, until the desired volumes were achieved. This step was

necessary to minimise the area that the samples penetrate onto the nitrocellulose membrane.

Next, membrane was blocked with 30 mL of 5% (v/v) milk solution for an hour at room temperature. The membrane was then incubated overnight with primary antibody, MUC5AC (ab3649) at 1:1000 dilution (Abcam, Cambridge, UK) at 4°C. Following washing (3 x 15 minutes with TBST buffer), the membrane was exposed with secondary antibody, goat anti-mouse IgG (IRDye[®]680CW Conjugate) at 1:10,000 dilution for an hour at 37°C. The membrane was washed again (3 x 15 minutes with TBST buffer) and then dots on the membrane were detected and their fluorescence intensities quantified using a LI-COR Image Studio infrared imaging system (Lincoln, NE).

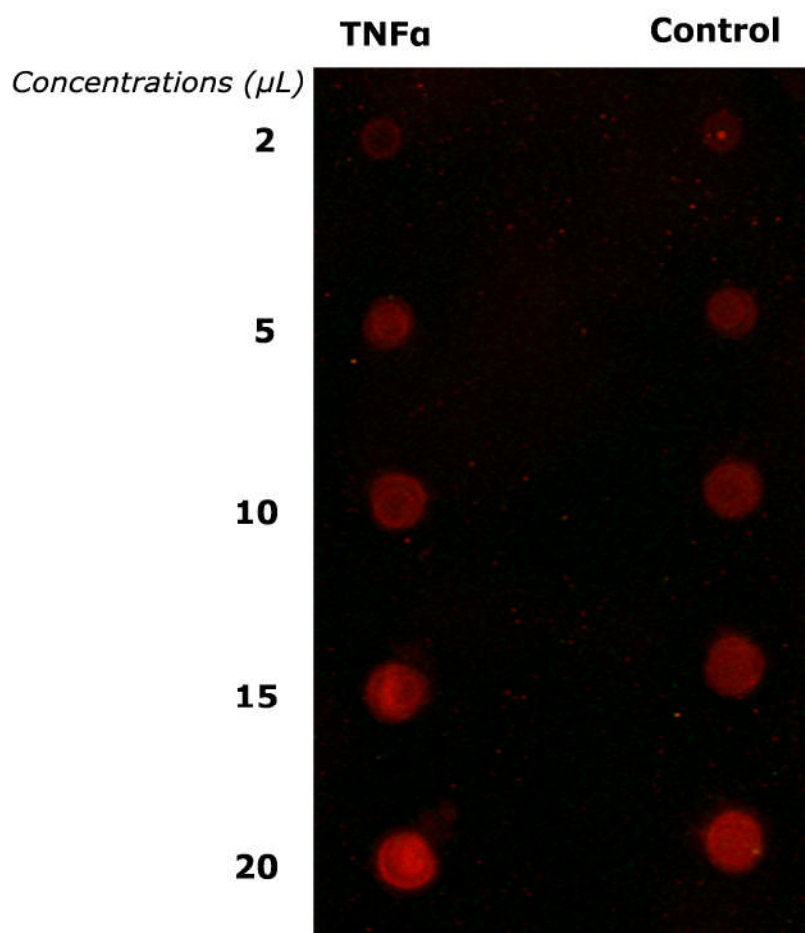


Figure 2-6 Both samples of the cytokine, TNFα (10 ng/mL) and control (no drug) groups were dotted onto a 5 x 10 cm nitrocellulose membrane at volumes 2, 5, 10, 15 and 20 μL. Fluorescence intensities of these dots were directly proportional to the increasing concentration of samples.

Based on *Figure 2-6*, a concentration (or volume) of 10 μL for both TNFα and control groups was deemed the optimised concentration as the fluorescence intensities of the blots were not excessive, yet clear.

2.7.3 Modifications to the Dot Blotting Protocol

Subsequent dot blotting experiments were carried out using a 96-well Bio-Dot[®] Microfiltration apparatus (Bio-Rad, Hercules, CA, USA). The apparatus was more efficient than manual dotting as the area of sample can be contained within a vacuumed, microfiltration unit. As previously described in *section 2.7.2*, the concentration of sample loaded was 10 μL per microfiltration unit, in steps of 5 μL each time. Stages for blocking, primary and secondary antibody incubation were conducted as *section 2.7.2*.

Figure 2-7 illustrates the setup and assembly of the 96-well Bio-Dot[®] Microfiltration apparatus.

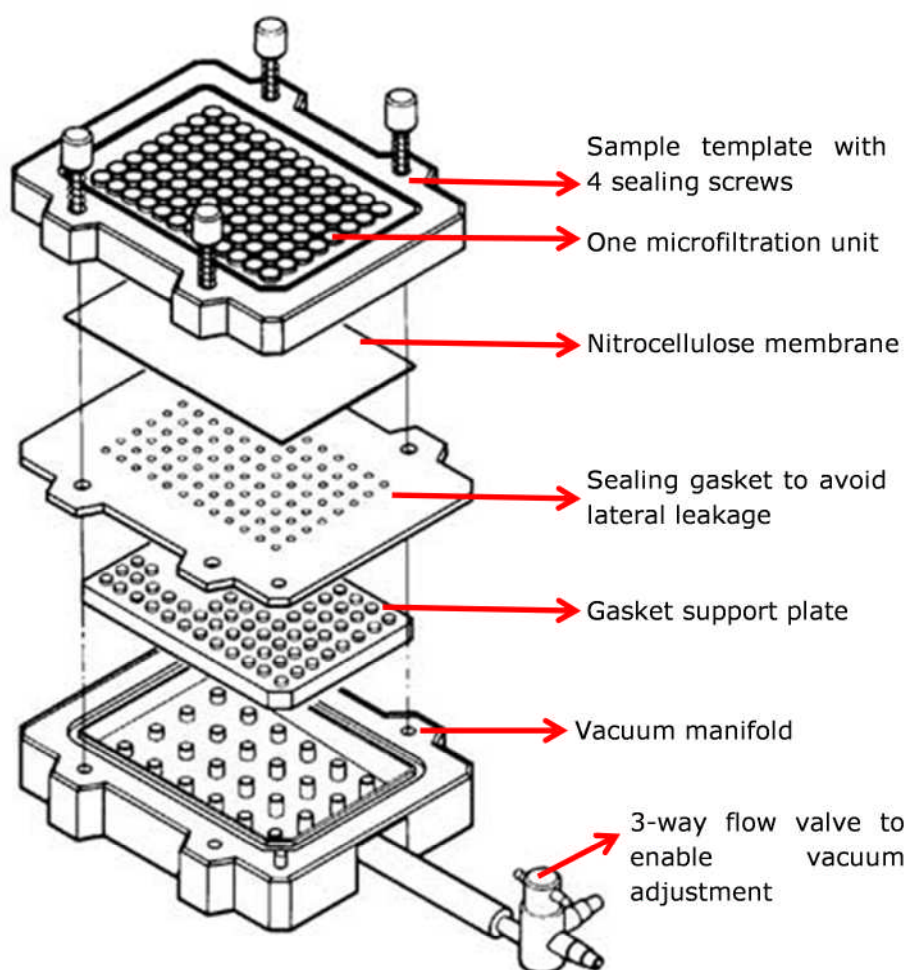


Figure 2-7 (a) A typical set up of a 96-well Bio-Dot[®] Microfiltration apparatus used in the laboratory. **(b)** The separate components which were assembled within the dot blotting apparatus. (Adapted from the official website of (Bio-Rad, 2015))

2.8 Radioligand-Binding Studies

2.8.1 Preparation of Membranes

Calu-3 cells were cultured in T125 flasks (CoStar, Corning, UK) for 7 days until approximately 90% confluent. Cells were then scraped from the flasks and homogenised in Tris buffer (50 mM Trizma[®] base) using a Polytron handheld homogeniser. Homogenates were washed with Tris buffer and centrifuged at 30 000 x g for 10 minutes at 4⁰C. The washing and centrifugation processes were repeated three times.

2.8.2 Radioligand-binding Assay

Specific binding to either CB₁ or CB₂ receptors was assessed by measuring the amount of [³H]-CP 55,940 bound in the presence of saturating concentrations of HU-210 (1 µM), a non-selective CB_{1/2} agonist, and JWH133 (500 nM), a selective CB₂ receptor agonist. Membranes were placed in separate LP4 tubes into which 1 mL of assay buffer (containing 2 mM EDTA, 5 mM magnesium chloride, 50 mM Trizma base and 0.2% BSA), [³H]-CP 55,940 and unlabelled cannabinoid receptor ligand (either HU-210 and JWH133) were added. Samples were incubated for 1.5 hours at 30⁰C then filtered using a 24-well Brandell Harvester. The GFB filter paper was rinsed with cold assay buffer. Radioactivity of each piece of filter paper was measured by liquid scintillation spectroscopy in 3 mL scintillation cocktail. Specific binding (expressed in disintegration per minute, DPM) was obtained by subtracting the value for the non-specific binding (in the presence of HU-210 or JWH133) from total [³H]-CP 55,940.

2.9 Investigating Cannabinoid Receptor Expression and Signalling Pathways underlying TEER changes with Western Blotting

2.9.1 Western Blotting Protocol

Samples stored in the -20°C freezer (refer *section 2.7.1*) were selected according to the appropriate experimental plan and warmed at 95°C for 5 minutes. Once thawed and boiled, these samples were dispersed with a Vortex mixer, then centrifuged at $7500 \times g$ in a bench top centrifuge for 1 minute. Samples were then loaded into designated wells of a 4%-20% precast SDS-PAGE gel in a volume of $10 \mu\text{L}$, for all experiments. Protein concentrations were not measured to determine the amount of samples to be loaded onto the gels as Calu-3 cells were all seeded at a fixed density of 100,000 cells per well. Next, electrophoresis was conducted in electrophoresis buffer at 200 V for 35 minutes. Separated proteins were transferred onto a nitrocellulose membrane in a blotting chamber at 100 V for 60 minutes. The nitrocellulose membrane was then blocked in approximately 25 mL of 5% milk solution for an hour to minimise non-specific binding. The following step involved overnight incubation with a selected primary antibody, in the presence or absence of a loading control antibody (refer to individual chapters). The next day, membranes were blotted with selected secondary antibodies (refer to individual chapters). Membranes were then washed (for 3 x 15 minutes) with approximately 25 mL TBST. Bands were detected and their fluorescence intensities quantified using a LICOR Image Studio infrared imaging system (Lincoln, NE).

2.10 Cytotoxicity Studies

2.10.1 Resazurin Assay

Background Previously known for its use in detecting bacterial contamination in dairy products, the resazurin assay is a simple, safe and reliable technique, commonly used to assess *in vitro* cell toxicity (Fields and Lancaster, 1993). The presence of viable cells reduces the blue, oxidised compound, resazurin, to pink resorufin which is highly fluorescent (*Figure 2-8*). Hence, the more viable cells found in a sample, the higher the fluorescence intensity (in arbitrary units) detected. The resazurin assay was therefore, chosen as a means to detect any cytotoxicity induced by THC or TNF α in this study.

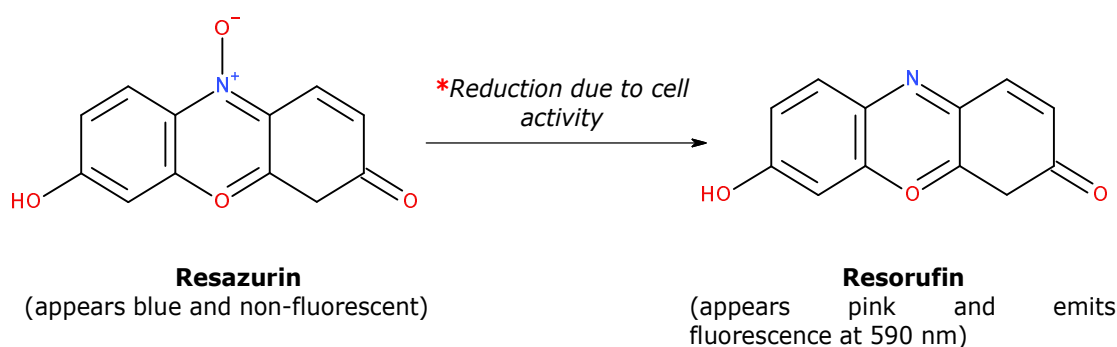


Figure 2-8 Chemical reaction involving reduction of resazurin to resorufin, which is likely to occur due to oxygen consumption in viable cells (O'Brien and Pognan, 2001).

Method Calu-3 cells, cultured in Transwells[®] (refer to *section 2.4.1*), were treated with basolateral administration of THC concentrations, including 3 to 30 μ M for 48 hours. Only a single concentration of EtOH (0.3% v/v), reflecting the amount of ethanol in the highest concentration of THC studied (30 μ M) was studied as vehicle

control in this experiment. Untreated Calu-3 cells were included as a universal control.

A 1 mg/mL stock resazurin solution was prepared in distilled water. The solution was filter sterilised into a universal tube and wrapped in aluminium foil as resazurin is photosensitive. A working solution was subsequently prepared by performing a 1 in 10 dilution of the stock resazurin solution (1 mg/mL), with warmed medium (37°C). The apical and basolateral compartments of the Transwells[®] were then filled with 500 µL and 1500 µL of working resazurin solution respectively. The plates were left to incubate for an hour in the incubator at 37°C, with 5% carbon dioxide. Next, 100 µL of the working resazurin solution from both compartments in the Transwell[®] were transferred into a black 96-well plate. The optical density was measured using a FluoStarGalaxy[®] fluorometer at an excitation wavelength of 530 nm.

2.10.2 MTT Assay

Background MTT assay is another colorimetry study used in this study to confirm the cytotoxicity effect of THC treatment at a concentration of 30 µM in addition to resazurin assay. Besides that, MTT assay was also employed to assess Calu-3 cell proliferation following an extended treatment period with the phytocannabinoid. MTT assay measures the extent of enzymatic conversion from yellow (3-[4,5-dimethylthiazol-2-yl]-2,5 diphenyl tetrazolium bromide) MTT compound, to purple formazan crystals (refer *Figure 2-9*).

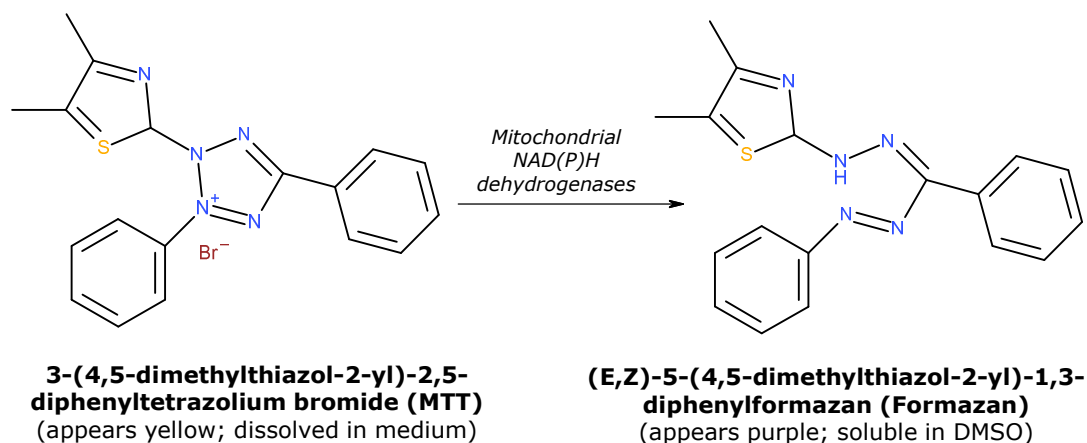


Figure 2-9 Chemical reaction involving the reduction of yellow MTT compound to purple formazan crystals reflects the mitochondrial activity in dividing cells.

Previous study by (Berridge and Tan, 1993) had demonstrated that NADH and NADPH dehydrogenase enzymes, found on the inner mitochondrial membrane, are responsible for this reaction. Thus, a change in the number of viable cells can be detected by measuring formazan concentration; i.e. an indication of cell proliferation when comparing the treated and control cells.

Method Calu-3 cells were cultured according to *section 2.4.1*. TNF α (10 ng/mL), THC 30 μ M or a combination treatment of TNF α and THC were applied to the basolateral side of Transwells for an extended duration of 10 days, with EtOH (0.3% v/v) as vehicle control. The MTT assay commenced after TEER readings were recorded. The medium from each apical side of the Transwells[®] was removed and the apical face of Calu-3 cells washed with 500 μ L of PBS. Then 500 μ L of 1 mg/mL MTT solution (in warmed medium) was added for 4 hours, in the incubator, at 37⁰C with 5% carbon dioxide. One Transwell[®] from each of the treatment group was not

incubated with MTT solution to serve as a negative control. The experiment was conducted in the dark from this stage onwards as MTT is photosensitive. Next, the MTT solution was aspirated from all Transwells[®] and replaced with an equal volume of 100% DMSO. Plates were covered in aluminium foil and placed on a shaker, at room temperature for 10 minutes, to promote dissolution of formazan crystals. 100 μ L from each of the Transwells[®] were transferred into a black 96-well plate and formazan concentrations measured at 570 nm using a Dynex absorbance microplate reader (Dynex Technologies, USA).

2.11 Bronchial Contractility Studies

2.11.1 *Tissue Preparation*

Lungs from pigs (aged less than 6 months, both sexes) were obtained from G Wood & Sons Ltd, (Mansfield) and transported on ice to the laboratory. Lower bronchioles from either side of the lungs were identified by cutting horizontally across the anterior basal segment, approximately 1.5 cm above the lung apex. A crude dissection was performed to isolate about 3 to 4 cm lengths of bronchioles, with diameters ranging from 3 to 6 mm and thickness of approximately 1 mm. Bronchiole segments were then placed in a universal tube in 2% w/v Ficoll[®] PM70 solution and refrigerated overnight at 4°C. Fine dissection was carried out the next day in a Petri dish, containing warmed (37°C) Krebs-Henseleit buffer. Each bronchiole was divided into four rings of 5 mm in length to provide two paired preparations (with and without epithelium). Denudation of the epithelium was achieved by inserting a wet, fine stainless steel forcep into the lumen of each ring, and pressing gently onto a moistened tissue paper in a corkscrew motion. This was repeated twice. Epithelium denudation was verified when a thin yellow sheet of tissue within the lumen was removed. This step was done by examining the bronchiole segment under a dissecting microscope, at 40x magnification.

2.11.2 Organ Bath Experiments

Each bronchiole segment was suspended on a parallel hook in a 5 mL tissue bath containing warmed (37°C) Krebs-Henseleit buffer, with constant gassing with 95% oxygen and 5% carbon dioxide. An initial tension of 2 grams was applied for all bronchiole segments which were left to equilibrate for about 10 minutes. Tissues were then exposed to three challenges of 60 mM potassium chloride (KCl) to assess their viability. They were then washed with fresh warm Krebs-Henseleit buffer (three times). Tension was readjusted to 2 grams after each KCl washout and tissues equilibrated in Krebs-Henseleit buffer for 30 minutes. Cumulative additions of the cholinergic receptor agonist, carbachol (1 to 100 μ M) were performed to achieve a contraction corresponding to 60% to 80% of the third KCl response in all tissues. This was to ensure that the anticipated bronchodilatory response could be detected when THC was added into the organ bath. Once a steady contractile response was achieved, one segment from each of the epithelium-intact and denuded-epithelium pairs was treated with either THC 30 μ M or vehicle control (EtOH, 0.3% v/v). Tissues were incubated for a minimum of 30 minutes to allow THC-treated tissues to exhibit a full response. *Figure 2-10* illustrates the experimental setup:-

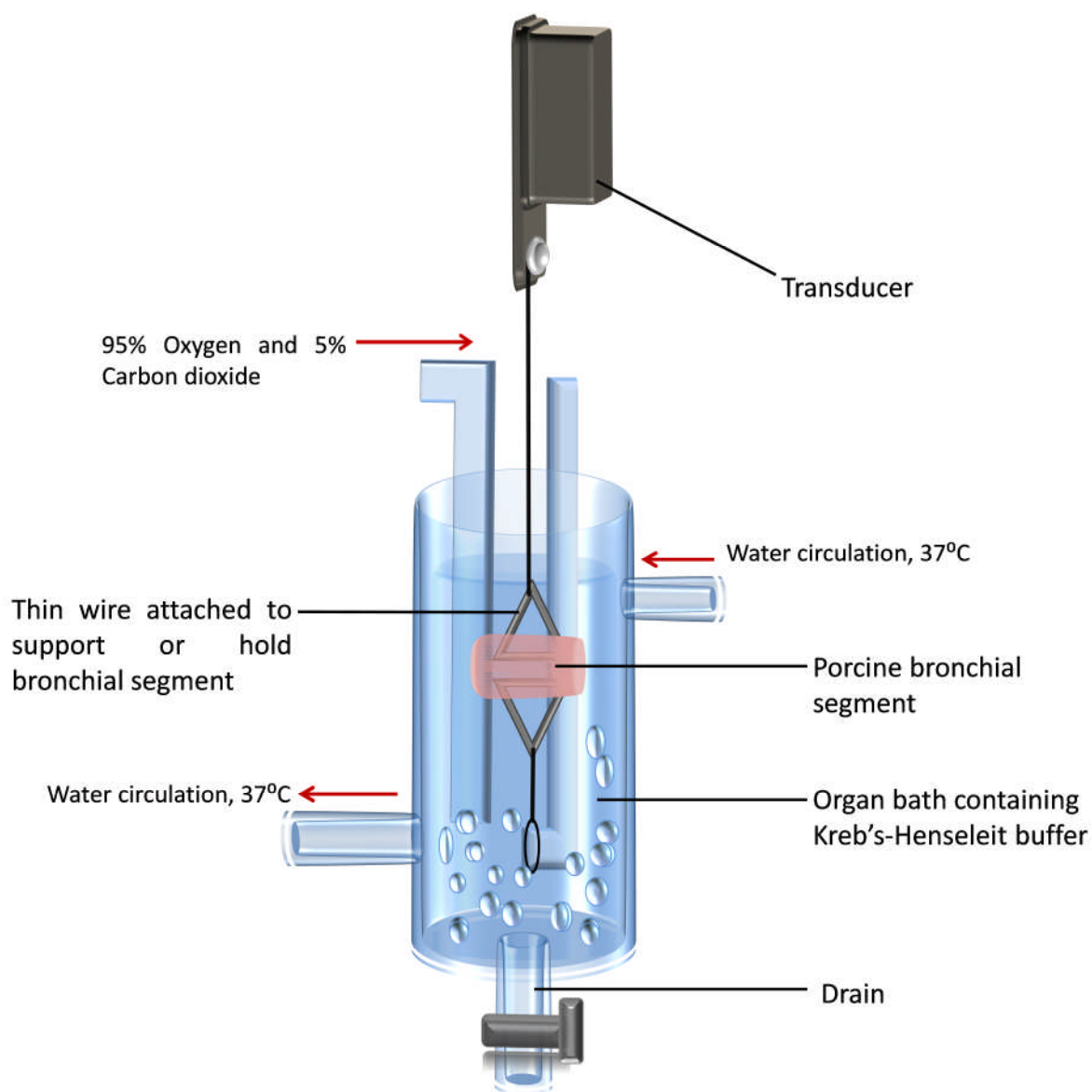


Figure 2-10 Experimental organ bath set-up for porcine bronchial smooth muscle contractility studies. THC ($30\ \mu\text{M}$) was added into a 5 mL organ bath containing warmed (37°C) Kreb's-Henseleit buffer following contractile response to carbachol.

2.12 Statistical Analysis

Time-dependent changes in TEER were analysed using 2-way ANOVA, followed by a Bonferroni post-hoc test. The use of 2-way ANOVA was necessary owing to the presence of two independent variables; i.e. different drug treatments and the various individual time points studied (usually lasted up to 8 hours or 48 hours).

Dot blotting, Western blotting and data from the cytotoxicity studies were analysed by 1-way ANOVA followed by a Bonferroni post-hoc test. 1-way ANOVA was used in these studies to compare the changes in protein expression between more than two treatment groups at a fixed time point.

The present study solely employed Bonferroni correction to results that were earlier analysed with either 2-way or 1-way ANOVA. It is also worth noting that results that were detected to display ‘statistical significant differences’ following post-hoc Bonferroni were in agreement even when results were analysed using either 2-way or 1-way ANOVA analysis alone. Nonetheless, post-hoc Bonferroni test was conducted to reduce possibility for false-positive results (i.e. declaring statistical significant difference even when null hypothesis was true). Post-hoc Bonferroni is the preferred choice as it provides flexibility to allow multiple comparisons to be made within the same set of data. For example, post-hoc Bonferroni detects differences in TEER readings or protein expression between vehicle control and treated groups, as well as between two treated groups, at a specific time point.

Other post-hoc tests are not considered due to the following reasons; First, Dunnett’s test limits only to pairwise comparison with the control group. Hence, this restricts the option to compare results from two different treatment groups. For instance, whether a change in protein expression existed between cells treated with an enzyme

inhibitor alone and in the presence of a cannabinoid ligand (refer *Figure 4-6B* for an example). In addition, Tukey's test allows the comparison between means of a treatment and every other means of a different treatment group. This signifies that Tukey's test only takes account of a selected number of data, hence is undesirable in experiments with small sample sizes.

Student t-test is used for the analysis of Western blotting which involved the comparison between two treatment groups. For instance, to determine changes in the stimulation of intracellular signalling proteins (i.e. ERK1/2 and MYPT1) between cells treated with the cytokine TNF α alone and TNF α in the presence of a cannabinoid ligand.

Results of $P < 0.05$ were considered significant.

2. The Effects of Endocannabinoids on Human Bronchial Epithelial Permeability

3.1 Introduction

Broncheaveolar lavage in patients with allergic asthma demonstrated an elevated level of anandamide, which was suggested to have contributed to the pathogenesis of airway inflammation (Zoerner et al., 2011). However, little is known so far about the role of anandamide on the airway, especially on the epithelium structure. In comparison, there are no reports of the detection of 2-AG within the airway structures. A previous study in Caco-2 intestinal epithelial cells had demonstrated that both endogenous cannabinoids, anandamide and 2-AG, resulted in a decrease in transepithelial resistance, which was mediated through CB₁ receptor activation (Alhamoruni et al., 2010). Experiments presented in this chapter thus aimed to evaluate the effect of anandamide and 2-AG in mediating airway epithelial permeability, using Calu-3 bronchial epithelial cell line as an *in vitro* model. In addition to these findings, the study of the effects of endocannabinoids on the barrier function of airway epithelial structure could provide a clearer indication of whether the presence of these endogenous ligands can cause detrimental consequences or have potential therapeutic uses.

Mucins hypersecretion is one of the key pathological features in airway inflammatory diseases, such as asthma and COPD. Mainly the MUC5AC glycoprotein has been detected in healthy and diseased human expectoration (Thornton et al., 1996, Groneberg et al., 2002, Caramori et al., 2004), as well as normal and fully-differentiated bronchial epithelium (Gray et al., 2004a, Abdullah et

al., 2012). In addition to its housekeeping role in providing a chemical barrier on the bronchial epithelium during normal conditions, MUC5AC secretion is acutely responsive to environmental or chemical insults (Shao et al., 2004). Previous biochemical assays of bronchoalveolar lavage (BAL) in asthmatic subjects (Tillie-Leblond et al., 1999) revealed that the amount of MUC5AC glycoprotein detected was directly proportional to the expression of various pro-inflammatory mediators, including TNF α . Quantitative analysis of MUC5AC production is, thus, beneficial as an additional approach in identifying dysregulation of the bronchial epithelium physiology.

3.1.1 Aims

The aims of this study were:

1. To develop a reliable and robust protocol for epithelial permeability measurements using the bronchial epithelial cell line, Calu-3, cultured at an air-liquid interface (ALI) as an *in vitro* model of human epithelium.
2. To measure the effects of cytokines and various endocannabinoids (listed in *Table 3-1*) on trans-epithelial electrical resistance (TEER),
3. To determine the effects of endocannabinoids and the cytokine TNF α on mucin secretions in Calu-3 cells.

3.2 Materials and Methods

3.2.1 Materials

Materials used for cell culture are listed in *section 2.1.1*; TEER experiment in *section 2.1.2*; dot blotting and Western blotting in *section 2.1.4* with the list of primary and antibodies used in *section 2.1.5*.

3.2.2 Methods

TEER readings during the pilot studies (described in *section 2.5.1*) had failed to show any difference in TEER between the control and treated groups, as readings were unstable. This issue was rectified and the protocol was successfully optimised after changes were implemented according to *section 2.5.3*; which reduced temperature fluctuations during TEER recording. The rationale for the concentrations of the compounds used in TEER experiments is listed in *Table 3-1*.

Following TEER measurements, samples from these experiments were used for sample preparation for dot blotting studies to quantify MUC5AC expression (refer to *section 2.7.1*). This provided consistency in results for these parallel functional studies and reduced wastage of materials. Method for dot blotting studies is described in *section 2.7.2 and section 2.7.3*. Concentrations of the primary and secondary antibodies used are listed in *section 2.1.5*.

Compound	Concentration studied	Evidence on concentration studied	Notes on site(s) of action/ K_i or IC_{50} values relevant to studied concentration
2-arachidonoylglycerol (2-AG)	30 μ M	TEER decreased to approximately 40% with 2-AG (30 μ M) in Caco-2 intestinal epithelial cells (Alhamoruni et al., 2012).	An endocannabinoid. Metabolised by MAGL to arachidonic acid (Nomura et al., 2008). Affinity for $CB_1R > CB_2R$ / K_i (CB_1R) > 10 μ M in low detectable CB_1R efficacy model, human neocortical (Steffens et al., 2005).
AM251	100 nM	Inhibition of THC-mediated effects in maintaining Caco-2 intestinal epithelial cell permeability with AM251 (100 nM) (Alhamoruni et al., 2010).	CB_1R (antagonist)/ K_i value (CB_1R): 7.5 nM. K_i value (CB_2R): 2290 nM (Pertwee, 2010).

Anandamide	30 μ M	TEER decreased to approximately 40% with anandamide (30 μ M) in Caco-2 intestinal epithelial cells (Alhamoruni et al., 2012).	An endocannabinoid. Metabolised by FAAH to arachidonic acid (Maccarrone et al., 1998). Affinity for CB ₁ R > CB ₂ R / K _i (CB ₁ R): 61 to 543 nM. K _i (CB ₂ R): 579 to 1940 nM (Pertwee, 2010).
Arachidonic acid	30 μ M	Concentration of 30 μ M was chosen assuming anandamide (30 μ M) were converted to arachidonic acid.	Not applicable
EDTA	1 mM	Chelating agent for Ca ²⁺ . EDTA (1 mM) was used as a positive control in Calu-3 cells – induced significant decrease in TEER by approximately 50% (Petecchia et al., 2012).	Not applicable

Indometacin	10 μ M	Indometacin (at concentration up to 20 μ M) prevented IL-1 β induced increase in mucin secretion in primary bronchial epithelial cells, which was mediated by COX-2 enzymes (Gray et al., 2004b).	IC ₅₀ value for COX in A549 alveolar epithelial cells: was approximately 13 nM. COX-2 to COX-1 selectivity was shown to be 1.9-fold (Range et al., 2000).
Nordihydroguaiaretic acid (NDGA)	10 μ M	NDGA (10 μ M) was shown to inhibit IL-4-induced cell apoptosis in A549 alveolar epithelial cells (Shankaranarayanan and Nigam, 2003).	IC ₅₀ value was approximately 2.6 to 11 μ M for 12- and 15-LOX1 and 15-LOX2 derived from human prostrate epithelial cells (Vasquez-Martinez et al., 2007).
SR144528	1 μ M	SRR144528 (1 μ M) prevented the increase in cAMP levels induced by the selective CB ₂ R agonist, JWH133 in CHO cells (Taylor et al., 2015). Its effect on epithelial permeability is still unknown.	CB ₂ R (antagonist)/ K _i (CB ₁ R):70 nM. K _i (CB ₂ R):0.6 nM expressed in cloned human CB ₂ R on CHO cells (Rinaldi-Carmona et al., 1998).

TNF α	10 ng/ml	<p>Dose-response studies in Caco-2 epithelial cells showed that TNFα (10 ng/ml) was the lowest, most effective dose in causing significant decreases in the transepithelial resistance (to approximately 60%) (Ma et al., 2004).</p> <p>TNFα (10 ng/ml) induced 50% drop in TEER in Calu-3 bronchial epithelial cells, compared to untreated cells (Peticchia et al., 2012).</p>	Not applicable
URB597	1 μ M	URB597 (1 μ M) prevented anandamide-induced cell death which indicated the presence of FAAH activity in rat hepatocyte cells (Siegmund et al., 2006).	IC ₅₀ value was approximately 5 nM in FAAH enzymes derived from the rat brain (Piomelli et al., 2006).

Table 3-1 List of the drugs used in this chapter and the rationales for the concentrations used.

3.2.3 Statistical Analysis

Data are presented as the mean \pm standard error of mean (S.E.M). Western blotting data were analysed by 1-way ANOVA followed by a Bonferroni post-hoc test. Alternatively, Western blotting analysis to detect differences in fold change of a specific protein expression between two treatment group at a fixed time point were compared using paired, Student's t-test. Results of $P < 0.05$ were considered significant.

3.3 Results

3.3.1 Pilot Experiments

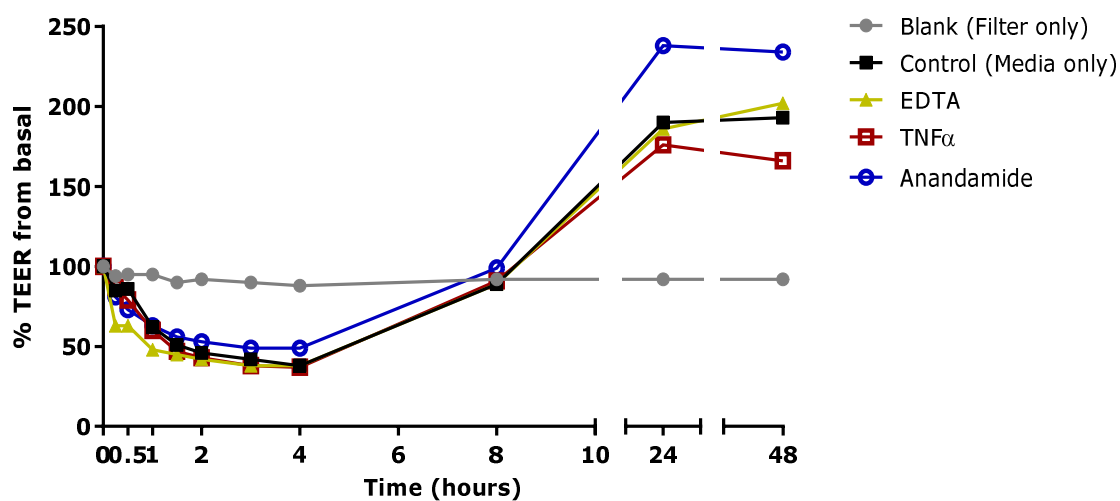


Figure 3-1 Effects of apical administration of EDTA (1 mM), TNF α (10 ng/mL) and anandamide (10 μ M) on 21-day old Calu-3 cells grown at ALI. Data are reported as means of TEER expressed as percentage of basal level of individual Transwells[®] measured in triplicate. (n=1).

A reduction in TEER levels over 4 hours was seen in Calu-3 cells exposed to EDTA, TNF α or anandamide added onto the cells' apical side. However, a similar decrease was seen in control cells which were exposed to media only on the apical side.

3.3.2 Optimisation of TEER Measurement Protocol

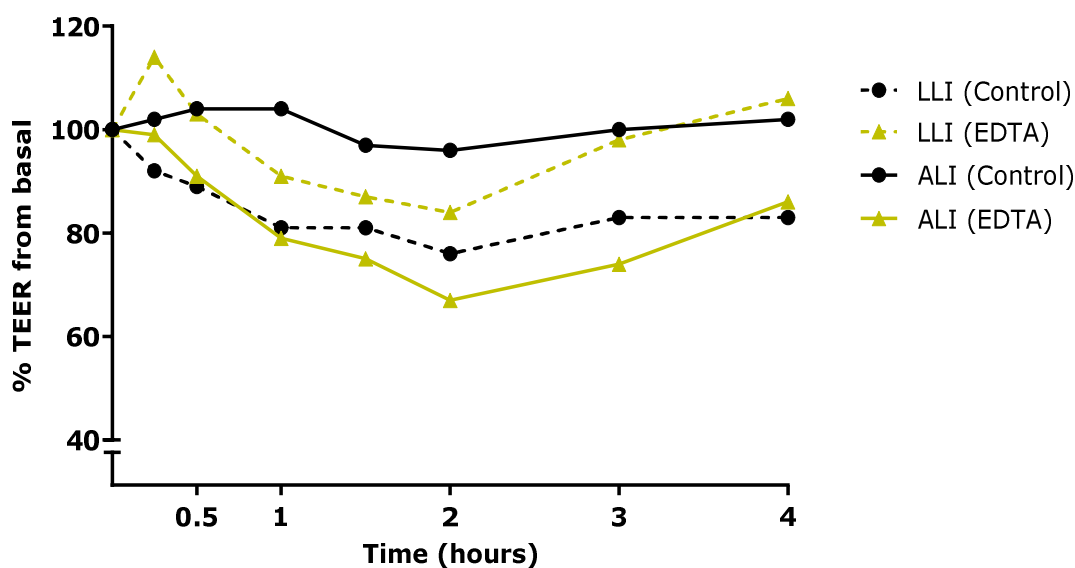


Figure 3-2 Time-related responses to control (no drug) and EDTA (1 mM) when TEER readings were measured on a hot plate warmed to 37°C at either LLI or ALI, $n=1$. Data are reported as means of TEER changes of individual Transwell® measured in triplicate. ($n=1$).

In this experiment, it was tested whether the addition of medium to the apical side and leaving it in the Transwells® for the entire duration of TEER measurements would result in an initial drop in TEER in the control cells as seen in *Figure 3-1*. *Figure 3-2* shows a reduction in TEER readings when cells were continuously exposed to liquid on the apical side (LLI (Control)). In comparison, cells kept at ALI, except for the brief period of TEER measurements, showed no significant changes in TEER (ALI (Control)) and an evident decrease in TEER in the presence of EDTA. These data indicate that addition of media to the apical side of the cells results in a drop in TEER levels. Therefore, in subsequent experiments, ALI was maintained and drugs applied to the basolateral side.

3.3.3 The Impact of Disrupted Bronchial Epithelial Barrier on TEER Measurement by EDTA

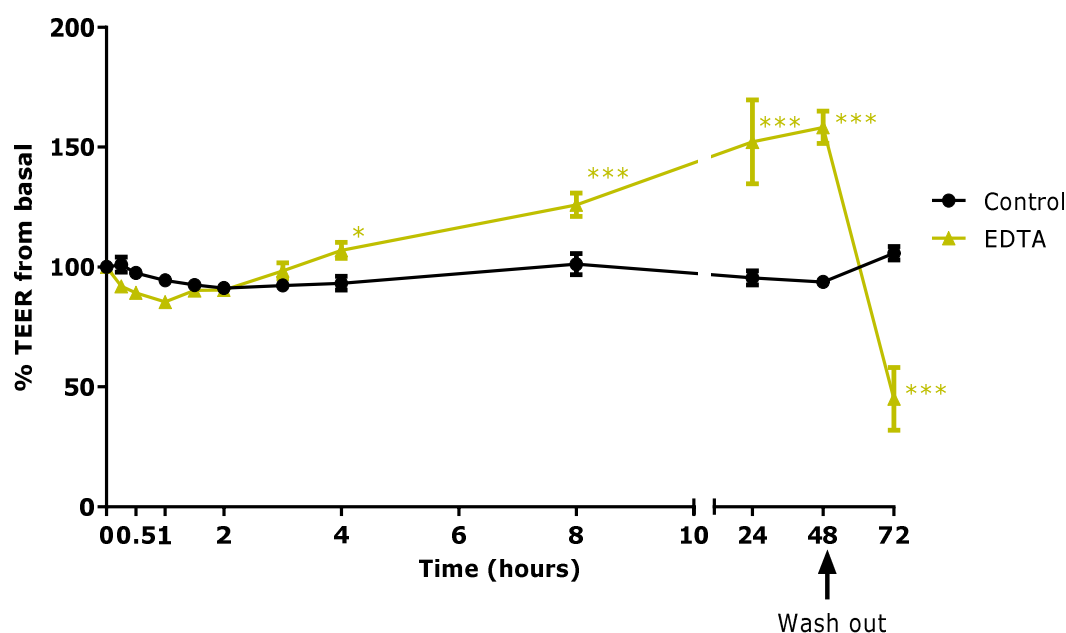


Figure 3-3 TEER changes following basolateral application of a positive control, EDTA (1 mM) with that of control (untreated). Calu-3 cells were cultured for 21-days at ALI. Data are expressed as percentage TEER by calculating the relative change in resistance at various time points from basal reading, and are presented as mean \pm SEM; $n=5$, * $P<0.05$, ** $P<0.01$, *** $P<0.001$, 2way ANOVA followed by a Bonferroni post-hoc test, compared to control.

Figure 3-3 shows that the TEER values of the untreated (control) cells were maintained throughout the duration of assay when experiments were repeated in the ALI condition. Treatment with a chelating agent, EDTA (1 mM) was included as a positive control to induce increased permeability across the Calu-3 cells layer. An initial decrease up to an hour was observed in cells treated with EDTA (1 mM), followed by an unanticipated increase in TEER.

3.3.4 Alterations in Bronchial Epithelial Cell Permeability following Basolateral Application of the Endocannabinoids or TNF α

Consistent TEER readings were seen in vehicle controls which only fluctuated between $91 \pm 9.2\%$ and $101 \pm 8.5\%$ (*Figure 3-4A*). Both TNF α (10 ng/mL) and anandamide (30 μ M) showed significant decreases in TEER from their basal values and these were maintained for 48 hours. Reduction in TEER with TNF α was observed at an earlier time point, 1.5 hours, compared to anandamide at 4 hours. It is also noted that TNF α produced a greater drop in TEER than anandamide. Removal of the drugs from the cells allowed TEER recovery which was evident at the 72 hour point.

In comparison, basolateral administration of the endocannabinoid 2-AG (30 μ M) or methanandamide (100 nM), a stable analogue of anandamide, (see *Figure 3-4B*) had no effect on the control responses.

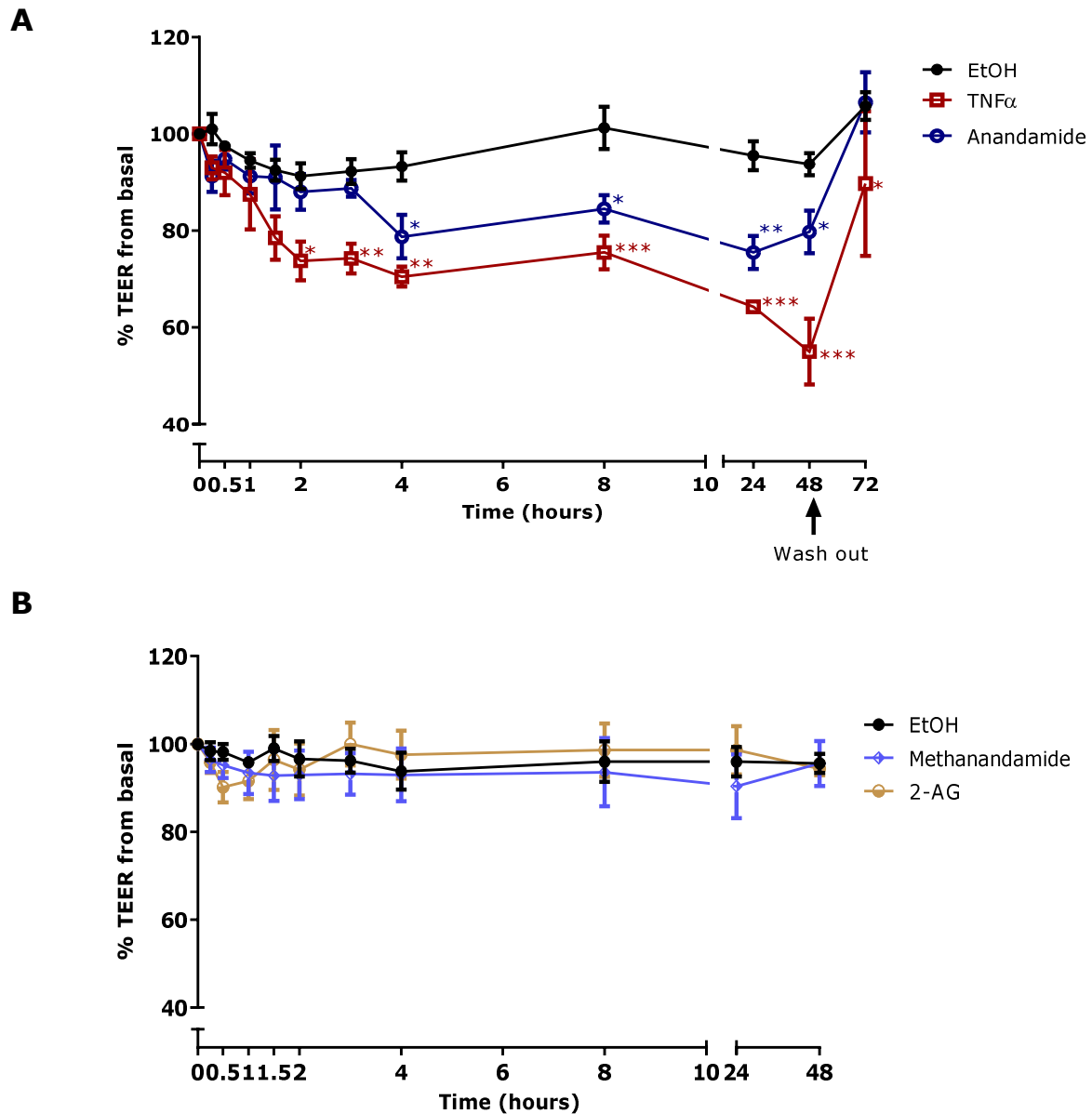


Figure 3-4 A. Effects of basolateral application of TNF_{α} (10 ng/mL), anandamide (30 μ M); **B.** 2-AG (30 μ M) or methanandamide (100 nM) onto 21-day old Calu-3 cells cultured at ALI. Data are expressed as percentage TEER by calculating the relative change in resistance at various time points from basal reading, and are presented as mean \pm SEM; $n=3-5$, $*P<0.05$, $**P<0.01$, $***P<0.001$, 2way ANOVA followed by a Bonferroni post-hoc test, compared to vehicle control (0.3%v/v) EtOH.

3.3.5 Interaction of Endocannabinoids with the Cytokine, TNF α

Stable TEER readings were observed for both vehicle controls, (0.3% v/v) EtOH (*Figure 3-5A*) and (0.1% v/v) EtOH (*Figure 3-5B*) throughout the whole duration of the experiment. TNF α (10ng/mL) also provoked reproducibly decreased TEER throughout 48 hours in both sets of experiments.

The application of the endocannabinoids, anandamide (30 μ M) or 2-AG (30 μ M) in the presence of TNF α (10 ng/mL) did not cause any changes to the magnitude of TNF α -induced TEER reduction (*Figure 3-5A*).

As previously shown in *Figure 3-4B*, TEER of cells treated with methanandamide (100 nM) alone did not significantly differ compared to vehicle control (0.1% v/v EtOH). Interestingly, TEER recorded from the combination treatment of methanandamide and TNF α were generally similar to TNF α -treated cells, except briefly between 4 and 5 hours when a modest reduction was seen ($P<0.01$) (*Figure 3-5B*).

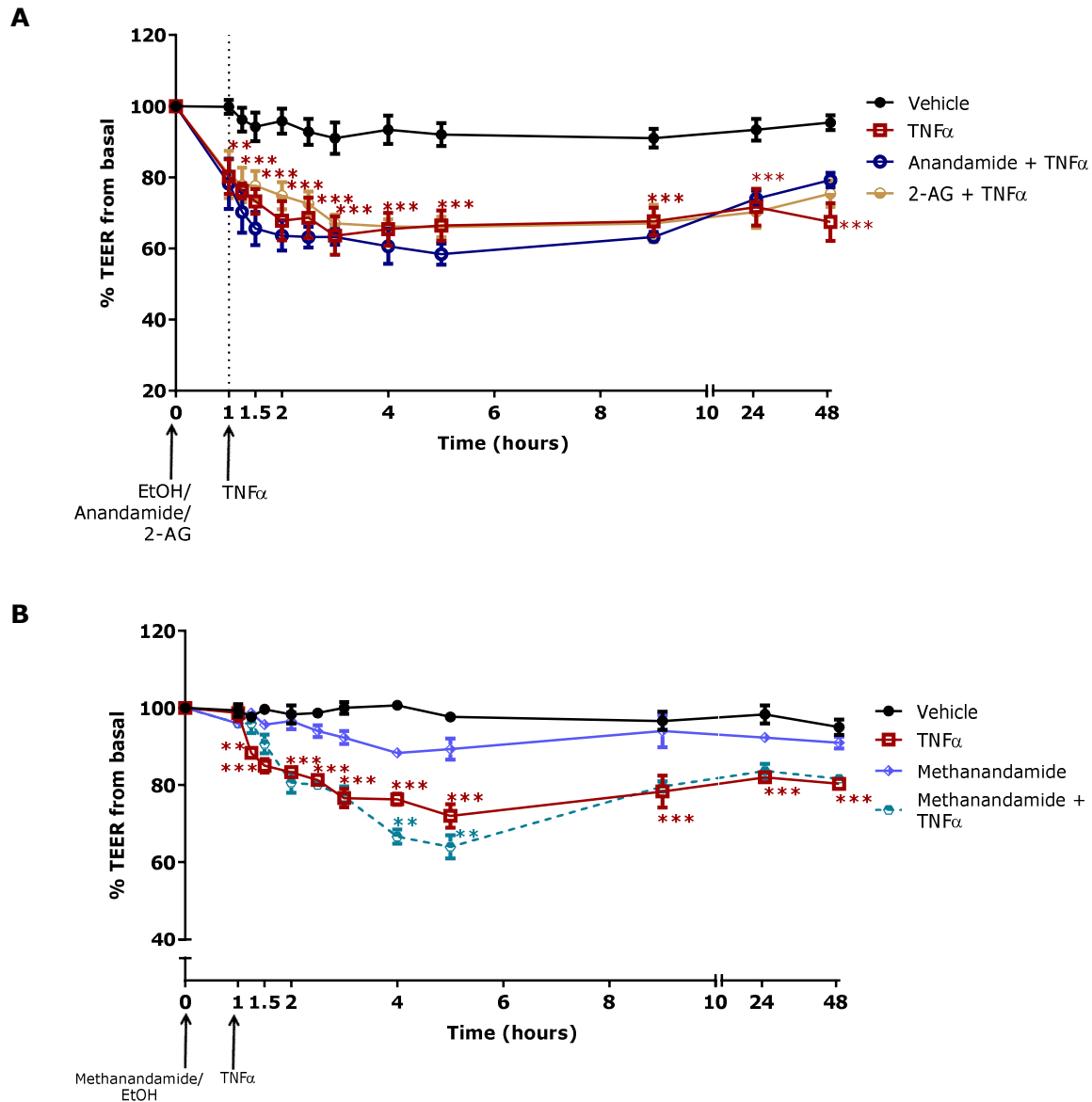


Figure 3-5 Effects of basolateral application of **A.** anandamide (30 μ M) or 2-AG (30 μ M); **B.** methanandamide (100 nM) in the presence of TNF α (10 ng/mL) onto 21-day old Calu-3 cells cultured in ALI. Data are expressed as percentage TEER by calculating the relative change in resistance at various time points from basal reading, and are presented as mean \pm SEM; $n=3$, * $P<0.05$, ** $P<0.01$, *** $P<0.001$, 2way ANOVA followed by a Bonferroni post-hoc test, compared to TNF α (10ng/mL); except **A.** TNF α which is compared to vehicle control, (0.3% v/v) EtOH; **B.** TNF α and methanandamide which is compared to vehicle control, (0.01% v/v) EtOH.

3.3.6 Cannabinoid Receptor Antagonists Did Not Alter Anandamide-induced Increased Permeability

Figure 3-6 shows that TEER for vehicle control (0.31% v/v EtOH) treatment were generally consistent, although there was an initial decrease from basal which might be due to the presence of EtOH. Neither AM251 (100 nM) nor SR144528 (1 μ M) had any effect on anandamide-induced TEER reduction.

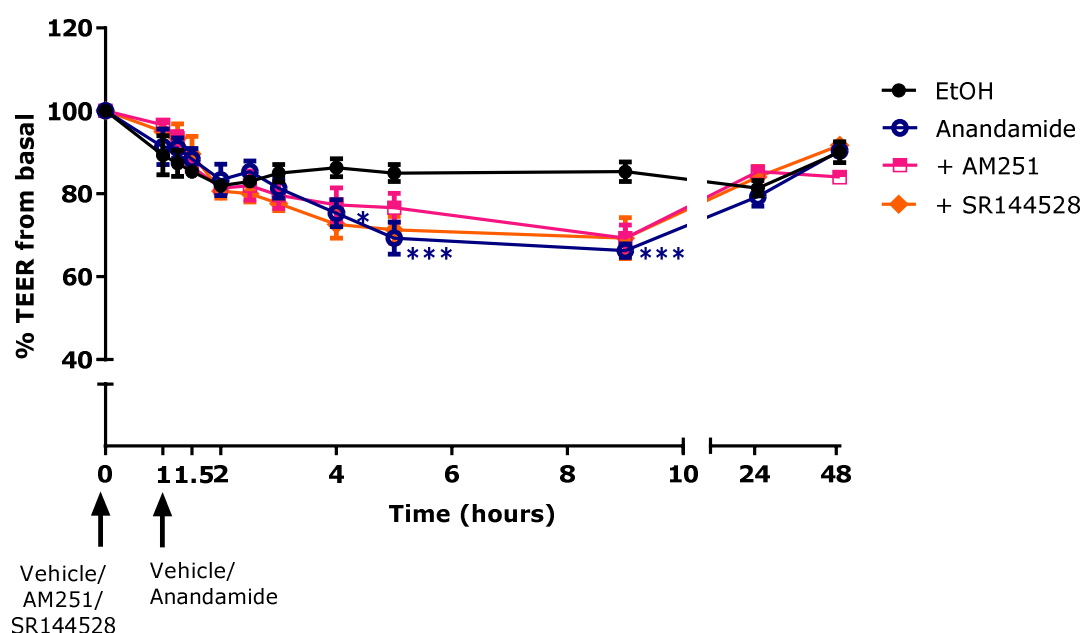


Figure 3-6 Effects of basolateral application of the selective CB_1 antagonist, AM 251 (100 nM) or the selective CB_2 antagonist, SR144528 (1 μ M) in the presence of anandamide (30 μ M). Data are expressed as percentage TEER by calculating the relative change in resistance at various time points from basal reading, and are presented as mean \pm SEM; $n=3$, * $P<0.05$, ** $P<0.01$, *** $P<0.001$, 2way ANOVA followed by a Bonferroni post-hoc test, compared to anandamide (30 μ M), except for anandamide, which is compared to vehicle control (0.31% v/v) EtOH.

3.3.7 Inhibitors of Enzymes FAAH, and Combined COX and LOX Inhibition Prevents Anandamide-Induced Increased Permeability

Previous studies have shown that FAAH selectively hydrolyse anandamide to arachidonic acid in various systems such as the porcine and rat brain preparations, as well as human neuroblastoma (NI8TG2) cells [review by (Blankman and Cravatt, 2013)]. Hence, the present study aimed to investigate the involvement of FAAH enzyme in anandamide-mediated response in Calu-3 bronchial epithelial cell line. *Figure 3-7* shows that pre-incubation with the FAAH enzyme inhibitor URB597 (1 μ M) alone had no effect on the control responses. In comparison, TEER for a combination of vehicle controls (0.3% v/v EtOH) and (0.1% v/v DMSO) (*Figure 3-8A*) were fairly consistent over the first 8 hours. However, a drop in resistance was observed at 24 and 48 hours which was probably due to the presence of DMSO (the vehicle control for URB597). Anandamide again caused a significant drop in TEER which was prevented by pre-incubation with URB597.

In addition to FAAH, anandamide is also a substrate for the COX and LOX enzymes which either directly metabolise anandamide into arachidonic acid or further metabolise arachidonic acid into various other active metabolites (Kozak et al., 2002a). Thus, this study aimed to investigate the role of COX and LOX in anandamide-induced increase in epithelial permeability. Vehicle control showed an initial drop in TEER which was likely due to the effect of EtOH (*Figure 3-8A*). Cells treated with anandamide displayed reproducible TEER reduction which persisted for 48 hours. Interestingly, individual administration of either

the COX inhibitor, indometacin (10 μ M) or the LOX inhibitor, NDGA (10 μ M) did not prevent TEER reduction associated with anandamide.

As URB prevented the decrease in TEER caused by anandamide, the effect of the anandamide metabolite on TEER was determined. The experiment shown in *Figure 3-8B* was terminated at 8 hours as a higher concentration (0.4% v/v) of EtOH caused monolayer perforation, resulting in a rapid drop in resistance. TEER readings for vehicle control up to 8 hours were still maintained, ranging between $85 \pm 9.2\%$ and $99 \pm 9.8\%$. Similar to that seen with anandamide, arachidonic acid alone significantly reduced TEER, an effect which lasted for the whole duration of the experiment. Combination treatment with indometacin and NDGA fully inhibited TEER reduction associated with both anandamide and arachidonic acid.

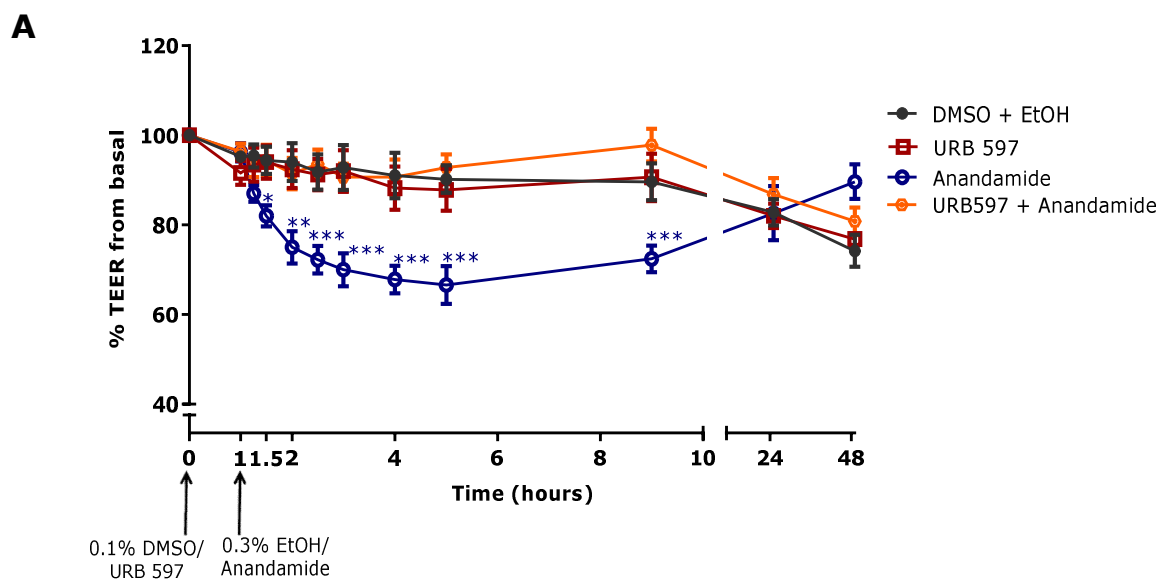


Figure 3-7 Effects of basolateral application of the selective inhibitor of FAAH, URB597 ($1\ \mu\text{M}$) in the absence and presence of anandamide ($30\ \mu\text{M}$). Data are expressed as percentage TEER by calculating the relative change in resistance at various time points from basal reading, and are presented as mean \pm SEM ($n=5$); * $P<0.05$, ** $P<0.01$, *** $P<0.001$, 2way ANOVA followed by a Bonferroni post-hoc test, compared to anandamide ($30\ \mu\text{M}$); except anandamide, which is compared to respective vehicle control, (0.3% v/v) EtOH + (0.1% v/v) DMSO.

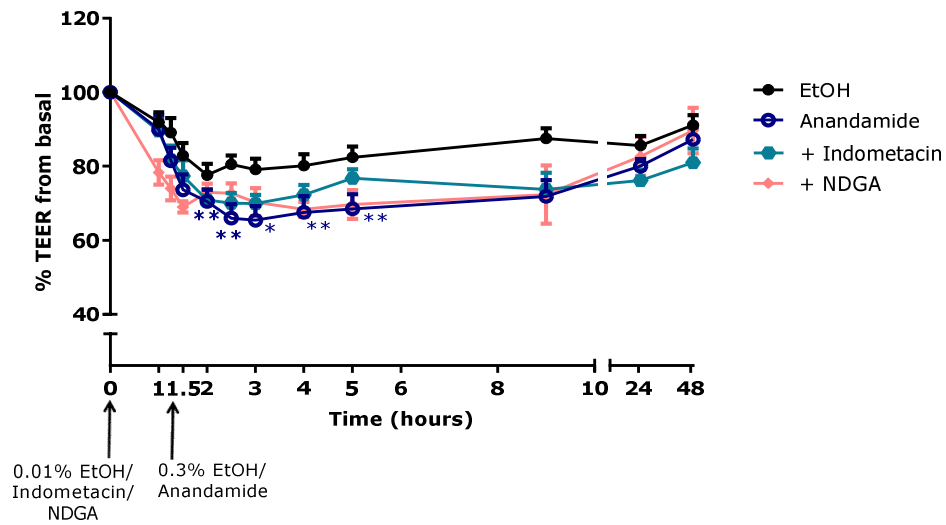
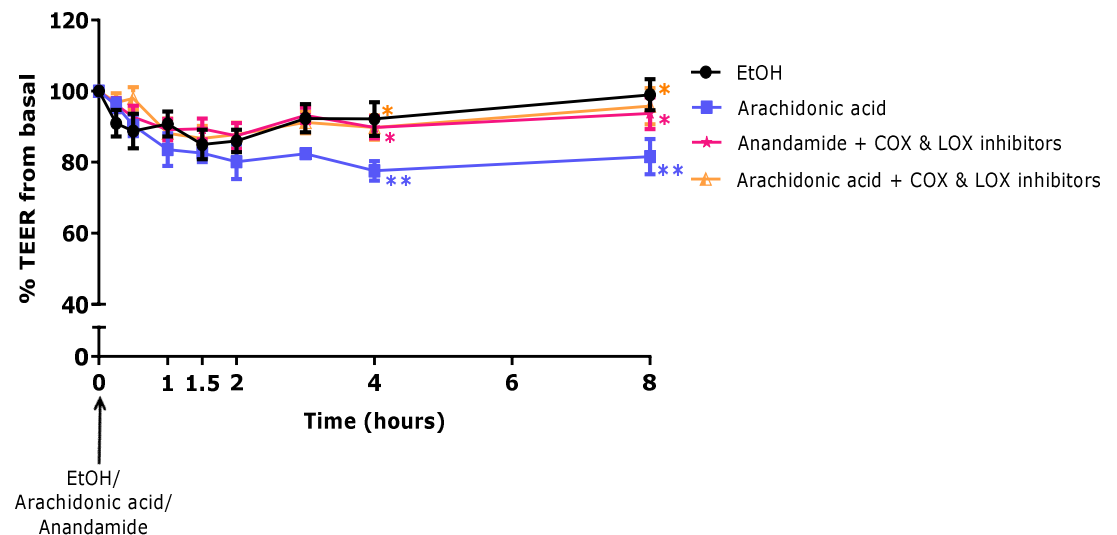
A**B**

Figure 3-8 Effects of basolateral application of the selective inhibitor of **A.** COX inhibitor, indometacin ($10\ \mu\text{M}$) or LOX inhibitor, NDGA ($10\ \mu\text{M}$) in the presence of anandamide ($30\ \mu\text{M}$); **B.** Combined application of COX inhibitor, indometacin ($10\ \mu\text{M}$) and LOX inhibitor, NDGA ($10\ \mu\text{M}$) in the presence of anandamide ($30\ \mu\text{M}$) or arachidonic acid ($30\ \mu\text{M}$). Data are expressed as percentage TEER by calculating the relative change in resistance at various time points from basal reading, and are presented as mean \pm SEM ($n=5-6$); $*P<0.05$, $**P<0.01$, $***P<0.001$, 2way ANOVA followed by a Bonferroni post-hoc test, compared to anandamide ($30\ \mu\text{M}$); except anandamide, which is compared to respective vehicle control **A.** (0.31% v/v) EtOH, **B.** (0.4% v/v) EtOH

3.3.8 MUC5AC Protein Expression following Treatment with Anandamide and the Cytokine, TNF α

Protein expression of MUC5AC was investigated in dot blot studies. Drugs were administered into the basolateral compartment of the Transwells[®] for a total duration of 48 hours. Samples were collected following the completion of TEER experiments. Note that control represents untreated Calu-3 cells.

The data presented in *Figure 3-9A* reveals that cells treated with TNF α alone showed significant increase in MUC5AC expression level compared to the untreated (control) group. MUC5AC glycoprotein expression was also increased in cells treated with anandamide alone. However, results were not significantly different compared to its vehicle control, as (0.3% (v/v)) ethanol was shown to modestly stimulate MUC5AC expression. An example of the dot blot image shows clear signals for the expression of MUC5AC protein (*Figure 3-9B*).

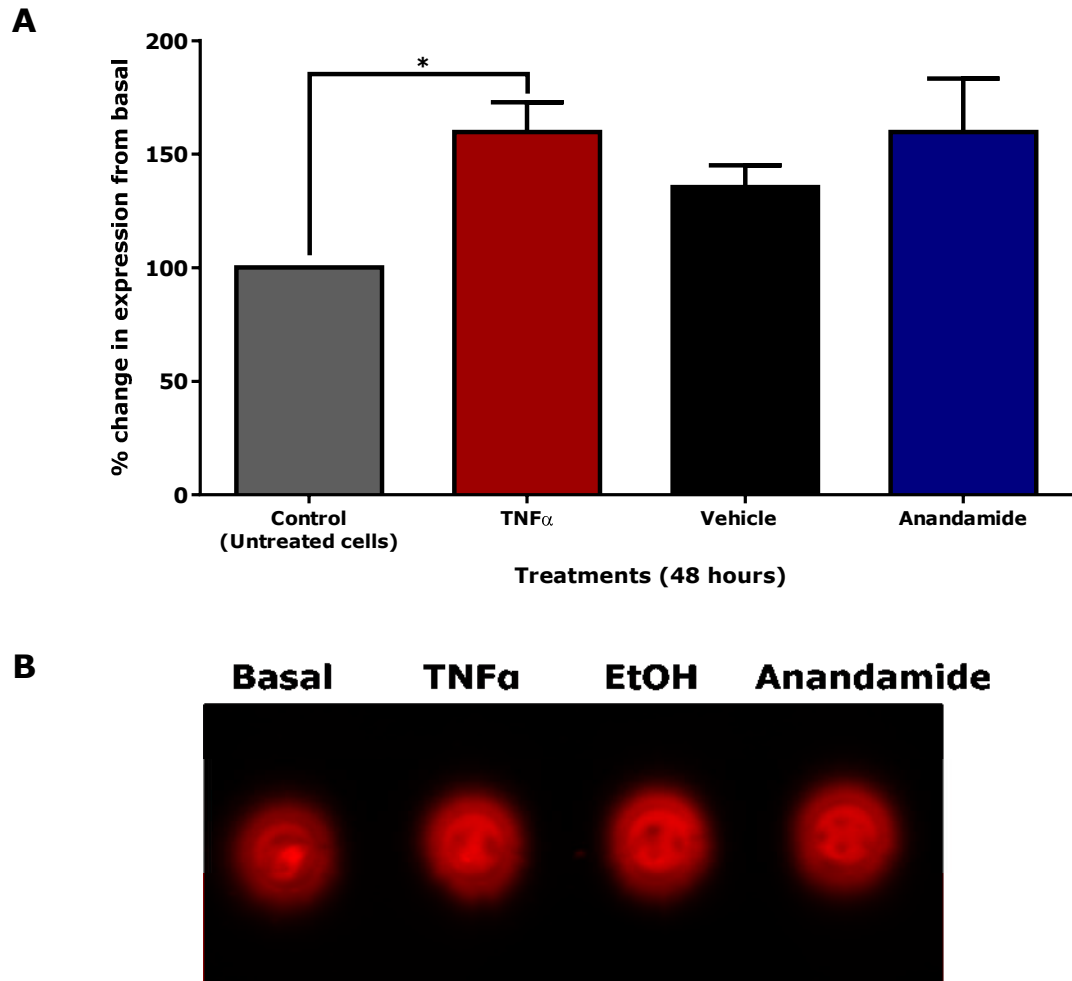


Figure 3-9 A. Fluorescence intensity quantification for MUC5AC expression following treatments of TNF α (10ng/mL), 0.3(v/v) EtOH or anandamide (30 μ M) on Day 21 Calu-3 epithelial cells cultured at ALI. Data are expressed as percentage change of fluorescence intensity and are presented as mean \pm SEM (n=6); *P<0.05, 1way ANOVA followed by a Bonferroni post-hoc test. TNF α -treated cells were compared to control (untreated), whereas anandamide was compared to vehicle control; **B.** Fluorescence signals for MUC5AC protein expression were detected using dot blotting technique.

3.4 Discussion

Calu-3 cells have previously been shown as a robust *in vitro* model to detect changes in cell permeability due to the development of tight junctions when cultured and maintained at ALI (Wan et al., 2000, Stewart et al., 2011). Results obtained from the TEER experiments in this study confirmed the usefulness of Calu-3 cells as a pharmacological screening tool based on the changes in permeability following drug treatments. The optimised TEER protocol in the present study revealed that treatment with the cytokine TNF α caused reproducible increases in Calu-3 epithelial cell permeability, which was consistent with the data shown in other studies (Coyne et al., 2002, Petecchia et al., 2012). Similarly, the endogenous cannabinoid anandamide also promotes epithelial leakiness in Calu-3 cells which effect was found to be independent of cannabinoid receptors activation, but mediated through its metabolite, arachidonic acid instead.

During the initial stages of TEER protocol development, drugs were initially administered to the apical compartment of Transwells[®] (Figure 3-1) in order to simulate the exposure to noxious stimuli from the environment. However, leaving the medium on the apical side represents a change in the culture condition from ALI to LLI, which led to a decrease in TEER, even in non-treated controls.

The need for repetitive removal of the apical medium for TEER measurement also posed an additional challenge to drug application. *In vitro* experiments involving human airway epithelial cells have generally administered drugs onto the apical side as, allergens or drugs are more commonly exposed to lung tissue through inhalation (Coyne et al., 2002, Petecchia et al., 2012). Nevertheless, all drugs were applied basolaterally in this project to ensure that steady TEER readings were obtained. The

experiments then model the exposure of drugs delivered to the bronchial epithelium systemically.

All TEER experiments were conducted by placing Transwells[®] plates on a 37°C heating block to minimise temperature fluctuations that were previously shown to distort TEER readings (*Figure 3-1*). The DMEM F12-Ham's medium used contains a buffering agent, 15 mM 4-(2-hydroxyethyl)-1-piperazineethanesulfonic acid (HEPES), that effectively conserves the physiological pH when placing the cells onto a heating block during TEER measurement (Baicu and Taylor, 2002).

The use of the chelating agent, EDTA (1 mM) as a positive control for TEER experiments was supported by evidence from experiments involving bronchial and intestinal epithelial cells which showed robustly reduced barrier integrity (Kibangou et al., 2008, Petecchia et al., 2012). A previous study on the effect of EDTA on epithelial tight junctions revealed that chelation of ions such as Ca^{2+} and Mg^{2+} from the medium caused immediate disruption of tight junctions attributable to dissociation of their protein complexes including zona-occludens-1 (ZO-1) and occludin (Klingler et al., 2000). The apparent TEER fluctuations observed for the response of Calu-3 cells to EDTA (*Figure 3-3*) could be due to earlier chelation of ions from the medium that subsequently disrupted the tight junction proteins making the epithelial layer leaky. It is possible that TEER readings were increased afterwards because metal-EDTA complexes that formed on the basolateral side reversibly clogged the pores of the Transwells[®] filters, producing an artefactual increase in resistance. This observation fits with the hypothesis made by Klingler *et al*, as removal of these complexes following washout immediately disrupted the cell monolayer. An increase in TEER following the addition of EDTA has never been reported in the literature as most previous experiments using various epithelial cell

models EDTA applied onto the apical side or for a much shorter duration of up to 2 hours (Tomita et al., 1996, Wang et al., 2000, Petecchia et al., 2012).

Ethanol was frequently used as the vehicle control in the present study to solubilise lipophilic compounds such as anandamide, indometacin and NDGA. However, the presence of ethanol at high concentrations was thought to exert detrimental effects on epithelial permeability. A study in primary human bronchial epithelial cells and BEAS2B bronchial epithelial cell line revealed that ethanol administered at 20, 50 or 100 mM caused a concentration-dependent decrease in transepithelial resistance (Simet et al., 2012). In the present study, similar phenomenon was observed especially in vehicle controls containing more than (0.3% (v/v)) ethanol (i.e. more than 52 mM) which TEER readings reduced to a minimum point of approximately 80% (for example, *Figure 3-6* and *Figure 3-8A&B*). Despite the ethanol-induced TEER decrease, the effects between vehicle control group (which contain ethanol) and other treatments groups were still distinguishable.

Levels of the endogenous cannabinoid, anandamide are raised in the bronchioles of patients with asthma (Zoerner et al., 2011), suggesting that the endocannabinoid may be involved in the inflammatory response. Inflammation in the airways increases bronchial epithelial permeability [review by (Lambrecht and Hammad, 2012)] leading to a reduction in epithelial barrier function. Similarly, the cytokine TNF α and anandamide have previously been shown to be present at elevated levels in the BALF of asthmatic and COPD patients (Rouhani et al., 2005, Iwamoto et al., 2014), which were thought to have contributed to the loss of bronchial epithelium barrier function. Although there are currently limited data on anandamide, the effect of TNF α on the epithelium structure has been extensively investigated in various *in vitro* experiments using Calu-3 or primary human bronchial epithelial cells (HBECS).

Published data indicate the association of bronchial epithelium disruption with decreased TEER when stimulated with TNF α (10 ng/mL) for up to 72 hours (Coyne et al., 2002, Petecchia et al., 2012) when the cytokine was administered into the apical side of the Transwells[®]. However, one study reported similar observations when TNF α (10 ng/mL) was applied to the basolateral side of primary human bronchial epithelial cells (Hardyman et al., 2013). Hence, this revealed a consistent effect of TNF α on bronchial epithelial permeability, regardless of the site of treatment within the Transwell[®].

Arguably, detection of the endocannabinoid anandamide in asthmatic bronchoalveolar lavage fluid reported by Zoerner *et al* (2011) also indicates an apical (i.e. luminal) site of action. The anandamide precursor, NAPE, was reported to be present at higher levels during airway inflammatory state (Calignano et al., 2000). Unless hydrolysed by oxidising enzymes such as fatty acid amide hydrolase (FAAH), anandamide binds to albumin in the culture medium, which further enhances its hydrophobicity (Bojesen and Hansen, 2003) potentially assisting internalisation through the cell membrane. It is, however, beyond the scope of this project to determine the mechanism of transport of anandamide in epithelial cells in detail.

The fall in transepithelial resistance as a consequence of basolateral application of TNF α or anandamide alone (*Figure 3-4A*) was an indication of increased bronchial epithelial permeability. *Figure 3-4A* showed consistent observation with that from previous *in vitro* studies by Coyne *et al* (2002) and Petecchia *et al* (2012), as exposure to TNF α on Calu-3 bronchial epithelial cells caused a similar TEER reduction. Similar investigation of the effect of anandamide and TNF α on tight junction protein expression in this study will be presented in *chapter 4*. Combined

treatment with anandamide and TNF α showed no cumulative fall in TEER (*Figure 3-5A*). Hence, the finding suggests that the presence of anandamide does not cause any additional effect to TNF α -induced increase in bronchial epithelial leakiness. However, this is the first time that anandamide has been shown to alter airway epithelial cell permeability. Recovery of TEER after the removal of these drugs shown in *Figure 3-4A* indicate that the effects of anandamide and TNF α on Calu-3 epithelial cell permeability were reversible. Therefore, this suggests that the endocannabinoid anandamide, in this context, behaves as a pro-inflammatory mediator similar to the cytokine, TNF α . Thus, this indicates that the overproduction of anandamide as observed in patients with allergic asthma (Zoerner et al., 2011) could subsequently lead to disruption of the bronchial epithelial barrier function.

Interestingly, basolateral administration of the endocannabinoid 2-AG did not cause any significant change in TEER (*Figure 3-4B*). Neither did 2-AG prevent or enhance TNF α -induced increased epithelial permeability (*Figure 3-5A*). Unlike anandamide, this study shows that 2-AG does not appear to have any direct role in controlling bronchial epithelium permeability. 2-AG could, however, have other roles in airway diseases and an *in vitro* study using EoL-1 cells, a human eosinophilic cell line, demonstrated that 2-AG acts as a chemotactic agent through CB₂ receptor activation (Oka et al., 2004). The latter investigators thus concluded that 2-AG affects the immune response by promoting the migration of eosinophils to the sites of inflammation and postulated that inhibiting the action of 2-AG would be beneficial in attenuating airway inflammation. Therefore, this highlights one of the limitations in the TEER experiment due to the absence of leukocytes in the isolated, bronchial epithelial *in vitro* model used in our study. The addition of leukocytes onto T84 intestinal epithelial cell line was shown to enhance cell permeability due to the

increased production of various cytokines, such as IL-4, IL-10 and interferon- γ (IFN γ) (Colgan et al., 1993). However, the mechanism of tight junction disruption induced by these cytokines was not studied by the investigators. A recent study has also ruled out any effect of 2-AG on the bronchial tone as it failed to reverse acetylcholine-induced bronchoconstriction *in vitro* using normal human bronchi (Grassin-Delye et al., 2014).

The addition of a 2-methyl group to the anandamide structure yields a stable analogue, methanandamide (refer *Figure 1-7* of *section 1.11.1* for chemical structure). This modification significantly increases the availability of the compound *in vitro* as methanandamide is resistant to enzymatic hydrolysis, mainly via FAAH, to which endocannabinoids are subject (Abadji et al., 1994). This explains the methanandamide concentration (100 nM) used in the present experiments, which is considerably lower than that employed for other endocannabinoids (30 μ M) which are FAAH substrates. Interestingly, methanandamide had no effect on bronchial epithelial permeability (*Figure 3-4B*), contrasting with the reduction seen with anandamide. Furthermore methanandamide had no effect on the TNF α -induced decrease in TEER (*Figure 3-5B*).

The involvement of CB₁ and CB₂ receptors in the anandamide-mediated effect was evaluated using CB₁ receptor antagonist, AM251 and CB₂ antagonist, SR144528 respectively. In a previous study using mouse brain, AM251 displayed 300-fold affinity to the CB₁ over the CB₂ receptor (Gatley et al., 1996). In addition, concentration-response studies in Caco-2 epithelial cells revealed that treatment with AM251 at 100 nM was sufficient to antagonise the anandamide and 2-AG- induced colonic epithelial permeability, whilst devoid of its own effect on mediating the epithelial permeability (Alhamoruni et al., 2010). The CB₂ receptor antagonist

SR144528, on the other hand has an affinity for the CB₂ receptor at low nanomolar range with an inhibitor constant (K_i) value of 0.28 nM, compared to CB₁ (K_i of approximately 70 nM) (Rinaldi-Carmona et al., 1998). Within the same study, SR144528 at 1 μ M (or up to 10 μ M) was shown to completely selectively block CB₂-mediated cAMP activation in transfected CHO cells. Hence, competitive antagonism experiment conducted in the present study employed AM251 at a concentration of 100 nM and SR144528 at 1 μ M to demonstrate selective antagonistic activity in CB₁ and CB₂ receptors expressed in Calu-3 cells. Results from the TEER experiment shown in *Figure 3-6* revealed that the effect of anandamide-induced effect was unaffected despite the presence of CB₁ receptor antagonist, AM251 or CB₂ receptor antagonist, SR144528. However, it is noted that the response of Calu-3 epithelial cell permeability to either AM251 or SR144528 was overlooked, hence such effect will be investigated in future experiments. Taken together with the lack of effect of the stable analogue methanandamide, this suggests that anandamide-induced TEER reduction may be mediated by a metabolite with no effect on CB₁ or CB₂ receptors. The present data contrast with those generated in experiments investigating the intestinal epithelium, as activation of CB₁ receptors by methanandamide is reported to increase intestinal permeability (Alhamoruni et al., 2012). Similarly, the endogenous cannabinoid, 2-AG was shown to decrease Caco-2 intestinal epithelial permeability (Alhamoruni et al., 2010) but showed no effect in the present study in Calu-3 cells.

The presence of the FAAH enzyme inhibitor URB597 alone did not affect Calu-3 cell epithelial permeability, but prevented the fall in TEER following basolateral application of anandamide (*Figure 3-8A*). This implies that the reduction in TEER is mediated by a metabolite of anandamide, possibly arachidonic acid, which is widely

known for its role in inducing inflammatory responses via downstream metabolites such as prostaglandins and leukotrienes. Previous work by Cravatt *et al* demonstrated the hydrolysis of anandamide, a fatty acid amide, to arachidonic acid by FAAH isolated from solubilised plasma membranes of rat liver (Cravatt et al., 1996). It is also possible that the activity of FAAH enzyme is increased as part of a feedback mechanism to dampen elevated levels of anandamide during active inflammatory responses. Such a mechanism is seen in other inflammatory disorders such as arthritis (Richardson et al., 2008) and colitis (de Fillippis et al., 2008), but is yet to be described for airway inflammatory conditions.

Besides FAAH, earlier enzymatic assays using isolated COX has demonstrated that the endogenous cannabinoid anandamide is metabolised specifically by COX-2 enzyme, and not COX-1 to form its metabolite, arachidonic acid (Kozak et al., 2002a). On the other hand, studies using porcine brain (Hampson et al., 1995) and rabbit reticulocytes (Ueda et al., 1995) confirmed the presence of 12- and 15-lipoxygenases respectively that were found to directly metabolise anandamide into 12- and 15-hydroxyanandamide. It was reported in these studies that the rate of conversion of anandamide into 12- and 15-lipoxygenases and arachidonic acid were near equal. Subsequent mass spectroscopy analysis revealed that arachidonic acid derived from anandamide was metabolised into a variety of active metabolites such as prostaglandin E₂ (PGE₂) by COX-2 (Almada et al., 2015) and hydrolysis by LOX was thought to lead to the production of hydroperoxyeicosatetraenoic acids (HPETEs) (van der Stelt et al., 2002). Based on these findings, it was thus postulated that inhibition of the COX and or LOX enzymes may have beneficial effect in preventing anandamide-induced increase in bronchial epithelial permeability, such as that seen in URB597-treated cells. The rationale of investigating the effect of COX

and LOX inhibition was further supported by previous studies which demonstrated the expression of these hydrolysing enzymes in the human bronchial epithelial structure, and the presence of COX-2 in Calu-3 bronchial epithelial cell line (Jayawickreme et al., 1999, Waskewich et al., 2002, Fukunaga et al., 2005). Results in *Figure 3-8B* indicate that inhibition of either COX or LOX showed no effect on the reduction in TEER caused by anandamide. However, simultaneous inhibition of both enzymes prevented the reduction in TEER, suggesting that metabolites of both COX and LOX mediate the action of anandamide. The present study thus hypothesises that blocking COX and LOX separately shunts the metabolism of anandamide through the other pathway. Inhibition of both COX and LOX also inhibited the reduction in TEER caused by arachidonic acid (*Figure 3-8B*) consistent with the proposal that anandamide is first converted to arachidonic acid via FAAH, prior to metabolism by COX and LOX enzymes. Such observation also supports a role for arachidonic acid/COX/LOX metabolites in the reduction in TEER by anandamide. The efficiency of anandamide conversion to arachidonic acid has never been explored. Hence, the arachidonic acid concentration of 30 μM was used in this study assuming that anandamide (30 μM) was fully metabolised into arachidonic acid.

Nevertheless, future experiments would include complete dose-response studies for all the compounds used. It is acknowledged that the effect of each drug may differ in variable concentrations used. The range of concentrations to be studied should be linear; for example, 3, 10 and 30 μM for all cannabinoid ligands, as well as the anandamide metabolite, arachidonic acid. The optimal concentration would be decided based on the concentration that showed approximately 50% reduction in TEER, i.e. the EC_{50} . Results from the TEER experiments shown in *Figure 3-4A*

indicate that, anandamide exerts a pro-inflammatory-like response on the human bronchial epithelial layer, similar to that seen with TNF α . Previous studies have proven that TNF α (Levine et al., 1995) and the metabolites of arachidonic acid (Zhao et al., 2009) increases MUC5AC mRNA expression in primary human bronchial epithelial cells using enzyme-linked immunosorbent assay (ELISA) and quantitative real time PCR technique (qPCR) respectively. Based on these findings, an initial hypothesis was made that both TNF α and anandamide might cause an increase in MUC5AC glycoprotein expression, as mucus hypersecretion is known to be one of the clinical feature observed in airway inflammatory diseases like asthma and COPD. It is also noted that MUC5AC was the chosen mucin subtype of study as studies have previously shown that MUC5AC is highly expressed in Calu-3 cells (Berger et al., 1999, Stewart et al., 2011).

In the present study, MUC5AC expression was investigated using dot blotting due to the limitation of Western blotting in separating high molecular weight proteins of more than 250 kDa, such as that for MUC5AC mucins. In addition, previous reports revealed that the molecular weights of MUC5AC vary depending on the length of their oligomeric glycoprotein chains, ranging between 250 kDa to 40 MDa (Sheehan et al., 2004, Ryan et al., 2015).

Results in *Figure 3-9* showed that exposure to TNF α enhanced MUC5AC protein expression in Calu-3 cells. The level of MUC5AC glycoprotein expression was also elevated in cells treated with anandamide. However, a comparison to its vehicle control, (0.3% v/v) EtOH showed no statistical difference in the amount of MUC5AC secreted. This finding suggests that anandamide may have promoted airway mucins secretion. However, further investigations such as quantification of MUC5AC gene expression using qPCR or ELISA may be beneficial in verifying

anandamide role in mucins production. Nevertheless, results obtained from the dot blotting experiment add strength to the earlier findings from TEER experiment conducted in this study, supporting the fact that the endogenous cannabinoid, anandamide behaves as a pro-inflammatory mediator, much like so for the cytokine, $\text{TNF}\alpha$.

3.5 Conclusion

Following the successful development of a TEER measurement protocol, this study has demonstrated that Calu-3 cells cultured at ALI are useful as *in vitro* pharmacological screening tool, owing reproducible effects following various drug treatments. *Figure 3-10* (on page 144) summarises the findings obtained following the optimisation of the TEER method in measuring changes to Calu-3 transepithelial resistance following various drug treatments:

The increase in anandamide detected in bronchoalveolar lavage fluid from asthmatic patients has been suggested to be an inhibitory feedback response (Zoerner et al., 2011), as activation of the cannabinoid receptors was expected to relieve airway inflammation (Stengel et al., 2007, Makwana et al., 2015). However, the data presented here suggest that the increase in anandamide in asthmatic patients may contribute to increased permeability of the epithelium through degradation to arachidonic acid metabolites. Therefore, preventing anandamide hydrolysis by FAAH or subsequent metabolism by COX and LOX enzymes in the airways may help to prevent epithelial permeability in asthma. It is noted that the presence of FAAH, COX and LOX enzymes on the Calu-3 bronchial epithelial cell line remained to be investigated in future experiments. Identification of the metabolites formed from anandamide within the bronchial epithelial structure will also add value to understanding the underlying mechanism of anandamide-induced increase in epithelial permeability.

It is also concluded from this study that the other endogenous cannabinoid, 2-AG showed no role in regulating the bronchial epithelial permeability. Future

investigation in intact airway epithelium models would be beneficial to identify 2-AG expression and its possible role in airway inflammation.

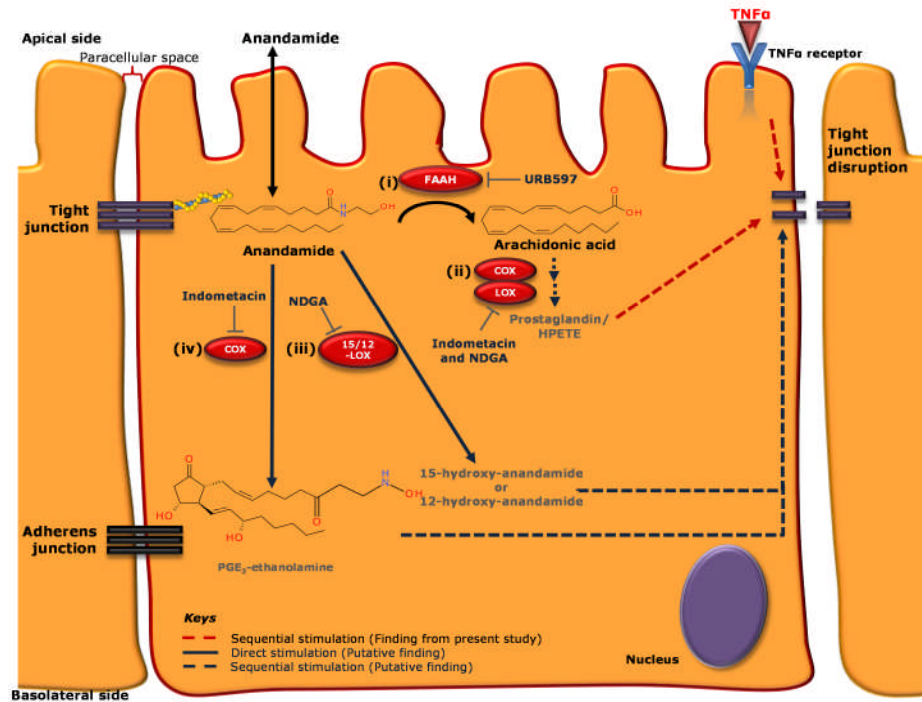


Figure 3-10 Changes to the bronchial epithelial cell permeability following the treatment of the endogenous cannabinoid, anandamide in comparison to the pro-inflammatory cytokine, TNF α . Red coloured arrows represent intracellular signalling steps involved in tight junction disruption, whereas arrows in black denote the cascades associated to anandamide metabolism. T-shaped lines indicate inhibition. Exposure to anandamide increases Calu-3 cell permeability that was similarly observed in when the cells were treated with TNF α . Further investigations revealed that anandamide-induced decrease in transepithelial permeability was not due to anandamide itself, but through its metabolites which can be produced following catabolism by different intracellular enzymes. (i) The fatty acid amide hydrolase (FAAH) enzyme metabolises anandamide to arachidonic acid. Inhibition of the FAAH activity by URB597 was shown to prevent the decrease in transepithelial resistance caused by anandamide. (ii) Subsequently, arachidonic acid was thought to be metabolised by cyclooxygenase (COX) and lipoxygenase (LOX) to form prostaglandins (PG) and 5-hydroperoxyeicosatetraenoic acid (5-HPETE). Such reaction was inhibited when cells are treated with combined treatment of COX inhibitor, indomethacin and LOX inhibitor, nordihydroguaiaretic acid (NDGA). Alternatively, anandamide can be directly broken down by LOX or COX to prostaglandin-E₂ (PGE₂)-ethanolamine and 15- and 12-LOX to 15- and 12-hydroxyanandamide respectively.

4. Mechanisms of Anandamide-induced Increases in Human Bronchial Epithelial Permeability

4.1 Introduction

The continuity of the bronchial epithelial layer depends on the structural integrity of the tight junction protein complex. The tight junctions play a significant role in filtering paracellular entry of foreign particles or pathogens, whilst maintaining cell polarity by regulating transcellular transport of nutrients and water into the airway submucosa.

As previously described in *section 1.3.1*, the tight junction structure is an assembly of two distinct types of protein complexes. First, the scaffolding proteins, ZO-1, ZO-2 and ZO-3 that link to the actin filament on the intracellular side while attaching themselves onto the intercellular membrane proteins. Second, these membrane-spanning proteins which include occludin, claudin and junctional adhesion molecule (JAM), anchor neighbouring ciliated columnar, mucus-producing Goblet and surfactant-secreting Clara cells. Arrangement of the different types of tight junction proteins that underlie the gating function of the airway epithelium is illustrated in *Figure 1.3 of section 1.3.1*.

Previous immunohistochemical studies revealed that confluent and fully-differentiated Calu-3 cells cultured at ALI express similar tight junction proteins compared to intact human bronchial epithelial cells (Wan et al., 2000, Stewart et al., 2011). These authors also reported that the level of expression of these proteins and their ability to assemble into tight junction complexes at the epithelial cell membrane corresponds to their barrier function in the Calu-3 cell layer.

Pharmacological studies in various epithelial cell models revealed that expression of tight junction proteins is regulated by a cascade of intracellular events that transmit signals to mediate epithelial permeability in response to environmental stimuli (Matter and Balda, 2003, Gonzalez-Mariscal et al., 2008). Activation of the MAP kinases, mainly of the classical extracellular signal-regulated kinases (ERKs) (Lu et al., 1998, Chen et al., 2000, Wang et al., 2004, Petecchia et al., 2012) and p38-MAP kinase (Garcia et al., 2002, Oshima et al., 2008) is associated with decreased epithelial barrier function as intracellular signals for tight junction protein expression are reported to be impaired. However, most studies reported in the current literature were conducted in non-airway epithelial cells, such as the gut and MDCK epithelial cells.

4.1.1 Aims

Results in *chapter 3* demonstrated that the endogenous cannabinoid, anandamide increases bronchial epithelial permeability, probably through its metabolite, arachidonic acid, independent of stimulation of cannabinoid receptors. Therefore, the aims for the study reported in this chapter were:

- i. To characterise the signalling pathway(s) involved in anandamide-induced increases in bronchial epithelial cell permeability.
- ii. To test the role of MAP kinase signalling in $\text{TNF}\alpha$ -induced tight junction disruption.

4.2 Materials and Methods

4.2.1 Materials

Materials used for cell culture are listed in *section 2.1.1*; TEER experiment in *section 2.1.2*; dot blotting and Western blotting in *section 2.1.4* with the list of primary and antibodies used in *section 2.1.5*. Enzymes inhibitors including PD98059, U0126 and SB203580 that were also purchased from Sigma Aldrich were dissolved in DMSO to a stock concentration of 10 mM before administration into the cells.

4.2.2 Methods

TEER experiments were conducted according to the optimised protocol in *section 2.5.2* and justification for the drug concentrations used in this chapter is presented in *Table 4-1*. As discussed in *section 3.3.7*, damage to Calu-3 cell layers was observed when DMSO was present beyond 8 hours. Hence, all TEER measurements presented in this chapter were made at or before 8 hours post-drug or vehicle addition.

Following TEER experiments, Calu-3 cells were harvested from the Transwells[®] and samples for Western blotting were prepared according to *section 2.7.1*. The same batches of cells were used in TEER and Western blot experiments to ensure consistency in results in these parallel functional studies and to reduce wastage of materials.

Gel electrophoresis for the investigation of ZO-1 protein expression was conducted at 200 V, for a duration of 50 minutes. This was to ensure a thorough separation of the proteins of interest, owing to the high apparent molecular weight of ZO-1 of 225 kDa. Information regarding the primary and secondary antibodies used is listed in *Table 2-5* in *section 2.1.5*.

Compound	Concentration studied	Evidence on concentration studied	Notes on site(s) of action/ K_i or IC_{50} values relevant to studied concentration
Anandamide	30 μ M	Refer <i>Table 3-1</i>	
PD98059	10 μ M	PD98059 (10 μ M) was shown to significantly reduce adenosine-induced ERK1/2 phosphorylation by approximately 50% in Calu-3 cells (Sun et al., 2008).	IC_{50} values of PD98059 for MEK1 and MEK2 are 4 μ M and 50 μ M respectively (Alessi et al., 1995).
SB203580	10 μ M	SB203580 (10 μ M) prevented <i>Pseudomonas aeruginosa</i> -mediated IL-8 release in Calu-3 cells (Bezzetti et al., 2011). Though TEER was not measured in the investigation by Bezzetti <i>et al</i> , a separate study revealed that the presence of IL-8 was associated to decreased TEER readings in the same cell	SB203580 at 10 μ M was shown to selectively inhibit isolated MAPK p38 enzyme activity by approximately 98% (Davies et al., 2000).

		model. (Zhu et al., 2010).	
TNF α	10 ng/ml	Refer <i>Table 3-1</i>	
U0126	10 μ M	U0126 (25 μ M) inhibited decreases in TEER by TNF α , IFN γ and IL-4- in Calu-3 cells (Petecchia et al., 2012). Concentration of 10 μ M was previously shown to prevent IL-6 release in Calu-3 cells caused by adenosine (Sun et al., 2008).	IC ₅₀ of U0126 ranges from 0.07 to 13 μ M for MEK1, whilst MEK2 was noted to be 0.06 μ M (Duncia et al., 1998).

Table 4-1 List of the drugs used in this chapter and the rationales for the concentrations used.

4.2.3 Statistical Analysis

Data are presented as the mean \pm standard error of mean (S.E.M). Western blotting data were analysed by 1-way ANOVA followed by a Bonferroni post-hoc test. Alternatively, Western blotting analysis to detect differences in fold change of a specific protein expression between two treatment group at a fixed time point were compared using paired, Student's t-test. Results of $P < 0.05$ were considered significant.

4.3 Results

4.3.1 Anandamide Decreases Expression of Tight Junction Proteins, Occludin and ZO-1

The target tight junction proteins investigated in this project included the membrane-spanning protein, occludin and scaffolding protein ZO-1. Changes to the expression of these proteins were evaluated in cells treated with either TNF α (10 ng/mL) or anandamide (30 μ M) for 48 hours, with (0.3% v/v) EtOH as the vehicle control. The basal condition represents untreated Calu-3 cells to allow for quantitative comparison in the relative changes in protein expression following drug treatments.

Western immuno-blotting for occludin detected a major band at approximately 64 kDa (*Figure 4-1A*). Similarly, Western blotting for ZO-1 detected a major band of about 225 kDa (*Figure 4-2A*). The presence of vehicle control for anandamide, (0.3% v/v EtOH) did not affect the expression of occludin or ZO-1.

In comparison, the amount of both tight junction proteins was significantly reduced by approximately 50% when treated with either anandamide (30 μ M) or TNF α (10 ng/ml) for 48 hours.

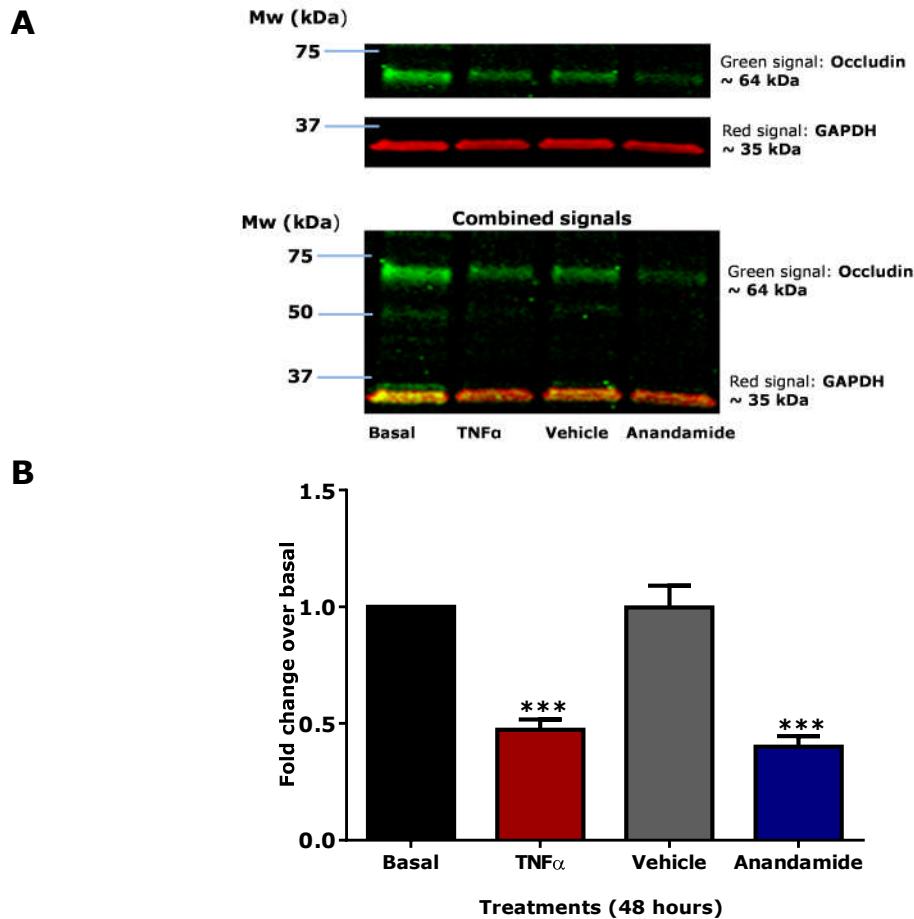


Figure 4-1 A. Western blot images and **B.** analysis of the changes in tight junction proteins expression, occludin following basolateral administration of TNF α (10 ng/mL), (0.3% v/v) EtOH or anandamide (30 μ M) in Calu-3 cells for 48 hours. Basal group represents untreated 21-day old Calu-3 cells cultured at air-liquid interface; i.e. no drug. GAPDH was used as a reference protein (or loading control) as its level of expression remained similar in all treatment groups, whilst occludin expression varied. 'Fold change from basal' labelled on the Y-axis in figure B. was derived by dividing the ratio of occludin to GAPDH expression for the respective treatment groups with the ratio of occludin to GAPDH of basal. Data are presented as means \pm SEM of fold changes in protein expression compared to vehicle, (0.3% v/v) EtOH; $n=3$, *** $P<0.001$, 1-way ANOVA followed by a Bonferroni post-hoc test, compared to vehicle control, (0.3% v/v) EtOH. Refer appendix for original blot images (Appendix- Chapter 4(1))

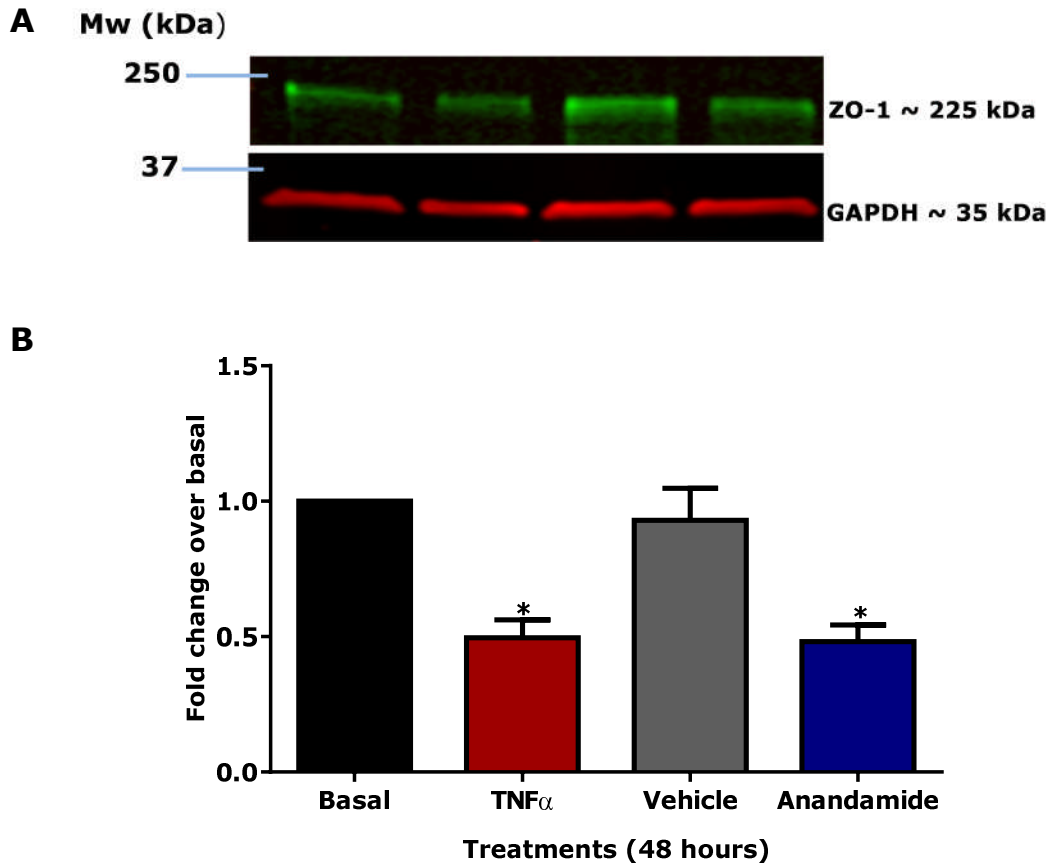


Figure 4-2 A. Western blot images and **B.** analysis of the changes in tight junction proteins expression, ZO-1 following basolateral administration of TNF α (10 ng/mL), (0.3% v/v) EtOH or anandamide (30 μ M) in Calu-3 cells for 48 hours. Basal group represents untreated 21-day old Calu-3 cells cultured at air-liquid interface; i.e. no drug. GAPDH was used as a reference protein (or loading control) as its level of expression remained similar in all treatment groups, whilst occludin expression varied. 'Fold change from basal' labelled on the Y-axis in figure B. was derived by dividing the ratio of ZO-1 to GAPDH expression for the respective treatment groups with the ratio of ZO-1 to GAPDH of basal. Data are presented as means \pm SEM of fold changes in protein expression compared to vehicle, (0.3% v/v) EtOH; $n=8$, $*P<0.05$, 1-way ANOVA followed by a Bonferroni post-hoc test, compared to vehicle control, (0.3% v/v) EtOH. Refer appendix for original blot images (Appendix- Chapter 4(2)).

4.3.2 Inhibition of ERK Activation Prevents Increased Epithelial Permeability due to Anandamide or TNF α

The presence of the vehicle control of MEK1/2 inhibitor alone, (0.1% v/v) DMSO (*Figure 4-3A&B*), or vehicle controls for MEK1/2 inhibitors and anandamide, (0.1% v/v) DMSO + (0.3% v/v) EtOH (*Figure 4-4B* and *Figure 4-5*), or did not significantly affect the resistance of the Calu-3 cell layer throughout the 8-hour duration of the experiment. Nevertheless, the presence of (0.1% v/v) DMSO as vehicle control for PD98059 in *Figure 4-4A* caused a transient drop in TEER for up to 4 hours, though TEER readings were generally maintained 90% or higher.

Inhibition of ERK activation using the MEK1/2 inhibitor PD98059 (10 μ M) alone resulted in a modest TEER increase which was maintained for 8 hours (*Figure 4-3A*, *Figure 4-4A* and *Figure 4-5*). In contrast, treatment with a highly selective MEK1/2 inhibitor, U0126 (10 μ M) alone caused a significant increase in TEER compared to cells treated with its vehicle control (0.1% v/v) DMSO (*Figure 4-3B* and *Figure 4-5B*).

Activation of ERK is thought to be involved in the disruption of tight junction permeability by TNF α (Petecchia et al., 2012). The use of PD98059 and U0126 was chosen based on their high selectivity for MEK1 and MEK2 which was previously demonstrated by Davies *et al* (2000). TEER experiments conducted in the present study (*Figure 4-3A&B*) produced results consistent with this proposal, as pre-incubation with either PD98059 or U0126 fully prevented TNF α -induced decreases in bronchial epithelial resistance.

As with TNF α , the increase in epithelial permeability induced by the endocannabinoid anandamide was also prevented by prior incubation with PD98059

for an hour (*Figure 4-4A*). A similar inhibition was seen using the other MEK1/2 inhibitor, U0126 (10 μ M) (*Figure 4-4B*).

Results displayed in *Figure 4-5* confirm that the TEER decrease caused by the anandamide metabolite arachidonic acid (30 μ M) was also prevented by the MEK1/2 inhibitor, PD98059.

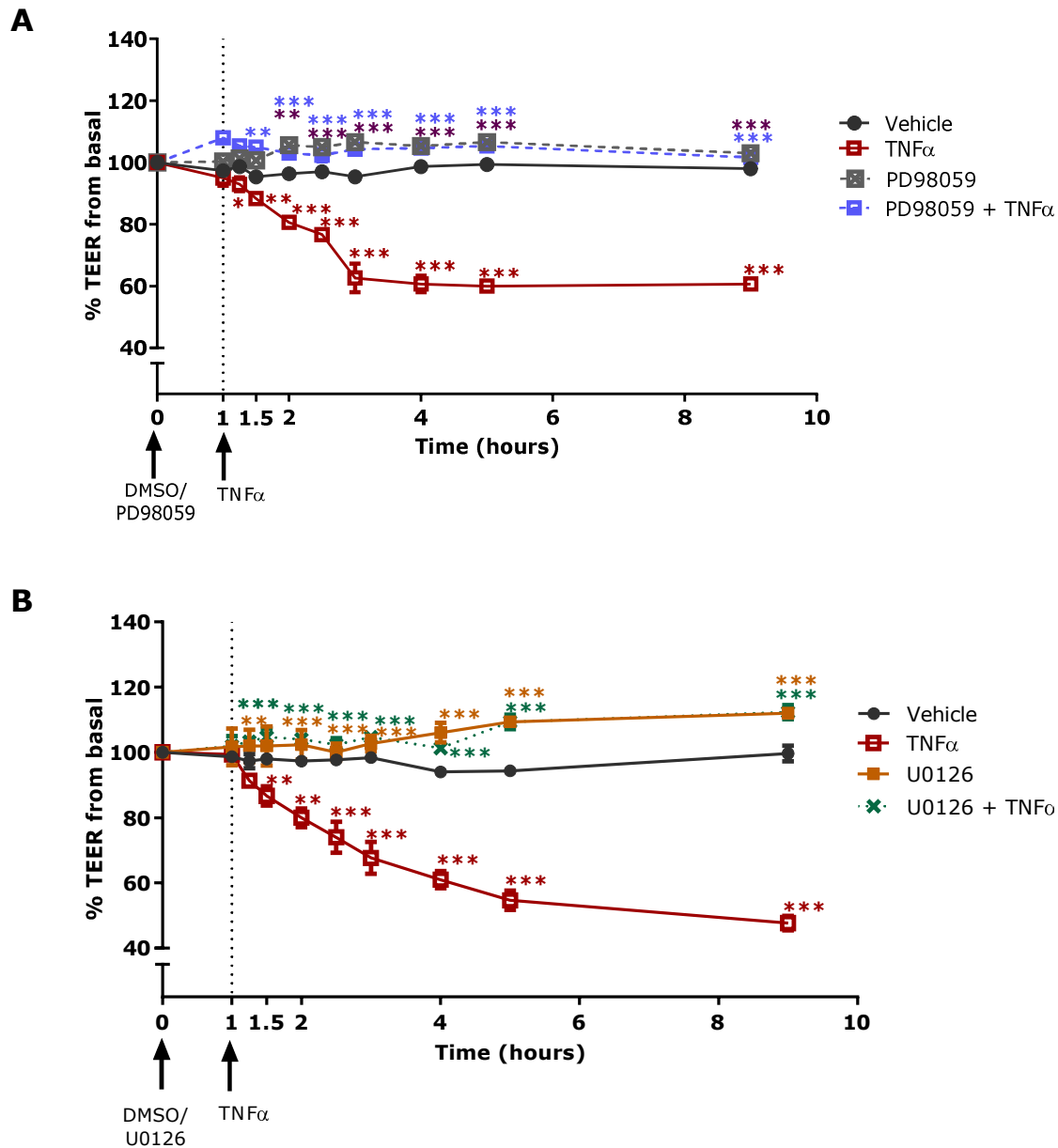


Figure 4-3 Effect of basolateral application of **A.** MEK1/2 inhibitor, PD98059 (10 μ M); **B.** a highly selective MEK1/2 inhibitor, U0126 (10 μ M); on TEER in 21-day old Calu-3 cells cultured at air-liquid interface, in the presence of TNF α (10 ng/ml). Data are presented as means \pm SEM; $n=3$, * $P<0.05$, ** $P<0.01$, *** $P<0.001$, 2way ANOVA followed by a Bonferroni post-hoc test, compared to anandamide (30 μ M); except anandamide, which is compared to vehicle control, (0.1% v/v) DMSO.

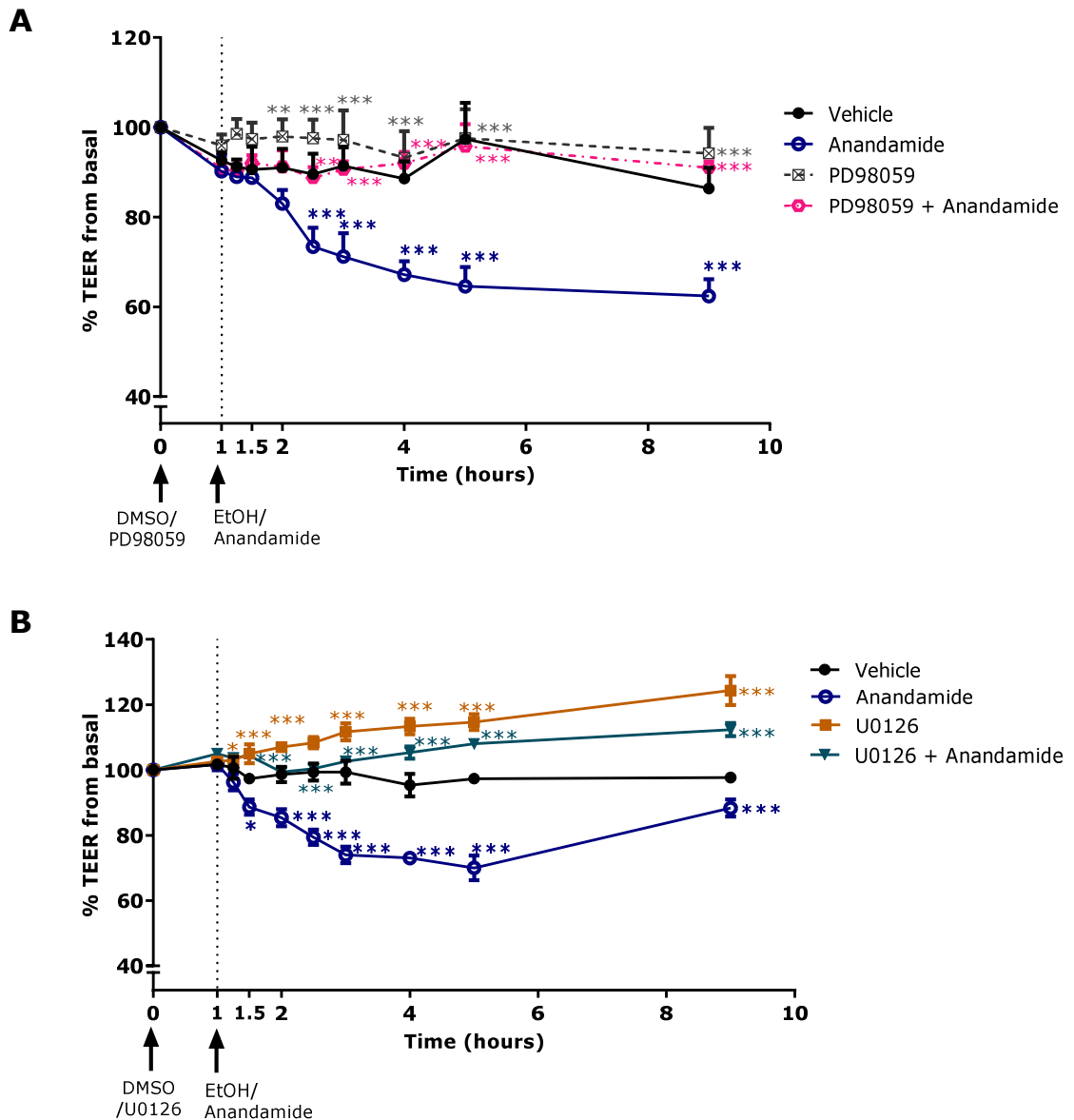


Figure 4-4 Effect of basolateral application of **A.** MEK1/2 inhibitor, PD98059 (10 μ M); **B.** a highly selective MEK1/2 inhibitor, U0126 (10 μ M); on TEER reading in 21-day old Calu-3 cells cultured at air-liquid interface, in the presence of anandamide (30 μ M). Data are presented as means \pm SEM; $n=3-5$, * $P<0.05$, ** $P<0.01$, *** $P<0.001$, 2way ANOVA followed by a Bonferroni post-hoc test, compared to anandamide (30 μ M); except anandamide, which is compared to vehicle control, (0.1% v/v) DMSO and (0.3% v/v) EtOH.

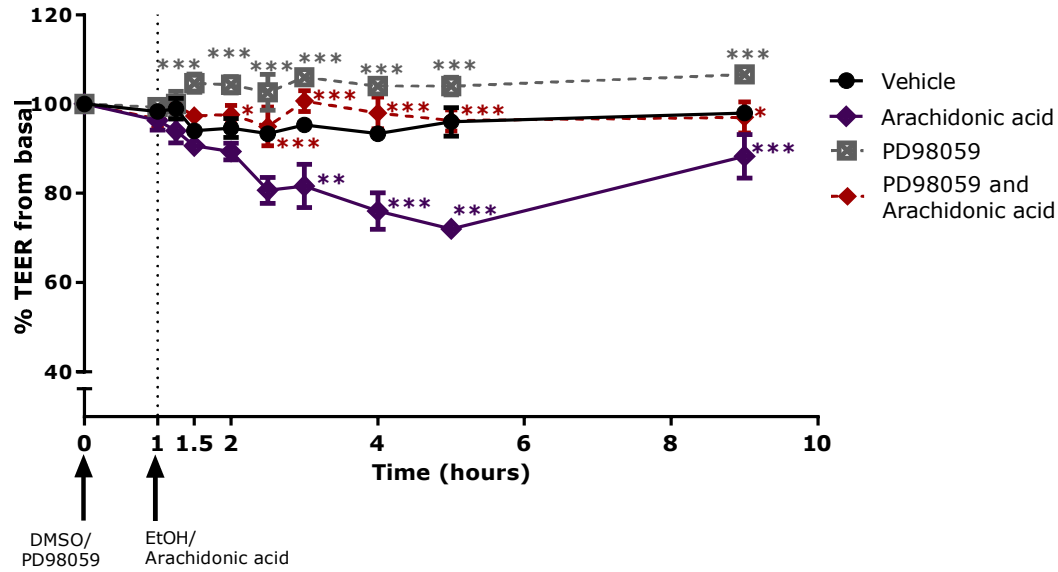


Figure 4-5 Effect of basolateral application of A. MEK1/2 inhibitor, PD98059 (10 μ M) on TEER in 21-day old Calu-3 cells cultured at air-liquid interface, in the presence of arachidonic acid (30 μ M). Data are presented as means \pm SEM; $n=3$, * $P<0.05$, ** $P<0.01$, *** $P<0.001$, 2way ANOVA followed by a Bonferroni post-hoc test, compared to anandamide (30 μ M); except anandamide, which is compared to vehicle control, (0.1% v/v) DMSO and (0.3% v/v) EtOH.

4.3.3 Inhibition of ERK Activation Prevented Decreased Expression of the Tight Junction Protein, Occludin in Anandamide-Treated Cells

The involvement of ERK MAP kinase signalling in the effects of anandamide and TNF α on epithelial permeability were further determined via semi-quantitative measurement of occludin expression using Western immunoblotting following parallel functional measurements of TEER (discussed in *section 4.3.2*).

The expression of the tight junction protein, occludin was the focus of the present series of experiments since a previous study revealed that its expression in human umbilical vein endothelial cells was significantly downregulated by 8 hours of TNF α stimulation (McKenzie and Ridley, 2007).

Administration of vehicle control (0.1% v/v) DMSO alone (*Figure 4-6* and *Figure 4-7*) had no effect on the expression level of occludin. However, prior administration of the MEK1/2 inhibitors, PD98059 (*Figure 4-6*) or U0126 (*Figure 4-7*) (both 10 μ M) prevented the 50% reduction in occludin expression due to TNF α stimulation.

Application of a combination of (0.1% v/v) DMSO and (0.3% v/v) EtOH as vehicle controls for the enzyme inhibitors and anandamide respectively, did not alter occludin expression. However, as was the case with TNF α , pre-treatment with PD98059 (*Figure 4-8*) or U0126 (*Figure 4-9*) prevented the decrease in occludin expression due to anandamide.

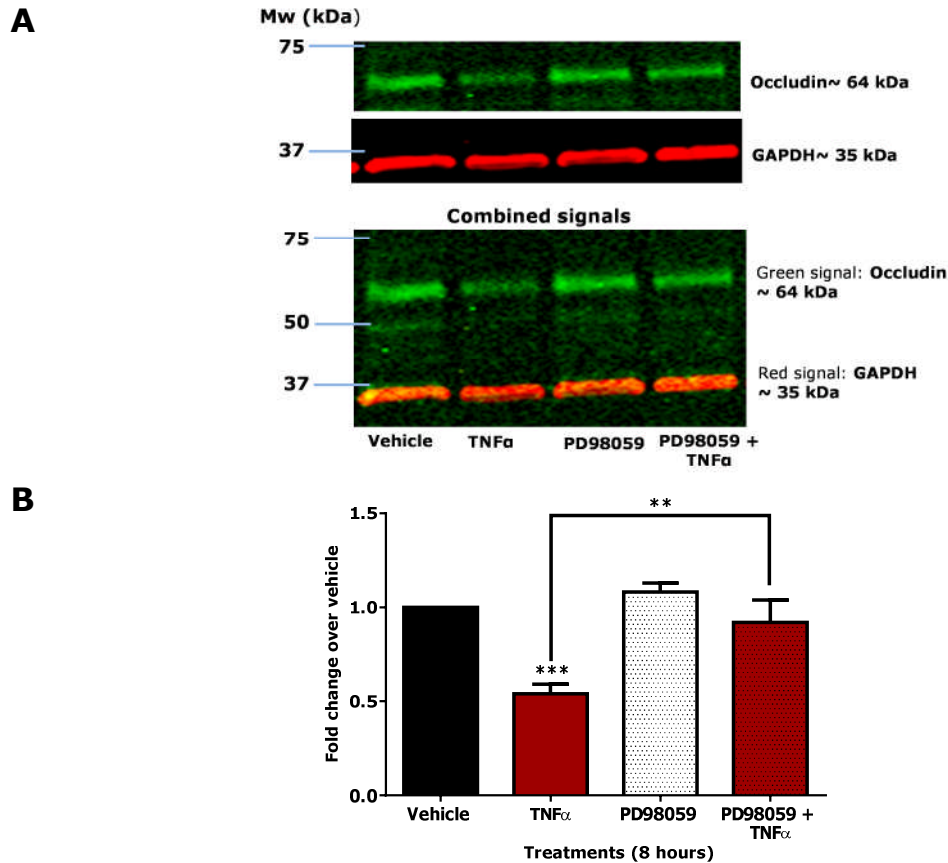


Figure 4-6 A. Western blot images and **B.** analysis of the changes in occludin expression following basolateral administration of PD98059 (10 μ M) in the presence of TNF α (10 ng/ml) in Calu-3 cells for 8 hours. GAPDH was used as a reference protein (or loading control) as its level of expression remained similar in all treatment groups, whilst occludin expression varied. 'Fold change from vehicle' labelled on the Y-axis in figure B. was derived by dividing the ratio of occludin to GAPDH expression for the respective treatment groups with the ratio of occludin to GAPDH for vehicle control. Data are presented as means \pm SEM of fold changes in protein expression compared with vehicle for the enzyme inhibitors, (0.1% v/v) DMSO; $n=3$, * $P<0.05$, ** $P<0.01$, *** $P<0.001$, 1way ANOVA followed by a Bonferroni post-hoc test, compared to vehicle control, (0.1% v/v) DMSO, whereas combined PD98059+TNF α which is compared to TNF α (10 ng/ml) alone. Refer appendix for original blot images (Appendix- Chapter 4(3)).

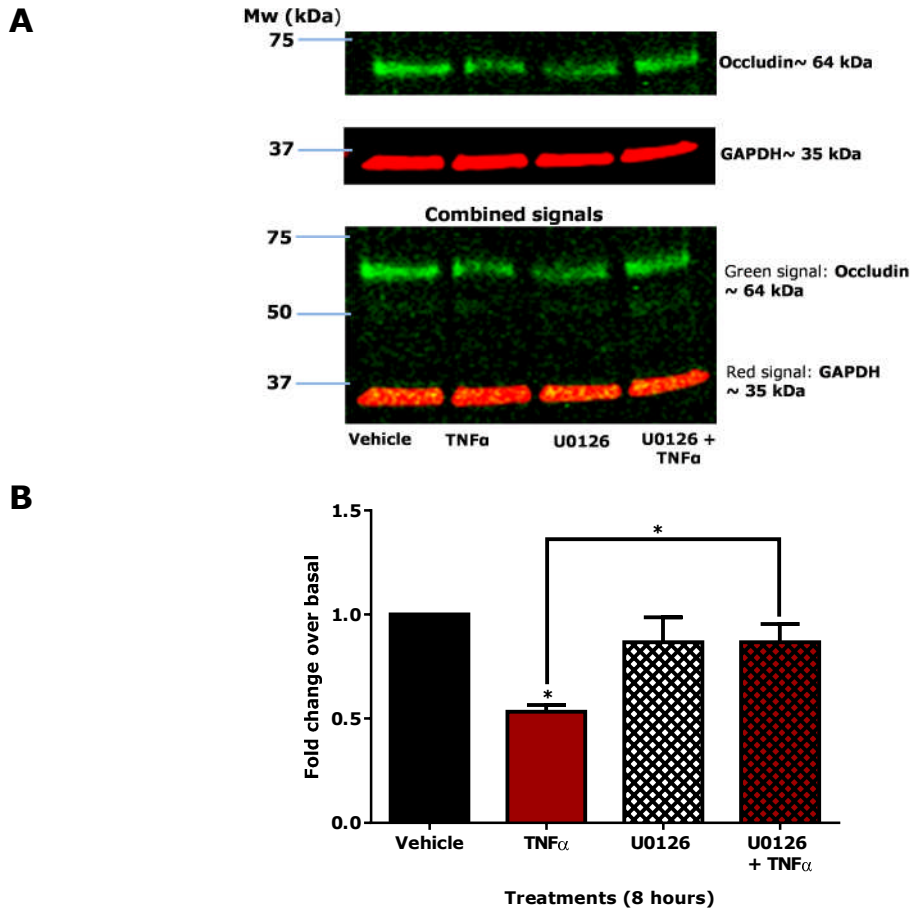


Figure 4-7 A. Western blot images and **B.** analysis of the changes in occludin expression following basolateral administration of U0126 (10 μ M) in the presence of TNF α (10 ng/ml) in Calu-3 cells for 8 hours. GAPDH was used as a reference protein (or loading control) as its level of expression remained similar in all treatment groups, whilst occludin expression varied. 'Fold change from vehicle' labelled on the Y-axis in figure B. was derived by dividing the ratio of occludin to GAPDH expression for the respective treatment groups with the ratio of occludin to GAPDH for vehicle control. Data are presented as means \pm SEM of fold changes in protein expression compared with vehicle for the enzyme inhibitors, (0.1% v/v) DMSO; $n=3$, * $P<0.05$, ** $P<0.01$, *** $P<0.001$, 1way ANOVA followed by a Bonferroni post-hoc test, compared to vehicle control, (0.1% v/v) DMSO, whereas combined U0126+TNF α which is compared to TNF α (10 ng/ml) alone. Refer appendix for original blot images (Appendix- Chapter 4(4)).

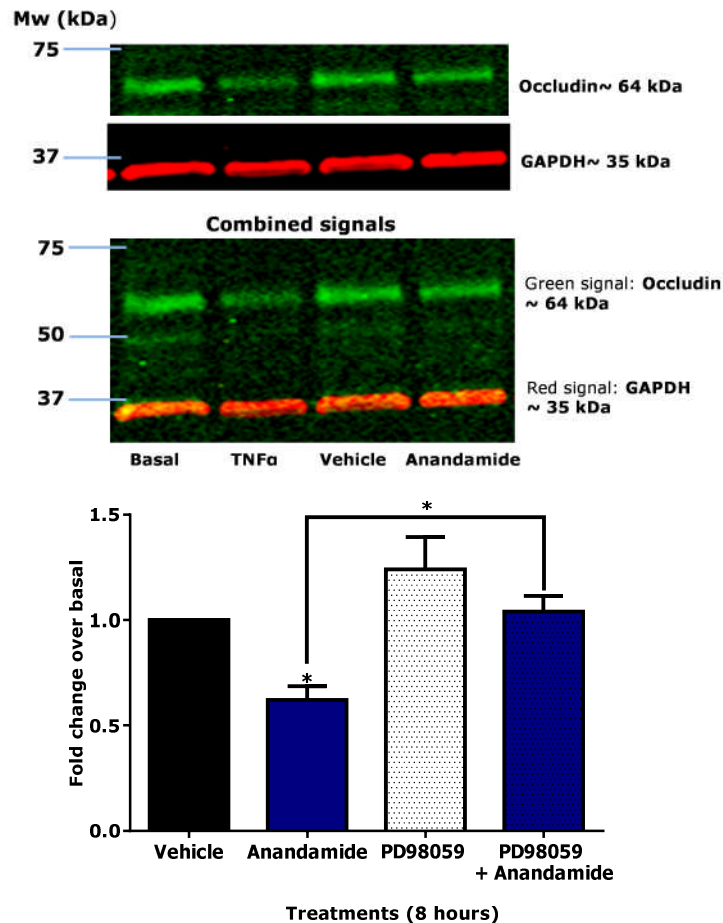
A

Figure 4-8 A. Western blot images and **B.** analysis of the changes in occludin expression following basolateral administration of PD98059 (10 μ M) in the presence of anandamide (10 μ M) in Calu-3 cells for 8 hours. GAPDH was used as a reference protein (or loading control) as its level of expression remained similar in all treatment groups, whilst occludin expression varied. 'Fold change from vehicle' labelled on the Y-axis in figure B. was derived by dividing the ratio of occludin to GAPDH expression for the respective treatment groups with the ratio of occludin to GAPDH for vehicle control. Data are presented as means \pm SEM of fold changes in protein expression compared with vehicle for the enzyme inhibitors, (0.1% v/v) DMSO; $n=3$, * $P<0.05$, ** $P<0.01$, *** $P<0.001$, 1way ANOVA followed by a Bonferroni post-hoc test, compared to vehicle control, (0.1% v/v) DMSO, whereas combined PD98059+anandamide which is compared to anandamide (30 μ M) alone. Refer appendix for original blot images (Appendix- Chapter 4(5)).

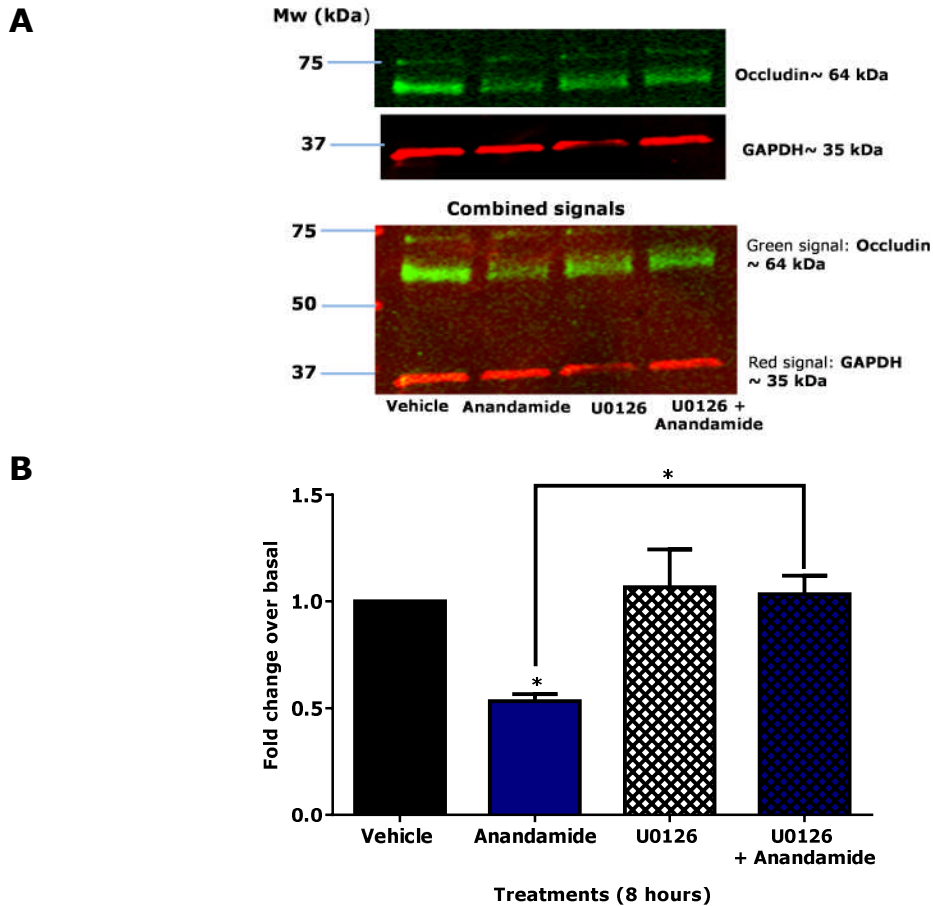


Figure 4-9 A. Western blot images and **B.** analysis of the changes in occludin expression following basolateral administration of U0126 (10 μ M) in the presence of anandamide (10 μ M) in Calu-3 cells for 8 hours. GAPDH was used as a reference protein (or loading control) as its level of expression remained similar in all treatment groups, whilst occludin expression varied. 'Fold change from vehicle' labelled on the Y-axis in figure B. was derived by dividing the ratio of occludin to GAPDH expression for the respective treatment groups with the ratio of occludin to GAPDH for vehicle control. Data are presented as means \pm SEM of fold changes in protein expression compared with vehicle for the enzyme inhibitors, (0.1% v/v) DMSO; $n=3$, * $P<0.05$, ** $P<0.01$, *** $P<0.001$, 1way ANOVA followed by a Bonferroni post-hoc test, compared to vehicle control, (0.1% v/v) DMSO, whereas combined U0126+anandamide which is compared to anandamide (30 μ M) alone. Refer appendix for original blot images (Appendix- Chapter 4(6)).

4.3.4 Inhibition of p38 MAPK Activation also Prevents Anandamide- and TNF α -Induced Increased in Cell Permeability and Occludin Expression

To determine whether the role of MAP kinase signalling in the effects of anandamide and TNF α specifically involves ERK, the potential role of another element of the MAP kinase cascade, p38 MAPK, was investigated.

Inhibition of p38-MAP kinase activation with SB203580 (10 μ M) prevented the decrease in TEER due to TNF α (10 ng/ml) (*Figure 4-10*) and anandamide (30 μ M) (*Figure 4-11*). Basolateral application of SB203580 alone did not alter TEER responses in the absence of anandamide or TNF α . Consistent with these functional effects, pre-treatment with SB203580 prevented reductions in occludin expression caused by either TNF α exposure (*Figure 4-12*) or anandamide (*Figure 4-13*)

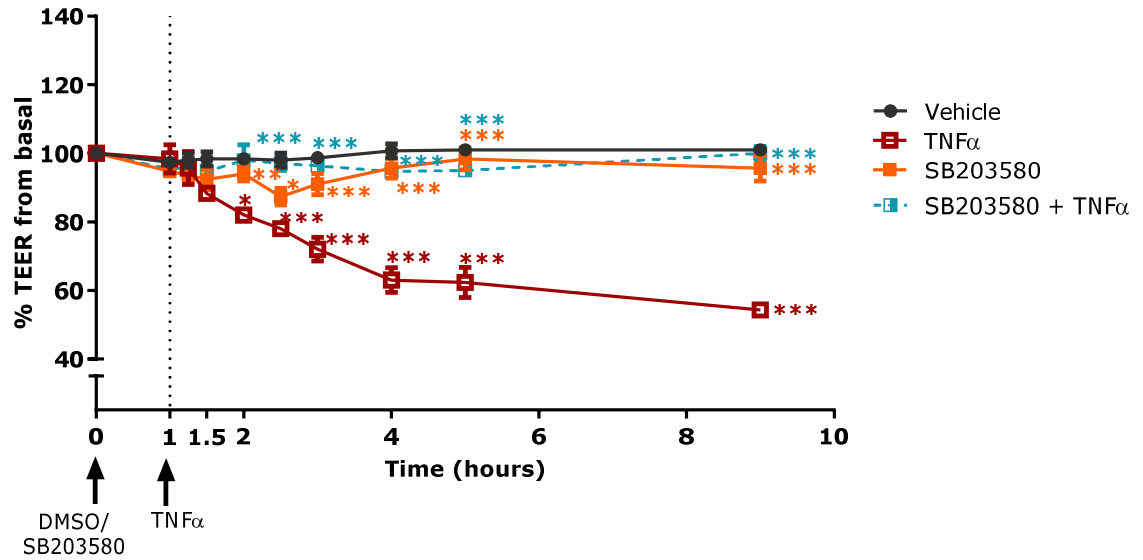


Figure 4-10 Effect of basolateral application of a selective MAPK p38 inhibitor, SB203580 (10 μ M) on TEER in 21-day old Calu-3 cells cultured at air-liquid interface, in the presence of TNF α (10 ng/ml). Data are presented as means \pm SEM; $n=3-5$, * $P<0.05$, ** $P<0.01$, *** $P<0.001$, 2way ANOVA followed by a Bonferroni post-hoc test, compared to TNF α (10 ng/ml); except TNF α , which is compared to vehicle control, (0.1% v/v) DMSO.

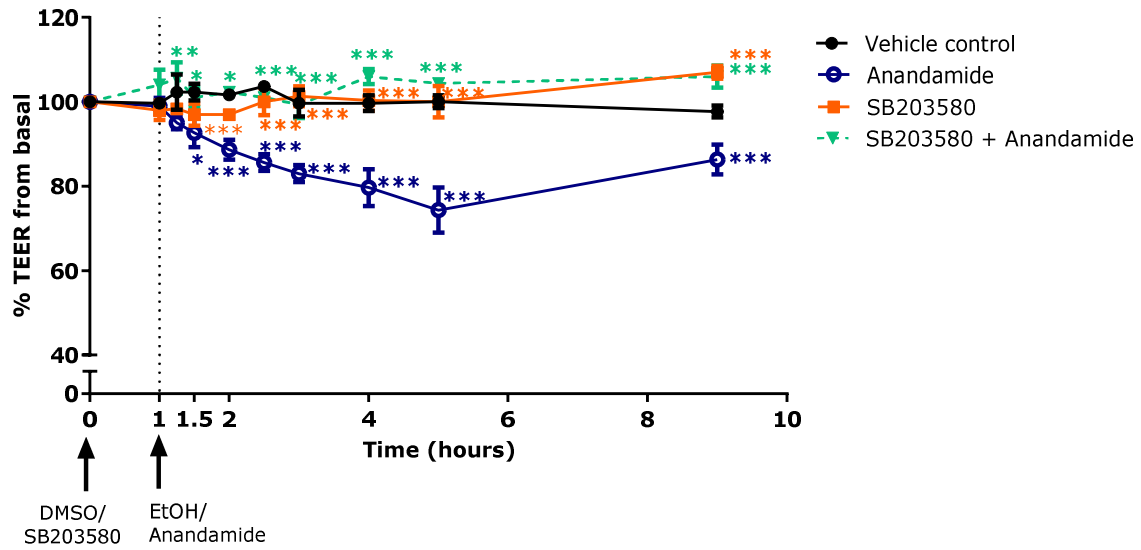


Figure 4-11 Effect of basolateral application of a selective MAPK p38 inhibitor, SB203580 (10 μ M) on TEER in 21-day old Calu-3 cells cultured at air-liquid interface, in the presence of anandamide (30 μ M). Data are presented as means \pm SEM; $n=3$, * $P<0.05$, ** $P<0.01$, *** $P<0.001$, 2way ANOVA followed by a Bonferroni post-hoc test, compared to anandamide (30 μ M); except anandamide, which is compared to vehicle control, (0.1% v/v) DMSO and (0.3% v/v) EtOH.

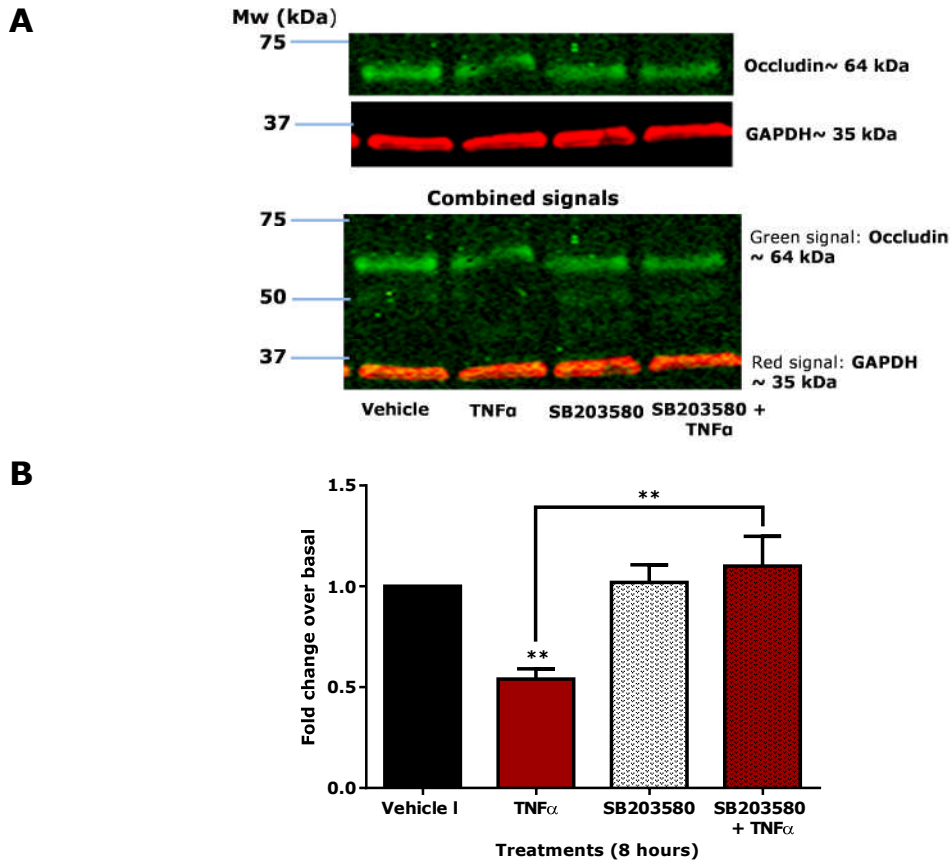


Figure 4-12 A. Western blot images and **B.** analysis of the changes in occludin expression following basolateral administration of SB203580 (10 μ M) in the presence of TNF α (10 ng/ml) in Calu-3 cells for 8 hours. GAPDH was used as a reference protein (or loading control) as its level of expression remained similar in all treatment groups, whilst occludin expression varied. 'Fold change from vehicle' labelled on the Y-axis in figure **B.** was derived by dividing the ratio of occludin to GAPDH expression for the respective treatment groups with the ratio of occludin to GAPDH for vehicle control. Data are presented as means \pm SEM of fold changes in protein expression compared with vehicle for SB203580, (0.1% v/v) DMSO; $n=3$, * $P<0.05$, ** $P<0.01$, *** $P<0.001$, 1way ANOVA followed by a Bonferroni post-hoc test, compared to vehicle control, (0.1% v/v) DMSO, whereas combined SB203580+TNF α which is compared to TNF α (10 ng/ml) alone. Refer appendix for original blot images (Appendix- Chapter 4(7)).

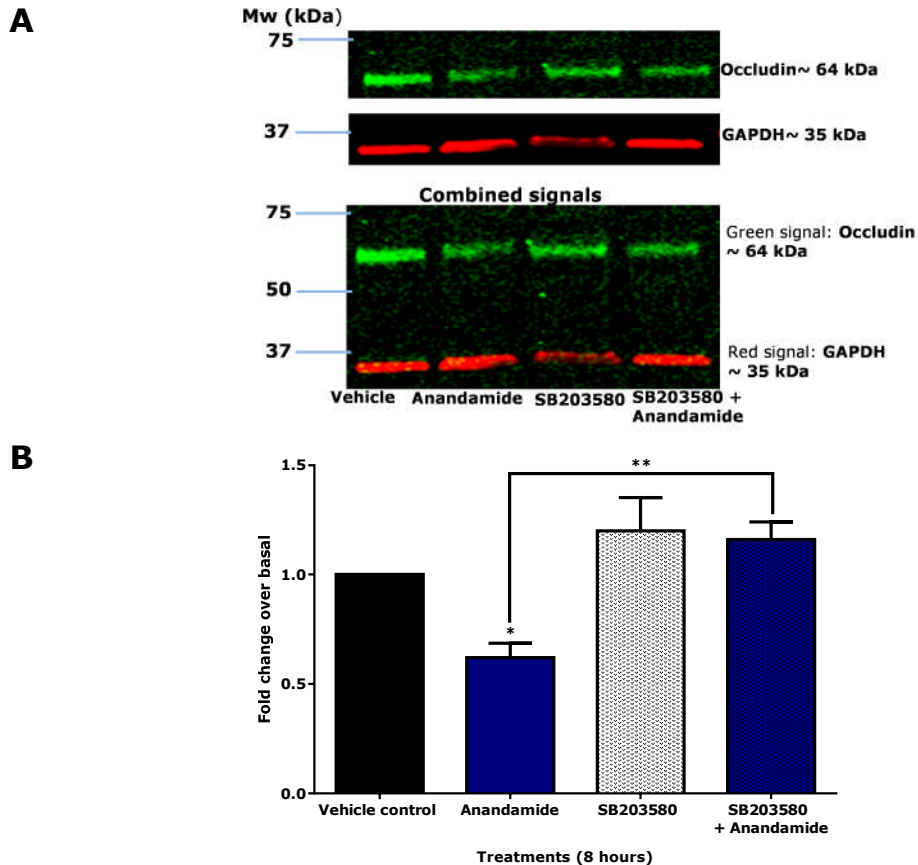


Figure 4-13 A. Western blot images and **B.** analysis of the changes in occludin expression following basolateral administration of SB203580 (10 μ M) in the presence of anandamide (30 μ M) in Calu-3 cells for 8 hours. GAPDH was used as a reference protein (or loading control) as its level of expression remained similar in all treatment groups, whilst occludin expression varied. 'Fold change from vehicle' labelled on the Y-axis in figure **B.** was derived by dividing the ratio of occludin to GAPDH expression for the respective treatment groups with the ratio of occludin to GAPDH for vehicle control. Data are presented as means \pm SEM of fold changes in protein expression compared with vehicle for SB203580, (0.1% v/v) DMSO; $n=3$, $*P<0.05$, $**P<0.01$, $***P<0.001$, 1way ANOVA followed by a Bonferroni post-hoc test, compared to vehicle control, (0.1% v/v) DMSO, whereas combined SB203580+anandamide which is compared to anandamide (30 μ M) alone.. Refer appendix for original blot images (Appendix- Chapter 4(8)).

4.4 Discussion

Findings from *chapter 3* revealed that the endogenous cannabinoid, anandamide and the cytokine, TNF α consistently resulted in enhanced Calu-3 cell permeability. Whilst measurement of the transepithelial resistance provides an indication of the tight junction integrity of epithelial cell layers, it is important to assess the effects of agents that change TEER on the expression of tight junction-associated proteins to probe their mechanism of action. An *in vitro* study in bronchial epithelial cells from normal subjects exposed to TNF α and IFN γ for 72 hours revealed decreases in TEER which corresponded with reductions in tight junction protein expression including occludin, claudin, JAM and ZO-1 (Coyne et al., 2002). Studies have demonstrated that mechanisms for the loss of the tight junction barrier function associated to the stimulation of MAP kinases, particularly ERK1/2 and p38 (Petcchia et al., 2012, Wu et al., 2013). Findings from the present study showed similar observation in which both occludin and ZO-1 expression were significantly reduced following the treatment of either TNF α or anandamide that also involved ERK1/2 and p38 activation

Tight junction proteins, including occludin and ZO-1, are known to be abundantly expressed in Calu-3 cells (Wan et al., 2000, Stewart et al., 2011). In the present study, basolateral application of the endocannabinoid, anandamide or the pro-inflammatory cytokine, TNF α for 48 hours caused a reduction in expression of both occludin and ZO-1. Therefore, this indicates that, as with TNF α , the decrease in TEER induced by anandamide (*Figure 3-4A*) is likely to be due to a reduction in tight junction protein expression. Expression of both of these tight junction-associated proteins were studied as occludin forms an anchorage between epithelial cells, while ZO-1 (Fanning et al., 1998) acts as a scaffold that connects occludin and

actin filament within the complex structure of epithelial tight junction. The expression of other membrane-spanning tight junction components such as claudin and JAM were excluded in the present study as previous work showed that occludin plays the most significant role in maintaining normal epithelial barrier function. For example, genetically-modified MDCK epithelial cells expressing truncated occludin showed increased epithelial permeability despite normal expression of other tight junction proteins (Balda et al., 1996).

The signal transduction pathways involved in modulating epithelial barrier function have only recently received much attention in the hope of gaining further insight into the pathology of diseases and to identify novel therapeutic targets. Several studies have reported that activation of the classical MAP kinase, ERK, was observed in common epithelial cell models, such as MDCK and gut-derived cells, such as primary intestinal epithelial cells, Caco-2 and T84 cell lines, following exposure to various extracellular stimuli that cause tight junction opening (Howe et al., 2005, Ulluwishewa et al., 2011, Lipschutz et al., 2005).

Data obtained from airway epithelial cell models are still lacking to date. The involvement of ERK phosphorylation in the human bronchial epithelial structure was described by Petecchia *et al* who revealed that decompensated tight junction barriers in various bronchial epithelial cell lines, including Calu-3, BEAS-2B and 16HBE14o-, were associated with an elevated phosphorylated ERK level when exposed to TNF α or cigarette smoke challenge (Petecchia et al., 2008, Petecchia et al., 2009, Petecchia et al., 2012). It was noted in these studies that ERK phosphorylation is associated to decrease in tight junction proteins expression that causes the increase in bronchial epithelium permeability. Although their observations have confirmed mechanistic similarities between epithelial cells from bronchial and

other origins, the cells cultured in their studies were not maintained at ALI in Transwell[®] inserts. Hence, the present study aimed to extend the findings reported by Petecchia *et al.* by employing fully differentiated Calu-3 cells, grown at ALI. Particularly, experiments discussed in this chapter aimed to investigate whether activation of ERK is responsible for the reductions in TEER caused by the endocannabinoid anandamide and by TNF α .

ERK activation occurs through its dual phosphorylation at threonine202/tyrosine204 by MEK. Therefore, inhibition of MEK prevents ERK activation. Presence of the MEK inhibitors, either PD98059 or U0126 alone which caused further increases in TEER (refer *Figures 4-3A&B* to *Figure 4-5*). Such observations had never been reported in the literature, though it is currently assumed that these MEK inhibitors may be involved in the production of basal tight junction proteins expression. This is supported by a previous finding in which treatment with PD98059 alone caused an increase in occludin expression in rodent salivary gland Pa-4 epithelial cells (Li and Mrsny, 2000). The MEK inhibitors PD98059 and U0126 prevented the anandamide-induced reduction in TEER. Pre-incubation with PD98059 also prevented the increase in epithelial permeability caused by the anandamide metabolite, arachidonic acid (*Figure 4-5*). Furthermore, the presence of these enzyme inhibitors also prevented the reduction in occludin expression caused by anandamide, suggesting that ERK activation is likely to mediate the effects of the anandamide metabolites on airway epithelial TEER by altering the expression of tight junction proteins. The role of ERK in anandamide-mediated responses is yet to be investigated in future studies. Nevertheless, a recent study using MDCK cells treated at toxic concentration of the Na⁺/K⁺-ATPase pump inhibitor, ouabain resulted in cell detachment (Rincon-Heredia et al., 2014). Subsequent immunohistochemistry experiment in their study

revealed that mechanism of epithelial tight junction disruption was due to internalisation and degradation of the tight junction proteins, such as occludin and ZO-1 that involved ERK activation. On the other hand, a separate study demonstrated increased human umbilical vein endothelial cell (HUVEC) permeability following exposure to hydrogen peroxide (H_2O_2) that was related to occludin hyperphosphorylation. The investigators then reported that the H_2O_2 -induced increase in endothelial cell permeability and occludin phosphorylation was attenuated by the MEK inhibitor, PD98059. Hence, it is speculated that ERK activation caused by anandamide may have similarly caused phosphorylation of the tight junction proteins, which then promoted their endocytosis and degradation hence increases bronchial epithelial cell permeability. However, future studies have yet to prove such speculation on anandamide mechanism.

Similar ERK inhibition with PD98059 and U0126 prevented the effects of on $TNF\alpha$ on epithelial permeability and occludin expression indicating that anandamide leads to activation of the same intracellular signalling pathway as the cytokine, $TNF\alpha$ in disrupting bronchial epithelial barrier function. The rationale for using two different MEK inhibitors was to reduce the likelihood that the effects by $TNF\alpha$ and anandamide-induced decrease in transepithelial resistance were due to inhibition of another enzyme. A comparison assay of multiple protein kinase inhibitors confirmed that PD98059 selectively inhibits the MAPK ERK1/2 pathway and U0126 specifically prevents MEK1 activation at a lower IC_{50} concentration compared to that of PD98059 (Davies et al., 2000). Hence, this suggests that the use of PD98059 and U0126 in this study verified the involvement of ERK activation in anandamide-mediated increase in bronchial epithelial cell permeability.

The involvement of another MAP kinase, p38 in influencing epithelial tight junction expression was also investigated. Pre-incubation with the p38-MAPK inhibitor, SB203580 on the other hand, impeded increased bronchial epithelial permeability and prevented reduced occludin expression due to anandamide. Results in *Figure 4-10* and *Figure 4-11* verified that, like TNF α , anandamide caused tight junction disruption via stimulation of a second route, the p38-MAP kinase cascade, in addition to ERK activation. This finding is supported by evidence from the T84 intestinal epithelial cell line in which there was decreased TEER following apical infection with the human enterocolitis-causing bacteria, *Campylobacter jejuni* (Chen et al., 2006). Subsequent Western blot experiments in their study then showed a similar reduction of occludin expression that was linked with increased phosphorylation of p38-MAP kinase.

Nevertheless, it is acknowledged that the lack of dose-response studies on the MEK and MAPK p38 inhibitors was the limitation in the present study. The experiment can be conducted in such a way that the lowest, most effective dose of the enzyme inhibitor to inhibit anandamide and TNF α at their optimal concentration (as previously discussed in *section 3.4*) will be chosen.

4.5 Conclusion

Dysfunction of the tight junction complex within Calu-3 cell treated with anandamide or TNF α for 48 hours was accompanied by reduced expression of the two key tight junction proteins, occludin and ZO-1. The loss of the membrane spanning protein, occludin and scaffolding protein, ZO-1 then weakens the barrier function of the bronchial epithelium. This confirmed the results obtained from earlier TEER experiments (in *chapter 3*) that demonstrated increased epithelial cell permeability in anandamide and TNF α -treated cells.

Findings reported in this chapter highlight the similarity in the mechanisms of anandamide and TNF α in disrupting the barrier function of bronchial epithelial cells. Increased epithelial permeability and decreased occludin expression induced by anandamide and TNF α were shown to be mediated through ERK MAP kinase signalling, as these responses were attenuated by MEK inhibitors, PD98059 and U0126. Subsequent experiments described in this chapter demonstrated the involvement of another MAP kinase, p38 in anandamide and TNF α -induced tight junction disruption.

Findings from this study thus revealed the involvement of ERK and p38-MAPK activation caused by anandamide and TNF α -induced increase in bronchial epithelial leakiness. However, future studies are still required to establish the relationship between these two kinases in the control of the human airway epithelial structure. Clarity is also needed in relation to the identity of the putative arachidonic acid metabolite that activates the kinase cascades and the link between kinase activation and tight junction protein gene expression.

Findings from this chapter is summarised in *Figure 4-14:-*

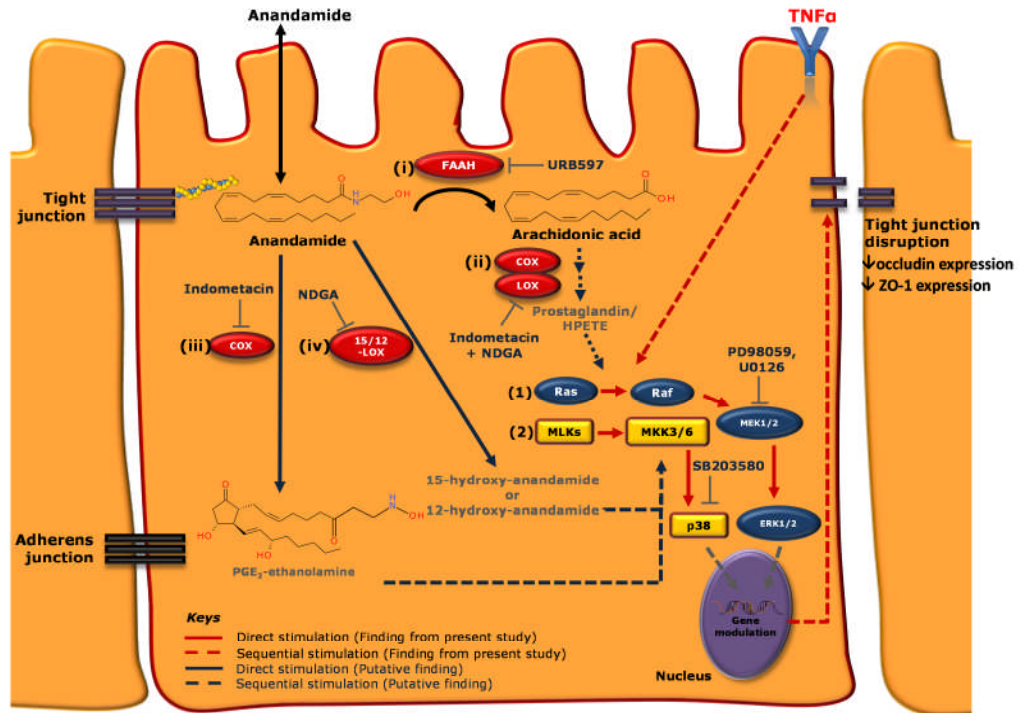


Figure 4-14 The diagram above illustrates the intracellular signalling pathways involved in the endogenous cannabinoid, anandamide and cytokine TNF α -induced increased in Calu-3 cell permeability, as reported in figure 3-10. Red coloured arrows represent intracellular signalling steps involved in tight junction disruption, whereas arrows in black denote the cascades associated to anandamide metabolism. T-shaped lines indicate inhibition. Results from chapter 3 confirmed that anandamide-induced increase in bronchial epithelial permeability was mediated through its metabolites. Hence, findings from this study indicated the involvement of MAPK ERK1/2 (pathway (1)) which can be stimulated by the putative metabolites of anandamide. Consequently, this is thought to modulate gene transcription within the nucleus. Data suggest that ERK activation leads to the decrease in the expression of tight junction proteins, occludin and ZO-1, hence increase in epithelial permeability as its barrier function has been impaired. Similarly, the MAPK p38 cascade (pathway (2)) has been shown to be involved in the anandamide-mediated effect, much like so for MAPK ERK1/2 pathway.

5. The Effects of Phytocannabinoids on Human Bronchial Epithelial Permeability

5.1 Introduction

Previous studies have demonstrated anti-inflammatory effects of phytocannabinoids, mainly Δ^9 -tetrahydrocannabinol (THC) and cannabidiol (CBD), within the respiratory tract following the stimulation of cannabinoid CB₁ and CB₂ receptors. It is noted that the present study focused on the involvement of classical cannabinoid receptors, although both phytocannabinoids are known to stimulate other putative cannabinoid receptors, such as GPR55, GPR18 and various subtypes of PPARs as well as TRP channels.

Evaluation of phytocannabinoids in the airway inflammatory response has predominantly aimed to reverse experimentally-induced bronchoconstriction caused by methacholine or histamine in *in vivo* studies, and exposure to cytokines such as TNF α in an *in vitro* setup. These studies have consistently shown that THC acts through the classical cannabinoid, CB₁ and CB₂ receptors, resulting in bronchodilatation, regardless of the type of allergen used. The effect of CBD in reversing airway inflammation had never been reported in the literature. Nevertheless, CBD has demonstrated its anti-inflammatory effect in other models, for example, by protecting coronary artery endothelial (Rajesh et al., 2007a) and intestinal epithelial (Alhamoruni et al., 2010, Alhamoruni et al., 2012) functions that may be dependent or independent of cannabinoid receptor stimulation. The study using Caco-2 intestinal epithelial cells revealed that the administration of THC or

CBD reversed $\text{TNF}\alpha$ and $\text{IFN}\gamma$ -induced increased cell permeability through an action on CB_1 and CB_2 receptors (Alhamoruni et al., 2012). The effect of both THC and CBD on airway epithelial permeability has never been investigated, although bronchial epithelial disruption is an important feature in asthma and COPD and is thought to play a role in the pathogenesis as well as disease progression.

Mucus hypersecretion is another common feature of asthma and COPD, as a feedback mechanism to minimise intraluminal mechanical stress during excessive coughing (Tarran et al., 2005, Button et al., 2007). MUC5AC and MUC5B glycoproteins, are the two major glycoforms expressed during healthy and inflamed conditions within the pulmonary structure (Kirkham et al., 2002). However, MUC5AC was the only glycoform investigated in the present study as it is mainly secreted by goblet cells within the epithelial layer, in contrast to MUC5B which is hypothesised to be primarily produced by the submucosal glands in the airway smooth muscle compartment (Voynow et al., 2006, Thornton et al., 2008). The effects of phytocannabinoids on airway mucus secretion have never been reported. Hence, a demonstration of an impact of phytocannabinoid(s) on airway mucin production in the present study could provide an interesting insight into an additional effect for treating airway inflammatory diseases.

5.1.1 Aims

This study aimed to identify;

- i. Any direct effects of phytocannabinoids or interactions with selected cytokines, in the human bronchial epithelial cell line, Calu-3.
- ii. Changes in the bronchial epithelial tight junction integrity by conducting FITC-dextran permeability experiments following treatment with a phytocannabinoid, in the presence and absence of a cytokine.
- iii. The possible involvement of cannabinoid receptors, CB₁ and CB₂ in any phytocannabinoid effects.
- iv. Changes in MUC5AC protein expression, following treatment of the phytocannabinoids, in the presence and absence of a cytokine.
- v. The role of the phytocannabinoids in the bronchial contractile responses of porcine lower bronchial sections.

5.2 Materials and Methods

5.2.1 Materials

Materials used for cell culture are listed in *section 2.1.1*; TEER experiment in *section 2.1.2*; FITC permeability in *section 2.1.3*; dot blotting and Western blotting in *section 2.1.4* with the list of primary and antibodies used in *section 2.1.5*; radioligand binding studies in *section 2.1.6*; resazurin assay in *section 2.1.7*; and organ bath studies in *section 2.1.8*.

5.2.2 General Methods

TEER measurements were conducted according to the revised protocol described in *section 2.5.4*. TEER experiments lasting for 48 hours included an hour's pre-incubation with a drug, before a second drug was added. In extended TEER experiments, lasting for 10 days, drugs were added basolaterally every two to three days. TEER readings were measured daily, except on days six and seven. Following TEER measurements, cells were harvested for Western and dot blotting (refer to *section 2.7.1* for sample preparation).

Repeated basolateral THC application was also investigated in this study to evaluate the effect of the phytocannabinoid over 10-days of treatment. The protocol for this experiment was similar to that described in *section 2.5.2* and *section 2.5.2*.

Standard protocol for FD permeability study is described in *section 2.6*; dot blotting in *section 2.7.2*; radioligand-binding studies in *section 2.8*; Western blotting in *section 2.9*; resazurin assay in *section 2.10.1* and bronchial contractility studies in *section 2.11*.

Compound	Concentration studied	Evidence on concentration studied	Notes on site(s) of action/ K_i or IC_{50} values relevant to studied concentration
AM251	100 nM	Refer <i>Table 3-1</i>	
ACEA	100 nM	ACEA (100 nM) inhibited HIV-1 Gp120 protein-induced increase in the permeability of human brain microvascular endothelial cell (Lu et al., 2008).	CB ₁ R agonist/ K_i (CB ₁ R): 1.4 to 5.49 nM. K_i (CB ₂ R): .>2000 nM. Data were obtained from rat brain or spleen samples expressing CB ₁ and CB ₂ receptors (Pertwee, 2010).
Cannabidiol	30 μ M	CBD (30 μ M) exhibited the highest efficacy in reversing TNF α -induced increase in Caco-2 intestinal epithelial permeability (Alhamoruni et al., 2012).	Phytocannabinoid. Lacks affinity for CB ₁ and CB ₂ R. GTP γ S binding studies revealed CBD as an antagonist at the putative cannabinoid receptor, GPR55 instead (Ryberg et al., 2007).
HU-210	100 nM	HU-210 (1 μ M) was shown to increase Caco-2 intestinal epithelial permeability, which further investigation within the same study showed this	Highly potent cannabinoid receptors agonist/ K_i (CB ₁ R): 0.8 nM. K_i (CB ₂ R): 0.6 nM. Data were established from radioligand binding studies,

		<p>was CB₁ receptor mediated (Muccioli et al., 2010).</p> <p>However, concentration used in the present study was 10-folds lower (i.e. 100 nM) owing to the subnanomolar affinity of HU-210 for CB₁ and CB₂ receptors.</p>	<p>measured according to the ability of HU-210 in displacing radiolabelled highly potent cannabinoid receptor agonists, [³H]-CP55,940 from CB₁ and CB₂ receptors (Pertwee, 2010).</p>
IL-1 β	1 ng/ml	<p>IL-1β (1 ng/ml) promoted the endogenous release of pro-inflammatory cytokines, such as GM-CSF, IL6 and IL-8 in primary bronchial epithelial cells (Newton et al., 2007).</p> <p>Although TEER was not measured, a separate study has shown that presence of these cytokines had led to airway epithelial damage (Seagrave et al., 2007).</p>	Not applicable.

JWH133	3 μ M	JWH-133 showed a dose-dependent response (ranging from 0.1 to 4 μ M) in inhibiting vascular smooth muscle cells migration caused by TNF α (Rajesh et al., 2008); indicating 3 μ M was a pharmacologically effective concentration. Its effect on epithelial permeability is still unknown.	CB ₂ R agonist/ K _i (CB ₁ R): 680 nM. K _i (CB ₂ R): 3.5 nM. Data were obtained from rat brain membrane expressing CB ₁ and CB ₂ receptors (Huffman et al., 1999).
SR144528	1 μ M	Refer <i>Table 3-1</i>	
THC	30 μ M	THC (30 μ M) exhibited the highest efficacy in reversing TNF α -induced increase in Caco-2 intestinal epithelial permeability (Alhamoruni et al., 2012)	Phytocannabinoid, also partial CB ₁ and CB ₂ R agonist/ K _i (CB ₁ R): 0.8 nM. K _i (CB ₂ R): 75 nM. Data were established from radioligand binding studies, measured according to the ability of THC in displacing radiolabelled highly potent cannabinoid receptor agonists, [³ H]-CP55,940 or [³ H]-HU243

		from CB ₁ and CB ₂ receptors (Pertwee, 2010).
TNF α	10 ng/ml	Refer <i>Table 3-1</i>

Table 5-1 *List of the drugs used in this chapter and the rationales for the concentrations used.*

5.2.3 Statistical Analysis

Data are presented as the mean \pm standard error of mean (S.E.M). Time-dependent changes in TEER were analysed using a 2-way ANOVA, followed by a Bonferroni post-hoc test. Western blotting data were analysed by 1-way ANOVA followed by a Bonferroni post-hoc test. Results of $P < 0.05$ were considered significant.

5.3 Results

5.3.1 Phytocannabinoids Did Not Directly Affect Bronchial Epithelial Permeability

In contrast to the previously reported effects of anandamide (*chapter 3 & 4*), neither THC (30 μ M) nor CBD (30 μ M) had any effect on TEER readings (*Figure 5-1*) which fluctuated between $87 \pm 8.0\%$ and $104 \pm 8.7\%$ for THC while TEER ranged from $94 \pm 9.9\%$ to $107 \pm 10.4\%$ for CBD. Similarly, resistance readings for vehicle control (0.3% v/v) EtOH and control (no drug) were maintained throughout the whole duration of experiment.

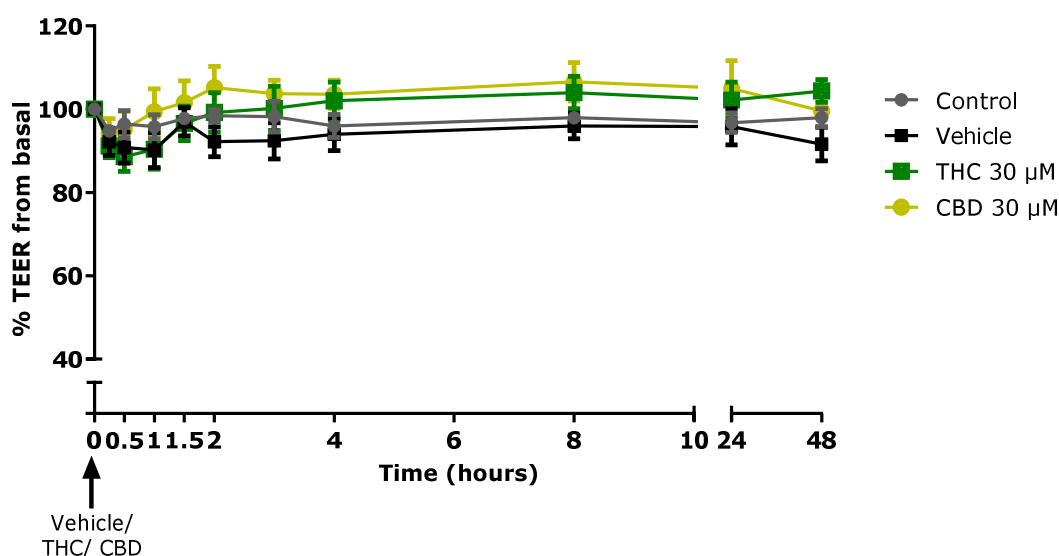


Figure 5-1 Effects of basolateral application of THC (30 μ M) and CBD (30 μ M) alone. Data are expressed as percentage TEER by calculating the relative change in resistance at various time points from basal reading, and are presented as mean \pm SEM; $n=5$. No statistical difference was detected in all treatment groups compared to the control (untreated) cells when data was analysed using 2way ANOVA followed by a Bonferroni post-hoc test.

5.3.2 Phytocannabinoids Reversed Cytokine-Induced Increases in Bronchial Epithelial Permeability

The experiment shown in *Figure 5-2A* involved pre-incubation with the cytokine, TNF α (10 ng/mL), followed by the basolateral addition of phytocannabinoids, THC (30 μ M) or CBD (30 μ M), on the next day. Results from this experiment revealed an initial decrease in TEER at 24 hours, ranging between $72 \pm 10.5\%$ and $76 \pm 7.8\%$, due to TNF α . The decreases in TEER readings were fully reversed by both phytocannabinoids to $105 \pm 10.0\%$ for THC and $103 \pm 4.5\%$ for CBD, and they were maintained at 72 hours following TNF α exposure.

Basolateral pre-administration of TNF α (10 ng/mL) in the presence of EtOH (0.3% v/v) showed the anticipated reduction in TEER (*Figure 5-2B*). Pre-treatment with THC (30 μ M) completely prevented TNF α -induced TEER reduction which persisted for 48 hours. TEER was also significantly maintained throughout 48 hours after TNF α exposure, when treated with CBD (30 μ M).

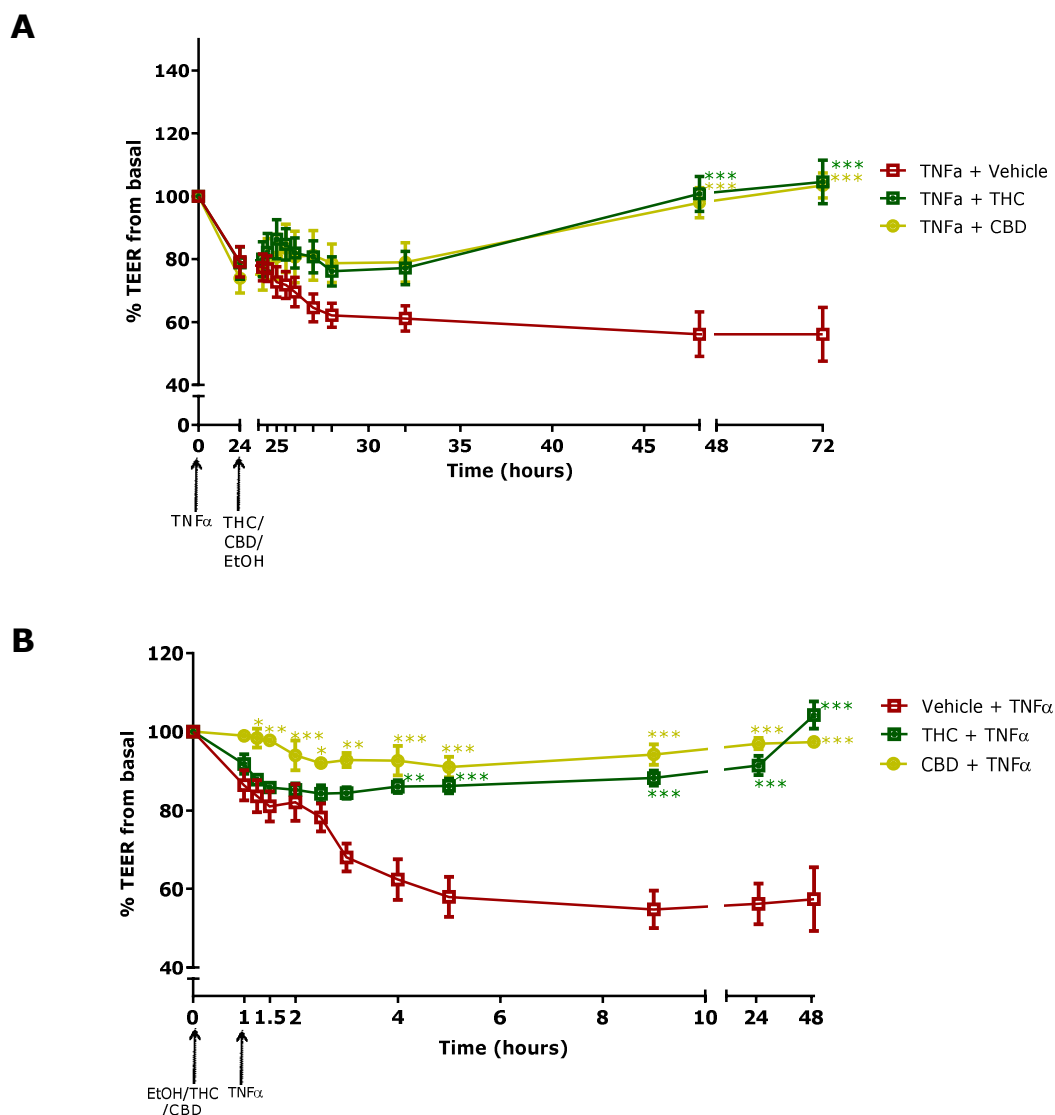


Figure 5-2 Effects of basolateral application of THC (30 μ M) and CBD (30 μ M) in the presence of TNF α onto 21-day old Calu-3 cells cultured in ALI. **A.** Change in TEER following 24 hour incubation of TNF α (10 ng/mL). **B.** The effect on TEER when Calu-3 cells were pre-incubated with the phytocannabinoids for an hour, before TNF α was administered following an hour's incubation with THC (30 μ M). Data are expressed as percentage TEER by calculating the relative change in resistance at various time points from basal reading, and are presented as mean \pm SEM; $n=3-5$, * $P<0.05$, ** $P<0.01$, *** $P<0.001$, 2way ANOVA followed by a Bonferroni post-hoc test, compared to A. control (no drug); B. 0.3% v/v EtOH and TNF(10 ng/mL).

5.3.3 THC Prevents Calu-3 Epithelial Permeability in the Presence of Other Pro-inflammatory Mediators

Experiments shown in *Figure 5-3A* and *B* demonstrate the ability of THC to reverse the increases in bronchial epithelial permeability caused by IL-1 β , another pro-inflammatory mediator involved in airway inflammation.

The addition of IL-1 β (1 ng/mL) into the basolateral side of Transwells® produced a similar effect to that of TNF α , as TEER readings were significantly reduced throughout the experiment (see *Figure 5-3A*). Pre-incubation with THC (30 μ M) prevented the IL-1 β -induced fall in TEER for 48 hours.

Treatment with anandamide (30 μ M) again produced a significant decrease in TEER throughout the 48-hour experiment, as seen in *Figure 3-8A* and this was fully prevented by pre-incubation with THC (30 μ M). It is worth noting that the concentration of EtOH (0.6% v/v) used as drug vehicle in this experiment (*Figure 5-3B*) was twice that employed in other TEER assays, owing to the presence of both anandamide (30 μ M) and THC (30 μ M). Despite the relatively high EtOH content, TEER remained steady, with only slight fluctuations ranging between $87 \pm 6.0\%$ and $100 \pm 2.3\%$.

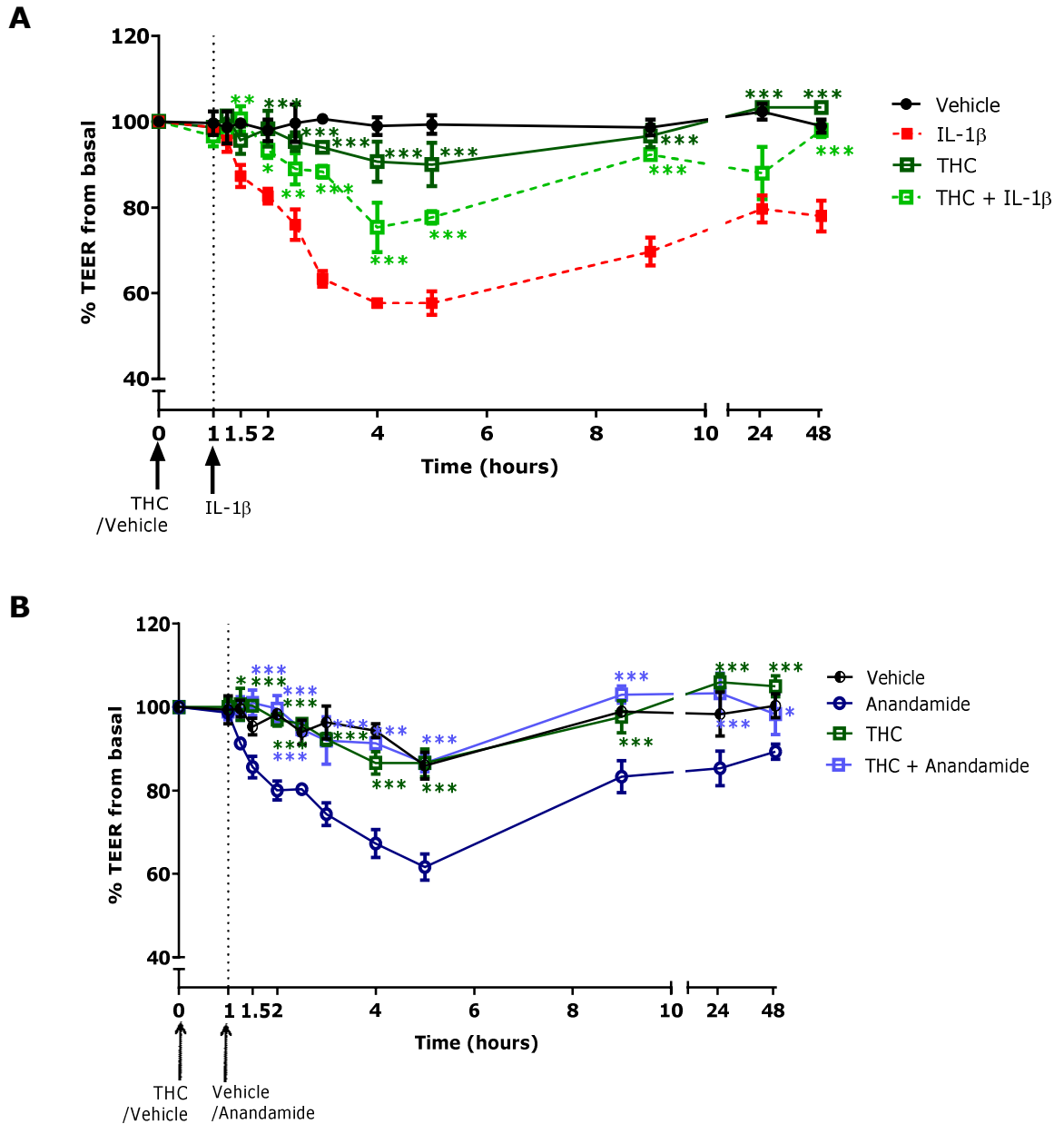


Figure 5-3 Effects of basolateral application of THC (30 μ M) in the presence of **A.** IL-1 β (1 ng/mL) or; **B.** anandamide (30 μ M). Data are expressed as percentage TEER by calculating the relative change in resistance from basal at various time points, and are presented as mean \pm SEM; $n=3$, * $P<0.05$, ** $P<0.01$, *** $P<0.001$, 2way ANOVA followed by a Bonferroni post-hoc test, compared to **A.** IL-1 β (1 ng/mL) **B.** (0.3% v/v) EtOH and anandamide (30 μ M); except anandamide which is compared to vehicle control (0.6% v/v) EtOH.

5.3.4 Effect of THC on P_{app} (Epithelial Permeability) in TNF α -treated Calu-3 Cells

The bar chart in *Figure 5-4B* demonstrates that treatment with TNF α alone showed a drastic increase in FD4 dextran paracellular permeability ($P < 0.001$ compared to vehicle control, 1-wayANOVA). The basolateral application of THC alone did not alter FD4 dextran permeability rate through the Calu-3 cell layers. Results also revealed that the increase in P_{app} caused by TNF α was prevented in the presence of THC ($P < 0.001$ compared to TNF α alone, 1-wayANOVA).

Data from this experiment thus confirmed the correlation that a decrease in TEER is mirrored by an increase in P_{app} .

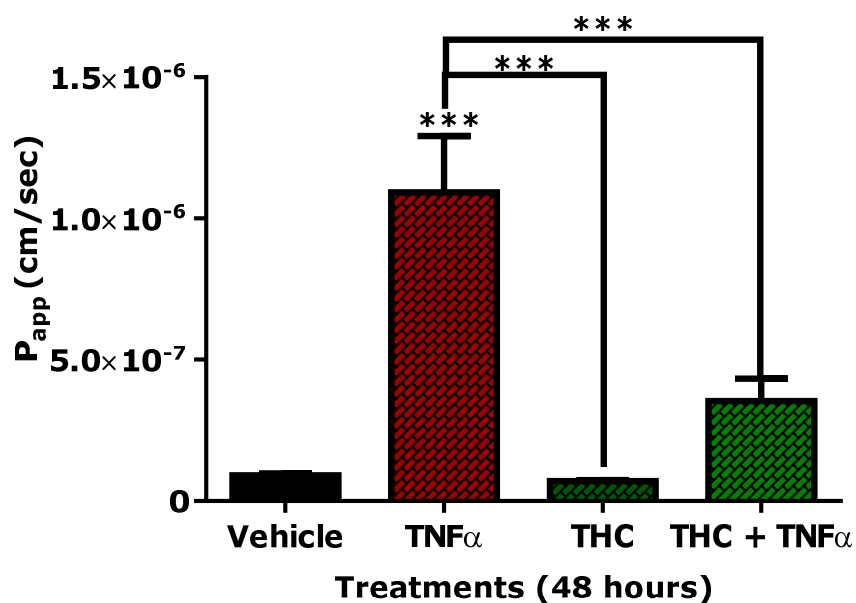


Figure 5-4 Effect of the corresponding treatments on FD4 paracellular permeability in Calu-3 cells. Epithelial permeability is represented as apparent permeability coefficient (P_{app}) calculated according to the equation in section 2.6.3. Data are presented as mean \pm SEM; $n=3$; *** $P<0.001$ 1way ANOVA followed by a Bonferroni post-hoc test, compared to $TNF\alpha$, except $TNF\alpha$ against the vehicle control, (0.3%v/v) EtOH.

5.3.5 The Effect of Cannabinoid Receptor Antagonism on THC-mediated Reversal of TNF α -induced Increase in Permeability

Vehicle control (0.31% v/v) EtOH alone produced a gradual decrease in resistance up to 2.5 hours (*Figure 5-5*). Treatment with TNF α alone was not included in this set of experiment. It is noted that TNF α caused consistent drop in TEER to a minimum of 50 to 65% after 4 hours (refer *Figure 5-2B*) THC prevented the decrease in TEER with TNF α . However, in the presence of the CB₁ antagonist, AM251 (100 nM) or the CB₂ antagonist, SR144528 (1 μ M), the ability of THC (30 μ M) to reverse the TNF α (10 ng/mL)-induced decrease in TEER was inhibited.

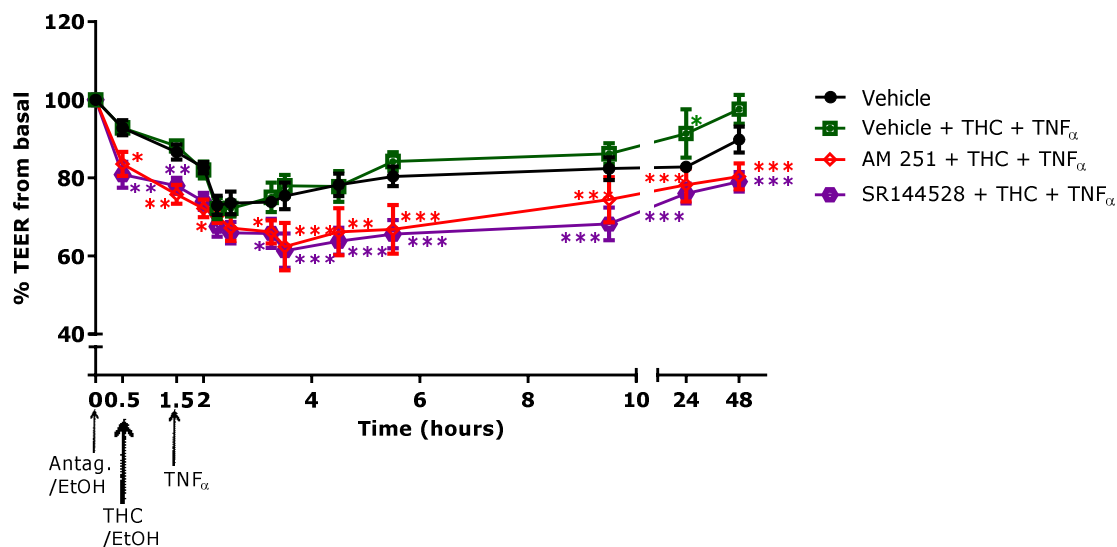


Figure 5-5 Effect of basolateral application of either the selective CB₁ antagonist, AM 251 (100 nM) or the selective CB₂ antagonist, SR144528 (1 μM) in the presence of THC (30 μM) and TNF_α (10 ng/mL); Data are expressed as percentage TEER by calculating the relative change in resistance at various time points from basal reading, and are presented as mean ± SEM; n=3-5, *P<0.05, **P<0.01, ***P<0.001, 2way ANOVA followed by a Bonferroni post-hoc test, compared to (0.01% v/v) EtOH, THC (30 μM) and TNF_α (10 ng/mL) treatment combination; except THC (30 μM), which is compared to vehicle control (0.31% v/v) EtOH.

5.3.6 The Effect of Competitive Antagonism with Cannabinoids Receptors Antagonists on CBD Action

Treatment with CBD (30 μ M) also prevented the reduction in TEER due to TNF α (10 ng/mL) (*Figure 5-6A and B*). However, neither the CB₁ antagonist, AM251 (100 nM), CB₂ antagonist, SR144528 (1 μ M) nor a combination of the two antagonists together reversed this effect of CBD (*Figure 5-6B*).

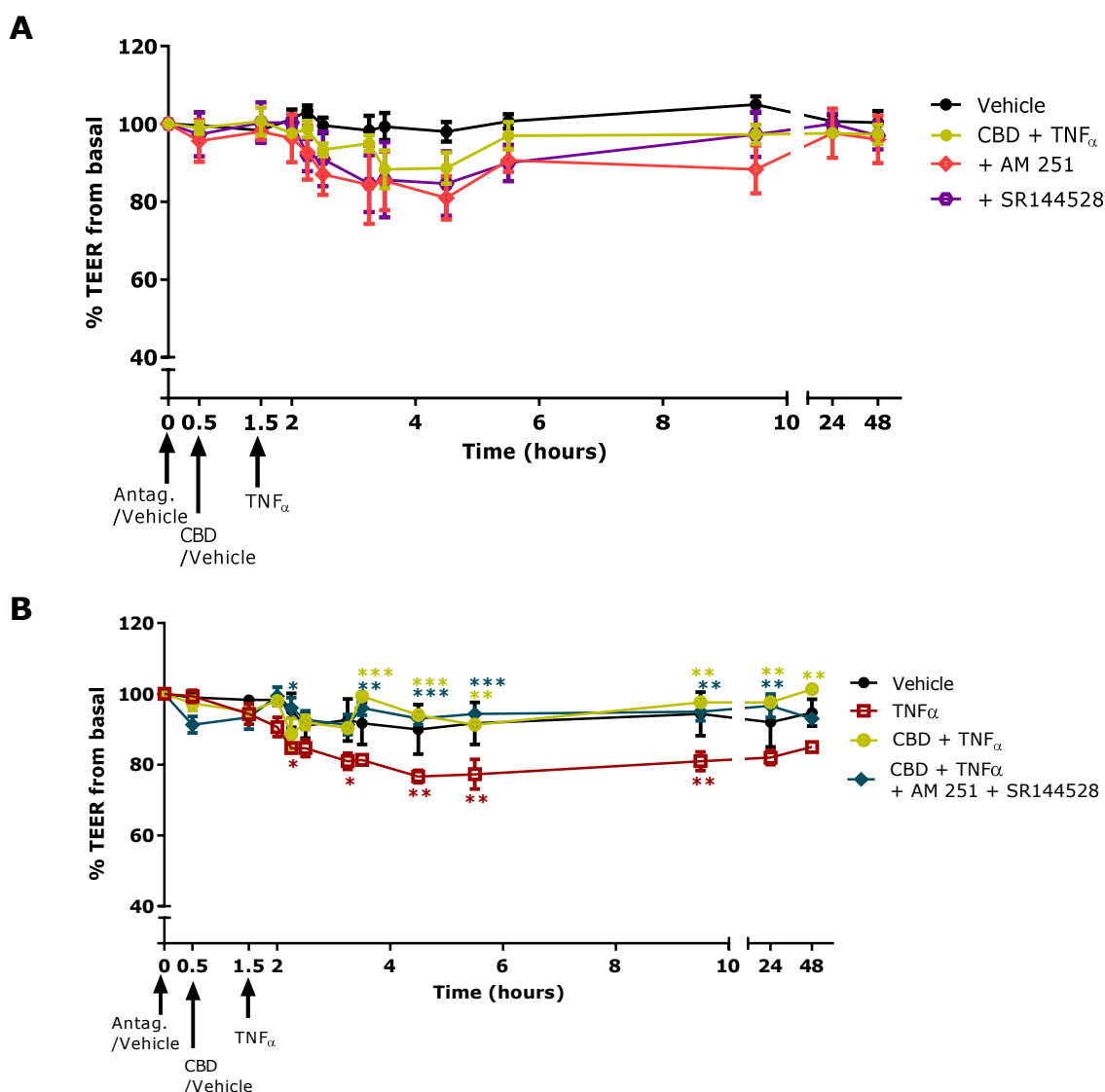


Figure 5-6 Effect of basolateral application of **A.** either the selective CB_1 antagonist, AM 251 (100 nM) or the selective CB_2 antagonist, SR144528 (1 μ M) in the presence of CBD (30 μ M) and TNF α (10 ng/mL); **B.** Effect of combination basolateral application of AM251 and SR144528 with CBD and TNF α . Data are expressed as percentage TEER by calculating the relative change in resistance at various time points from basal reading, and are presented as mean \pm SEM; $n=3$, * $P<0.05$, ** $P<0.01$, *** $P<0.001$, 2way ANOVA followed by a Bonferroni post-hoc test, compared to **A.** CBD (30 μ M)+TNF α (10 ng/mL) treatment combination; except CBD (30 μ M), which is compared to vehicle control (0.31% v/v) EtOH; **B.** TNF α (10 ng/mL); except TNF α which is compared to vehicle control (0.32% v/v).

5.3.7 Investigation of Cannabinoid Receptor Expression in Calu-3 Cells

5.3.7.1 Radioligand Binding Studies

Homogenised rat brain tissues samples were used as a positive control in this investigation as it is known that cannabinoid receptors are abundantly expressed in the central nervous system.

Results in *Figure 5-7* indicate significant displacement of [3 H]-CP 55,940 by HU-210, but not JWH133, in rat brain membranes. On the contrary, Calu-3 cells showed a significant increase in [3 H]-CP 55,940 binding in the presence of HU-210 and JWH133.

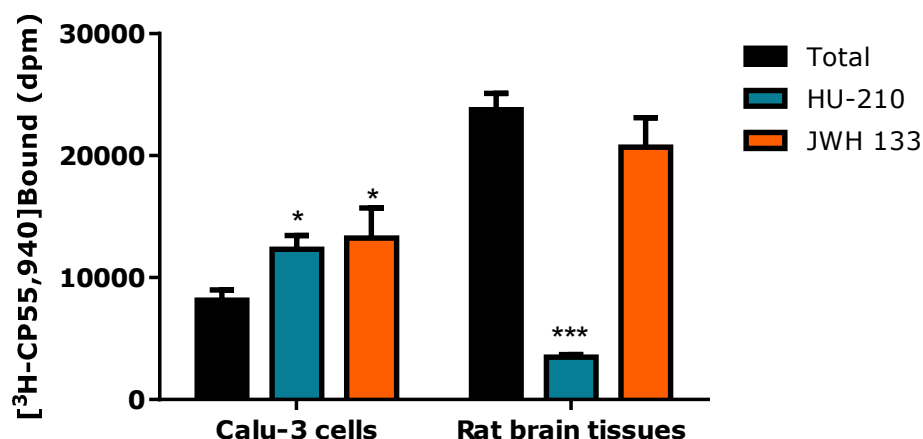


Figure 5-7 Measurement of [3 H-CP 55,940] binding shown in Calu-3 and rat brain tissue membranes. Non-specific binding was measured in the presence of HU-210 and JWH133 at saturating concentrations of 1 μ M and 500 nM respectively. Data are presented as mean \pm SEM; $n=3$, * $P<0.05$, *** $P<0.001$, 2-way ANOVA followed by a Bonferroni post-hoc test, compared to total [3 H-CP 55,940] binding.

5.3.7.2 Western Blotting Studies

Following the unsuccessful attempt to demonstrate the presence of CB₁ or CB₂ receptors by radioligand-binding studies, expression of the CB₁ and CB₂ receptors was probed using Western blotting studies. In this investigation, Calu-3 cells samples cultured in different conditions were compared; i.e. ALI versus LLI.

i. CB₁ Receptor Expression

Rat cerebellum was used as a positive control in the investigation of CB₁ receptor expression in Calu-3 cells, as it is known that these receptors are abundantly expressed in the central nervous system. BV-2 cells, a murine microglial cell line, were used as a negative control since it was previously reported (Hassan et al., 2014) that the cells express neither CB₁ nor CB₂ receptors. A comparison of CB₁ receptor expression was also made between Calu-3 cells grown at ALI and LLI (see *Figure 5-8*).

The expression of CB₁ receptor was significantly greater in cells grown at ALI compared with LLI (see *Figure 5-8A*). The apparent molecular mass for CB₁ receptor was detected at approximately 54 kDa, close to its predicted molecular weight of 60 kDa. It is noted that the expression of CB₁ receptor in the negative control, BV-2 cells was minimal.

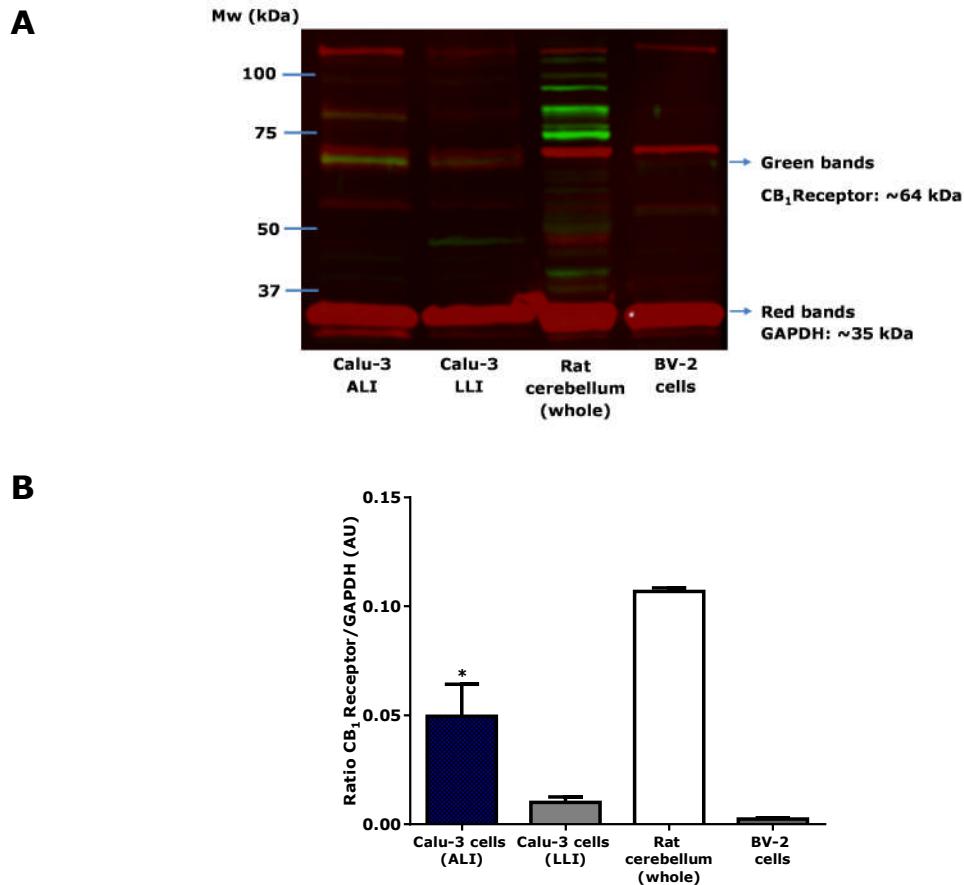


Figure 5-8 A. Western blot image showing samples that were treated with polyclonal anti-CB₁ receptor rabbit antibody and with anti-GAPDH mouse antibody as a loading control. Samples of Calu-3 cells grown at ALI were harvested at day 21 of culture; whereas cells of the LLI were obtained at day 5 of culture, when cells were 100% confluent in Transwell[®] inserts. Expression of CB₁R was confirmed by comparing immunoblotting of whole rat cerebellum sample as positive control, and BV-2 cells as negative control. Predicted molecular weight of CB₁R was approximately 64 kDa. **B.** Fluorescence intensity was recorded for the respective samples. Data are presented as mean \pm SEM; $n=3$, $*P<0.05$, $**P<0.01$ 1way ANOVA followed by a Bonferroni post-hoc test. AU: arbitrary units. Data obtained for CB₁R expression in Calu-3 cells cultured at ALI was compared against cells that were grown in LLI. Refer appendix for original blot images (Appendix- Chapter 5(1))

ii. CB₂ Receptor Expression

Spleen is reported to express CB₂ receptor highly, hence rat spleen was used as a positive control, while the human neuroblastoma SH-SY5Y cells were chosen as a negative control based on the evidence of low mRNA expression of CB₂ receptor in these cells (Dionisi et al., 2007).

As was the case for CB₁ receptor, CB₂ receptor expression was increased in Calu-3 cells grown in ALI compared to LLI (*Figure 5-9A and B*). The apparent molecular mass for CB₂ receptor was detected at 43 kDa, close to its predicted molecular weight of 35 kDa.

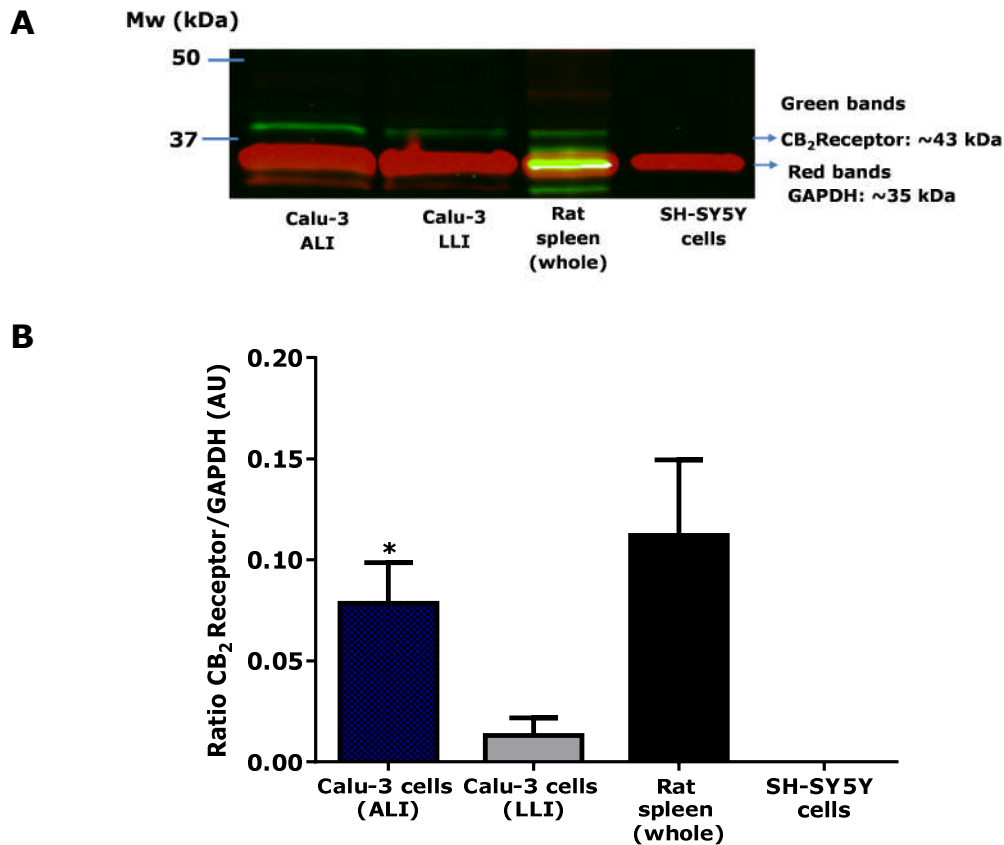


Figure 5-9 A. Western blot image showing samples that were treated with polyclonal anti-CB₂ receptor rabbit antibody with anti-GAPDH mouse antibody as loading control. Samples of Calu-3 cells grown at air-liquid interface (ALI) were harvested at day 21 of culture; whereas cells of the liquid-liquid interface (LLI) was obtained at day 5 of culture, when cells were 100% confluent in Transwell® inserts. Expression of CB₂R was confirmed by comparing immunoblotting of whole rat spleen samples as positive control, and SH-SY5Y cells as negative control. Predicted molecular weight of CB₂R was approximately 43 kDa. **B.** Fluorescence intensity was recorded for the respective samples. Data are presented as mean \pm SEM; n=3, *P<0.05, **P<0.01 1way ANOVA followed by a Bonferroni post-hoc test. AU: arbitrary units. Data obtained for CB₂R expression in Calu-3 cells cultured at ALI was compared against cells that were grown in LLI. Refer appendix for original blot images (Appendix- Chapter 5(1)).

5.3.8 Cannabinoid Receptor Agonists Reverse TNF α -induced Increases in Bronchial Epithelial Permeability

This series of TEER experiments using cannabinoid receptor agonists was included to test further the potential involvement of cannabinoid receptors in control of epithelial cell permeability.

Stimulation of both CB₁ and CB₂ receptors with HU210 or each one individually with JWH133 (CB₂R) or ACEA (CB₁R) had no significant effect on Calu-3 cell permeability when added alone (*Figure 5-10A*).

As expected, the presence of TNF α (10 ng/mL) in the basolateral side of Transwells[®] caused reproducible reduction in TEER (*Figure 5-10B*). TEER recovered more promptly in the presence of JWH133 (3 μ M) and HU210 (100 nM) than with ACEA (100 nM), returning to control values at 8 hours.

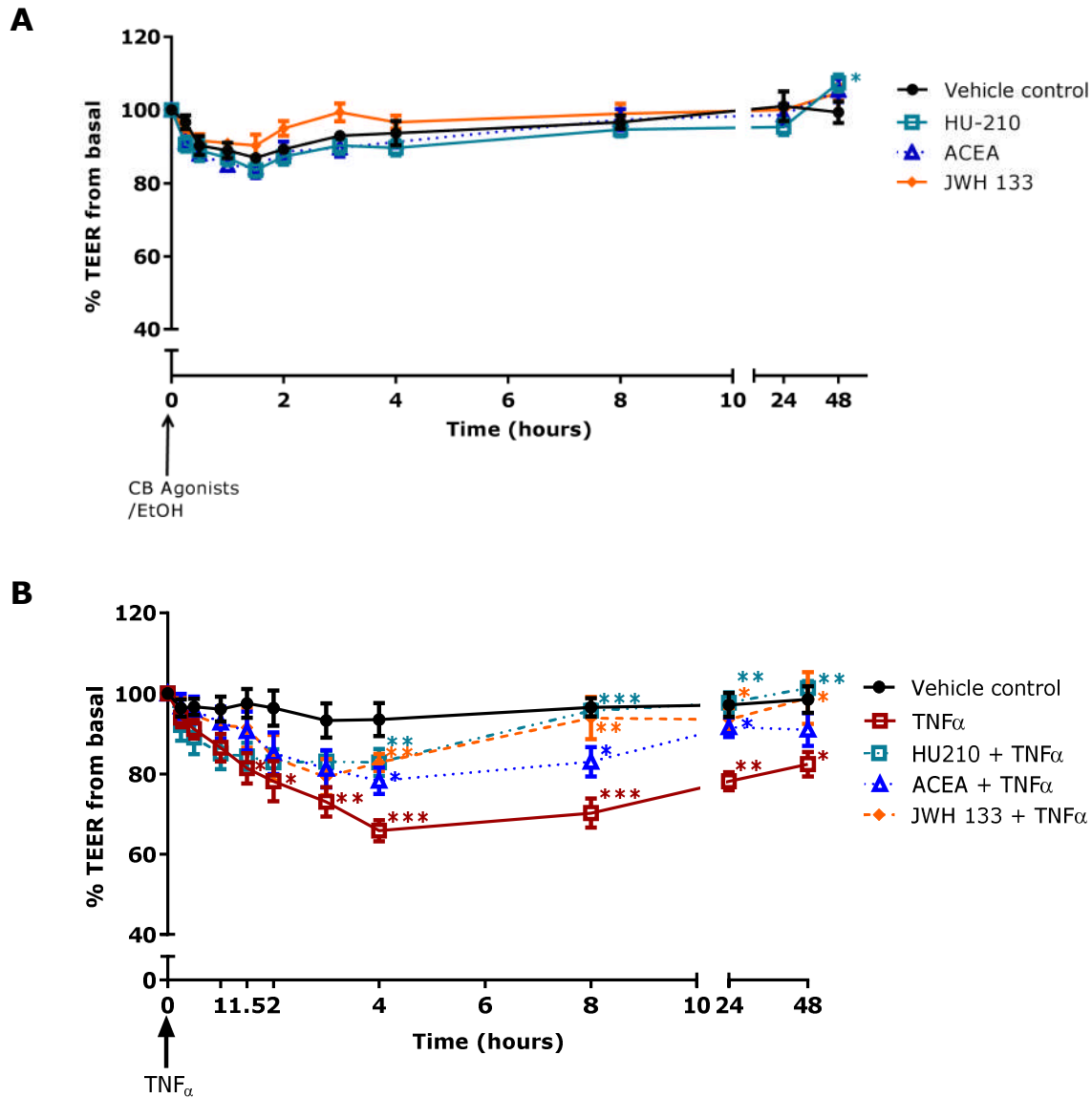


Figure 5-10 Effects of basolateral application of **A.** A highly potent cannabinoid CB_1/CB_2 receptor agonist HU-210 (100 nM), a selective CB_1R agonist ACEA (100 nM) or a selective CB_2R agonist JWH 133 (3 μ M) alone and; **B.** ACEA and JWH 133 in the presence of $TNF\alpha$ (10 ng/mL). Data are expressed as percentage TEER by calculating the relative change in resistance at various time points from basal reading, and are presented as mean \pm SEM; $n=3-8$, * $P<0.05$, ** $P<0.01$, *** $P<0.001$, 2way ANOVA followed by a Bonferroni post-hoc test, compared to: **A.** vehicle control (0.01% v/v) EtOH; **B.** $TNF\alpha$ (10 ng/mL); except $TNF\alpha$, which is compared to vehicle control (0.01% v/v) EtOH.

5.3.9 THC Decreases Mucin (MUC5AC) Protein Expression

As previously described in *section 2.7.1*, samples for this assay were harvested from Calu-3 cells after the completion of TEER studies. Vehicle indicated in *Figure 5-11A* represents the vehicle control used for THC, (0.3% v/v) EtOH. Untreated cells were included as a neutral (control) to measure the relative change in MUC5AC protein expression in the presence of drugs.

0.3% v/v EtOH (vehicle control for THC) alone produced an apparent increase ($135 \pm 14.2\%$), in MUC5AC protein expression, although this was not statistically different from the untreated (control) group (see *Figure 5-11A*). TNF α significantly increased MUC5AC protein expression and this was completely prevented by pre-exposure of the cells to THC. It is noted that THC alone had no effect on MUC5AC expression.

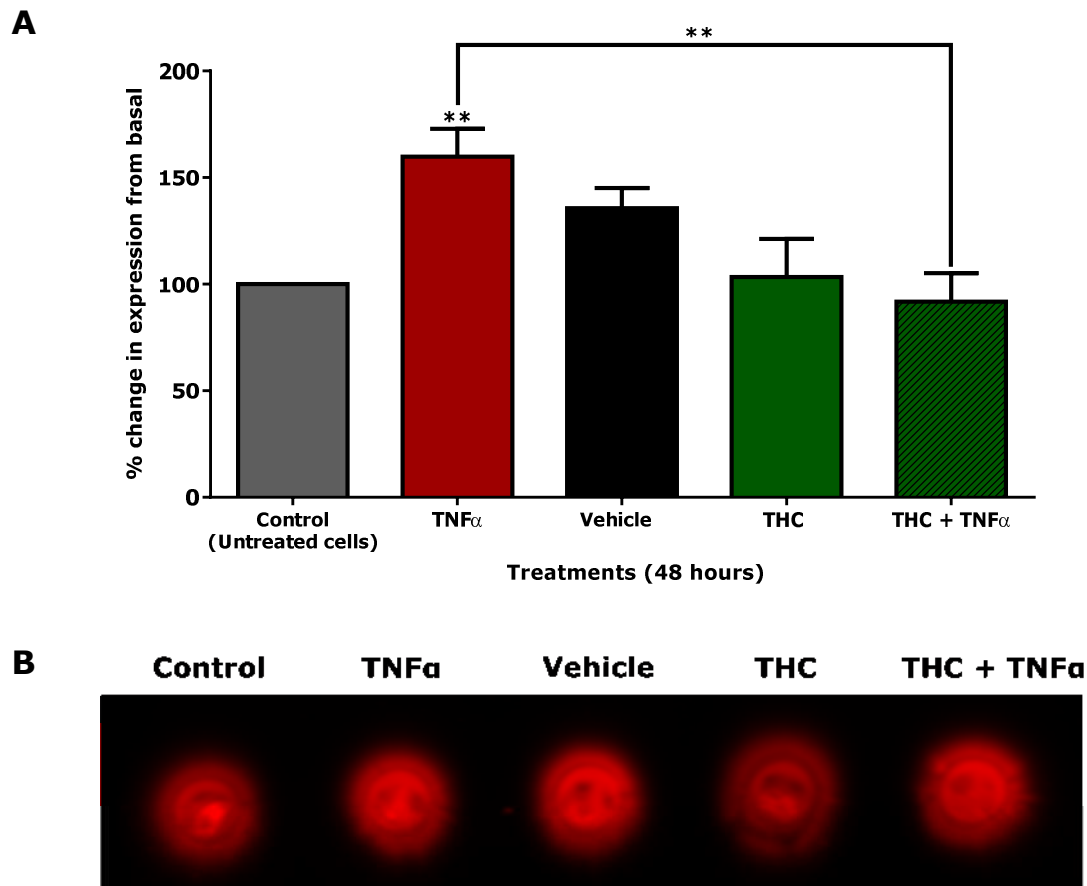


Figure 5-11 A. Fluorescence intensity quantification for MUC5AC expression measured by dot blotting (fluorescent images shown in panel **B.** following treatments of TNF α (10ng/mL), 0.3(v/v) EtOH, THC (30 μ M) or combination treatment of THC (30 μ M) and TNF α (10 ng/mL) on Day 21 Calu-3 epithelial cells, cultured at ALI. Data are expressed as percentage change of fluorescence intensity and are presented as mean \pm SEM (n=6), ***P<0.01, 2way ANOVA followed by a Bonferroni post-hoc test. Cells treated with TNF α was compared with the control (untreated) group and combined treatment of THC and TNF α . Treatment with THC alone was compared to its vehicle control (0.3% v/v) EtOH.

5.3.10 THC Concentrations Up to 30 μ M Do Not Affect Calu-3 Cell Viability

Assessment of Calu-3 cell viability following treatment with increasing concentrations of THC for 48 hours was conducted using the fluorescence-based, resazurin assay. Resorufin concentrations in the medium from the basolateral and apical sides of Transwells[®] were quantified using a fluorometer.

Figure 5-12 shows the resorufin concentrations (represented as arbitrary optical densities (ODs) in both, apical and basolateral sides of Transwells[®], in cells treated with increasing THC concentrations. Neither the vehicle control (0.3% EtOH) nor THC at concentrations up to and including 30 μ M affected Calu-3 cell viability.

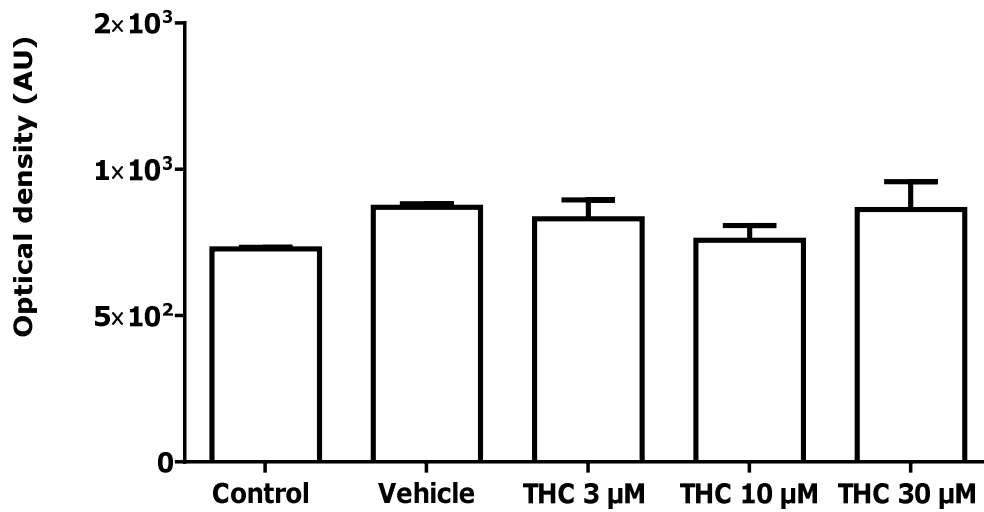


Figure 5-12 No effect on viability of Calu-3 cells treated with increasing concentrations of THC (3, 10 and 30 μ M) for 48 hours. 'Control' group represents untreated 21-day old Calu-3 cells cultured in ALI; (0.3% v/v) EtOH was included as a vehicle control for the highest THC concentration, 30 μ M. Results for cell viability are presented as optical density at an excitation wavelength of 530 nm (in arbitrary units) which reflects resorufin concentration detected in the medium of apical and basolateral compartments. Data are expressed as mean \pm SEM; $n=3$; $P>0.05$, 1way ANOVA followed by a Bonferroni post-hoc test. There are no significant differences due to THC (at all of the concentrations) compared to the untreated group (control).

5.3.11 The Effect of Repeated THC Treatment on Bronchial Epithelial Permeability

5.3.11.1 Repeated THC Treatment Maintains and Prevents TNF α - induced Increased Epithelial Permeability

TEER measurements were taken for an extended period of 10 days to investigate the effects of repeated THC treatment (*Figure 5-13A*) and to simulate a chronic exposure of Calu-3 cell layer to the cytokine, TNF α (*Figure 5-13B*). This experiment included the study of increasing concentrations of THC up to and including 30 μ M, with (0.3% v/v) EtOH as the vehicle control representing the highest THC concentration used. Drugs were administered basolaterally, every two to three days. The experiment shown in *Figure 5-13B* includes addition of TNF α (10 ng/mL) administration following an hour incubation of THC (30 μ M) or vehicle control, (0.3% v/v) EtOH.

TEER readings for vehicle control, (0.3% v/v) EtOH were consistently maintained throughout the duration of the 10-days experiment (*Figure 5-13A and B*).

Treatment with THC alone over 10 days showed a concentration-dependent increase in TEER with a rise to a maximum of $161 \pm 11.9\%$ of control on day 10 in the presence of 30 μ M THC (*Figure 5-13A*). In this experiment, TNF α (10 ng/mL) produced a modest decrease in TEER (*Figure 5-13B*), which was maintained for 10 days and was abolished by repeated application of THC to the cells.

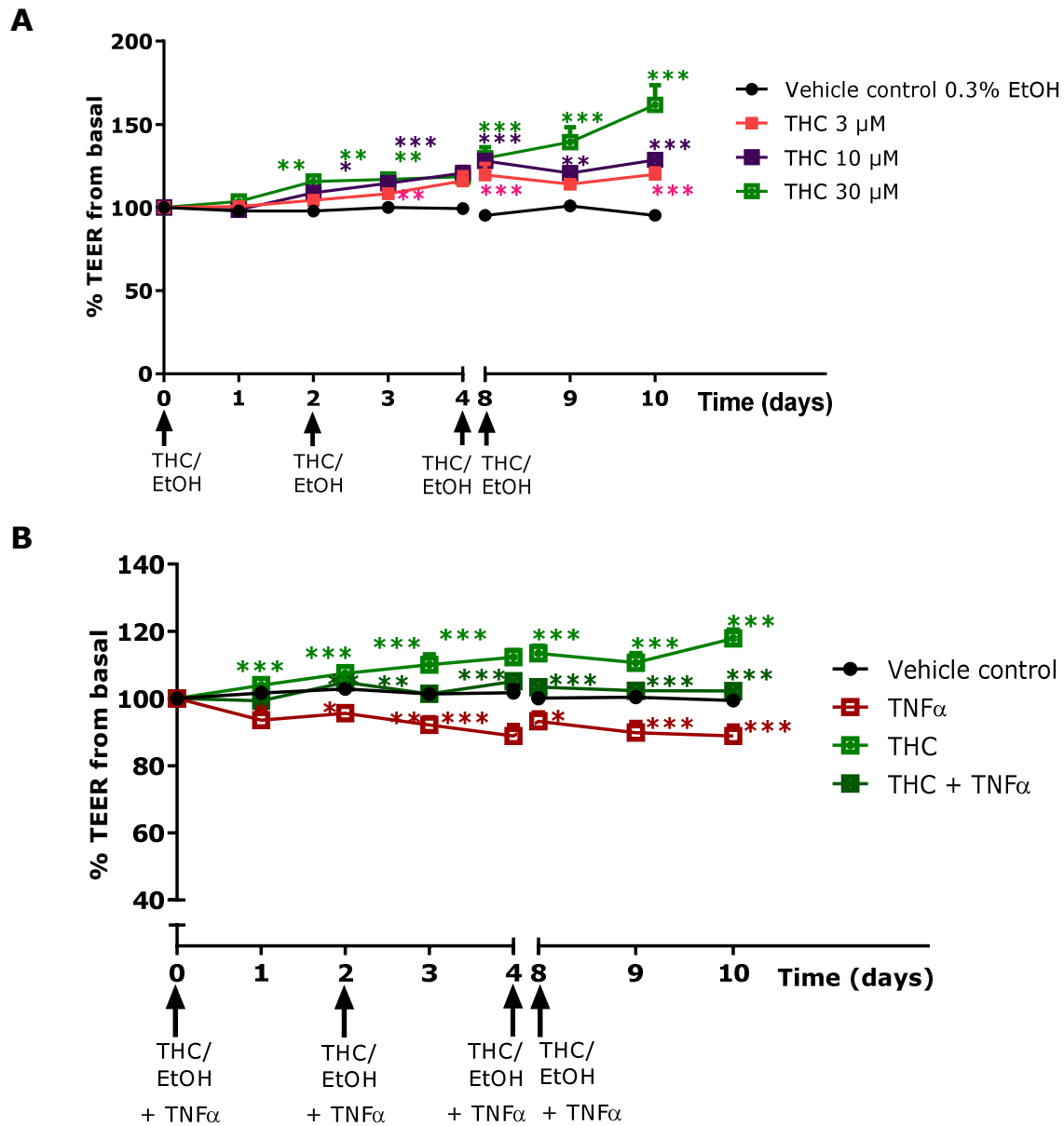
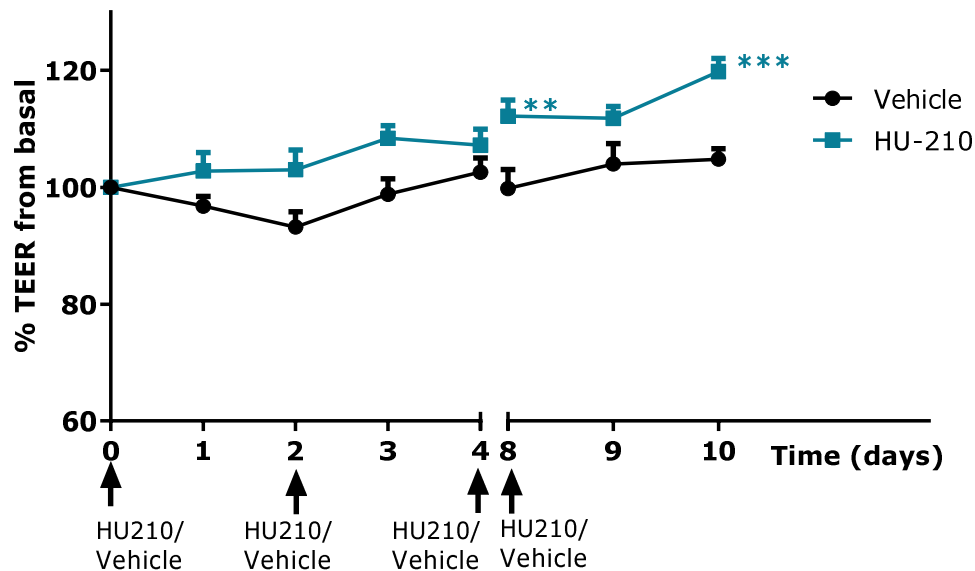


Figure 5-13 Effects of repeated basolateral application of **A.** various concentrations of THC (3, 10 and 30 μ M) alone; **B.** a single concentration of THC (30 μ M), with or without $TNF\alpha$ (10 ng/mL) for 10 days. Data are expressed as percentage TEER by calculating the relative change in resistance at various time points from basal reading, and are presented as mean \pm SEM; $n=3-9$, * $P<0.05$, ** $P<0.01$, *** $P<0.001$, 2way ANOVA followed by a Bonferroni post-hoc test, compared to **A.** vehicle control (0.3% v/v) EtOH; **B.** $TNF\alpha$ (10 ng/mL); except $TNF\alpha$, which is compared to vehicle control (0.3% v/v) EtOH.

5.3.12 Effect of Long-term Exposure to a Cannabinoid Receptor Agonist on Calu-3 cell Permeability

As repeated administration of THC produced increases in TEER, this experiment was repeated with a CB receptor agonist. Repeated administration of HU-210 for 10 days produced increases in TEER similar to those seen for THC (*Figure 5-14*). Calu-3 epithelial cell resistance was significantly elevated, compared to vehicle control (0.01% v/v) EtOH. Data show that TEER was increased to a maximum of $120 \pm 2.3\%$ of control on Day 10.



*Figure 5-14 Effects of repeated basolateral application of a highly potent cannabinoid CB₁/CB₂ receptor agonist, HU-210 (100 nM) for 10 days. Data are expressed as percentage TEER by calculating the relative change in resistance at various time points from basal reading, and are presented as mean \pm SEM; $n=5$, * $P<0.05$, ** $P<0.01$, *** $P<0.001$, 2way ANOVA followed by a Bonferroni post-hoc test, compared to vehicle control (0.01% v/v) EtOH.*

5.3.13 Repeated THC (30 μ M) Treatment Does Not Alter Proliferation Rate in Calu-3 Epithelial Cells

As previously demonstrated in *Figure 5-15*, treatment with THC increased TEER readings. The MTT assay was, therefore, employed to address the possibility that THC induces cell proliferation, which could reduce cell permeability by thickening of the Calu-3 cell layer.

Results in *Figure 5-15* show the absorbance due to formazan, which reflects the number of proliferating Calu-3 cells, when treated with THC (30 μ M) or TNF α (10 ng/ml) alone, or in combination. Regardless of treatment groups, there was no significant difference in cell proliferation.

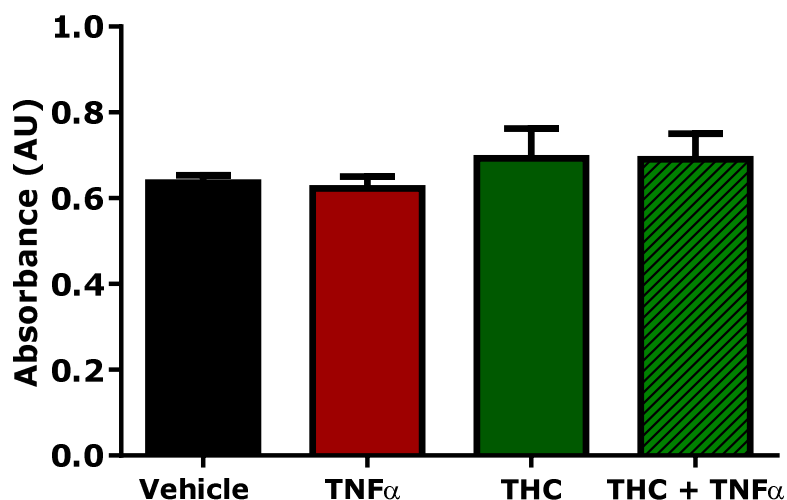


Figure 5-15 Effects of THC (30 μ M) or TNF α (10 ng/mL) alone, or in combination for 10 days on the proliferation of 19-day old Calu-3 cells cultured at ALI. EtOH (0.3% v/v) was included as the vehicle control for THC (30 μ M). Results representing the number of proliferating cells are presented as optical density (in arbitrary units) and reflect the concentration of formazan detected in DMSO applied on the apical side of Transwells[®], at an excitation wavelength of 570 nm. Data are expressed as mean \pm SEM; n=3; $P>0.05$, 1-way ANOVA followed by a Bonferroni post-hoc test; no treatment showed any significant difference compared to vehicle control.

5.3.14 THC Does Not Reverse Carbachol-induced Bronchoconstriction in Porcine Tissue

Having observed decreases in Calu-3 cell permeability due to THC, *in vitro* organ bath experiments using porcine bronchial tissue were conducted to explore the possibility that THC produces bronchodilator responses through effects on the epithelium. In some experiments the porcine bronchial epithelium was denuded (described as ‘without epithelium’ group in *Figure 5-16*).

Carbachol concentrations (from 1 μ M up to 100 μ M) were administered to induce tissue contraction. The effect of THC (30 μ M) to reverse carbachol-induced contraction in porcine bronchial tissue was investigated with or without epithelium (*Figure 5-16*). Exposure to vehicle control, (0.3% v/v) EtOH, produced modest reduction, although not significantly different ($P>0.05$, paired Student’s t-test), in the contractile response to carbachol in the presence or absence of intact epithelium. Addition of THC (30 μ M) did not produce any significant modification of the effect of carbachol.

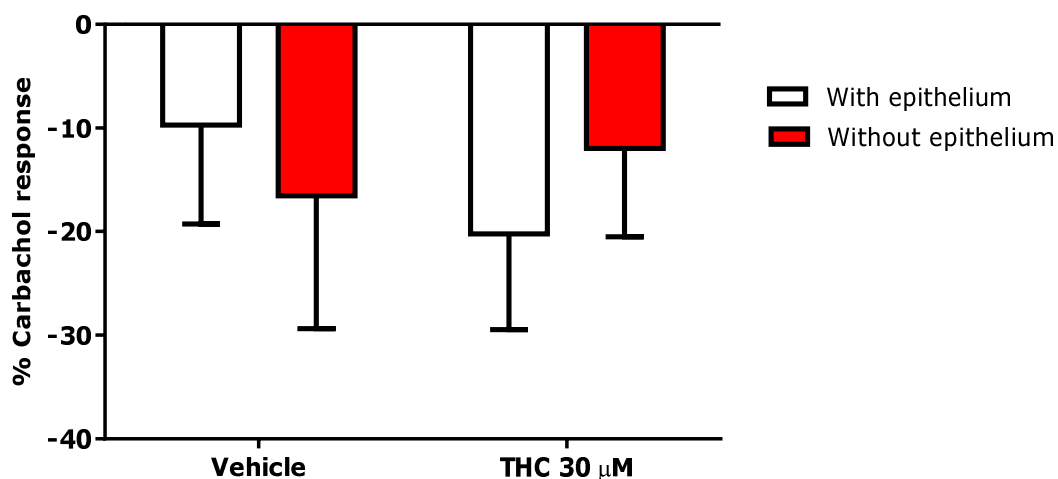


Figure 5-16 Effect of porcine bronchial epithelium denudation on the relaxation to carbachol-induced contraction following the addition of THC (30 μ M) or its vehicle control, (0.3% v/v) EtOH. Results are expressed as percentage of the carbachol response; in which a negative value denotes relaxation, and vice versa. Data are presented as mean \pm SEM; $n=10$; $P>0.05$, paired Student's t -test, removal of epithelium has no significant difference effect compared to its control condition (with epithelium) in cells treated with either vehicle control (0.3% v/v) EtOH or THC (30 μ M).

5.4 Discussion

Earlier *chapters 3* and *4* reported in this study had further confirmed the usefulness and the reproducibility of Calu-3 bronchial epithelial cells as a pharmacological screening tool owing to the expression of tight junctions that regulate the epithelial cell permeability. Hence, though earlier findings showed that phytocannabinoids caused the reversal and prevention of cytokines-induced increase in bronchial epithelial permeability, the effect of THC, but not CBD on Calu-3 transepithelial resistance was mediated through CB₁ and CB₂ receptors stimulation. It is noted that both THC and CBD can also bind to other receptors, such as GPR55, TRP channels and PPARs receptors. It is noted that subsequent experimental investigations in the present study focused mainly on THC due to time constraint within the project, and to allow further exploration into understanding the role of CB₁ and CB₂ receptors as a potential site of target to treat airway inflammatory diseases, such as asthma and COPD.

Initial studies to determine CB receptor expression using radioligand binding with Calu-3 cells grown at LLI. Under these conditions, there was no evidence for expression of either receptor. Subsequent investigations using Western blotting experiment demonstrated expression of both CB₁ and CB₂ receptors. Interestingly, receptor expression was increased in air-liquid conditions, which was the underlying reason that the cannabinoid receptors expression could not be detected using radioligand binding (*section 5.3.7*). This also strengthened the choice of using Calu-3 bronchial epithelial cell as an *in vitro* model for this study. However, issues on the specificity of the commercial antibodies against CB₁ receptor were raised in previous studies (Suarez et al., 2008, Grimsey et al., 2008). These investigations revealed staining patterns obtained from Western blotting were variable between samples

from different species. It was reported that bands detected also did not appear at the predicted molecular weight even in CB₁-transfected HEK293 cells or rat brain of which the receptor was known to be abundantly expressed. Thus, expression of the cannabinoid receptors in Calu-3 bronchial epithelial cell line, especially CB₁, needs to be further validated using other techniques in future studies (discussed in *section 7.3*).

As with TEER and immunoblotting experiments described in previous chapters, cannabinoid ligands, with or without the presence of a cytokine, were applied into the basolateral compartment of the Transwell[®]. This was necessary to maintain Calu-3 cells at ALI throughout the duration of the experiments. Hence, such experimental design postulates that the phytocannabinoids, cannabinoid receptor agonists or antagonists were introduced into the submucosal layer, indicated as the basolateral side of Transwells[®].

As previously discussed in *section 3.4*, presence of ethanol as vehicle control consistently caused decrease in TEER readings that were not less than 80% when concentrations of more than 0.3%(v/v) ethanol was used. Nevertheless, the high ethanol concentrations in these vehicle control groups (refer *Figure 5-3B*, *Figure 5-5* and *Figure 5-6 A&B*) still enable differences in the treatment groups distinguishable. Although the mechanism for the ethanol-induced increase in airway epithelial permeability was not investigated in the present study, Simet *et al* (2012) suggested that such effect occurred due to stimulation of the protein kinase C (PKC) pathway that subsequently reduced claudin and ZO-1 expression. A recent study in Caco-2 intestinal epithelial cell line had also demonstrated that ethanol at 0.2%(v/v) (i.e. approximately 40 mM) led to increase in epithelial permeability and reduced ZO-1 and adherence junctional proteins expression that was mediated by RhoA/ROCK

pathway stimulation (Elamin et al., 2014). Results obtained in *Figure 5-1* demonstrated that THC (30 μ M) or CBD (30 μ M) alone did not alter the permeability of the Calu-3 cells. Investigations conducted in the present using the resazurin assay also showed that the concentration of the phytocannabinoid, THC at 30 μ M did not alter cell viability. Cytotoxicity assays conducted in other epithelial models have never been reported in the literature. However, it is noted that studies in Caco-2 intestinal epithelial cells treated with either THC or CBD (of 100 nM up to 30 μ M) demonstrated a concentration-dependent response in restoring reduced transepithelial resistance caused by the cytokines TNF α and IFN γ (Alhamoruni et al., 2010). Hence, this excludes the possibility of the phytocannabinoids exerting toxicity effects when used at a concentration of 30 μ M.

As previously discussed in *section 2.3.2*, TNF α plays a major role in mediating airway inflammation. Elevated levels of TNF α are usually found in the sputum and bronchoalveolar lavage of patients with asthma or COPD (Cembrzynskanowak et al., 1993, Keatings et al., 1996). Introduction of a different pro-inflammatory cytokine, IL-1 β alone produced a similar increase in Calu-3 epithelial cell permeability (*Figure 5-3A*), such as that seen in TNF α . The rationale for the use of IL-1 β was based on evidence from previous histological studies that detected an increase in IL-1 β expression in the epithelial compartment of bronchial biopsy samples and bronchoalveolar lavage fluid of patients with either extrinsic (Sousa et al., 1996) or intrinsic (Mattoli et al., 1991, Mickleborough et al., 2005) asthma as well as COPD (Culpitt et al., 2003). Further investigations in these studies have demonstrated that IL-1 β behaves similarly to TNF α in the inflammatory response by stimulating inflammatory mRNA, in activating macrophages, and promoting the release of other chemokines and cytokines. The use of an IL-1 β receptor antagonist

attenuated experimentally-induced airway hyperresponsiveness in rodents (Gershenwald et al., 1990, Ramadas et al., 2006), but clinical trial reported that the humanised monoclonal antibody against IL-1, Anakinra, did not reverse airway inflammation in human asthmatics (Rosenwasser, 1998). The fall in TEER readings following the exposure of these pro-inflammatory mediators may be due to tight junction opening which will be investigated in the next chapter.

Introduction of one of the phytocannabinoids, THC or CBD demonstrated complete reversal of the TNF α -induced increased in epithelial cell permeability when added 24 hours after the cytokine (*Figure 5-2A*). Pre-exposure to THC or CBD prevented the reduction in TEER by TNF α (*Figure 5-2B*). Such observations were consistent to that reported by Alhamoruni *et al* (2010, 2012) in intestinal epithelial cells as TNF α and IFN γ -induced increased Caco-2 intestinal cell permeability which was reversed by THC and CBD. The present study has demonstrated that bronchial epithelial disruption caused by a different cytokine, IL-1 β (*Figure 5-3A*) and the endogenous cannabinoid, anandamide (*Figure 5-3B*) were also prevented by THC. Thus, this highlights the therapeutic potential of THC to treat disordered airway epithelial permeability conditions, like asthma and COPD. It is noted that this study did not investigate the effect of CBD in inhibiting IL-1 β and anandamide-mediated epithelial disruption, as THC had shown a better profile in maintaining its protective effect on the bronchial epithelial permeability than CBD in the initial experiments (*Figure 5-2B*).

Further investigations were conducted to confirm that the changes in TEER measurements following drug treatments were due to the alteration of paracellular permeability of the Calu-3 cells. High concentrations of FD4 dextran detected within the basolateral compartment of the Transwell[®] signify increased permeability; as a

leaky epithelial layer allows the dextran molecules to be transported more efficiently across the Calu-3 cell layer. Results from this experiment showed a marked increase in paracellular permeability in Calu-3 cells treated with TNF α only (*Figure 5-4B*). Whilst treatment with the phytocannabinoid THC alone maintained the epithelial permeability, the TNF α -induced increase in paracellular permeability was significantly attenuated in the presence of THC ($P<0.001$ compared to TNF α alone, 1-wayANOVA). Thus, a correlation between TEER and permeability studies are established – as elevated transepithelial resistance reading reflects limited paracellular permeability of the bronchial cells, and *vice versa*.

TEER readings that were measured before the permeability studies were generally increased by the end of the 3-hour permeability assay. It is noted that medium containing FD4 dextran immersed the apical side of the Calu-3 cell throughout the duration of the permeability studies and the increase in TEER is likely to be due to the presence of this liquid-liquid environment. The reason behind the increment in transepithelial resistance despite the brief period at LLI is unknown, although other studies using Calu-3 cells (Vllasaliu et al., 2011) and other bronchial epithelial cell line, 16HBE14o- cells (Ahsan et al., 2003) had reported the same observation. TEER measurement in *Figure 5-7A* revealed the lowest transepithelial resistance reading in cells treated with TNF α , whilst TEER for cells treated with THC alone or in combination with TNF α were higher. Statistical analysis for the TEER measurements taken before and after the permeability studies were not conducted. TEER readings measured at these time points may be invalid due to the need to maintain culture condition at LLI during the permeability studies. Hence, TEER readings were taken solely for monitoring purposes.

The involvement of CB₁ and CB₂ receptors in the THC and CBD-mediated effects were then investigated. TEER experiments demonstrated that the cannabinoid receptor antagonists, AM251 and SR144528 inhibited THC-induced TEER recovery (*Figure 5-5*). Therefore, this suggests that the action of THC in maintaining bronchial epithelial permeability was mediated through both CB₁ and CB₂ receptors. However, limitation with these experiment designs includes the lack of study on the effect of either AM251 or SR144528 on TEER as internal drug controls. Such an observation is consistent with the findings reported by Alhamoruni *et al* in Caco-2 intestinal epithelial cells (Alhamoruni et al., 2010) that epithelial permeability was restored with THC through CB₁ and CB₂ receptor stimulation. Subsequent TEER measurements were conducted to further confirm the presence and role of cannabinoid receptors in mediating the human bronchial epithelial permeability. According to the literature, HU-210 binds to both cannabinoid receptors at low nanomolar ranges, with approximate K_i values of 0.4 and 0.35 in displacing radiolabelled potent cannabinoid agonist, [³H CP55,940] from CB₁ and CB₂ receptor binding sites respectively (Pertwee, 2010). Its ability to demonstrate high selectivity for CB₁ and CB₂ receptors thus is the preferred choice for this study, compared to other currently available potent cannabinoid receptor agonists CP55,940 and WIN55212-2. ACEA is an analog of anandamide and is one of the most selective CB₁ receptor agonist available thus far. The presence of the chlorine atom on the amide structure (refer *Figure 1-6* for chemical structures) increases the affinity of ACEA to CB₁ receptor to the lower nanomolar range (K_i approximately 1.0 nM), and a lower affinity for CB₂ receptor (approximate K_i value 3.0 μM) (Hillard et al., 1999). On the other hand, JWH133 demonstrates high selectivity for CB₂ receptor

with the approximate K_i value of 3.5 nM compared to its affinity for CB₁ receptor (approximate K_i value 680 nM) (Huffman et al., 1999).

In the present study, treatment with cannabinoid ligands alone including full agonist HU-210 (100 nM), CB₁ receptor agonist, ACEA (100 nM) or CB₂ receptor agonist, JWH133 (3 μ M) alone did not alter Calu-3 cell permeability (*Figure 5-10A*). Pre-treatment with either HU-210 or JWH133 caused complete inhibition of TNF α -induced increase in permeability. Interestingly, selective stimulation of the CB₁ receptor with ACEA displayed a slight delay in exerting full TEER recovery as TEER reading was completely restored post-24 hours of TNF α challenge. This indicates that both CB₁ and CB₂ receptor activation can prevent TNF α -induced bronchial epithelial disruption.

THC is also known to stimulate other non-cannabinoid receptor targets. Petrocellis *et al* (2010) reviewed the list of THC targets in human and rat dorsal root ganglion neurons, where various transient receptor potential (TRP) channels are abundantly distributed, including TRPV1 and TRPV2 (vanilloid), TRPA1 (ankyrin), TRPM8 (mucopilin) as well the putative cannabinoid receptor GPR55 (De Petrocellis and Di Marzo, 2010). The peroxisome proliferator-activated receptor (PPAR) receptors, mainly the PPAR γ subtype are associated to airway inflammation (Honda et al., 2004). Evidence also suggests that the PPAR γ receptor is also activated by THC which caused vasorelaxation in rodent blood vessels (O'Sullivan et al., 2006). However, it is not the current interest of this project to investigate the role of these receptors that may or may not be expressed in the Calu-3 epithelial cell model.

Although CB₁ and CB₂ receptors appear to mediate the THC effect, single (*Figure 5-5A*) or dual (*Figure 5-5B*) pharmacological blockade of the cannabinoid receptors did

not block the effect of CBD in preventing cytokine-induced increases in bronchial epithelial permeability. This suggests that other potential CBD target receptors that may be present in Calu-3 cells. CBD has been previously demonstrated to activate purinergic receptors (Sun et al., 2008, Castillo et al., 2010) and TRP channels (Costa et al., 2004, McGarvey et al., 2014), or attenuation of oxidative stress induced by the cytokine TNF α (Booz, 2011). Nevertheless, it has been shown that CBD acts as an antagonist at the GPR55 receptor (Ryberg et al., 2007) which functional role remained to be evaluated. Further investigations are therefore, needed to determine the CBD mechanism of action on airway epithelium permeability. Following the exclusion of the involvement of classical cannabinoid receptors in mediating effect by CBD, subsequent experiment conducted in this study was focused mainly on evaluating THC action to allow further investigation into the pharmacological effect of CB₁ and CB₂ receptors as potential therapeutic target in airway inflammation. In addition, future investigations will include the study of the effect of cannabinoid ligands and CB₁ as well as CB₂ receptor antagonists at various concentrations when they are administered alone or in the presence of a cytokine. The approach to the design of the experiment is as previously discussed in *section 3.4* and *section 4.4*. The optimal concentration of the phytocannabinoids, for example, can then be used for other parallel functional studies, such as Western blotting and dot blotting.

Calu-3 cells are reported to produce a significant level of MUC5AC when grown at ALI, as a proportion of the cells differentiate to form mucus-producing (goblet) cells (Grainger et al., 2006). It is noted that mucus production is also an important element of forming the chemical barrier on the apical face of the bronchial epithelium structure, thus preventing the invasion of noxious stimuli into the smooth muscle compartment to trigger subsequent inflammatory responses (Thornton et al., 2008).

However, overexpression of MUC5AC is observed in pathological conditions such as asthma and COPD, which thickens the mucus layer hence obstructing the airflow within the conducting airways (Kirkham et al., 2002). Dot blotting (*Figure 5-11A*) showed the expression of MUC5AC glycoprotein across the different types of treatments. The MUC5AC glycoprotein expression in the presence of TNF α was significantly increased compared to the untreated Calu-3 cells. The presence of THC, effectively lowered TNF α -induced MUC5AC expression to basal level (*Figure 5-11B*). Quantification analysis of the fluorescence signals in these dot blots showed consistency in an earlier study which demonstrated reduced MUC5AC mRNA expression in influenza A-infected mice, following systemic administration of THC (Buchweitz et al., 2007). Results observed from the present study thus highlight the potential role of THC in reducing mucus secretion, besides preventing cytokine-induced bronchial epithelial disruption. In addition, involvement of CB₁ and CB₂ receptor expression on goblet cells that mediates THC effect in reducing MUC5AC mRNA or functional protein expression remained to be investigated.

Majority of the published findings available in the literature were of acute models, rather than that of chronic condition which more accurately reflect the pathology of airway inflammatory diseases such as asthma and COPD. These experiments, which usually lasted for up to 72 hours, involved the exposure of one or a combination of pro-inflammatory mediators to cells, with or without drug treatments (Coyne et al., 2002, Olson et al., 2009, Alhamoruni et al., 2010, Fiorentino et al., 2013). The longest time course in a published study demonstrated that a single co-application of the cytokines TNF α and IFN γ to T84 intestinal epithelial cell line increased epithelial leakiness that was maintained for five days (Adams et al., 1993). An alternative experimental approach to establishing an *in vitro* chronic inflammatory model was to

culture epithelial cells from diseased subjects for subsequent TEER measurements (Yamada et al., 1993, Den Beste et al., 2013). Although such a method is an improvement on the use of cell lines, isolating and culturing primary epithelial cells can be practically challenging owing to human genetic variation. Hence, the following aim of this study was to evaluate the effect of basolateral application of THC on Calu-3 epithelial cell layer for an extended period (10 days), compared to the previous TEER studies which terminated at 48 hours. This study was also conducted to determine THC's ability to prevent TNF α -induced increased epithelial permeability without the development of tolerance and to explore the potential for developing a better *in vitro* chronic airway inflammatory model.

TEER experiments revealed that basolateral application of THC alone increased TEER readings over the 10-day treatment (*Figure 5-13A*). Results in *Figure 5-13B* revealed that exposure of the cells to TNF α alone for 10 days produced only a modest drop in TEER, unlike the effect seen when treating TNF α for 48 hours (*Figure 5-2B*). This could be due to the fact that the optimal point of TNF α -induced TEER decrease may have been missed as it was previously demonstrated to occur at an earlier time point; i.e. below 10 hours (*Figure 3-4B*). Repeated exposure of THC had similarly attenuated bronchial epithelial disruption caused by TNF α . Basolateral application of HU-210 alone for 10 days resulted in a similar increase in TEER (*Figure 5-14*), such as that seen for THC-treated cells. This suggests that long-term stimulation of both CB₁ and CB₂ receptor has a potential role in the development of the bronchial epithelial barrier function. The reason for the increase in TEER with THC over 10 days was then investigated. It was hypothesised that THC might be increasing cell proliferation. However, resazurin assays showed no difference in cell proliferation between any of the treatment conditions.

The use of porcine bronchial segments for organ bath studies was selected due to the physiological and genotypical similarities it shares with the human airway (Canning, 2003). Besides that, the sturdiness and size of the porcine bronchial structure aids in the practicality aspect in organ bath setup. The rationale for the organ bath studies was to determine whether the effect of THC on the epithelium, as determined in cell culture, could alter airway tone, for example, through the release of epithelium-derived relaxing factor (Vanhoutte, 2013).

Results revealed that administration of THC (30 μ M) did not reverse the bronchoconstriction caused by carbachol (*Figure 5-16*). Instead, relaxation in both types of bronchial segments (with or without epithelium) was observed when treated with the vehicle control for THC, (0.3% v/v) EtOH. A recent study using TNF α and lipopolysaccharide (LPS)-stimulated guinea pigs bronchial segments (Makwana et al., 2015) demonstrated that the application of THC (1 μ M) reversed nerve-evoked bronchoconstriction, mediated by CB₁ and CB₂ receptor activation. In addition, aerosol inhalation of 200 μ g THC in human asthmatic subjects has been proven to improve the respiratory function with minimal side effects, although the investigators from the clinical trial study claimed that salbutamol induced a more rapid bronchodilatation effect compared to THC (Williams et al., 1976). Despite the slower duration of action of THC, its use as an asthmatic relief would provide pharmaceutical alternative to patients who are intolerant of the β_2 -adrenoceptor agonist. The discrepancy of the results obtained from this study and that in the literature suggests that different mechanisms are involved in sensitivity and reactivity of bronchial structure with cholinergic agonist, carbachol and the pro-inflammatory mediators. The studies in the Calu-3 epithelial cells indicated that acute addition of THC had no effect on its own, but prevented the effects of the cytokines. Therefore,

THC may prevent cytokine-induced changes in airway tone and this should be considered for future studies.

5.5 Conclusion

In contrast to the action of the endogenous cannabinoid anandamide, basolateral application of the phytocannabinoids THC or CBD alone had no effect on epithelial permeability. Treatment with the cytokine, TNF α alone had shown a reproducible drop in TEER (previously demonstrated in *chapter 3*), indicating an increase in Calu-3 cell permeability. Both phytocannabinoids reversed and prevented such effect by TNF α . Data obtained from FD4 dextran permeability studies confirmed that the alteration in TEER reading was indeed due to changes in the epithelial permeability. Further TEER experiments also demonstrated that THC prevented the increase in Calu-3 permeability induced by other pro-inflammatory mediators, including the cytokines TNF α and IL-1 β , as well as the endocannabinoid anandamide. Thus, the ability of THC in blocking increased in epithelial permeability induced by various pro-inflammatory cytokines related to asthma and COPD suggests its potential therapeutic use in preventing airway hyperresponsiveness as the epithelial barrier function is preserved. Subsequent TEER experiments indicated that THC mediates its effect through both cannabinoid CB₁ and CB₂ receptors. Such conclusion was derived when THC action in preventing TNF α -induced increase in epithelial permeability was attenuated in the presence of CB₁ receptor antagonist, AM251 and CB₂ receptor antagonist, SR144528. Data from Western blotting studies then confirmed that CB₁ and CB₂ receptors are expressed in Calu-3 cells cultured in ALI. Stimulation of the cannabinoid receptors with full agonist, HU-210 or selective CB₁

or CB₂ receptor activation with ACEA and JWH133 respectively did not alter Calu-3 epithelial cell permeability when they were administered alone. Like the phytocannabinoids, combined application of one of the cannabinoid ligands with TNF α prevented the decrease in transepithelial resistance caused by the cytokine. These results suggest that THC reverses the reduction in transepithelial resistance caused by TNF α , through an effect at CB₁ and CB₂ receptors. Hence, the cannabinoid receptors expressed within the airway epithelium can be targeted for the prevention of epithelial leakiness without inducing undesirable effects on the central nervous system. However, there are also possibilities that other putative cannabinoid receptors are also involved in THC-mediated effect within the airway epithelium structure.

In contrast, the effect of CBD in TNF α -treated cells was unaffected by the CB₁ receptor antagonist, AM251, or CB₂ receptor antagonist, SR144528, or combination of the two antagonists. Hence, this indicates that CBD acts independently of the cannabinoid receptor activation. Like THC, future studies should investigate the stimulation of other receptors, mainly GPR18, GPR55, PPAR γ and various subtypes of TRP channels by CBD in regulating airway epithelium permeability. Particularly, TRPV1 channel has been frequently implicated in patients with asthmatic symptoms as its expression was shown to be upregulated in previous investigation (McGarvey et al., 2014).

Mucus hypersecretion is one of the distinct features of airway inflammation. Analysis of the sputum samples in asthma and COPD patients revealed increased MUC5AC glycoprotein (Kirkham et al., 2002) compared to healthy subjects. Dot blotting studies demonstrated that the presence of THC alone did not alter MUC5AC expression but its combined application with TNF α had shown to reduce MUC5AC

expression, compared to the level of MUC5AC expression in TNF α treatment alone. Thus, this experiment highlights the ability of THC in reducing MUC5AC glycoprotein expression, hence aids in decreasing the amount of mucins secreted during inflamed conditions and prevent mucus formation that can clog the lumen of the conducting airways

Repeated administration of THC alone revealed a concentration-dependent response in increasing the barrier function of the Calu-3 epithelial cells. Prolonged treatment with HU-210 exhibited a similar effect on TEER as THC. The effect of THC did not appear to be due to increased cell proliferation, suggesting that repeated stimulation of the CB₁ and CB₂ receptors may exert a positive impact on the bronchial epithelial tight junction proteins expression. However, further investigations are still needed to investigate the involvement of both cannabinoid receptors in THC-mediated effect in an extended treatment period.

Studies on the characterisation of subsequent cellular signalling pathways involved in regulating the bronchial epithelial permeability caused by THC in the presence and absence of the cytokine, TNF α will be studied in greater detail in *chapter 6*.

The figure below summarises the findings presented in this study:-

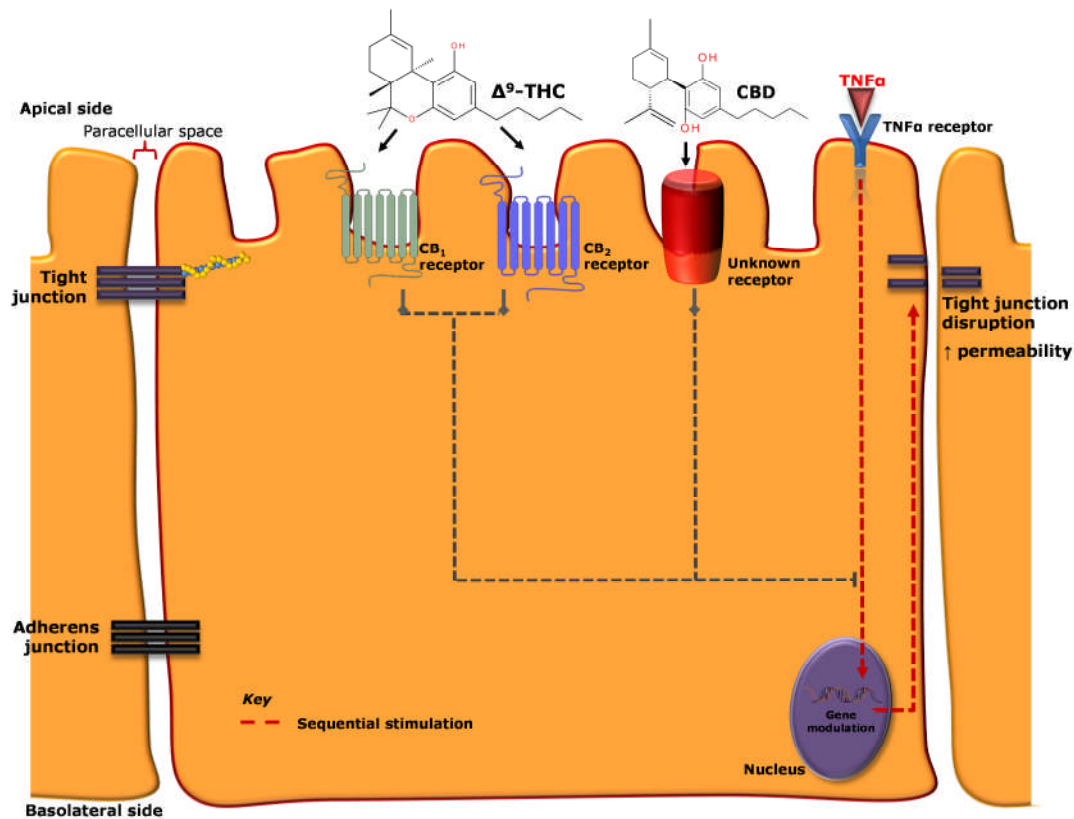


Figure 5-17 Changes to the bronchial epithelial cell permeability following the treatment of the phytocannabinoids, THC or CBD in the presence and absence of the pro-inflammatory cytokine, TNF α . Red coloured arrows represent intracellular signalling steps involved in tight junction disruption, whereas arrows in black denote the cascades associated to THC stimulation. T-shaped lines indicate inhibition. Exposure to TNF α alone increases Calu-3 cell permeability. Evidence suggests that TNF α exerts its effect through gene modulation within the nucleus. Its potential mechanism of action will be discussed in greater detail in chapter 6. Treatment with either THC or CBD restores or prevents the increase in epithelial permeability caused by TNF α . THC mediates such effect through stimulation of both CB₁ and CB₂ receptors, whereas CBD action is independent of the cannabinoid receptors activation.

6. The Mechanism Involved in THC-Mediated Response on the Bronchial Epithelial Tight Junction

6.1 Introduction

Results presented in *chapter 5* revealed that the action of THC in preventing cytokine and anandamide-induced increased bronchial epithelial permeability was mediated through CB₁ and CB₂ receptors. Studies in various human epithelial models, such as bronchial and intestinal epithelial cells as well as MDCK cells, have consistently shown that the measurement of epithelial resistance is dependent on the expression level of tight junction proteins, which then determines the integrity of the epithelial barrier function [reviews by (Terry et al., 2010, Shen, 2012, Matter and Balda, 2014)]. To date, changes in the expression of epithelial tight junction proteins following the treatment of THC or other cannabinoid ligands have never been investigated. Results described in *chapter 4* have demonstrated that the bronchial epithelial leakiness caused by anandamide was a result of a decrease in expression of the tight junction proteins, occludin and ZO-1, similar to the effect seen with TNF α as reported in the literature (Coyne et al., 2002, Petecchia et al., 2012). Therefore, in this chapter, further experiments were conducted to probe the effect of THC on the molecular composition of tight junctions, particularly occludin and ZO-1, with or without TNF α challenge.

Expression of the tight junction proteins is regulated by a complex array of intracellular cascades, which ultimately cause the tight junction structure to either assemble or disassemble. Two of the intracellular signalling pathways that are frequently linked to mediating epithelial and endothelial cell permeability in

response to extracellular stimuli are the MAP kinases, including ERK1/2, p38 and JNK, as well as the RhoA/ROCK cascade [reviews by (Terry et al., 2010, Zihni et al., 2014)]. Based on these review articles, activation of MAPK ERK1/2, p38 and JNK are commonly linked to disrupted epithelial barrier function. However, there are reports that contradict such findings as stimulation of these MAP kinases could also result in epithelial tight junction sealing (Gonzalez-Mariscal et al., 2008). Thus, the role of MAP kinase signalling, particularly ERK1/2 activation in mediating the effect of THC on bronchial epithelial barrier function was investigated in the present study.

In addition, the involvement of RhoA/ROCK signalling was also considered. There are currently limited number of studies that have linked the role of cannabinoid CB₁ and CB₂ receptors in the regulation of the RhoA/ROCK cascade. Therefore, understanding of such pharmacological association is still not well understood. Reports that are available thus far have only investigated the effect of cell migration following stimulation of either CB₁ or CB₂ receptor that would then activate or deactivate RhoA. A study using HL-60 neutrophilic cells have demonstrated that selective activation of CB₂ receptor promoted cell migration that is mediated by RhoA activation as part of the regulation of a general inflammatory response (Kurihara et al., 2006). On the other hand, stimulation of CB₁ receptor expressed in prostate carcinoma cells reported an opposing effect as ROCK activity diminishes, thus inhibiting cellular motility (Nithipatikom et al., 2012). Conflicting observations reported in these experiments proposed the need to investigate the involvement ROCK activity in regulating bronchial epithelial permeability following activation of the cannabinoid receptors by THC.

6.1.1 Aims

Therefore, this study aimed to;

- i. Identify the effect of THC on the level of expression of the tight junction proteins occludin and ZO-1.
- ii. Investigate the possibility for the involvement of ROCK signalling in THC-mediated effect in preventing airway epithelial leakiness caused by the cytokine, TNF α .
- iii. Establish the effect of CB₁ and CB₂ receptor activation in the regulation of ROCK signalling and subsequent regulation of Calu-3 bronchial epithelial cell permeability.

6.2 Materials and Methods

6.2.1 Materials

Materials used for cell culture in are listed in *section 2.1.1*, TEER experiment in *section 2.1.2*, Western blotting in *section 2.1.4* and the list of primary and secondary antibodies used in *section 2.1.5*.

6.2.2 Methods

After the TEER readings were collected, Calu-3 cells that had been treated with THC (30 μ M) alone, with or without the presence of TNF α (10 ng/mL) for 48 hours were harvested from the Transwells[®] for Western blotting experiments (refer *section 2.7.1*: samples preparation for Western blotting protocol). The levels of expression of the tight junction proteins occludin and ZO-1 were then quantified from the images obtained. Dilutions for the primary and secondary antibodies used for Western blotting are listed in *Table 2-5*.

Calu-3 cells used to investigate the involvement of ERK1/2 MAPK and MYPT1 activity were serum-starved for 4 hours to reduce the basal cellular signalling activity. Cells were then exposed to TNF α (10 ng/mL) basolaterally for up to 4 hours, with a prior incubation of either THC (30 μ M) or its vehicle control (0.3% v/v) EtOH for an hour.

TEER experiments to study the effect of TNF α in the presence of the ROCK inhibitor Y27632 (10 μ M) were conducted according to the revised protocol outlined in *section 2.5.4* and lasted for 48 hours. These experiments were conducted to confirm the involvement of ROCK signalling caused by TNF α . Again, samples from

this experiment were collected for subsequent Western blotting to study changes in occludin and ZO-1 expression.

Compound	Concentration studied	Evidence on concentration studied	Notes on site(s) of action/ K_i or IC_{50} values relevant to studied concentration
ACEA	100 nM	Refer <i>Table 5-1</i>	
JWH133	3 μ M	Refer <i>Table 5-1</i>	
SR144528	1 μ M	Refer <i>Table 3-1</i>	
THC	30 μ M	Refer <i>Table 5-1</i>	
TNF α	10 ng/ml	Refer <i>Table 3-1</i>	
Y27632	10 μ M	<p>Y27632 (10 μM) was shown to inhibit isolated ROCK enzyme activity by approximately 87% (Davies et al., 2000).</p> <p>Y27632 (10 μM) was also shown to prevent thrombin-induced increase in permeability in A549 alveolar epithelial cell line (Kawkitinarong et al., 2004).</p>	Y27632 displays high selectivity to ROCK enzyme, with K_i value of 800 nM (Davies et al., 2000).

Table 6-1 List of the drugs used in this chapter and the rationales for the concentrations used.

6.2.3 Statistical Analysis

Data are presented as the mean \pm standard error of mean (S.E.M). Western blotting data were analysed by 1-way ANOVA followed by a Bonferroni post-hoc test. Alternatively, Western blotting analysis to detect differences in fold change of a specific protein expression between two treatment group at a fixed time point were compared using paired, Student's t-test. Time-dependent changes in TEER were analysed using a 2-way ANOVA, followed by a Bonferroni post-hoc test. Results of $P < 0.05$ were considered significant.

6.3 Results

6.3.1 THC Prevents Reduced Tight Junction Proteins, Occludin and ZO-1 Expression Induced by TNF α

Following TEER measurements (as previously discussed in *section 5.3.2*), changes in the expression of tight junction proteins, occludin and ZO-1, were investigated in cells treated with THC alone or in the presence of TNF α for 48 hours. Western immunoblotting detected bands for occludin at approximately 64 kDa (*Figure 6-1A*), whereas ZO-1 was expressed at about 225 kDa (*Figure 6-2A*). It is noted that the predicted molecular weights for the bands corresponding to occludin and ZO-1 expression are 59 kDa and 225 kDa respectively.

Fluorescence quantification analysis of these images revealed that basolateral administration of TNF α (10 ng/ml) reduced the expression of both occludin (*Figure 6-1B*) and ZO-1 (*Figure 6-2B*) by half, compared to untreated (basal) Calu-3 cells. On the other hand, treatment with THC alone had no effect on the expression of either occludin or ZO-1 protein, but prevented the decrease in expression caused by TNF α .

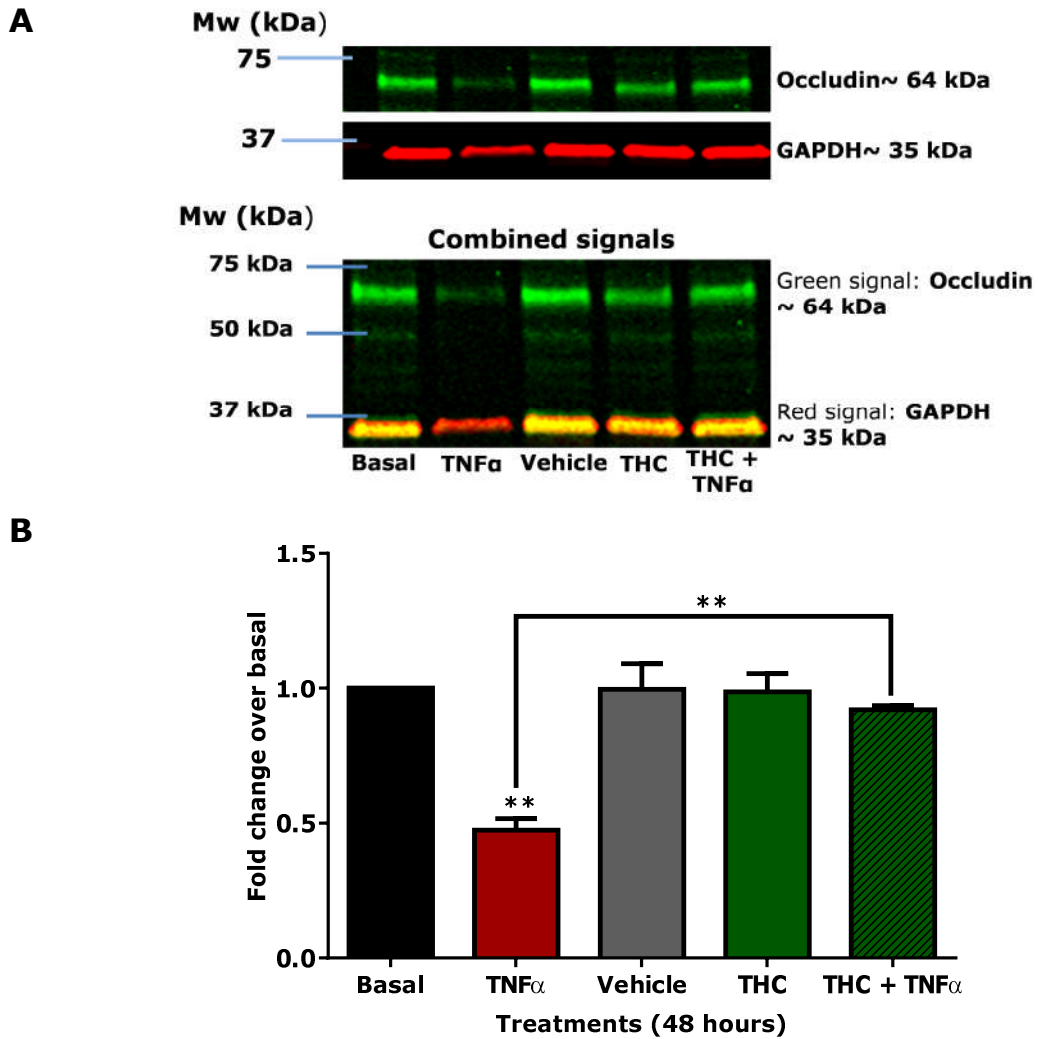


Figure 6-1 A. Western blot images and **B.** semi-quantitative analysis of the changes to tight junction protein, occludin expression (green signal) following basolateral administration of $\text{TNF}\alpha$ (10 ng/mL), (0.3% v/v) EtOH or anandamide in Calu-3 cells for 48 hours in Western blotting. Basal group represents untreated 21-day old Calu-3 cells cultured at air-liquid interface; i.e. no drug. Total protein loaded into the SDS-PAGE gel was determined with GAPDH antibody (red signal). Data are presented as mean of fold change to protein expression over basal \pm SEM; $n=3-8$, $**P<0.01$, 1-way ANOVA followed by a Bonferroni post-hoc test. $\text{TNF}\alpha$ is compared to basal as well as combined treatment of $\text{THC}+\text{TNF}\alpha$, whereas treatment with THC alone is compared to its vehicle control (0.3% v/v) EtOH. Refer appendix for original blot images (Appendix- Chapter 6(1)).

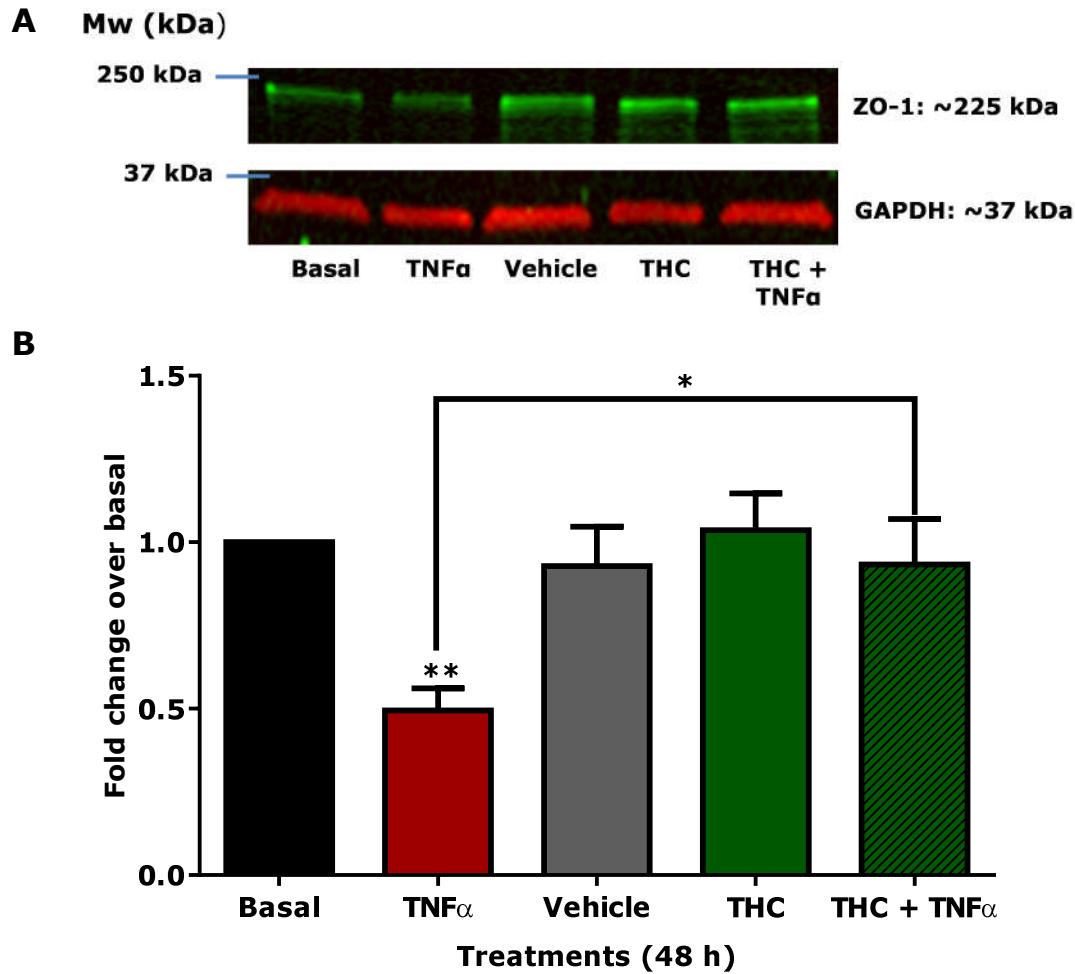


Figure 6-2 **A.** Western blot images and **B.** semi-quantitative analysis of the changes to tight junction protein, ZO-1 expression (green signal) following basolateral administration of TNF α (10 ng/mL), (0.3% v/v) EtOH or anandamide in Calu-3 cells for 48 hours in Western blotting. Basal group represents untreated 21-day old Calu-3 cells cultured at air-liquid interface; i.e. no drug. Total protein loaded into the SDS-PAGE gel was determined with GAPDH antibody (red signal). Data are presented as mean of fold change to protein expression over basal (\pm SEM; $n=3-8$, $*P<0.05$, $**P<0.01$, 1-way ANOVA followed by a Bonferroni post-hoc test. TNF α is compared to basal as well as combined treatment of THC+TNF α , whereas treatment with THC alone is compared to its vehicle control (0.3% v/v) EtOH. Refer appendix for original blot images (Appendix- Chapter 6(2)).

6.3.2 THC Increases ERK1/2 MAPK Phosphorylation

Previous studies in Calu-3 epithelial cells have indicated that activation of ERK-MAP kinase is involved in the disruption of tight junctions in the presence of TNF α (Petcchia et al., 2012). The present study demonstrated consistent observation as pre-incubation with one of the MEK1/2 inhibitors, either PD98059 or U0126, in Calu-3 cells prevented the decrease in TEER and expression of occludin caused by TNF α (refer *sections 4.3.2 and 4.3.3*).

TEER (refer *section 5.3.2*) and Western blotting (refer *section 6.3.1*) experiments conducted earlier in this study have shown that TNF α -induced tight junction disruption was fully prevented by THC. Thus, this formed the hypothesis that ERK1/2 stimulation caused by TNF α may be inhibited in the presence of the phytocannabinoid.

Figure 6-3A shows that phosphorylated ERK1/2 levels following the combination treatment with THC and TNF α treatment was visibly higher than that of TNF α -only treated cells. Semi-quantitative analysis of these bands at all time points (i.e. 0.5 to 4 hours) showed elevated phospho-ERK1 and ERK2 in the presence of THC (see *Appendix-Chapter 6 (3)*). In contrast, phospho-ERK1 and ERK2 level in cells treated with TNF α alone were not significantly raised from their basal time point.

Results revealed the increase in ERK1 (*Figure 6-3B*) and ERK2 (*Figure 6-3D*) phosphorylation level peaked at 1 hour in Calu-3 cells treated with THC and TNF α . It was noted that the level of ERK1 phosphorylation caused by THC and TNF α showed no statistical difference compared to TNF α alone, which may be due to low ERK1 expression (i.e. weaker fluorescence signals) in both treatment groups.

The expression levels of total ERK1 (*Figure 6-3C*) and ERK2 (*Figure 6-3E*) were unaltered, signifying that the fold change in ERK1 and ERK2 signalling was solely due to the variation in the activated, phosphorylated form.

Earlier experiments conducted in the present study have demonstrated that THC prevented the decrease in Calu-3 epithelial cell resistance (*section 5.3.2*) and tight junction protein expression associated to TNF α (*section 6.3.1*). However, the fact that THC stimulates ERK1 and ERK2 phosphorylation, rather than inhibiting the response suggests that inhibition of ERK MAPK activation is not the mechanism by which THC prevents the effects of TNF α . An alternative intracellular signalling pathway, the RhoA/ROCK cascade was subsequently explored to identify differences in the underlying mechanism of TNF α and THC.

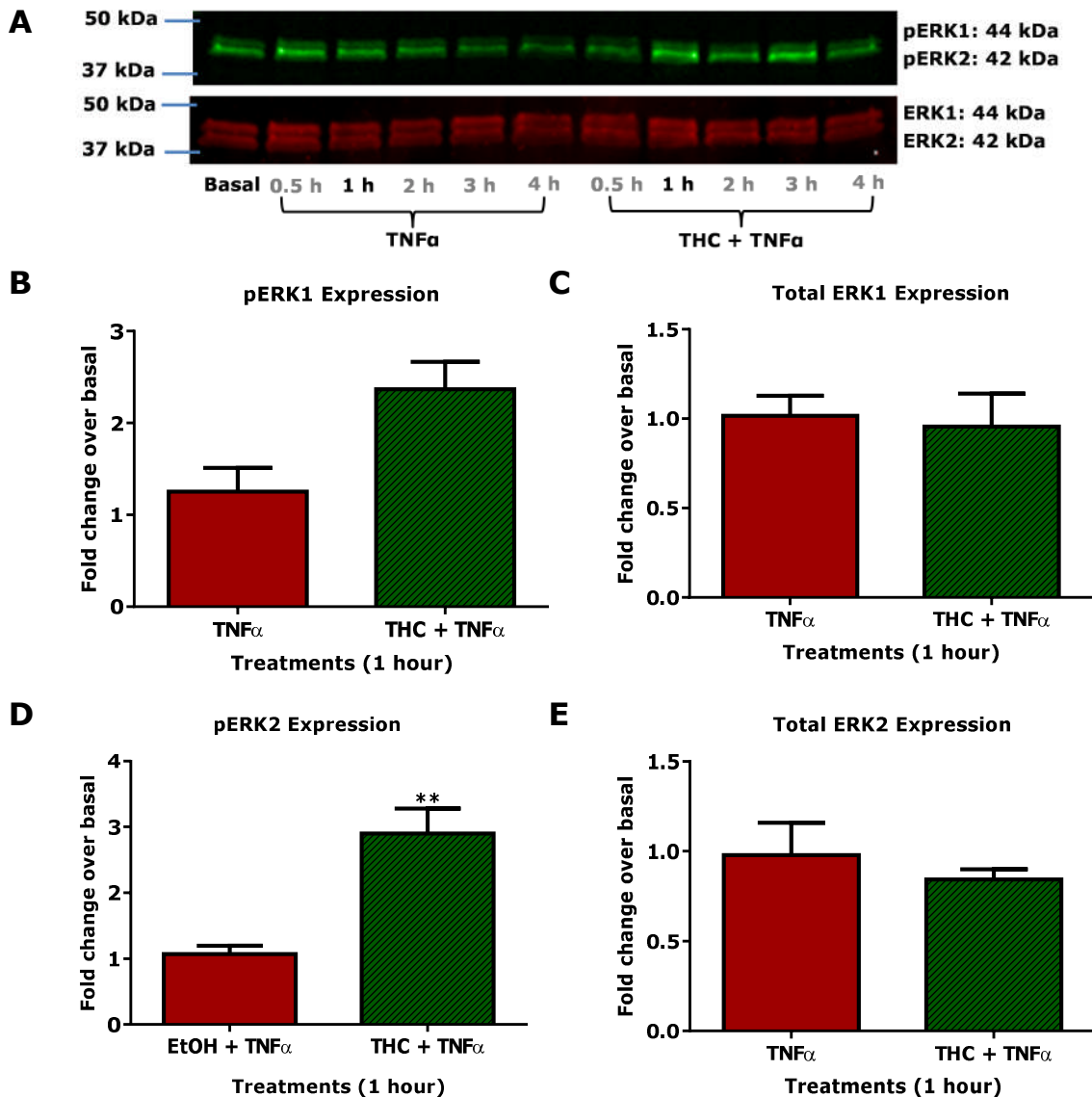


Figure 6-3 A. Western blot image of phospho- and total ERK1/2 MAPK signalling following basolateral application of TNF α (10 ng/ml) alone or in the presence of THC (30 μ M) up to 4 hours in serum-starved 21-day old Calu-3 cells, cultured in ALI. B. Semi-quantitative analysis of ERK1 expression level, which is normalised according to C. the total ERK1 expressed at 1 hour following TNF α exposure. D. Semi-quantitative analysis of ERK2 expression level, which is normalised according to E. the total ERK2 expressed at 1 hour following TNF α exposure. Data are presented as mean of fold change to protein expression over basal (untreated) cells \pm SEM; $n=4$, ** $P<0.01$, paired Student's t -test, compared to TNF α (10 ng/ml). Refer appendix for original blot images (Appendix- Chapter 6(3)).

6.3.3 Selective Inhibition of ROCK Prevents TNF α Effect on Epithelial Permeability and Tight Junction Proteins Expression

Previous study in the human umbilical vein endothelial cells (HUVEC) indicated increased cell leakiness caused by the cytokine TNF α was mediated through the RhoA/ROCK signalling pathway (McKenzie and Ridley, 2007). Hence, subsequent experiments conducted in this study aimed to investigate the role of ROCK stimulation in altering human bronchial epithelial cell permeability.

In the absence of drugs, TEER readings for the control cells were maintained throughout the 48-hour experiment (*Figure 6-4*). Vehicle control group was not included in this particular experiment as the ROCK inhibitor Y27632 was dissolved in sterile distilled water to obtain a stock concentration of 10 mM. A 1 in 1000 dilution was then performed by adding 1.5 μ L of Y27632 (10 mM) into 1.5 ml media on the basolateral side of the Transwell[®].

Treatment with Y27632 (10 μ M) alone did not significantly alter Calu-3 cell resistance. TNF α (10 ng/ml) consistently reduced TEER to its minimum of $61 \pm 5.5\%$ following 8 hours application. However, pre-incubation of Y27632 completely prevented TEER decrease caused by TNF α (*Figure 6-4*).

Western blotting revealed treatment with TNF α alone for 48 hours resulted in a reproducible decrease in occludin (*Figure 6-5A&B*) and ZO-1 (*Figure 6-6A&B*) expression. The presence of Y27632 attenuated the decrease in the expression of both tight junction proteins caused by TNF α .

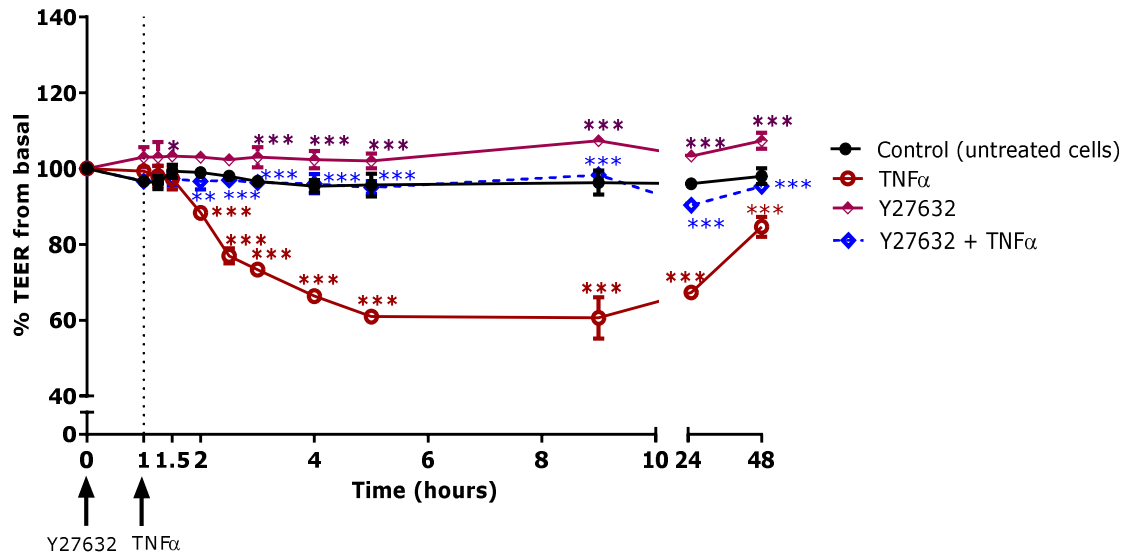


Figure 6-4 Effects of basolateral application of selective ROCK inhibitor, Y27632 (10 μ M) in the presence of TNF α (10 ng/mL) onto 21-day old Calu-3 cells cultured in ALI. Data are expressed as percentage TEER by calculating the relative change in resistance at various time points from basal reading, and are presented as mean \pm SEM; $n=3$, * $P<0.05$, ** $P<0.01$, *** $P<0.001$, 2-way ANOVA followed by a Bonferroni post-hoc test, compared to TNF α (10ng/mL); except TNF α which is compared to control (untreated cells).

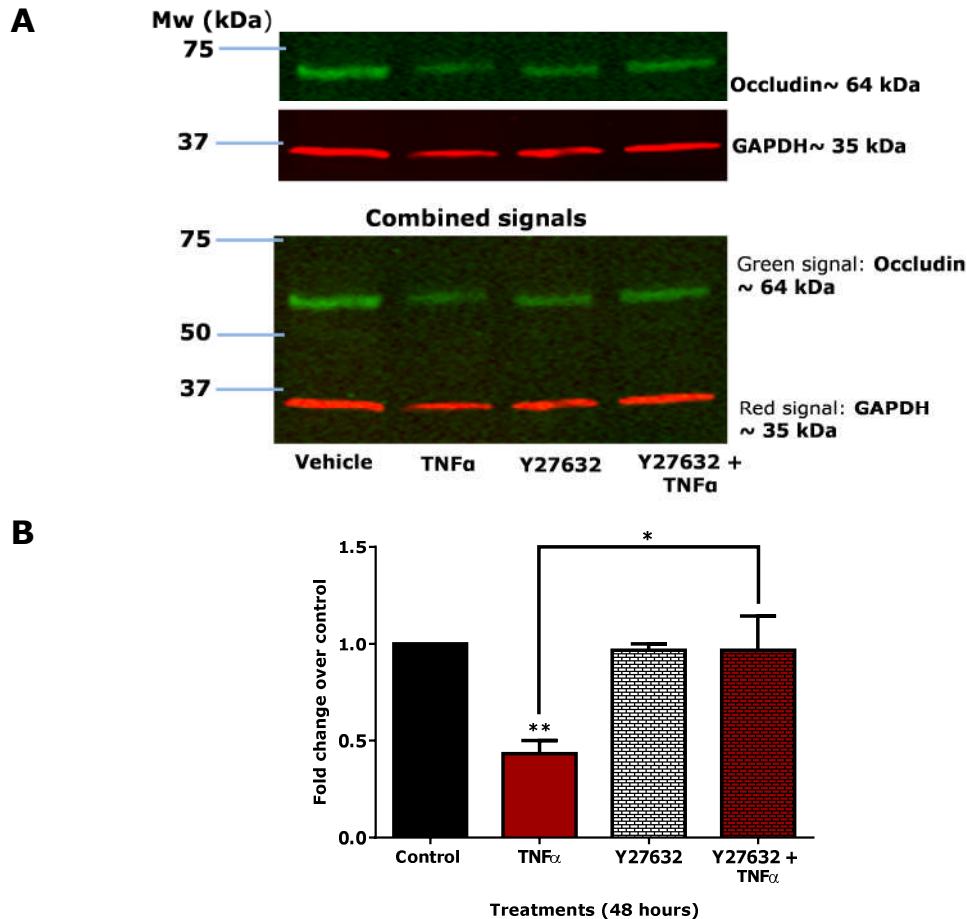


Figure 6-5 A. Western blot images and **B.** semi-quantitative analysis of the changes in the tight junction protein, occludin expression following basolateral administration of Y27632 (10 μ M) in the presence of TNF α (10 ng/ml) in Calu-3 cells for 48 hours. GAPDH was used as a reference protein (or loading control) as its level of expression remained similar in all treatment groups, whilst occludin expression varied. 'Fold change from vehicle' labelled on the Y-axis in figures B&D was derived by dividing the ratio of occludin to GAPDH expression for the respective treatment groups with the ratio of occludin to GAPDH for the control cells. Data are presented as means \pm SEM of fold changes in protein expression compared with control (untreated cells); $n=3$, $*P<0.05$, $**P<0.01$, 1-way ANOVA followed by a Bonferroni post-hoc test, compared to control, whereas combined treatment of Y27632 and TNF α is compared to TNF α alone. Refer appendix for original blot images (Appendix- Chapter 6(4)).

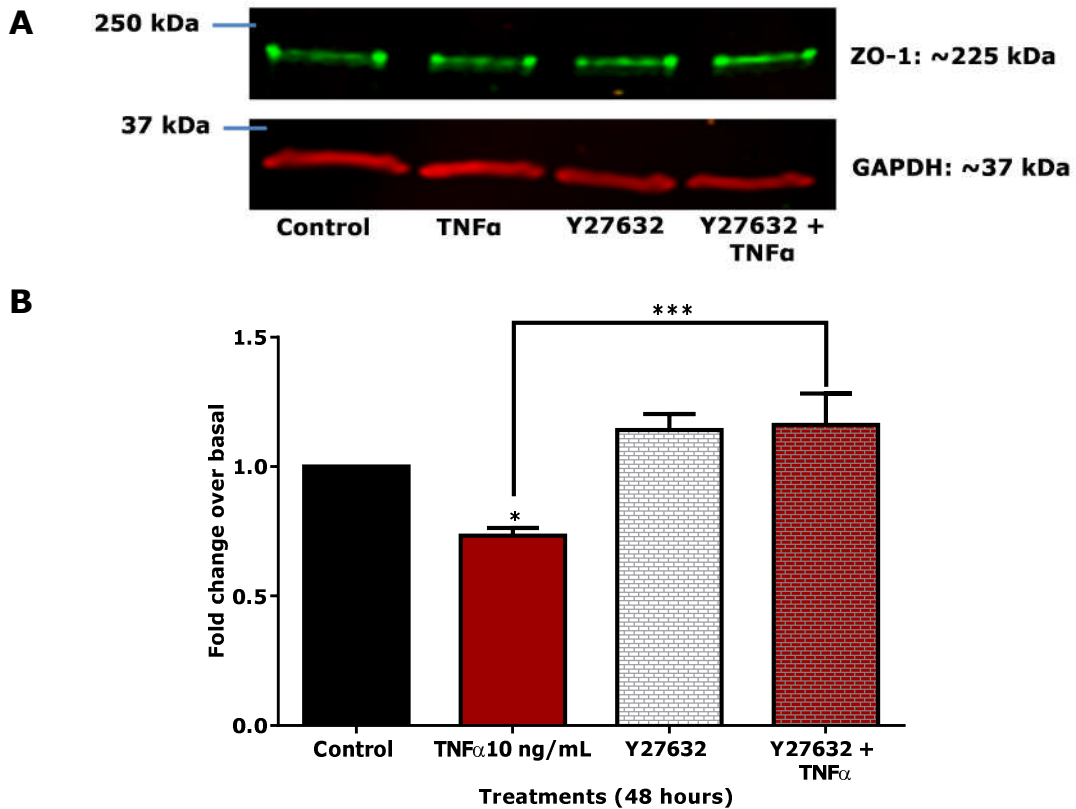


Figure 6-6 A. Western blot images and **B.** semi-quantitative analysis of the changes in the tight junction protein, ZO-1 expression following basolateral administration of Y27632 (10 μ M) in the presence of TNF α (10 ng/ml) in Calu-3 cells for 48 hours. GAPDH was used as a reference protein (or loading control) as its level of expression remained similar in all treatment groups, whilst occludin expression varied. 'Fold change from vehicle' labelled on the Y-axis in figures B&D was derived by dividing the ratio of occludin to GAPDH expression for the respective treatment groups with the ratio of occludin to GAPDH for the control cells. Data are presented as means \pm SEM of fold changes in protein expression compared with control (untreated cells); $n=6$, * $P<0.05$, ** $P<0.01$, 1-way ANOVA followed by a Bonferroni post-hoc test, compared to control,, whereas combined treatment of Y27632 and TNF α is compared to TNF α alone. Refer appendix for original blot images (Appendix- Chapter 6(5)).

6.3.4 Effect of THC on MYPT1 phosphorylation

Changes in Rho kinase activity were determined by measuring changes in the phosphorylation of the Rho kinase substrate, myosin phosphatase target subunit 1 (MYPT1) at Thr696. Total and phosphorylated MYPT1 at Thr696 were detected at earlier time points, from basal up to 20 minutes when cells were treated with TNF α only and in the combination of THC and TNF α (see *Appendices –Chapter 6(6)*).

The time points studied were then extended, ranging from time 0 (basal), 0.5, 1, 2, 3 and 4 hours (*Figure 6-7A*). These experiments revealed that TNF α caused an increase in MYPT1 phosphorylation at Thr696 at 3 hours (*Figure 6-7B*), which coincided with the reduction in TEER. The presence of THC in TNF α -treated cells significantly inhibited MYPT1 phosphorylation caused by TNF α alone ($P<0.001$, 1-wayANOVA). *Figure 6-7C* confirmed that total MYPT1 levels were unaltered in both treatments. It is noted that the results presented in *Figure 6-7B* were normalised to indicate the fold change in total MYPT1 level from that of cells at basal (i.e. time zero).

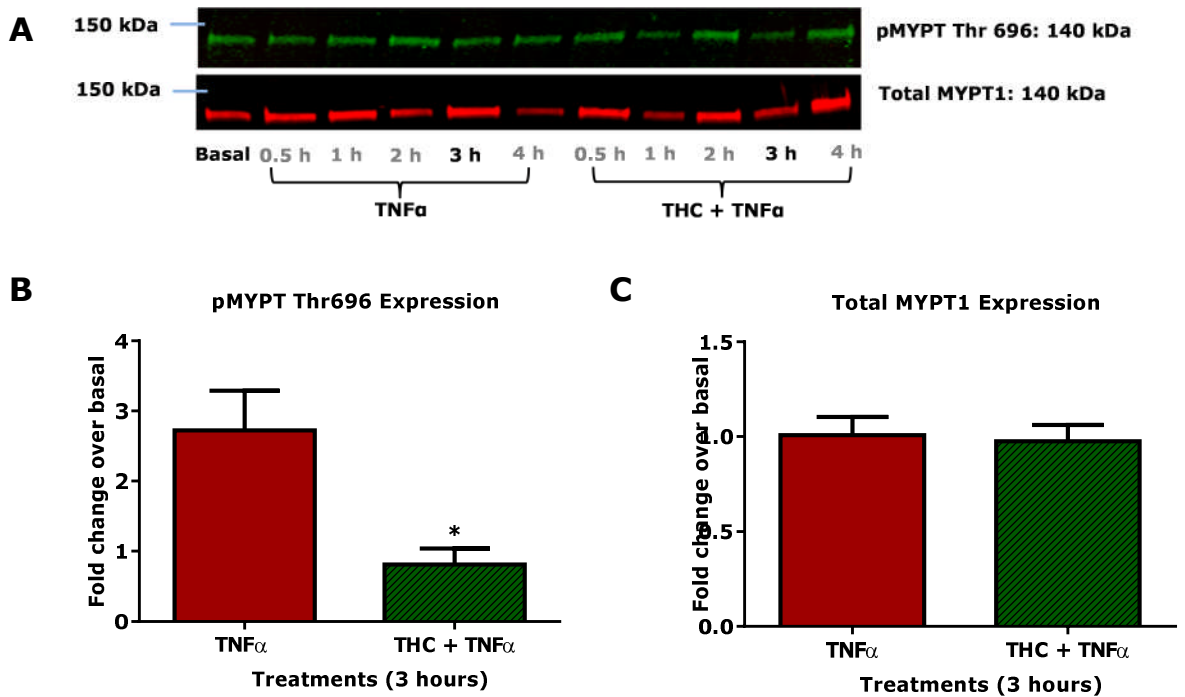


Figure 6-7 **A.** Typical immunoblot showing changes in phospho-MYPT1 (Thr696) (top) and total MYPT1 (bottom) expression following basolateral application of TNF α (10 ng/ml) alone or in the presence of THC (30 μ M) up to 4 hours in serum-starved 21-day old Calu-3 cells, cultured in ALI. **B.** Fold change of phospho-MYPT1 (Thr696) expression at 3 hours following TNF α exposure compared to fold change of phosphor-MYPT1 at basal (i.e. time zero); **C.** Semi-quantitative data of total MYPT1 expression remained similar whilst phosphorylated MYPT varied between treatments hence was used as a reference protein. Fold change from basal labelled on the Y-axis in figures B&C is expressed as the fold change of total MYPT1 expression at a 3 hours to total MYPT1 for the basal cells. Data are presented as mean of fold change over protein expression in basal (untreated) cells mean \pm SEM; $n=4$, $*P<0.05$, analysed using paired Student's t -test, compared to TNF α alone. Refer appendix for original blot images (Appendix- Chapter 6(7)).

6.3.5 The Role of CB₁ and CB₂ Receptors Activation in the Regulation of MYPT1 Signalling

The following Western blotting experiments aimed to evaluate the involvement of CB₁ and CB₂ receptors in regulating MYPT1 signalling as earlier TEER experiments from the present study demonstrated that THC acts through both CB₁ and CB₂ receptors to prevent TNF α -induced increased cell.

The effect of activation of CB₁ and CB₂ receptors was studied individually by stimulating cells with a selective CB₁ agonist, ACEA (100 nM) and CB₂ agonist JWH133 (3 μ M) for an hour, before exposing the cells with TNF α (10 ng/ml) for up to 4 hours.

In contrast to THC, treatment with ACEA did not prevent the TNF α induced phosphorylation of MYPT1 (*Figure 6-8B*). *Figure 6-8C* shows that the total MYPT1 level of the samples from both treatments were similar, thereby confirming that the amount of protein loaded onto the SDS-PAGE gel was near equal and total MYPT1 level were unaltered in both treatment groups.

On the other hand, selective activation of the CB₂ receptor with JWH133 prevented the increase in phosphorylated MYPT1 following the administration of TNF α at 3 hours ($P < 0.01$, 1-way ANOVA) (*Figure 6-9B*). Results in *Figure 6-9C* have yet again proven that approximately the same amount of protein from cells samples was loaded onto the SDS-PAGE gel and there was no change in total MYPT1 despite different treatments.

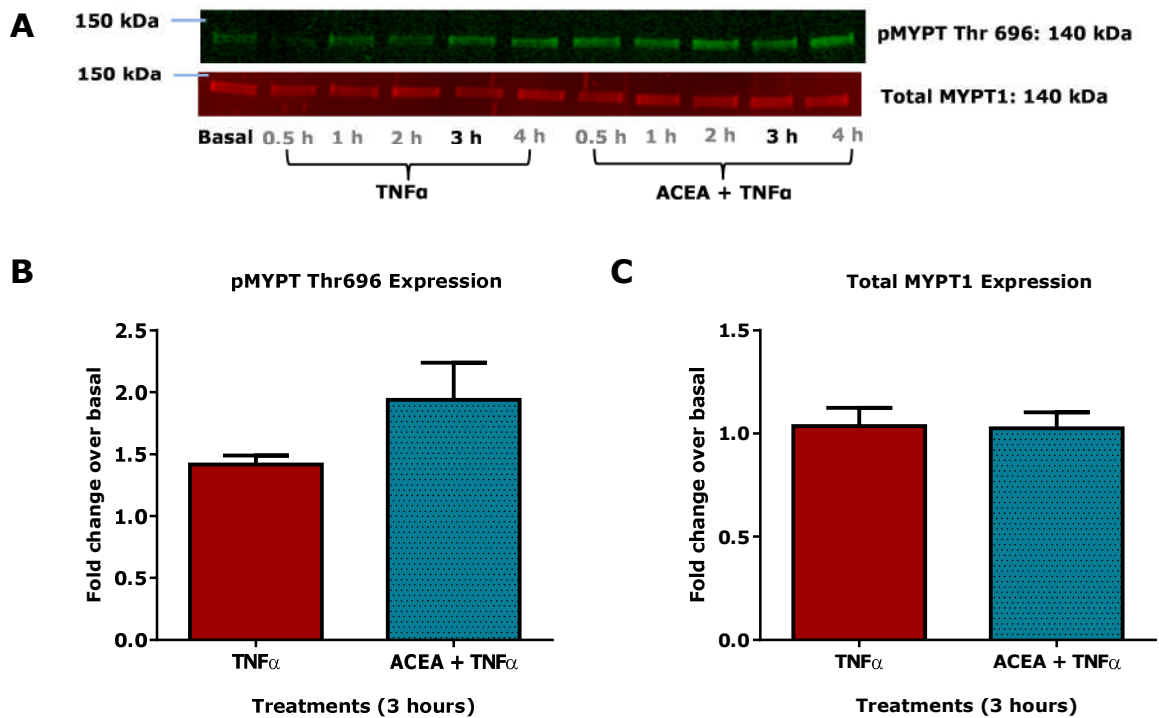


Figure 6-8 A. Typical immunoblot showing changes in phospho-MYPT1 (Thr696) (top) and total MYPT1 (bottom) expression following basolateral application of TNF α (10 ng/ml) alone or in the presence of ACEA (100 nM) up to 4 hours in serum-starved 21-day old Calu-3 cells, cultured in ALI. **B.** Fold change of phospho-MYPT1 (Thr696) expression at 3 hours following TNF α exposure compared to fold change of phosphor-MYPT1 at basal (i.e. time zero); **C.** Semi-quantitative data of total MYPT1 expression remained similar whilst phosphorylated MYPT varied between treatments hence was used as a reference protein. Fold change from basal labelled on the Y-axis in figures B&C is expressed as the fold change of total MYPT1 expression at a 3 hours to total MYPT1 for the basal cells. Data are presented as mean of fold change over protein expression in basal (untreated) cells mean \pm SEM; n=5, no statistical change was detected when results were analysed using paired Student's t-test, compared to TNF α alone. Refer appendix for original blot images (Appendix-Chapter 6(8)).

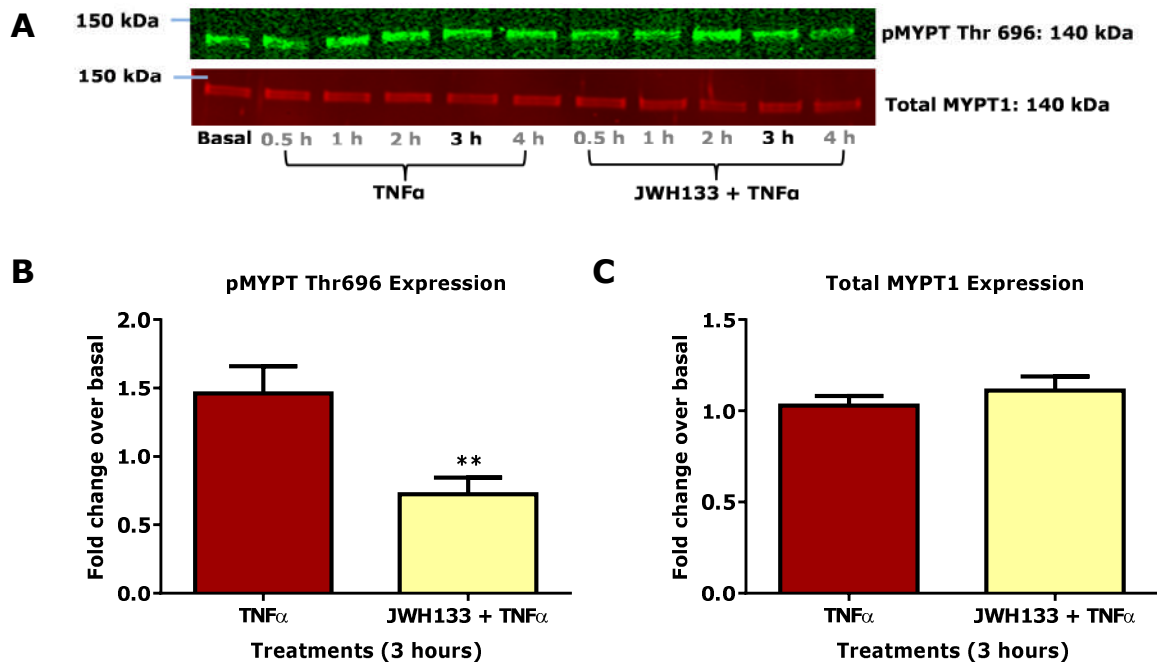


Figure 6-9 **A.** Typical immunoblot showing changes in phospho-MYPT1 (Thr696) (top) and total MYPT1 (bottom) expression following basolateral application of TNF α (10 ng/ml) alone or in the presence of JWH133 (3 μ M) up to 4 hours in serum-starved 21-day old Calu-3 cells, cultured in ALI. **B.** Fold change of phospho-MYPT1 (Thr696) expression at 3 hours following TNF α exposure compared to fold change of phosphor-MYPT1 at basal (i.e. time zero); **C.** Semi-quantitative data of total MYPT1 expression remained similar whilst phosphorylated MYPT varied between treatments hence was used as a reference protein. Fold change from basal labelled on the Y-axis in figures B&C is expressed as the fold change of total MYPT1 expression at a 3 hours to total MYPT1 for the basal cells. Data are presented as mean of fold change over protein expression in basal (untreated) cells mean \pm SEM; $n=4$, ** $P<0.01$, analysed using paired Student's t -test, compared to TNF α alone. Refer appendix for original blot images (Appendix- Chapter 6(9)).

6.4 Discussion

Studies in various epithelial cell models especially human intestinal and kidney epithelial cells (Schmitz et al., 1999, Chen et al., 2000, Ma et al., 2004) have linked the functional association of epithelial permeability to the change in expression of key tight junction proteins, such as occludin and ZO-1. Results presented in this chapter showed that the phytocannabinoid, THC prevented TNF α -induced decrease in occludin and ZO-1 expression by paradoxically caused a further increase in ERK1/2 phosphorylation compared to TNF α alone. Alternatively, THC was also found to dampen TNF α -induced ROCK activation which mediated selectively through CB₂ receptor stimulation.

Similarly, previous studies using epithelial cells derived from the airway including primary or Calu-3 and 16HBE14o- epithelial cell lines had demonstrated consistent outcome, as the expression of occludin and ZO-1 were reportedly to be directly proportional to TEER measurement (Wan et al., 2000, Coyne et al., 2002). The assembly of occludin and ZO-1 with the rest of the tight junction proteins including ZO-2, ZO-3 and claudin (Furuse et al., 1993, Anderson and Vanitallie, 1995, Fanning et al., 1998) are membrane-bound complexes that form the barrier against paracellular invasion of foreign particles and pathogens into the airway submucosal compartment to trigger inflammation.

In the present study, basolateral application of THC to Calu-3 cells had been shown to both restore and maintain bronchial epithelial resistance upon exposure to TNF α , IL-1 β or the endocannabinoid, anandamide (refer *chapter 5*). It is noted that TNF α was the chosen cytokine to represent the selection of pro-inflammatory mediators in this series of experiments. This is due to its reproducibility in inducing epithelial

leakiness and the fact that TNF α is one of the major cytokines in the pathogenesis of asthma and COPD.

Earlier TEER experiments have demonstrated that treatment with TNF α alone decreases Calu-3 epithelial resistance as cells became increasingly leaky. Parallel functional studies with Western blotting revealed significant reduction in the level of occludin and ZO-1 expression when cells were treated with TNF α (10 ng/ml) (refer *Figure 6-1* and *Figure 6-2*). The presence of THC prevented such phenomenon. This finding is also consistent with earlier results obtained in TEER and FITC-permeability experiments - as the decrease in TEER and increase in P_{app} value caused by TNF α were completely inhibited by THC (*section 4.3.2* and *section 4.5.2*). Hence, this supports the idea that the presence of occludin and ZO-1 is essential to maintain intercellular anchorage within the bronchial epithelium layer. Downregulated expression of these proteins by the cytokine TNF α signifies an undesirable increase in epithelial leakiness, which is counteracted by THC.

Previous finding presented in *chapter 4* also revealed that MAPKs including ERK1/2 and p38 activation are necessary in TNF α -induced increased bronchial epithelial permeability. However, the results displayed in *Figure 6-3* shows the presence of THC in TNF α -treated cells caused a further increase in ERK1 and ERK2 phosphorylation compared to TNF α alone, suggesting that ERK1/2 MAPK is activated rather than inhibited by THC. Indeed, there was no apparent increase in ERK with TNF α at the studied time points; i.e. up to 4 hours. This may be made possible as the cannabinoids CB₁ and CB₂ receptors are known to be positively coupled to MAP kinases (Pertwee, 2010). Hence, treatment with THC which stimulated both cannabinoid receptors expressed in Calu-3 cells promoted ERK2 phosphorylation.

This could indicate that ERK activation is involved in tight junction formation. Such phenomenon was previously observed in intestinal epithelial cell lines, such as T84 and HT-29 cells that were treated with the transforming growth factor β (TGF β). It was shown in these studies that ERK1/2 activation was essential to promote tight junction assembly (Howe et al., 2002, Howe et al., 2005). However, these data are at odds with the studies demonstrating that inhibition of ERK activation with PD98059 and U0126 prevented the TNF α -induced decrease in TEER (*section 4.3.2*). A potential explanation could be differences in the subcellular localisation (i.e. cytoplasmic or nuclear) of ERK1/2 MAPK activation. Raman *et al* reported that phosphorylation of the ERK1/2 MAPK leads to ERK dimerization, which is dependent on the availability of scaffold proteins (Raman et al., 2007). Whilst ERK dimers facilitate stimulation of cytoplasmic substrates, both scaffolds and the formation of ERK dimers are not essential for the stimulation of ERK signalling within the nucleus (Casar et al., 2008). In this study, samples used for Western blotting experiments were collected from the supernatant of the Calu-3 cell lysate (refer *section 2.4.1*). This signifies that the ERK1/2 signalling presented in *Figure 6-3* was derived from the cytoplasm. Whole cell lysates or different subcellular fractionation might identify differences in subcellular location of ERK activation depending on the stimulus. Future investigations should distinguish specific molecular characteristics of ERK1/2 activation involved in causing epithelial tight junction assembly and disruption.

Besides the MAP kinases, another intracellular transduction pathway that is commonly linked to the regulation of epithelial paracellular permeability is the RhoA/ROCK cascade. Previous studies have shown RhoA/ROCK-mediated epithelial tight junction disruption can be triggered by various pro-inflammatory

mediators, mainly cytokines such as TNF α (Cunningham and Turner, 2012) and IFN γ (Utech et al., 2005) as well as pathogenic toxins (Nusrat et al., 2001) or presence of bacteria or viruses (Nava et al., 2004, Boyle et al., 2006). The TEER experiment conducted in the present study has demonstrated that TNF α -induced increased epithelial cell permeability was fully inhibited by the ROCK inhibitor Y27632 (10 μ M) (*Figure 6-4*). Hence, this study indicates the involvement of ROCK in mediating the barrier function of bronchial Calu-3 cells following TNF α challenge. Previous study had shown that treatment with Y27632 at 10 μ M selectively inhibited ROCK enzyme, although it was also reported that another downstream RhoA effector, protein kinase C-related kinase 2 (PRK2) was also inhibited at similar IC₅₀ value to that of ROCK (Davies et al., 2000). The lack of concentration-response experiments has been addressed in *section 5.4*, therefore will be considered in future studies. Nevertheless, the use of Y27632 in the present study was necessary to identify the involvement of RhoA and ROCK activity. The increase in phosphorylation of MYPT1 at the ROCK phosphorylation site Thr696 in the presence of TNF α supports the idea that TNF α increases ROCK activity.

The mechanism of ROCK in regulating epithelial cell permeability is thought to be linked to the modification in tight junction proteins expression. Exposure of the renal HK-2 cell line to the cytokine, TGF β caused a decrease in occludin and ZO-1 protein expression which was attenuated by the ROCK inhibitor, Y27632 (Zhang et al., 2013). Similar phenomenon was observed in the present study as pre-incubation with Y27632 prevented the downregulation of occludin and ZO-1 expression caused by TNF α (*Figure 6-5* and *Figure 6-6*). These findings suggest that activation of ROCK by TNF α reduces the availability of occludin and ZO-1 as building blocks for tight junction assembly.

It is noted that several other mechanisms of ROCK on epithelial tight junction regulation have been described in the literature and were not evaluated in this study. For instance, internalisation of the epithelial tight junction proteins following RhoA/ROCK activation subsequently destabilise intracellular actin filaments that provide support to the tight junction protein complex. Immunofluorescence study in T84 intestinal epithelial cells exposed to the cytokine IFN γ revealed endocytosis of tight junction proteins, occludin, JAM and claudin that disrupted F-actin microfilament organisation within the cell (Utech et al., 2005). The loss of such protein interaction between the tight junction protein complex and actin filaments which led to increased epithelial permeability was related to an increased in activated RhoGTPases. Furthermore, stimulation of RhoA/ROCK activity can promote phosphorylation of tight junction proteins which consequently disorganises the tight junction complex structure, hence increases epithelial leakiness. Genetically modified MDCK cells overexpressing the activated form of RhoA caused phosphorylation of occludin and ZO-1 which delocalised both tight junction proteins from the membrane, causing renal epithelial leakiness (Gopalakrishnan et al., 1998). These alternative mechanisms observed mainly in intestinal and renal epithelial cell models are interesting for the future studies to further the understanding of Rho/ROCK cascade in the mediating airway epithelial barrier function.

Activation of ROCK by various pro-inflammatory cytokines results in an increase in epithelial leakiness that is associated with increased phosphorylation of the regulatory light chain, MLC2 [reviews by (Gonzalez-Mariscal et al., 2008, Terry et al., 2010)]. Activation of ROCK leads to phosphorylation of MYPT1 that inhibits myosin phosphatase, hence preventing a decrease in MLC2 phosphorylation (refer RhoA/ROCK cascade in *section 1.7.2*). TNF α and IFN γ -induced increased in

paracellular permeability in Caco-2 intestinal epithelial cells was related to an increased in MLC2 phosphorylation and inhibition of phosphorylation attenuated the epithelial barrier disruption caused by these cytokines (Turner et al., 1997). MLC phosphorylation was also associated with intestinal epithelial leakiness through redistribution of the tight junction proteins; occludin, ZO-1 and JAM from the cell membrane (Clayburgh et al., 2005). Electron microscopy examination then confirmed that this was linked to the contraction of actomyosin. Therefore, activation of MLC2 following an upstream stimulation of RhoA/ROCK would similarly increase bronchial epithelial permeability as the molecular compositions of the intestinal and bronchial tight junction are similar (Vilasaliu et al., 2011). Nevertheless, the involvement of MLC2 was not evaluated in this study, but would be interesting for future investigations.

Instead, the present study evaluated MYPT1 phosphorylation at Thr696 as a measure of ROCK activity. The hypothesis derived for this experiment was based on the fact that an increase in MYPT1 phosphorylation by the cytokine, TNF α would lead to inhibition of myosin phosphatase from converting phospho-MLC2 to MLC2. An accumulation of the activated, phosphorylated form of MLC2 is then expected to disrupt the epithelial barrier function by causing tight junction proteins disassembly. Contrary to such postulation, results reported in several research papers refuted the role of myosin phosphatase in regulating epithelial permeability. These studies which employed human intestinal MKN28 and T84 epithelial cells revealed that both total and phosphorylated MYPT1 expression levels remained unaltered despite expression of high or low epithelial resistance determined by TEER measurements (Utech et al., 2005, Samarin et al., 2007, Wroblewski et al., 2009). Nevertheless, the present study detected an increase in phosphorylated MYPT1 which peaked at 3 hours (*Figure 6-*

7B) in cells treated with TNF α (10 ng/ml). This finding suggests that the RhoA-ROCK-MYPT1 network is involved in TNF α -induced increase in bronchial epithelial permeability. Pre-incubation with THC (30 μ M) prevented TNF α -induced MYPT1 phosphorylation at 3 hours (*Figure 6-7D*), which could occur either by directly preventing MYPT1 phosphorylation caused by TNF α , or by stimulating dephosphorylation of phospho-MYPT1. This supports the hypothesis suggested by Gonzalez-Mariscal *et al* and Terry *et al* of the role of MYPT1 signalling in influencing the epithelial tight junction barrier function.

Further investigations using Western blotting were then conducted to probe for the receptor involved in mediating THC effect in inhibiting TNF α -induced MYPT1 activation. Previous functional bioassays have characterised THC as a partial agonist at both CB₁ and CB₂ receptors (Matsuda et al., 1990). Findings reported in *chapter 4* have demonstrated that THC prevents TNF α -induced increased bronchial epithelial permeability through CB₁ and CB₂ receptors stimulation. The fact that THC had subsequently shown to inhibit TNF α -mediated MYPT1 activation prompted the need to evaluate the intracellular transduction pathway undertaken by THC.

Upon activation, CB₁ and CB₂ receptors stimulate several intracellular signalling pathways through the G_{i/o} proteins, that are known to inhibit adenylyl cyclase but promote activation of mitogen activated protein kinases [reviews by (Pertwee, 2006)]. However, evidence on the association of the cannabinoid receptors to Rho-dependent responses is still limited and remains controversial. The literature reports a predominant role of G _{α 12/13} proteins in activation of the RhoA/ROCK pathway [reviews by (Schwartz and Shattil, 2000, Siehler, 2009)]. Nevertheless, Western blotting study with Swiss 3T3 fibroblast cells treated with the GPCR agonist, lysophosphatidic acid (LPA) demonstrated an increase in RhoA activity (Fleming et

al., 1996) that was attenuated following pre-incubation with pertussis toxin, a selective inhibitor of $G_{ai/o}$ proteins. Such evidence suggests that activation of the GPCRs through $G_{ai/o}$ proteins also participate in stimulating the RhoA/ROCK cascade.

Reports on the involvement of CB_1 and CB_2 in regulating the RhoA/ROCK cascade are still limited. Studies that were published thus far are of investigations on the effect of cannabinoid receptor(s) activation on cellular migration in immune cells, rather than epithelial or endothelial cell permeability. Exposure to $TNF\alpha$ in an *in vitro* co-culture model of human coronary artery endothelial cells and CB_2 receptor-expressing THP-1 monocyte cell line resulted in the stimulation of RhoA which promoted monocyte migration. $TNF\alpha$ -induced RhoA activation was reportedly diminished following activation with either the selective CB_2 agonist, JWH133 or HU-210 (Rajesh et al., 2007b). In addition, a recent study in murine macrophages expressing both CB_1 and CB_2 receptors showed an increase in RhoA-mediated phagocytosis when stimulated with selective CB_1 receptor ligand methanandamide (Mai et al., 2015), but treatment with JWH133 had no effect.

The present study evaluated the role of cannabinoid receptor(s) on RhoA-mediated epithelial cell permeability in Calu-3 cells. Pre-incubation with JWH133 (3 μ M) inhibited the increase in MYPT1 phosphorylation at Thr696 by $TNF\alpha$ (Figure 6-9) - indicating an upstream decrease in RhoA/ROCK activity. It is noted that such effect is similar to that of THC-treated cells.

Interestingly, selective activation of CB_1 receptor had no effect on MYPT1 phosphorylation caused by $TNF\alpha$ (Figure 6-8). It is thus tempting to conclude that inhibition of $TNF\alpha$ -induced increased cell permeability by THC was CB_2 receptor-

mediated, but not CB₁. The role of CB₁ receptor on Calu-3 epithelial cell permeability was therefore speculated. TEER results in *section 5.3.8* have shown a delayed effect of ACEA in inducing complete TEER recovery compared to CB₂ agonist, JWH133 and potent cannabinoid agonist, HU-210 when Calu-3 cells were exposed to TNF α . This suggests the possibility that ACEA inhibits the RhoA/ROCK/MYPT1 pathway at a later time point (i.e. more than 3 hours) than cannabinoid ligands that can more potently stimulate CB₂ receptor. The effect of the CB₁ and CB₂ selective ligands on expression of tight junction proteins was not investigated in this present study. Nevertheless, earlier TEER experiments presented in *chapter 4* showed that the action of THC in preventing TNF α -induced increased in Calu-3 cell permeability was antagonised by both CB₁ receptor antagonist, AM251 and CB₂ receptor antagonist, SR144528 (*section 5.3.6*). Subsequent Western blotting studies supported the inference that both cannabinoid receptors are expressed Calu-3 cells (*section 5.3.7*). These findings suggest that THC reverses the reduction in transepithelial resistance caused by TNF α , through an effect at CB₁ and CB₂ receptors. Thus, it is postulated that stimulation of the CB₂ receptor by THC occurs at the early phase in blocking the TNF α effect, whereas CB₁ receptor activation is involved at the later phase – i.e. suggesting a possibility that the activation of these cannabinoid receptors by THC may have happened sequentially.

Further hypothesis was then made that the presumably late onset of action by ACEA suggested the role of CB₁ receptor stimulation in mediating epithelial gene expression. One of the common pathways known to cause gene modulation following cytokine exposure such as TNF α and activation of GPCRs is the nuclear factor-kappaB (NF- κ B) transcription factor (Matsusaka et al., 1993, Ye, 2001). TNF α challenge, which produced an anticipated increase in Caco-2 intestinal cell

permeability, was demonstrated to be mediated through the ROCK-MLCK-MLC cascade that subsequently led to activation of NF- κ B. The authors then revealed that the decrease in functional tight junction protein expression including occludin, ZO-1 and claudin expression was due to alteration of their gene expression following activation of NF- κ B. Data obtained from murine derived BV2 microglial cells stimulated with endotoxin lipopolysaccharide (LPS) had showed resulting increase in cytokine release including IFN γ , IL-1 β and IL-6 that was related to the NF- κ B stimulation. Such effect was reportedly attenuated in the presence of the phytocannabinoid THC (Kozela et al., 2010). Ribeiro et al reported consistent observation as treatment using selective CB₁ receptor agonist, ACEA was shown to deactivate the NF- κ B pathway that had fully inhibited LPS-induced cytokines release from BV2 cells (Ribeiro et al., 2013). These evidences thus suggest that CB₁ receptor stimulation in Calu-3 cells may have inhibited the decrease in tight junction gene expression and increase in cytokines transcription associated with TNF α exposure. Data obtained from ELISA and microplex cytokine assays revealed that TNF α promoted the endogenous release of IL-1 β , IL-6 and IL-8, as well as further increase TNF α level from primary human bronchial epithelial cells (Hardyman et al., 2013).

The consideration of only the classical cannabinoids, CB₁ and CB₂ receptor is considered naïve as both ACEA and THC are known to stimulate to other receptors, such as the putative cannabinoid receptor, GPR55 and various subtypes of TRP channels (Ryberg et al., 2007, Sharir and Abood, 2010, De Petrocellis et al., 2011). However, owing to time limitations, it was decided to concentrate attention on the role of CB₁ and CB₂ receptors. To date no studies have attempted to detect GPR55 receptor expression in Calu-3 bronchial cells and whether stimulation of the receptor would lead to a change in epithelial permeability. Future studies, therefore, should

determine the role of other cannabinoid-like receptors in the control of airway epithelial permeability.

As previously mentioned in *section 1.13.4*, the human bronchial epithelial cells commonly express various sub-types of TRP channels, typically thermosensitive and chemosensitive TRPV1 channel (McKemy et al., 2002), the chemosensitive TRPA1 (Bessac and Jordt, 2008), and TRPV4 channel which have been proven thus far in murine model to regulate the ciliary beat of ciliated columnar cells (Lorenzo et al., 2008). Binding studies have demonstrated that the CB₁ receptor agonist, ACEA stimulates TRPV1 (Baker and McDougall, 2004) and TRPA1 channels (Ruparel et al., 2011). Although usually present in other airway epithelial cell models, TRPV1 channel is not expressed in Calu-3 cells (Hibino et al., 2011), excluding the possibility that the action of ACEA observed in the present study was due to TRPV1 activation. Nevertheless, the role of other TRP channels that can be stimulated by ACEA is an interesting area of study as these cationic channels are also known to mediate epithelial permeability (Corteling et al., 2004, Sidhaye et al., 2008).

6.5 Conclusion

Results from *chapter 5* revealed that treatment with TNF α (10 ng/ml) alone increased Calu-3 cell permeability, whilst the presence of phytocannabinoid, THC (30 μ M) before or after TNF α challenge had shown to prevent and reverse the cytokine effect. Subsequent studies in Western blotting revealed that the bronchial epithelial leakiness caused by TNF α was associated to downregulation of tight junction proteins, occludin and ZO-1. Such effect was attenuated in the cells treated with THC alone or in combination with TNF α .

Common intracellular pathways involved in regulating epithelial tight junction function were investigated. First, presence of THC in TNF α -treated cells caused a greater increase in ERK1/2 phosphorylation compared to TNF α alone. Such response was an unanticipated one, as treatment with one of the MEK1/2 inhibitor either PD98059 or U0126 had shown to attenuate TNF α -induced increase in Calu-3 cell permeability in earlier experiments conducted in the present study (*section 4.3.2*). The difference of effects observed in ERK1/2 involvement following THC and or TNF α administration is postulated to be site-specific as activation of the MAP kinase within the cytoplasmic or nuclear compartment had proven to yield different functional outcomes (Raman et al., 2007).

Second, decrease in bronchial epithelial resistance caused by TNF α was blocked by the ROCK inhibitor, Y27632 (*Figure 6-4*), indicating the role of ROCK activation in TNF α -induced effect. Hence, such phenomenon also suggests that THC may have prevented TNF α -induced TEER decrease possibly through an inhibitory effect on RhoA, ROCK or both RhoA and ROCK. Literature revealed that activation of the RhoA/ROCK cascade would subsequently lead to gene modulation within the

nucleus to alter tight junction protein expression (Terry et al., 2010). The phosphorylation of MYPT1 signalling was investigated in this study as a mean to evaluate the RhoA/ROCK activity in Calu-3 cells. Results revealed that the presence of THC had indeed diminished TNF α -induced MYPT1 phosphorylation at Thr696 which was most evident at 3 hours ($P<0.001$, 1-way ANOVA). The effect of TNF α on MYPT1 phosphorylation was also prevented by the CB₂ agonist, JWH133 (3 μ M). The CB₁ agonist ACEA, on the other hand, did not alter the level of MYPT1 phosphorylation caused by TNF α . Although these investigations confirmed that the involvement of CB₂ receptor in the THC-mediated effect on MYPT1 phosphorylation, further studies are needed to establish the involvement of CB₁ and other putative cannabinoid receptors in regulating airway epithelial permeability. Furthermore, the study of the interaction between RhoA/ROCK cascade with ERK1/2 MAPK pathway in the future will be beneficial to provide holistic signalling pathways involved in tight junction disruption and assembly in bronchial epithelial cells.

Figure 6-10 displays the schematic diagram of the summary of findings presented in this chapter:-

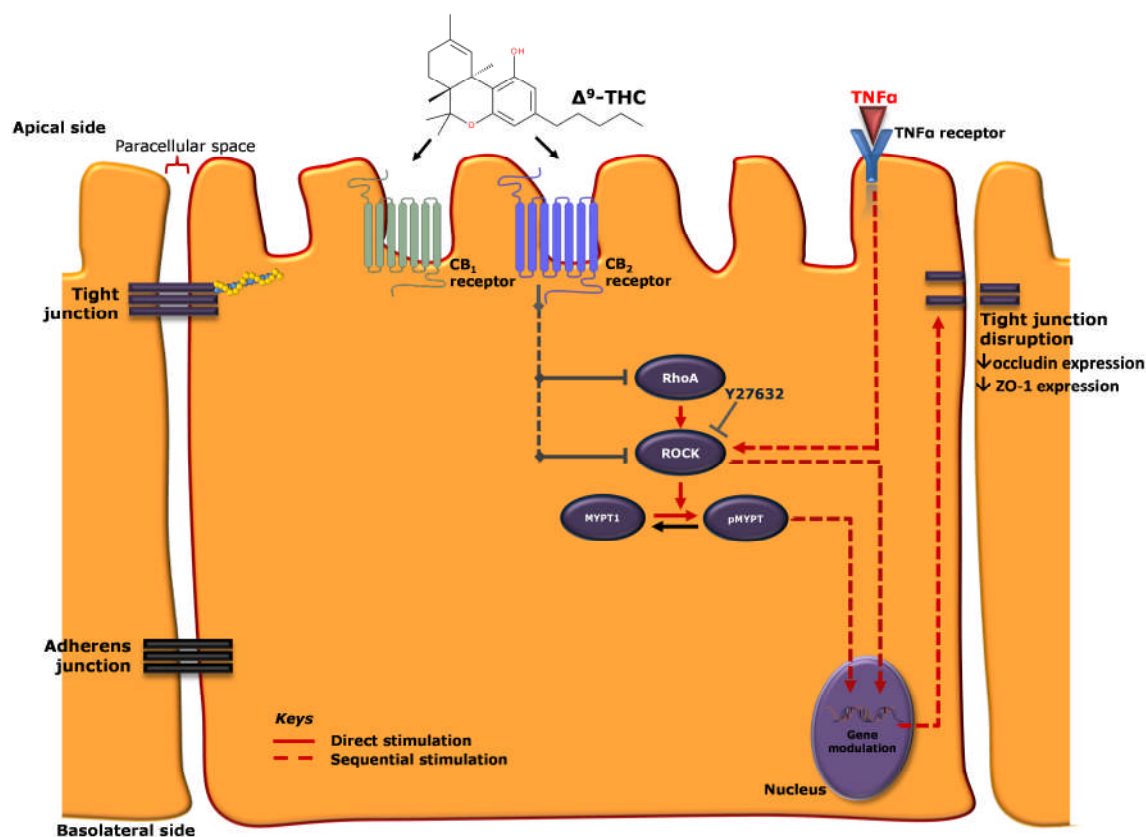


Figure 6-10 Regulation of the epithelial tight junction barrier structure in Calu-3 bronchial cells through the RhoA/ROCK cascade. Red coloured arrows represent intracellular signalling steps involved in tight junction disruption, whereas arrows in black denote the cascades associated to THC stimulation. T-shaped lines indicate inhibition. Activation of ROCK by TNF α promotes phosphorylation of MYPT1 at Thr696. Literature reported that stimulation of the MYPT1 leads to alteration in gene transcription within the nucleus. Subsequently, this leads to the decrease in functional downregulation of tight junction proteins, occludin and ZO-1, which were demonstrated in this study. The effect on tight junction permeability and proteins expression caused by TNF α was fully attenuated with ROCK inhibitor, Y27632. Treatment with THC stimulates both cannabinoid CB₁ and CB₂ receptors. However, only CB₂ receptor was involved in preventing TNF α -induced tight junction disruption which could occur due to the inhibition of either the RhoA GTPase or ROCK enzyme, or both.

7. General Discussion

7.1 The Proposed Hypothesis

Airway inflammation is a terminology umbrella used to describe heightened inflammatory response within the conducting airways, particularly the bronchial region that occurs chronically. The term 'airway' refers to the bronchus as the locus of inflammation. Conditions that are categorised as airway inflammatory diseases include asthma and COPD.

One of the mutual key features of patients with asthma and COPD is bronchoconstriction, a symptom which could be lethal due to blockage of the airflow, impeding the efficient exchange of oxygen and carbon dioxide during inhalation and exhalation reflexes. This is worsened when inflamed airway structures limit the airflow as the airway luminal opening becomes smaller. Bronchoconstriction is also a clinical evidence that the main site of inflammation is within the lower bronchial structures as these airways are less cartilaginous compared to the trachea and the primary bronchi, providing them the ability to respond to the environment by changing the bronchial smooth muscle tone (Monforte-Munoz and Walls, 2004). Exposure to various triggering factors such as plant pollens, house dust mites, cold air and exercise increases the release of pro-inflammatory cytokines in particular $\text{TNF}\alpha$ and $\text{IL-1}\beta$, thus causing the airway to constrict due to exaggerated stimulatory action at the airway sensory nerves. Such phenomenon is referred to as 'airway hyperresponsiveness', which is thought to occur due to the loss of the airway epithelium barrier function as demonstrated in various histological studies using airway samples of asthmatics and COPD patients

(Morrison et al., 1999, Hackett and Knight, 2007). Current pharmacological drugs such as the β_2 adrenoceptor agonists and anti-muscarinics show little or no anti-inflammatory action. On the other hand, corticosteroids, deemed to be the most effective drugs in reversing airway inflammation, also failed to prevent disease progression, especially in moderate to severe stages, or patients who are resistant to corticosteroid treatment (Sont et al., 1999). Since then, research for a new therapeutic treatment has been focusing on repairing airway epithelial injury to address the root cause involved in the manifestation of airway inflammation.

The endocannabinoid system (ECS) has been frequently linked to regulating inflammatory responses in various conditions such as neuropathic pain (Okine et al., 2012) and inflammatory bowel diseases (Massa et al., 2004). It is noted that the ECS involves the interaction of the endogenous cannabinoids anandamide and 2-AG with the classical cannabinoid CB₁ and CB₂ receptors, or, more recently, the putative cannabinoid GPR55 receptor is also included [review by (Henstridge, 2012, Pacher and Kunos, 2013)]. Hence, understanding the role of the ECS in mediating airway inflammatory disease could be an interesting area of study to probe for a new therapeutic target in restoring airway epithelium structure and functions. Current pre-clinical data have demonstrated that anandamide expression level is enhanced in the asthmatic state, suggesting its role in the pathogenesis of asthma (Zoerner et al., 2011). The presence of 2-AG in the airway structures however, has never been reported, thus its role in mediating airway inflammation is yet to be investigated.

Traditionally, the Cannabis plant was smoked or taken orally to treat diseases such as chronic cough and asthma (Nandakarni, 1976). However, the use of Cannabis has now been made illegal in most parts of the world. Indeed, there have been reports that Cannabis smoking increases the risk for lung cancer, but this was largely due to

the presence of the carcinogenic compound benzopyrene formed from burning the Cannabis leaves (Tashkin, 2013). Treatment with isolated constituents of the plant, i.e. phytocannabinoids, had shown positive outcomes in treating inflammation within the airway, mainly for its bronchodilatory effects and reduced immune response (Tashkin et al., 1974, Tashkin et al., 2002). The effect of phytocannabinoids on airway epithelial barrier function has never been investigated. Nevertheless, studies conducted in Caco-2 intestinal epithelial cells have shown that application of the inflammatory cytokines $\text{TNF}\alpha$ and $\text{IFN}\gamma$ increased epithelial cell permeability, indicating that the intestinal epithelial barrier function was impaired (Alhamoruni et al., 2010, Alhamoruni et al., 2012). The presence of the phytocannabinoids THC and CBD then reversed the cytokines' effects, which was mediated mainly through the CB_1 receptor. Although it was highlighted in their study that THC, CBD or other cannabinoid ligands could be useful for treating inflammatory bowel diseases, their finding also suggests the potential role of phytocannabinoids in treating other diseases with disordered permeability, such as asthma and COPD.

7.2 The Key Questions

Following the findings reported by Alhamoruni *et al* (2012) in Caco-2 intestinal epithelial cells, the present study aimed to address three main key questions to further understand the role of cannabinoids in airway inflammation, which is also a disease of disordered epithelial permeability:

- i. What is the effect of endogenous cannabinoids on airway epithelial barrier function as measured by the change in its permeability? The mechanism for its underlying response was also investigated.
- ii. Is there a change in airway epithelial permeability following the administration of phytocannabinoids, THC and CBD as well as selective cannabinoid ligands? This was to identify the effect of the phytocannabinoids on airway epithelial tight junction integrity and to evaluate the presence and function of CB₁ and CB₂ receptors in the *in vitro* model employed in this study, Calu-3 cells.
- iii. What is the effect of the endogenous cannabinoids and phytocannabinoids on MUC5AC protein expression?

7.3 Summary of Findings and Future Investigations

Calu-3 bronchial epithelial cells were the chosen *in vitro* model in this study owing to their ability to develop robust tight junctions and, hence, transepithelial resistance. Calu-3 cells also differentiate to cells that have similar phenotypical features as intact airway epithelium, when cultured at ALI, i.e. mainly ciliated columnar cells and mucus-secreting goblet cells. TEER studies presented here have also shown the usefulness of Calu-3 cells as a pharmacological screening tool. For instance, the application of the cytokine TNF α to the basolateral compartment of the Transwell[®] demonstrated a reproducible decrease in TEER such as that reported in the literature (Coyne et al., 2002, Petecchia et al., 2012), indicating that the epithelial tight junction barrier function was impaired. Furthermore, subsequent data obtained from Western blotting confirmed the expression of CB₁ and CB₂ receptors. The effect of cannabinoids on mucus secretion was also made possible as Calu-3 airway epithelial cells were known to produce the mucin glycoprotein MUC5AC, which is one of the monomers that form mucus. It has been demonstrated in other studies that MUC5AC is produced in response to the exposure of various pro-inflammatory cytokines and drugs [review by (Holgate, 2007)].

Figure 7-1 illustrates the summary of the findings obtained from this study:-

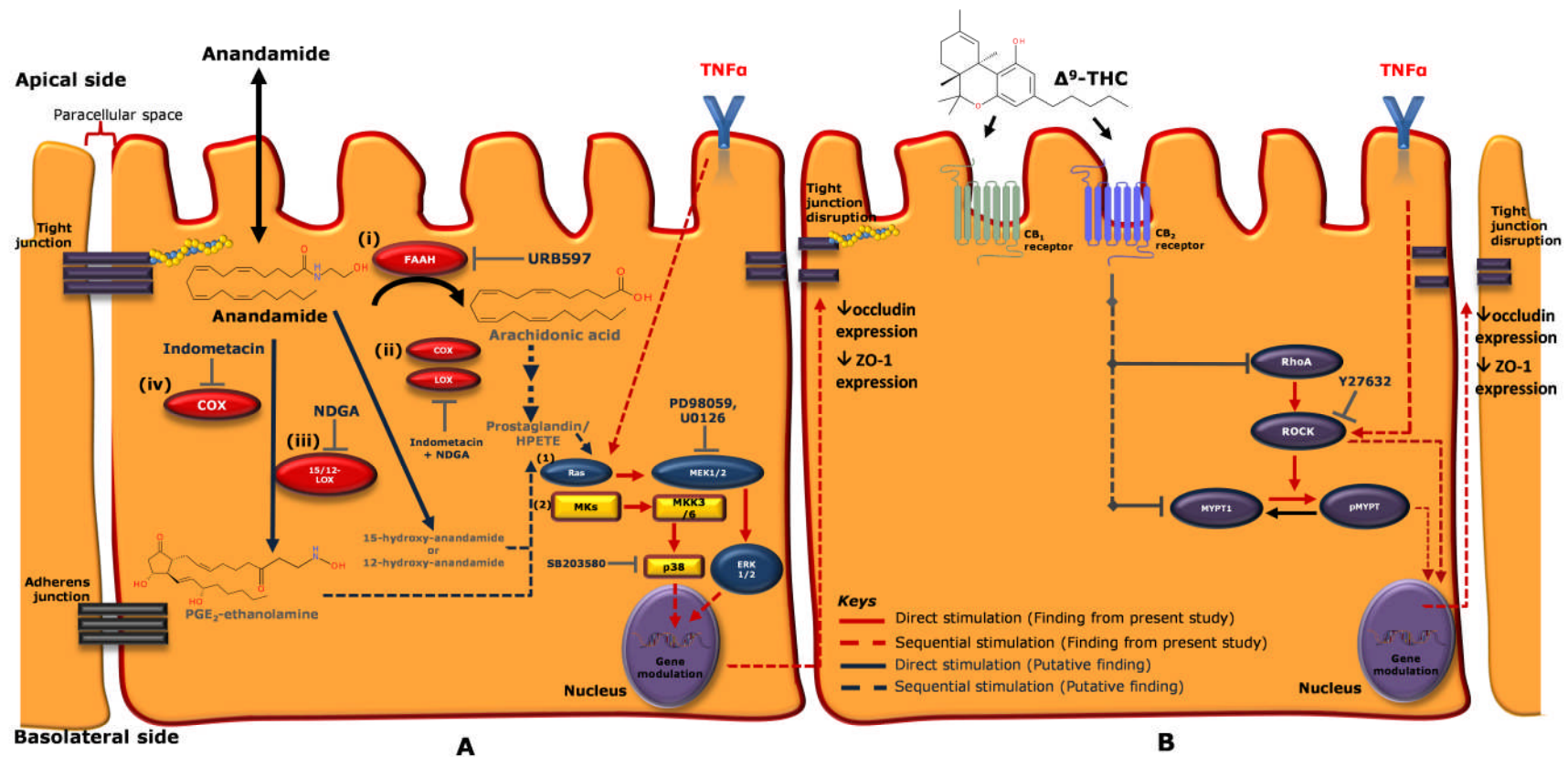


Figure 7-1 Schematic diagram of the findings obtained from the present study. Red coloured arrows represent intracellular signalling steps involved in tight junction disruption, whereas T-shaped lines indicate inhibition. Cell A illustrates that the endogenous cannabinoid, anandamide is metabolised by different intracellular enzymes (i) fatty acid amide hydrolase (FAAH). Arachidonic acid thus formed is metabolised by (ii)

cyclooxygenase (COX) and lipoxygenase (LOX) to various eicosanoids such as prostaglandins (PG) and 5-hydroperoxyeicosatetraenoic acid (5-HPETE). Alternatively, anandamide can be broken down directly by (iii) 15- and 12-LOX to 15- and 12- hydroxyanandamide respectively or by, (iv) COX to prostaglandin-E2 (PGE2)-ethanolamine. The eicosanoid metabolites formed from arachidonic acid or anandamide subsequently stimulate the (1) mitogen –activated protein kinase (MAPK) extracellular regulated kinases 1 or 2 (ERK1/2) through activation by the MAP/ERK1/2 kinases, MEK1/2 or (2) MAPK p38 pathway, through activation of MAPKKK, mixed lineage kinases (MLKs) and the MAPKK, MKK3/6 which leads to changes in gene transcription within the nucleus. Subsequently, this causes downregulation of the tight junction proteins occludin and ZO-1 leading to disruption of the tight junction structure. Similarly, tight junction disruption caused by the cytokine TNF α also involves activation of the MAPKs ERK1/2 and p38 cascades. Cell **B**: TNF α also stimulates RhoA cascade through activation of the Rho-associated protein kinase (ROCK) that leads to myosin phosphatase target subunit (MYPT1) phosphorylation. The present study hypothesises that this leads to alteration in gene transcription within the nucleus that decreases occludin and ZO-1 expression, hence impairing the epithelial tight junction structure. Administration of the phytocannabinoid, Δ^9 -tetrahydrocannabinol (THC) causes stimulation of the cannabinoid CB₁ and CB₂ receptors. Nevertheless, inhibition of the TNF α -induced tight junction disruption through ROCK activation by THC was mediated through CB₂ receptor stimulation, and not CB₁.

In the present study, basolateral application of the cytokine, TNF α (10 ng/ml) reduced transepithelial resistance in Calu-3 cells, indicative of an increased in bronchial epithelial leakiness (refer to *chapter 3*). Treatment with the endogenous cannabinoid anandamide (30 μ M) revealed a similar observation as that seen in TNF α , but 2-AG (30 μ M) showed no effect in altering bronchial epithelial permeability.

Subsequent investigations revealed that the anandamide effect does not appear to be mediated through cannabinoid receptors. In fact, inhibition of anandamide metabolism with a selective inhibitor of the anandamide catabolic enzyme FAAH, URB597 (1 μ M) prevented the effects of anandamide. It was previously reported that metabolism of anandamide by FAAH converts the endogenous cannabinoid to arachidonic acid and ethanolamine as its by-product (Di Marzo et al., 2005). Simultaneous inhibition of cyclooxygenase and lipoxygenase enzymes with indomethacin (10 μ M) and NDGA (10 μ M) was shown to prevent both anandamide and arachidonic acid-induced increased in epithelial permeability. These findings indicate that the increase in Calu-3 cell permeability caused by anandamide is mediated by its metabolite arachidonic acid. However, future work is still required to identify the type and role of arachidonic acid metabolites involved in mediating the structural integrity of the bronchial epithelial tight junction structures.

Further investigations in Western blotting revealed that the drop in transepithelial resistance caused by anandamide and TNF α was associated with a decrease in expression of tight junction proteins occludin and ZO-1. This suggests that the increase in bronchial epithelial permeability following exposure to anandamide and TNF α was due to the reduced availability of occludin and ZO-1 as the building blocks for tight junction assembly. The intracellular signalling pathway was also

investigated. Previous reports demonstrated that TNF α increased Calu-3 epithelial permeability through activation of the MAPK ERK1/2 cascade. Results from the present study revealed consistent observation with TNF α as pre-incubation with the MEK inhibitors PD98059 or U0126 attenuated the decrease in transepithelial resistance and prevented the decrease in expression of occludin caused by TNF α . In addition, inhibition of p38 MAPK with its selective inhibitor, SB203580 also prevented the effects of anandamide and TNF α -mediated responses in causing bronchial epithelial leakiness and decrease in occludin and ZO-1 expression. In conclusion, the endogenous cannabinoid anandamide and the cytokine, TNF α share common intracellular signalling pathways in increasing the Calu-3 epithelial cell permeability. Further work is needed to establish the interaction between MAPK ERK1/2 and p38 signalling in regulating the human bronchial epithelial cell permeability.

In contrast to the anandamide effects, basolateral administration of the phytocannabinoids THC (30 μ M) or CBD (30 μ M) alone did not alter the transepithelial resistance of Calu-3 cells (refer to *chapter 5*). The addition of THC or CBD following the exposure to TNF α (10 ng/ml) fully reversed the reduction in TEER caused by the cytokine. Pre-incubation of Calu-3 cells with either of the phytocannabinoids had also prevented TNF α -induced increase in epithelial permeability. Paracellular permeability assays verified that a reduction in transepithelial resistance measured in TEER experiments was correlated with an increase in paracellular permeability of the Calu-3 epithelial cell layer, and *vice versa*. Based on these findings, it is postulated that THC or CBD might have opposed the effect of TNF α by promoting tight junction proteins formation as data presented in *chapter 4* have demonstrated that TNF α -induced increase in epithelial

permeability was associated with the reduction in tight junction proteins expression. Such hypothesis was made based on the ability of the phytocannabinoids to reverse the drop in transepithelial resistance that had occurred following 24-hour incubation of TNF α . Alternatively, the phytocannabinoids may have interfered with the signalling pathway involved in TNF α -mediated effects, thus preventing the alteration in gene transcription of tight junction proteins expression within the nucleus. Exposure of Calu-3 cells to other pro-inflammatory cytokines known to cause airway inflammation was also evaluated. In this study, the cytokine IL-1 β and endogenous cannabinoid, anandamide showed an anticipated and reproducible decrease in transepithelial resistance. Pre-treatment with THC demonstrated complete inhibition of both the IL-1 β and anandamide effect, indicating that THC is not only effective in suppressing the effects by TNF α , but also other pro-inflammatory cytokines are involved in the pathogenesis of asthma and COPD.

The effects of THC on epithelial permeability are mediated through CB₁ and CB₂ receptors. Pre-incubation with either CB₁ receptor antagonist, AM251 (100 nM) or CB₂ receptor antagonist, SR144528 (1 μ M) inhibited THC-effect in preventing TNF α -induced TEER reduction. Coupled with the data reported in Western blotting experiment which confirmed the expression of both cannabinoid receptors in Calu-3 cells cultured at ALI, such observation has suggested the potential role of CB₁ and CB₂ in THC-mediated effect. Nevertheless, issues on specificity of the antibodies raised against these receptors presented limitation to findings obtained from Western blotting (refer *Figure 5-8* and *Figure 5-9*). Hence, the use of blocking peptide can be considered in future Western blotting experiments which help in detecting unspecific bands whilst silencing specific binding of protein of interest to antibody. In addition,

the detection of mRNA expression of CB₁ and CB₂ receptors using qPCR aids in providing confirmation the presence of cannabinoids receptor in Calu-3 cells.

Further to pharmacological blockade and Western blotting studies, selective cannabinoid ligands were also shown to prevent the effect of TNF α on epithelial permeability. These findings are beneficial in providing information on the structural-activity relationships of the cannabinoid receptors and its ligands for the development of future compounds that could reduce airway epithelial permeability without the undesirable side effects of THC on the central nervous system, such as hallucinations, anxiety attacks and psychosis.

On the other hand, the effects of CBD in preventing TNF α -induced TEER reduction appear to be independent of CB₁ or CB₂ receptors in the Calu-3 airway epithelial cells. Previous studies have demonstrated that CBD exerted its effect through binding to the putative cannabinoid receptor GPR55, various TRP channels and purinergic receptors (Castillo et al., 2010, Pertwee et al., 2010); which expression of these receptors is still yet to be determined in Calu-3 cells. In addition, it was suggested that CBD prevented oxidative stress caused by pro-inflammatory cytokines such as TNF α (Booz, 2011). Evidence has also demonstrated the ability of CBD in inhibiting the activity of FAAH enzyme (De Petrocellis et al., 2011), suggesting interesting future investigation to evaluate the effect of CBD on the endogenous cannabinoid, anandamide-induced increase in human bronchial epithelial cell permeability.

Besides reversing the increased in permeability caused by various pro-inflammatory cytokines, THC reduced expression of MUC5AC glycoprotein in the presence of TNF α . This suggests that THC has also a potential for treating mucus hypersecretion

in airway inflammatory diseases. Whether this effect is mediated through CB receptors was not investigated in this present study and should be addressed in future.

As the TNF α -induced increase in epithelial permeability was sensitive to inhibition of ERK1/2 activation, we hypothesised that THC might be inhibiting the TNF α effects through inhibition of ERK activation. However, administration of THC in TNF α -treated cells caused a further increase in ERK1/2 activation. This may be due to the fact that both CB₁ and CB₂ receptors are GPCRs that are coupled to G_{i/o} proteins which are known to stimulate MAP kinases (Pertwee, 2010). Although such findings contradict with earlier observations that the MEK inhibitors, PD98059 and U0126 prevented the decrease in transepithelial resistance caused by TNF α , it is speculated that spatial activation of ERK1 and ERK2 within the cytoplasm or nucleus (Raman et al., 2007) or the involvement of ERK scaffolds may have contributed to mediating the different outcomes to the changes in Calu-3 epithelial cell permeability. This can be investigated by determining the distribution of cytoplasmic and nuclear ERK scaffolding protein expression such as the Ras GTPase-activating-like protein IQGAP1 (IQGAP1), which is commonly associated to the regulation of cell-cell adhesion and actin-cytoskeleton rearrangement (Briggs and Sacks, 2003).

Data from the present study have also demonstrated that TNF α caused decrease in TEER and reduced occludin as well as ZO-1 expression that were attenuated by the ROCK inhibitor Y27632. Hence this finding suggests that TNF α -mediated epithelial tight junction disruption involves ROCK activation through the RhoA/ROCK pathway. Thus, it was postulated that THC may have a role in deactivating the RhoA/ROCK cascade through an inhibitory action at the small GTPase RhoA or

ROCK enzyme, or both. ROCK activation was determined by measuring changes in phosphorylation of MYPT1 at the ROCK phosphorylation site Thr696. Western blotting revealed that presence of THC significantly reduced MYPT1 phosphorylation especially at 3 hours after the exposure of TNF α . Pre-treatment with selective CB₂ agonist, JWH133 in TNF α -treated cells yielded similar observation, but not CB₁ agonist, ACEA. This finding suggests that the THC effect in preventing TNF α -induced MYPT1 phosphorylation was mediated through CB₂ receptor stimulation. MYPT1 phosphorylation was used as means of determining changes in ROCK activity. However, MYPT1 may not necessarily be involved in the changes in epithelial permeability. Further studies are required to determine how ROCK activation alters epithelial permeability. For example, siRNA silencing of MYPT1 may help determine whether this protein is involved. Phosphorylation of tight junction proteins could also be measured. This phosphorylation could be involved in internalisation of tight junction proteins, and subsequent reduction in protein expression. Immunocytochemistry could be employed to determine whether there is internalisation or co-localisation of occludin and ZO-1 and the effect of inhibition of the RhoA-ROCK-MYPT1 pathway.

The molecular mechanism underlying the role of CB₁ receptor stimulation in mediating Calu-3 cell permeability is unclear and needs to be determined in future experiments. For instance, exposure to TNF α had previously shown to increase endogenous release of cytokines in primary human bronchial epithelial cells. Thus, future experiment may include measurements of multiple cytokine levels in the absence and presence of a selective CB₁ receptor agonist using high throughput techniques, such as multiplex cytokine or cytometric bead arrays. This can be

investigated by comparing the effect of ACEA with another selective CB₁ agonist, arachidonylcyclopropylamide (ACPA).

One of the essential experiments to be considered for the future studies is to establish concentration-response for the cannabinoids compounds used in the present study. The range of concentrations to be studied should be linear. For example, this may include 0.1, 0.3, 1, 3, 10 and 30 μ M for the cannabinoid ligands. Such approach would enable the identification for the optimal concentrations for each of the compound used.

In addition to the findings obtained in Calu-3 cells, a selected series of experiments conducted in the present study can be reproduced in primary human bronchial epithelial cells derived from normal subjects or asthma and COPD patients. An example of a study worth repeating is the identification of CB₁ and CB₂ receptors expression using Western blotting to determine the protein expression of these cannabinoid receptors and reverse transcription polymerase chain reaction (RT-PCR) assay to confirm their mRNA expression. Alternatively, qPCR can be conducted to quantify and compare mRNA expression of CB₁ and CB₂ receptors in healthy and diseased states.

Besides cell-based models, the change in bronchial epithelial permeability can also be measured *in vivo* in guinea pigs, mice and rats. These animals are the appropriate model of study as it was previously report revealed similarity of their airway structures with that of human (Plopper et al., 1980). It is noted that most of the *in vivo* airway inflammatory models published in the literature were acute models, when airway inflammation as seen in asthma and COPD are chronic [review by (Kumar and Foster, 2002)]. Hence, future investigation for this study should adopt

chronic airway inflammatory model that can be created by exposing the animals to allergen challenge such as inhalation of histamine, methacholine or ovalbumin for long term. Previous study in mice had demonstrated that the exposure to aerosolised allergen for 30 minutes at each challenge on three times a week, for up to eight weeks caused airway remodelling that include structural impairment of the airway epithelium (Temelkovski et al., 1998). Subsequently, animals can be treated with cannabinoid ligands, such as THC, that has been demonstrated to potentially treat asthma and COPD in the current study due to its ability to preserve airway epithelial barrier function and indicated to prevent excessive mucus secretion. Dose-response studies can then be conducted to determine the therapeutic window of selected cannabinoid ligands in preventing or opposing the effect of aeroallergens from disrupting the airway epithelial structure. Thus, the airway barrier function is preserved, preventing overstimulation of the subepithelial afferent nerves; i.e. airway hyperresponsiveness. Successful attempts in *in vivo* testing can then lead to the eventual study in pre-clinical studies to explore the therapeutic benefits of cannabinoids in restoring impaired airway epithelium such as that seen in asthma and COPD.

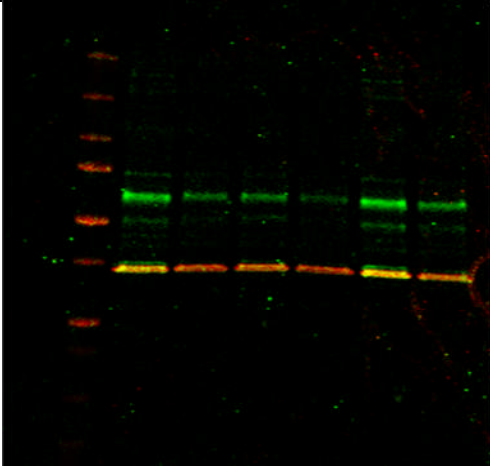
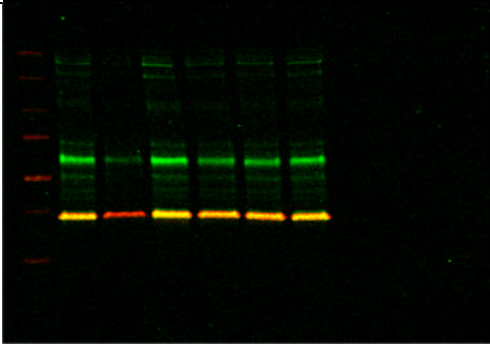
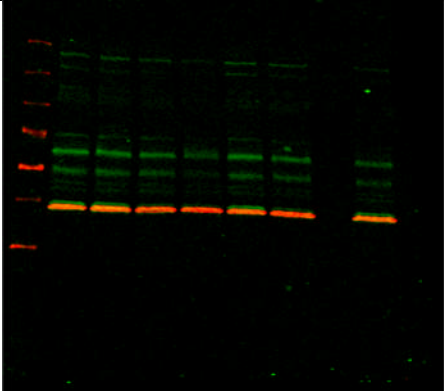
Nevertheless, limitations on the use of THC as possible therapeutic treatment for airway inflammatory conditions are acknowledged, mainly owing to its notorious psychotropic effect hence potential for abuse. THC-induced psychoactivity occurs due to its ability to stimulate CB₁ receptor, which is abundantly present in the brain [review by (Mechoulam et al., 2014)]. Studies have shown that CB₂ receptor predominantly mediates the immunomodulatory function [review by (Rom and Persidsky, 2013)], as CB₂ receptor is commonly distributed in the immune cells and the structures in various organs (refer *section 1.11.1*). Indeed, results from the

present study also suggest that CB₂ receptor may be a better potential site of target to hence supporting the further development of CB₂ receptor agonists in restoring airway epithelial damage, such as that seen in asthma and COPD.

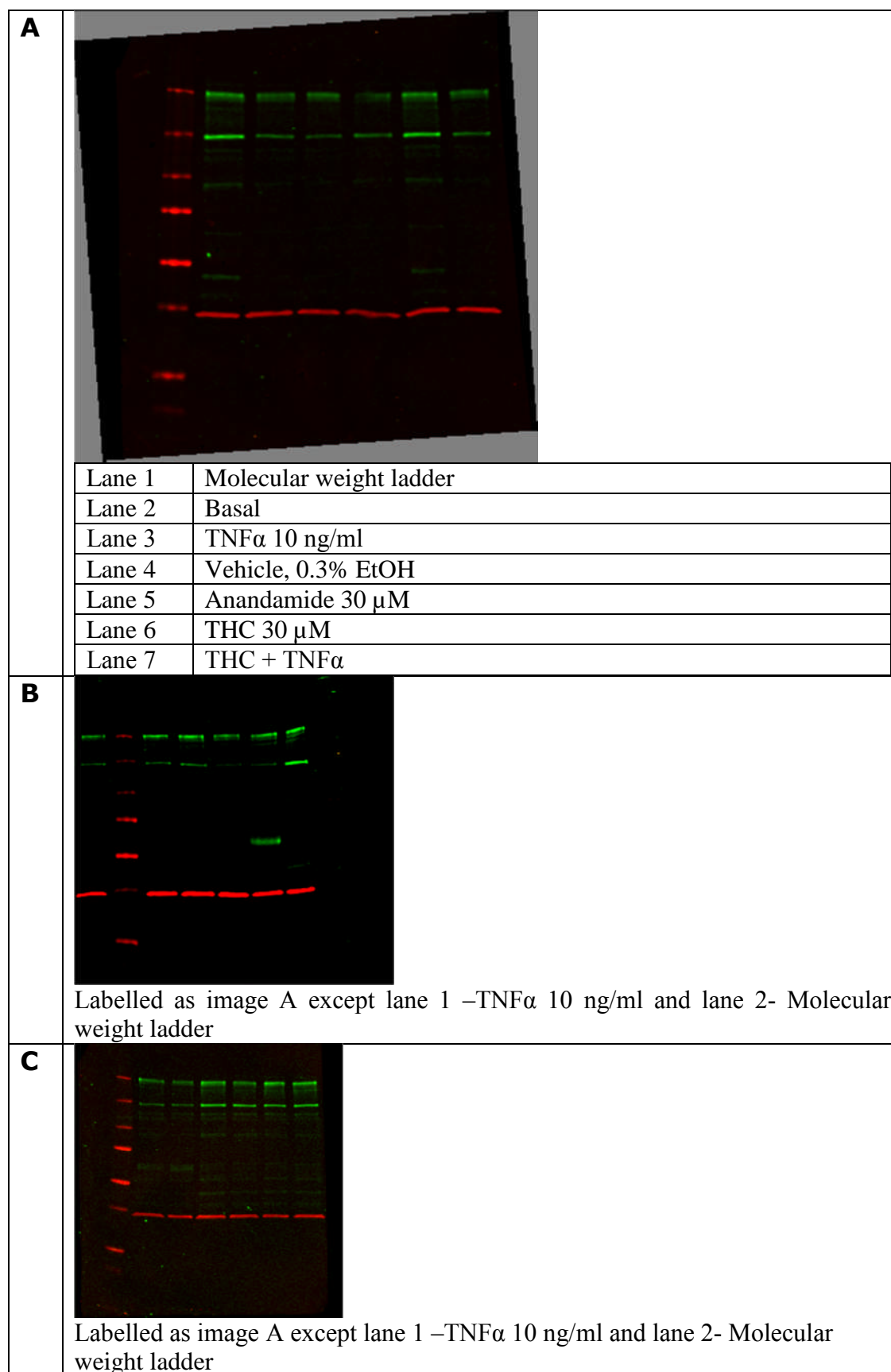
Appendix

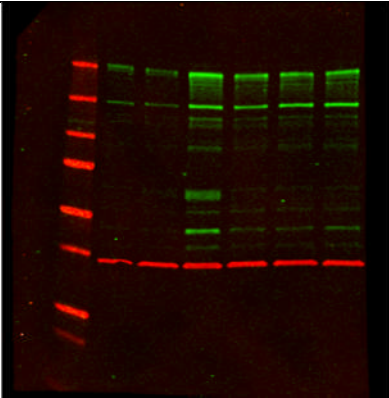
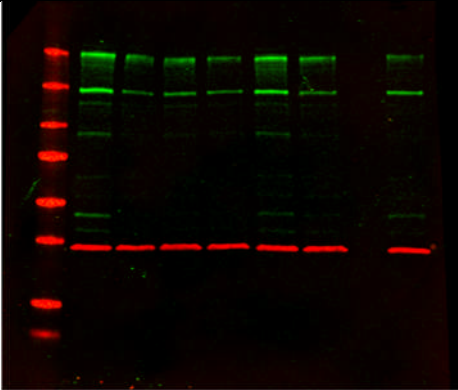
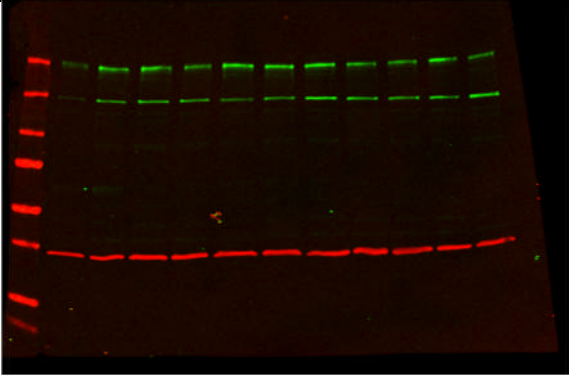
Chapter 4

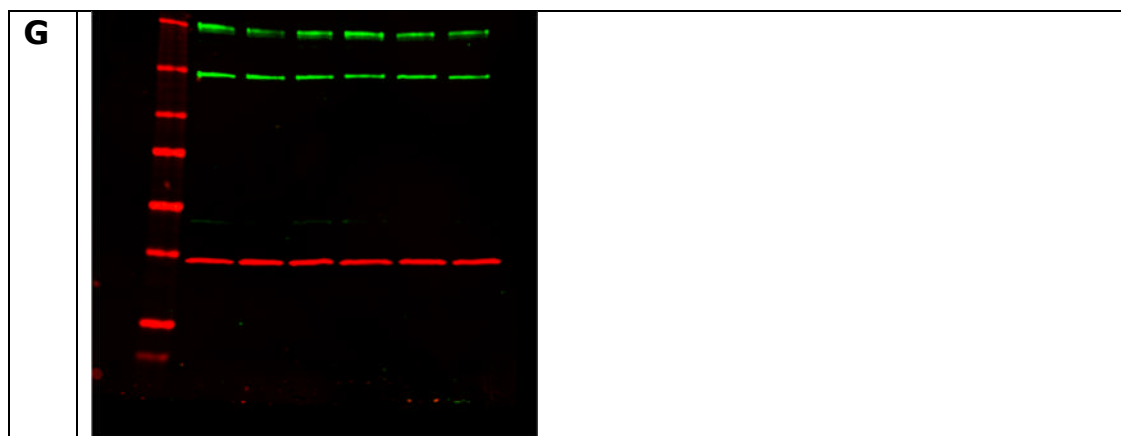
1. Original blot shown in *Figure 4-1*. Labelled as image A unless otherwise stated.

A		
	Lane 1	Molecular weight ladder
	Lane 2	Basal
	Lane 3	TNFα 10 ng/ml
	Lane 4	Vehicle, 0.3% EtOH
	Lane 5	Anandamide 30 μM
	Lane 6	THC 30 μM
	Lane 7	THC + TNFα
B		
	Labelled as image A.	
C		
	Labelled as image A, except lane 2 – untreated cells and lane 9 TNFα 10 ng/ml.	

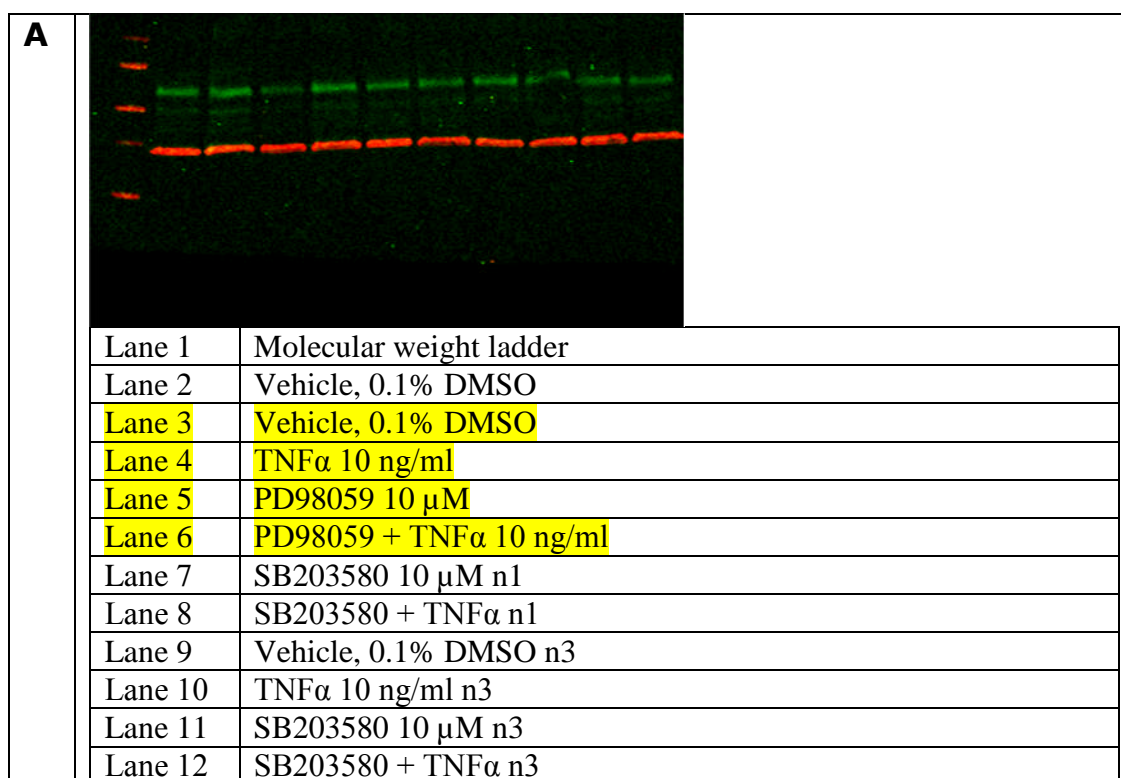
2. Original blot for *Figure 4-2*. Labelled as image A unless otherwise stated.

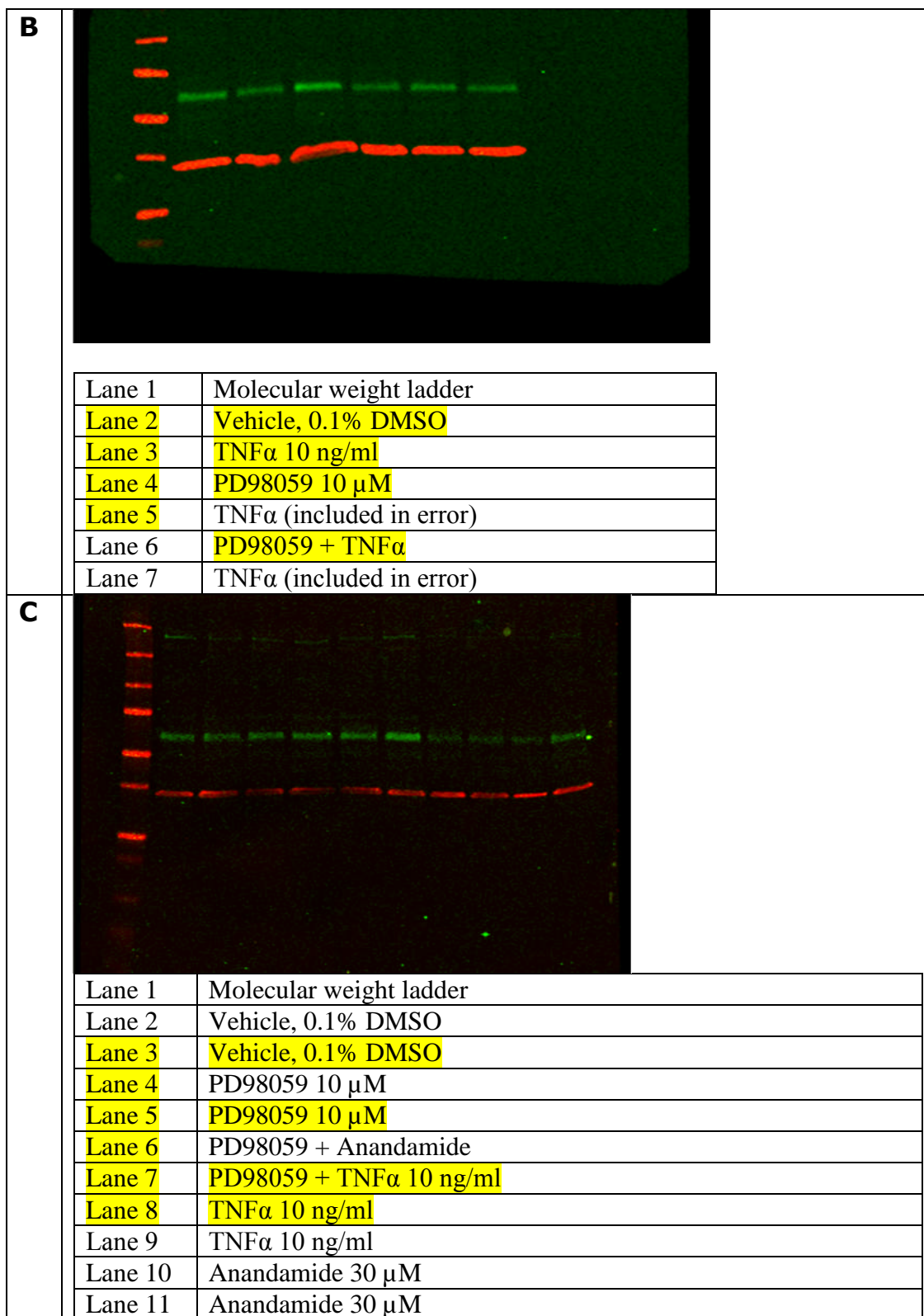


D	 <p>Labelled as image A except lane 2- TNFα and lane 3 -anandamide</p>																								
E	 <p>Labelled as image A, except lane 3 – TNFα 10 ng/ml and lane 9-Anandamide for image F.</p>																								
F	 <table border="1" data-bbox="371 1458 1407 1908"> <tbody> <tr> <td>Lane 1</td><td>Molecular weight ladder</td></tr> <tr> <td>Lane 2</td><td>TNFα 10 ng/ml</td></tr> <tr> <td>Lane 3</td><td>Basal</td></tr> <tr> <td>Lane 4</td><td>Vehicle, 0.3% EtOH</td></tr> <tr> <td>Lane 5</td><td>Anandamide 30 μM</td></tr> <tr> <td>Lane 6</td><td>THC 30 μM</td></tr> <tr> <td>Lane 7</td><td>THC + TNFα</td></tr> <tr> <td>Lane 8</td><td>Basal</td></tr> <tr> <td>Lane 9</td><td>Vehicle, 0.3% EtOH</td></tr> <tr> <td>Lane 10</td><td>Anandamide 30 μM</td></tr> <tr> <td>Lane 11</td><td>THC 30 μM</td></tr> <tr> <td>Lane 12</td><td>THC + TNFα</td></tr> </tbody> </table>	Lane 1	Molecular weight ladder	Lane 2	TNF α 10 ng/ml	Lane 3	Basal	Lane 4	Vehicle, 0.3% EtOH	Lane 5	Anandamide 30 μ M	Lane 6	THC 30 μ M	Lane 7	THC + TNF α	Lane 8	Basal	Lane 9	Vehicle, 0.3% EtOH	Lane 10	Anandamide 30 μ M	Lane 11	THC 30 μ M	Lane 12	THC + TNF α
Lane 1	Molecular weight ladder																								
Lane 2	TNF α 10 ng/ml																								
Lane 3	Basal																								
Lane 4	Vehicle, 0.3% EtOH																								
Lane 5	Anandamide 30 μ M																								
Lane 6	THC 30 μ M																								
Lane 7	THC + TNF α																								
Lane 8	Basal																								
Lane 9	Vehicle, 0.3% EtOH																								
Lane 10	Anandamide 30 μ M																								
Lane 11	THC 30 μ M																								
Lane 12	THC + TNF α																								

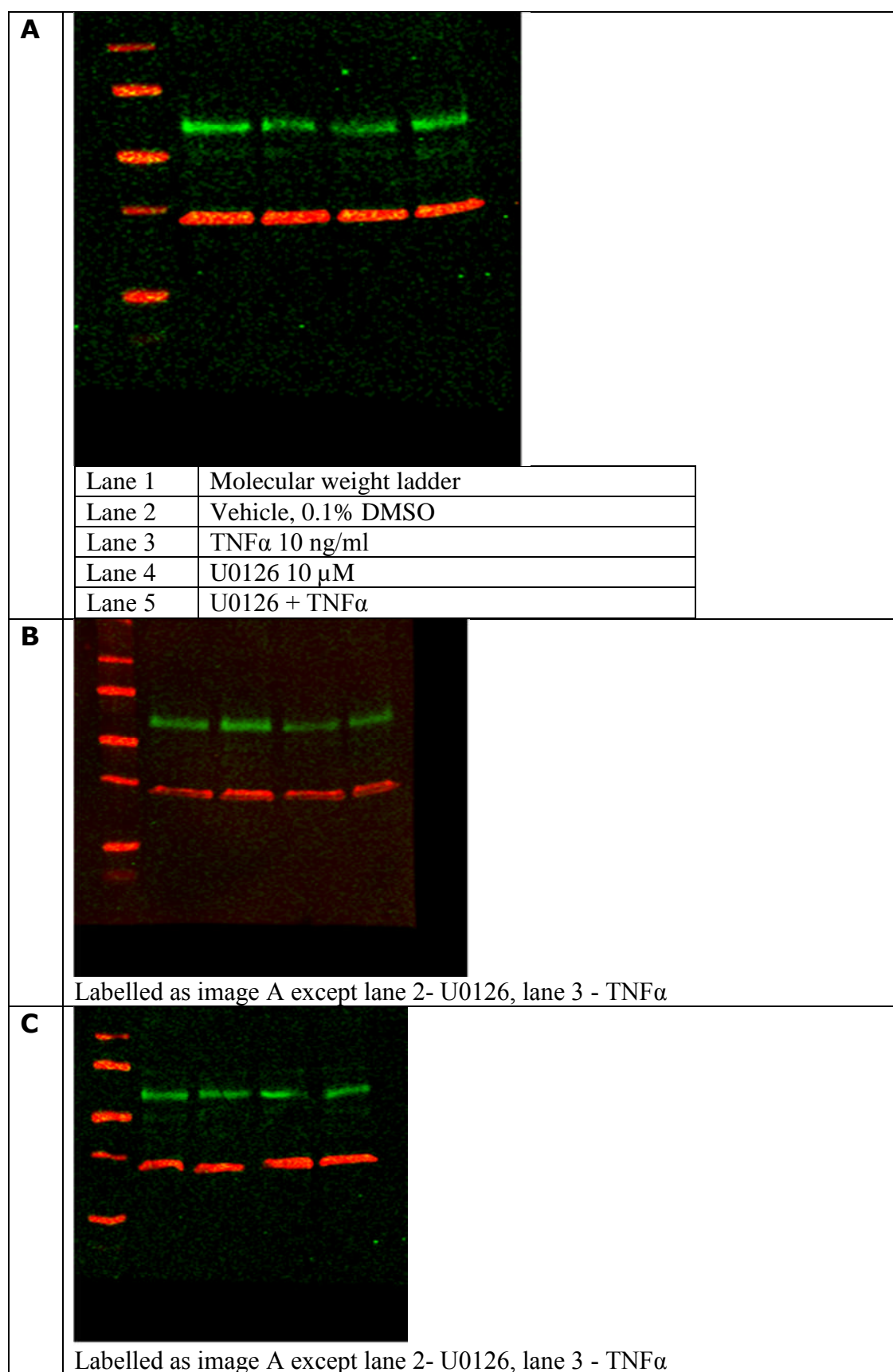


3. Original blot for *Figure 4-6*.

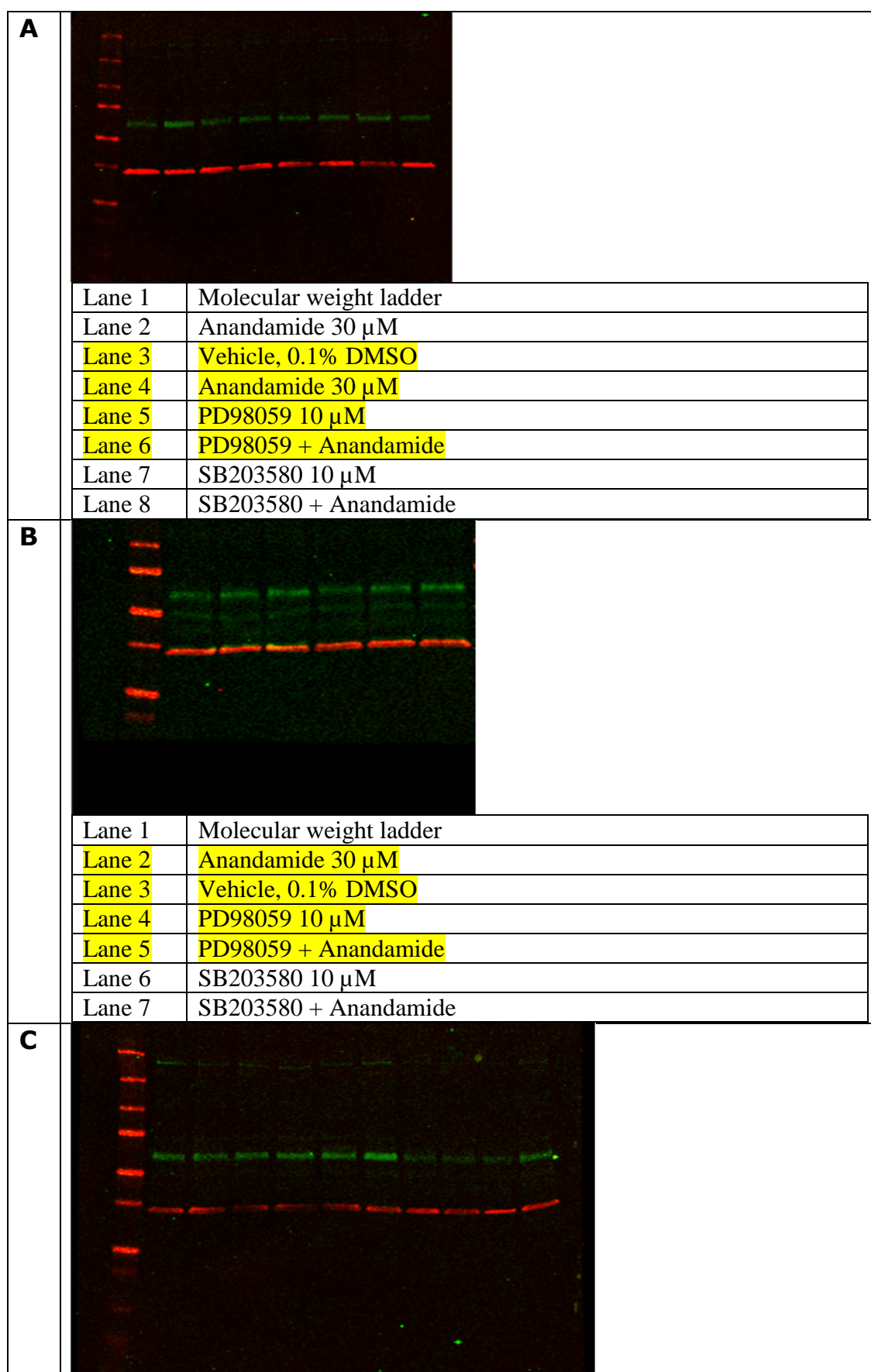




4. Original blot for *Figure 4-7*. Labelled as image A unless otherwise stated.

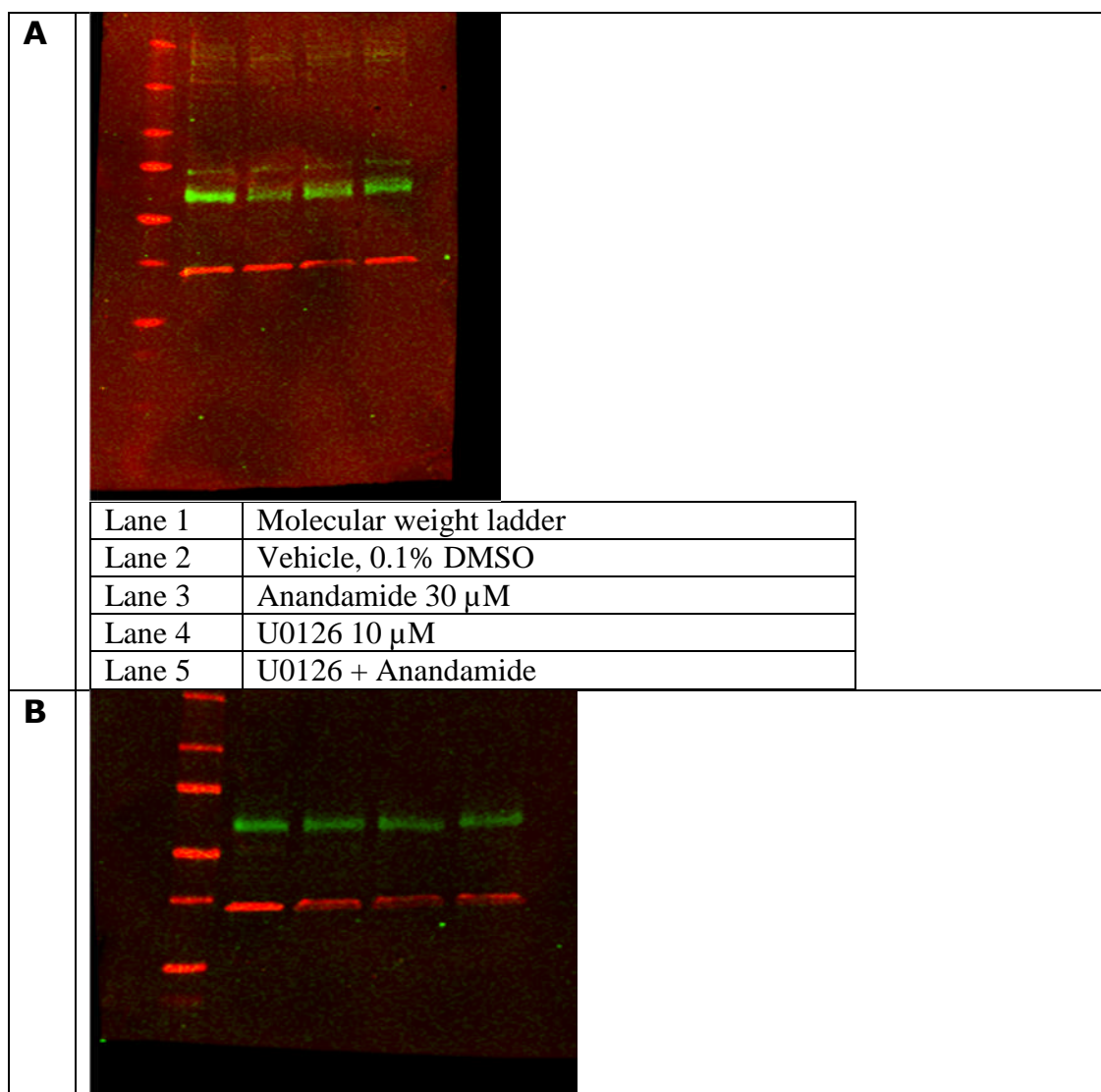


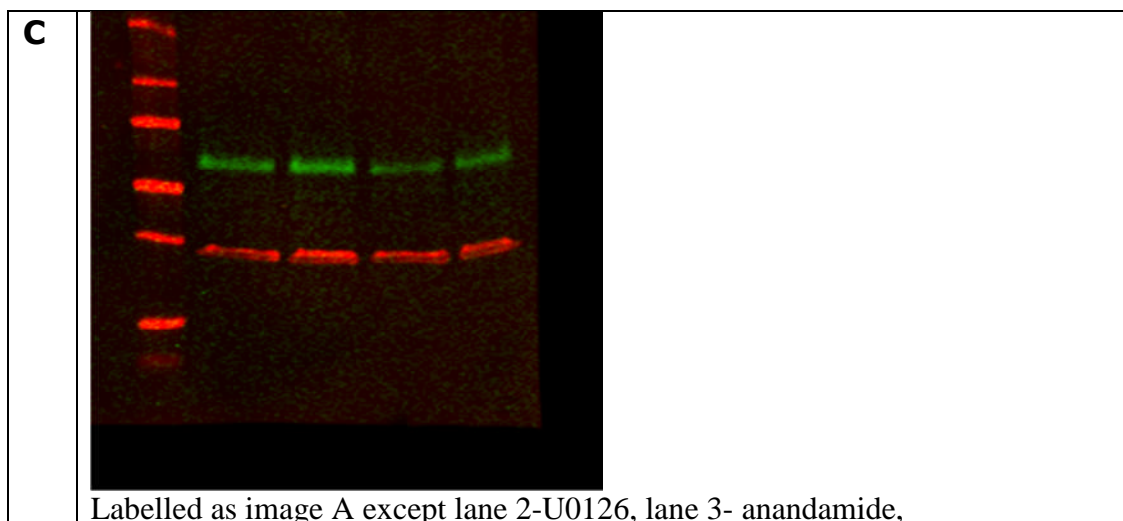
5. Original blot for *Figure 4-8*.



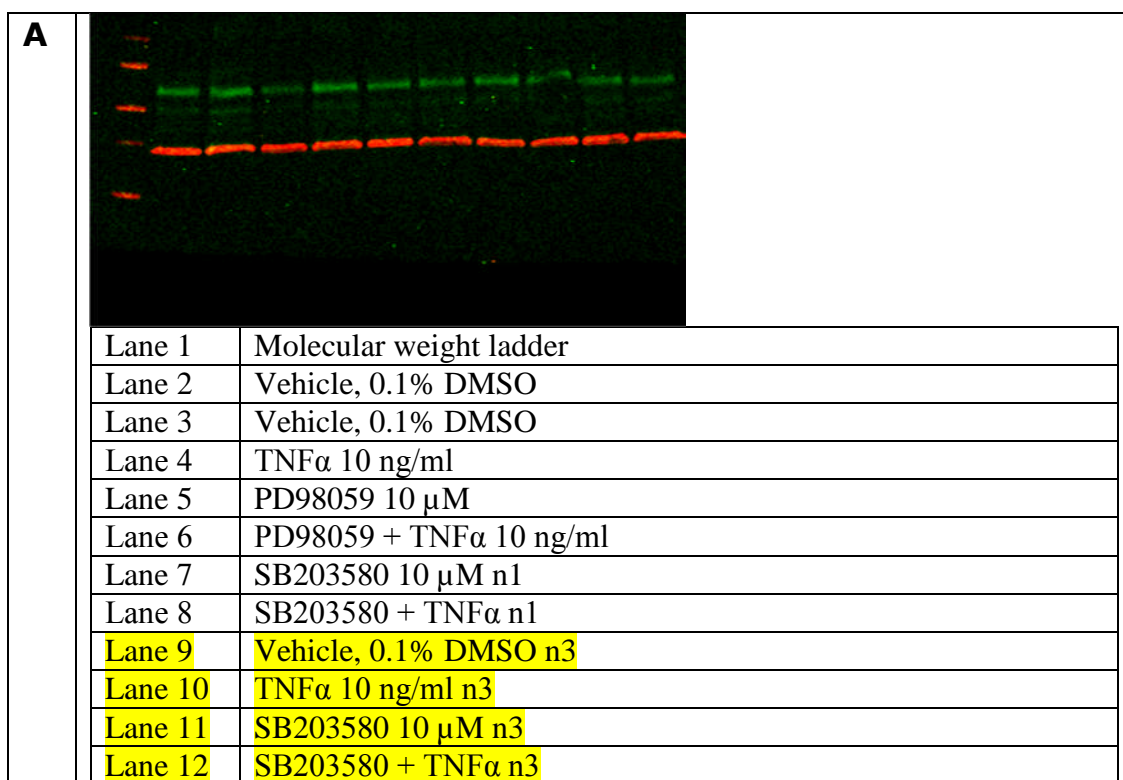
Lane 1	Molecular weight ladder
Lane 2	Vehicle, 0.1% DMSO
Lane 3	Vehicle, 0.1% DMSO
Lane 4	PD98059 10 μ M
Lane 5	PD98059 10 μ M
Lane 6	PD98059 + Anandamide
Lane 7	PD98059 + TNF α 10 ng/ml
Lane 8	TNF α 10 ng/ml
Lane 9	TNF α 10 ng/ml
Lane 10	Anandamide 30 μ M
Lane 11	Anandamide 30 μ M

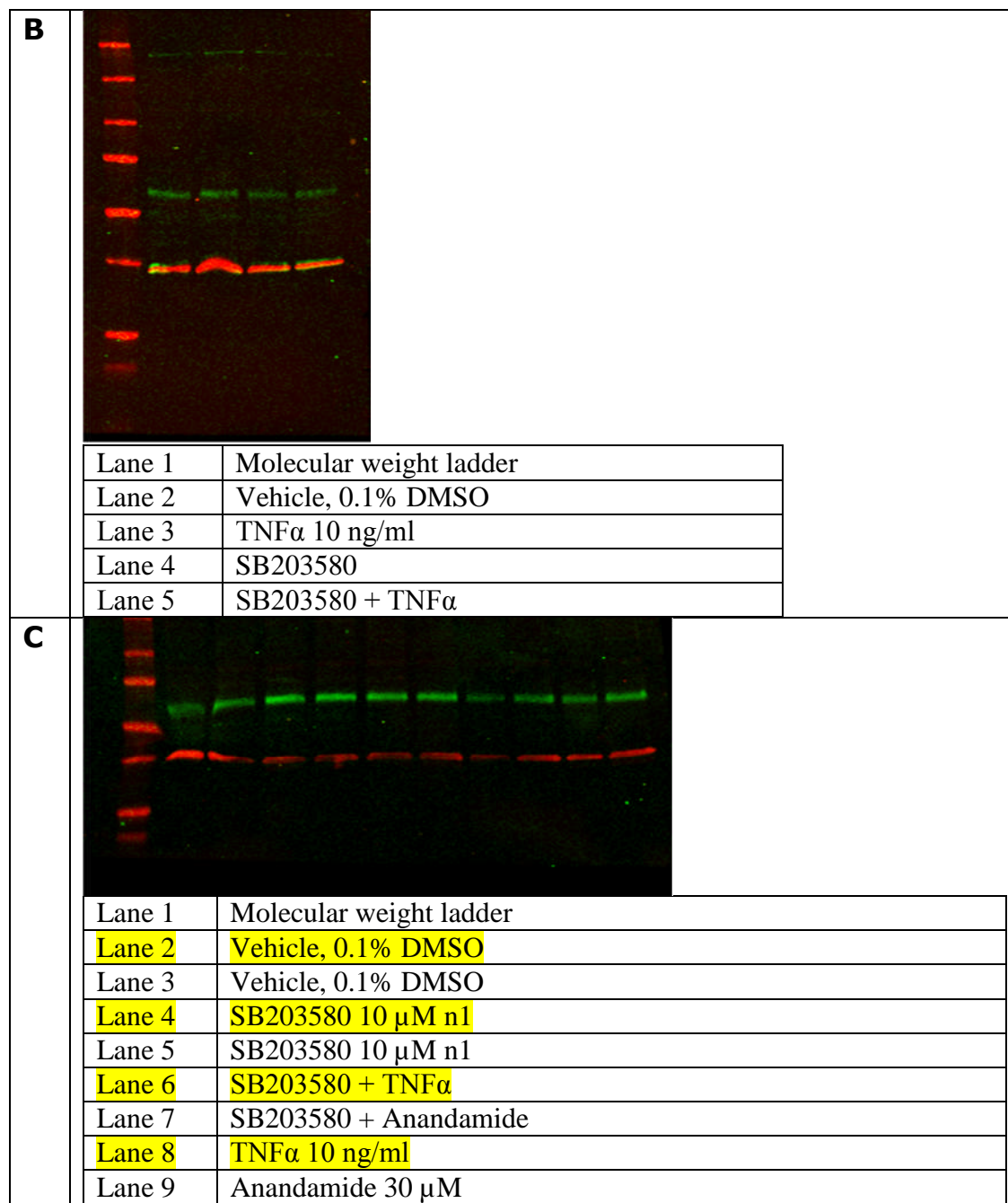
6. Original blot for *Figure 4-9*.



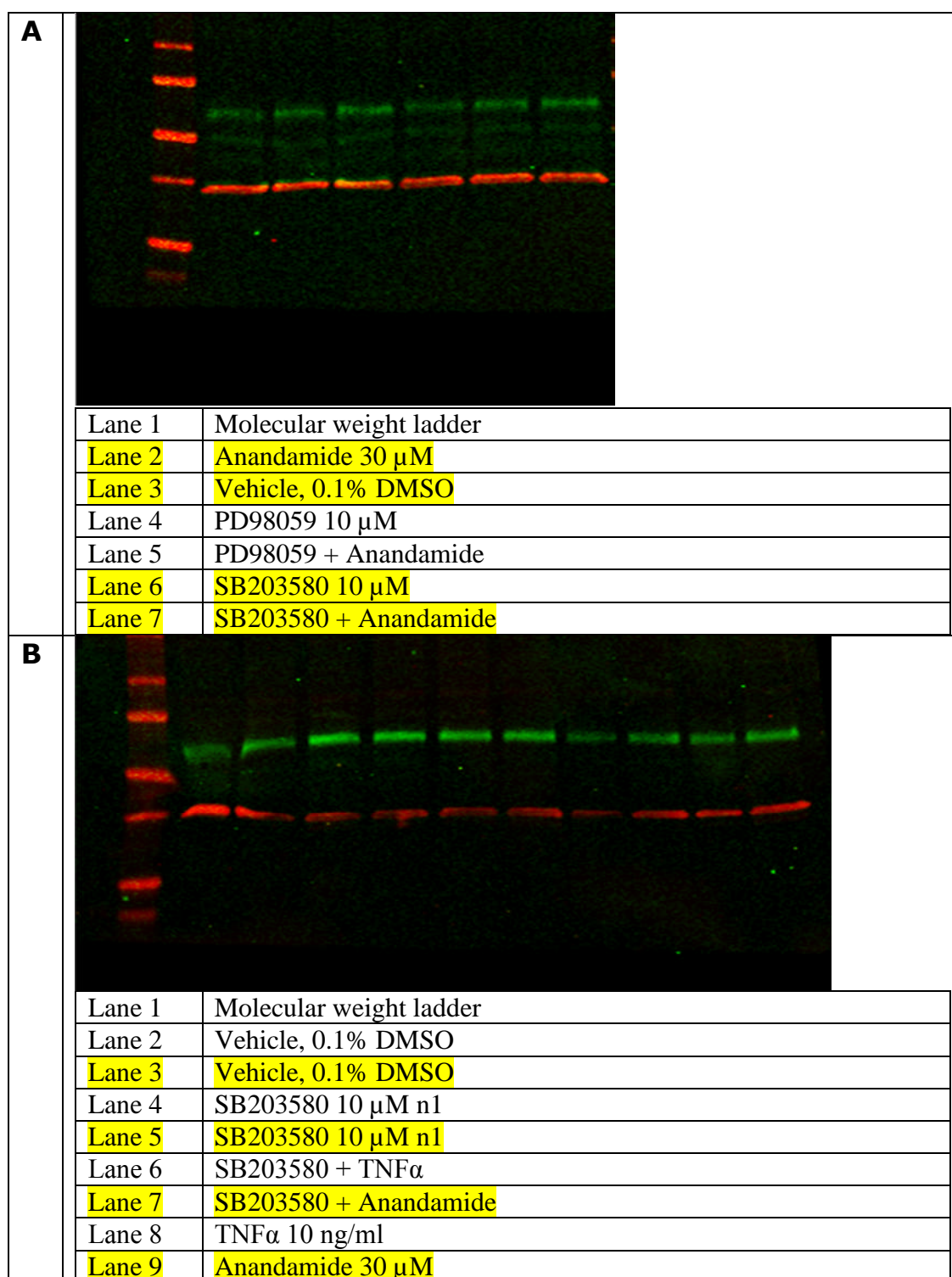


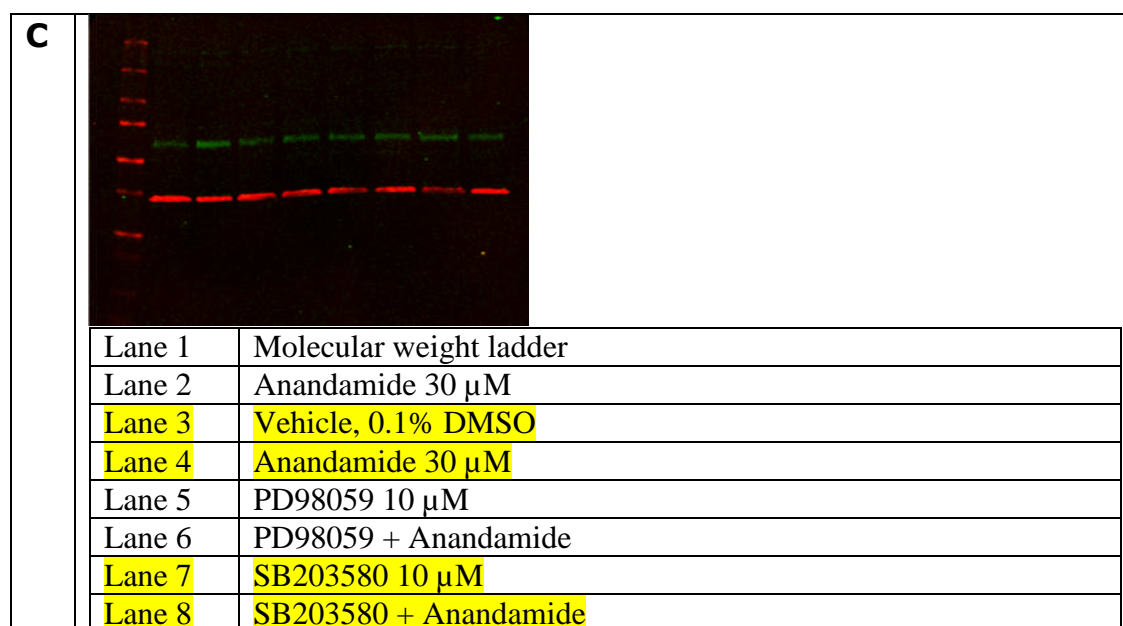
7. Original blot for *Figure 4-12*.





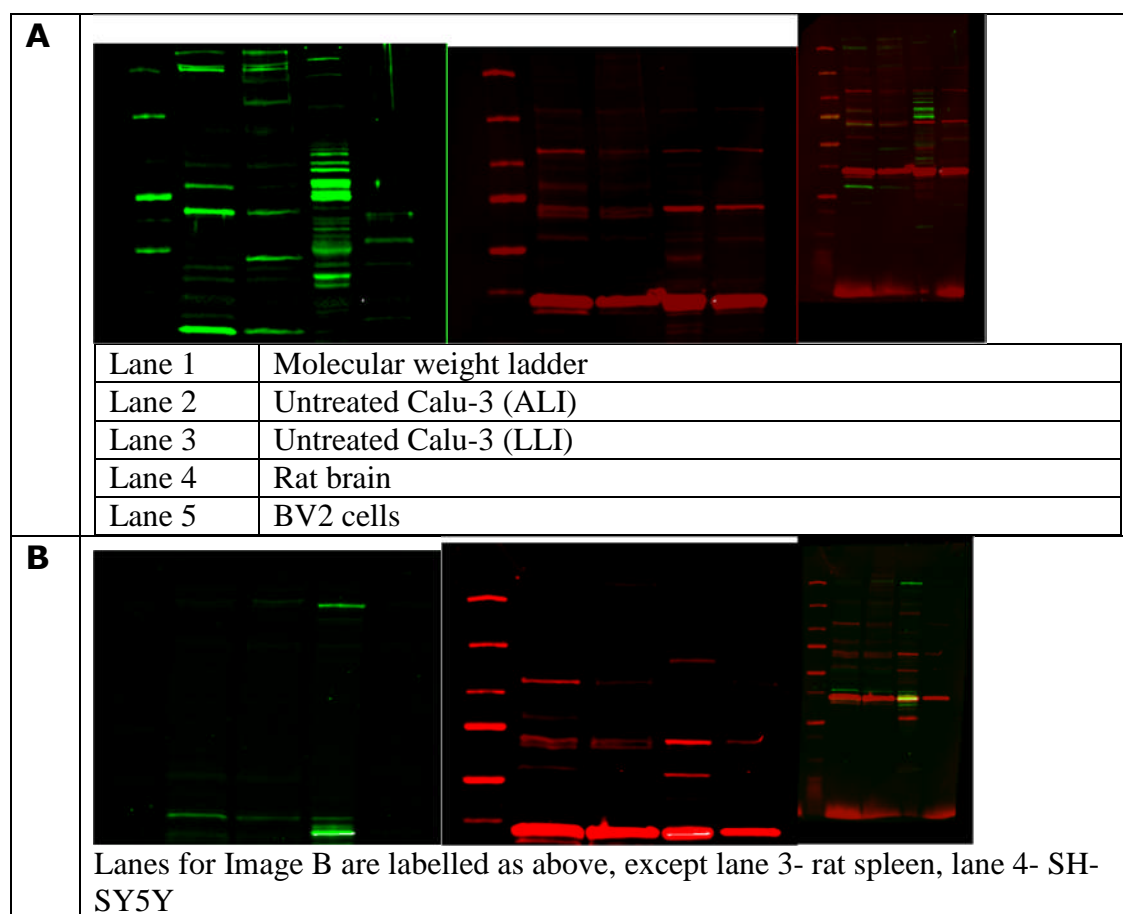
8. Original blot for *Figure 4-13*.





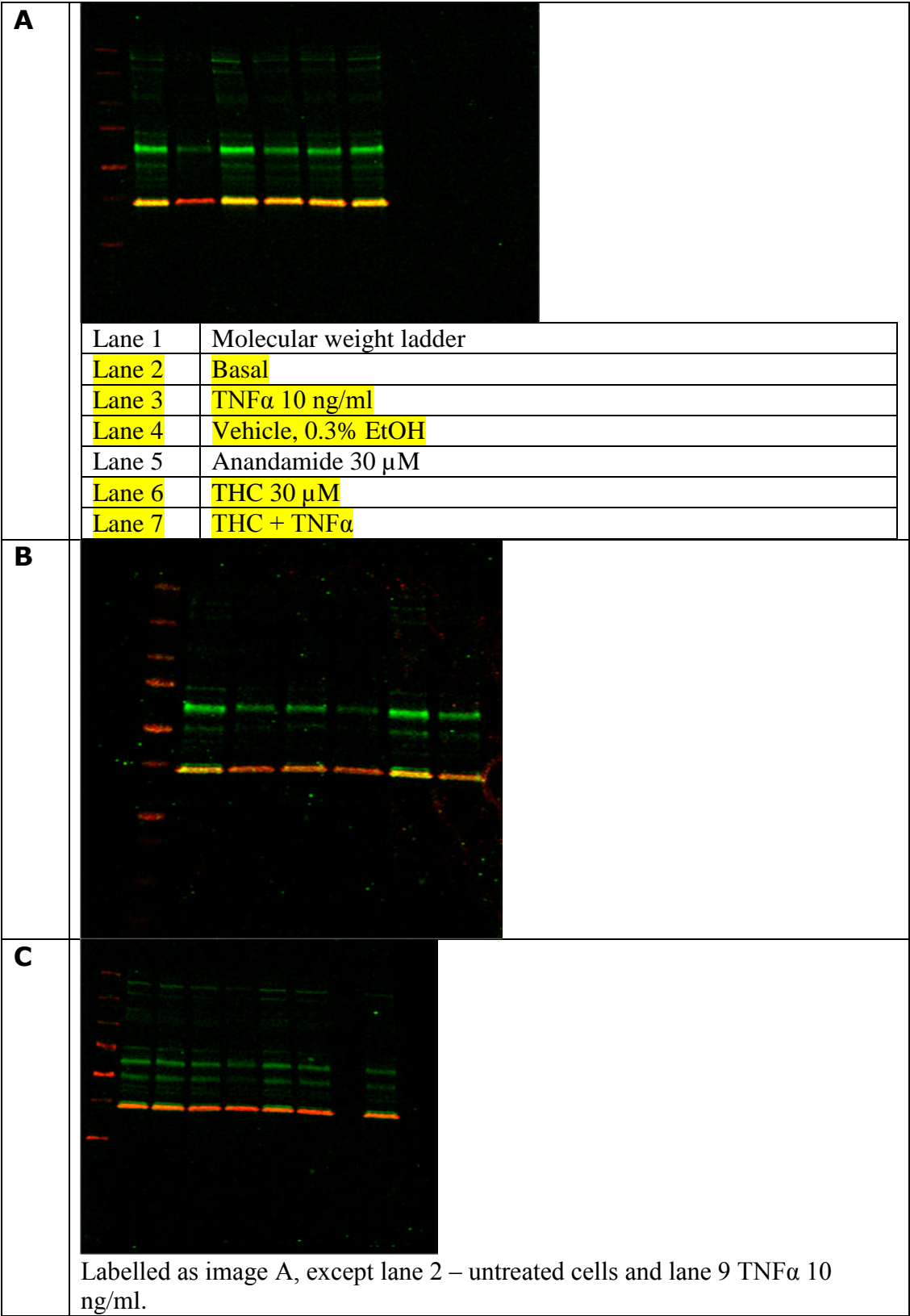
Chapter 5

- Other original blots, besides an example of the image shown in *Figure 5-8* and *Figure 5-9* are unavailable as files were lost during previous software update.

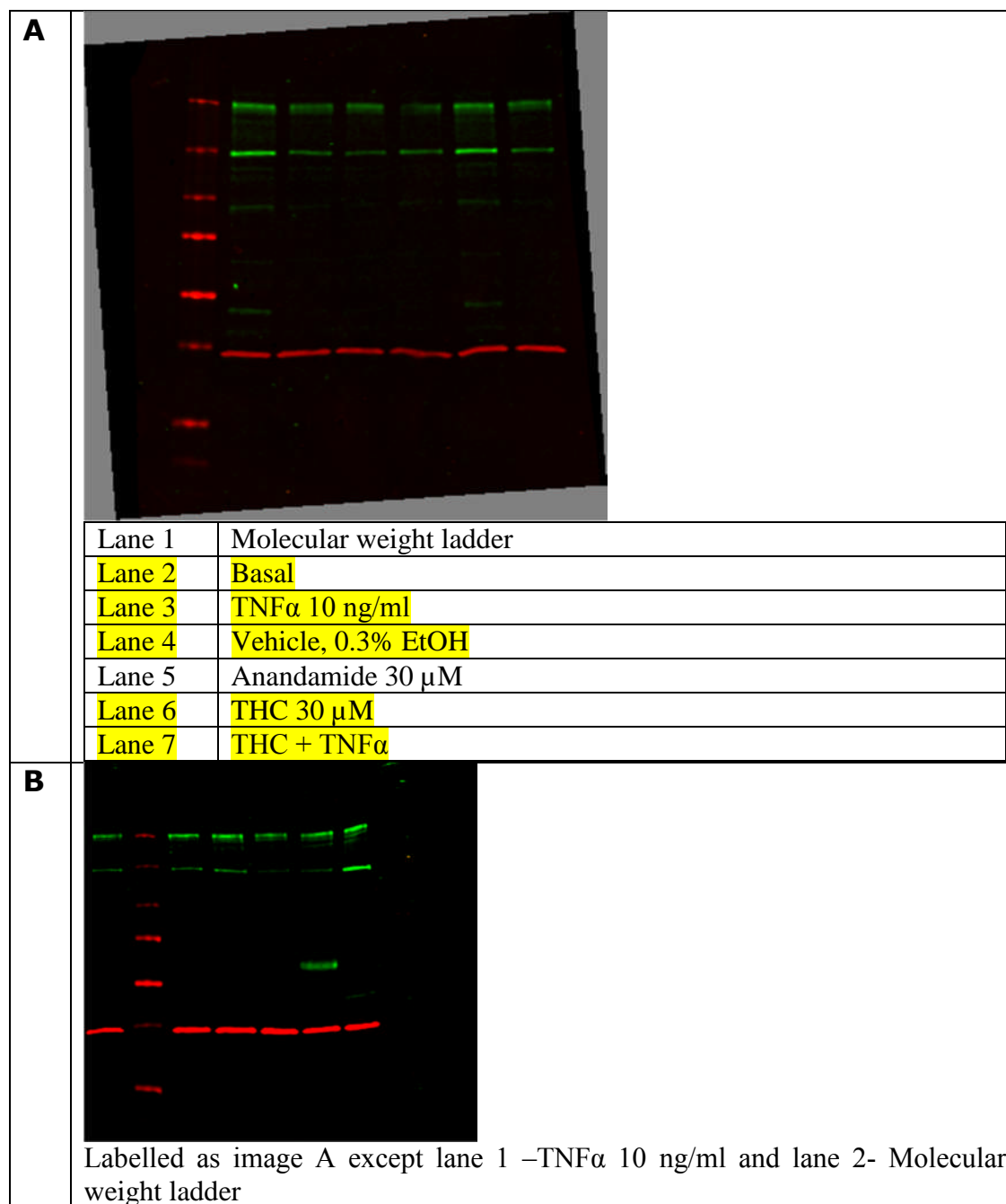


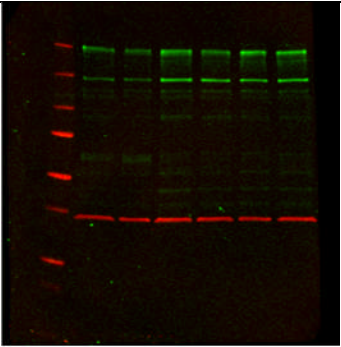
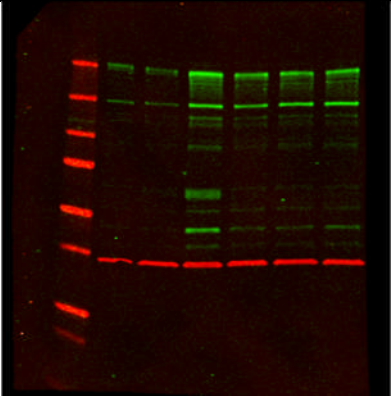
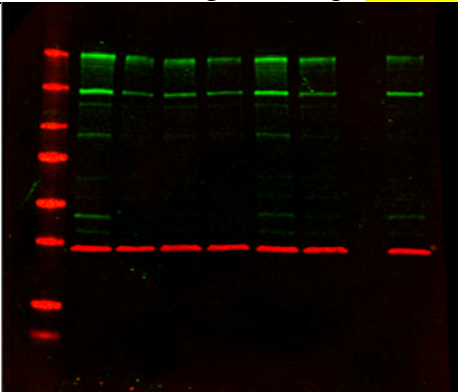
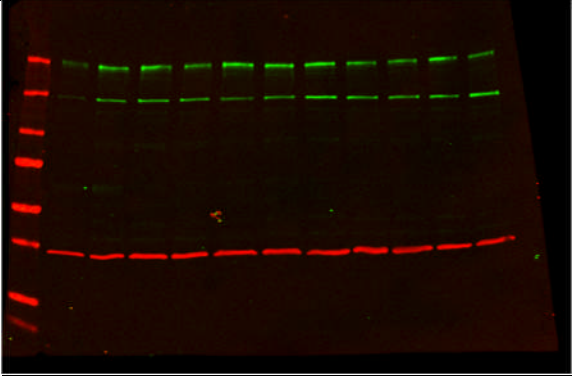
Chapter 6

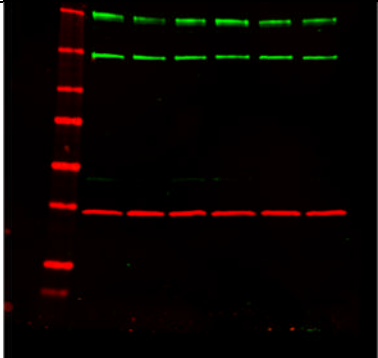
1. Original blot for *Figure 6-1*. Labelled as image A unless otherwise stated.



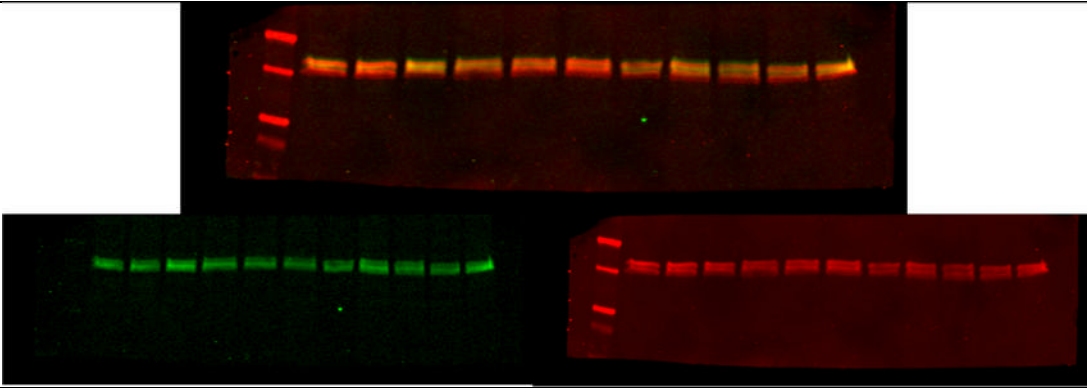
2. Original blot for *Figure 6-2*. Labelled as image A unless otherwise stated.

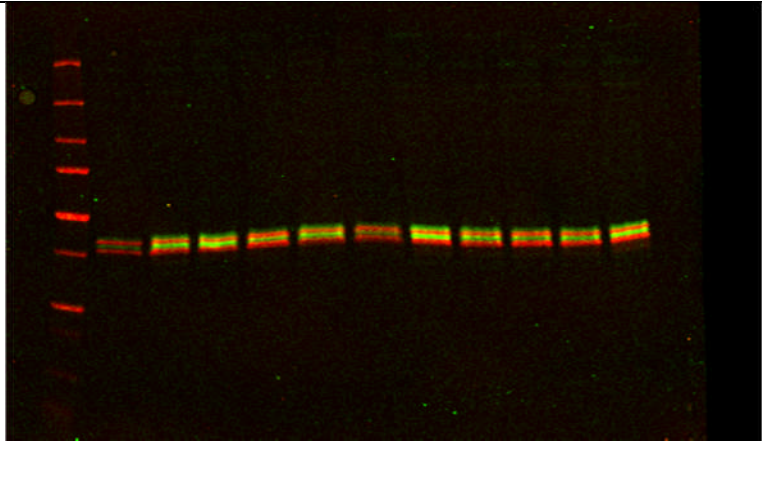
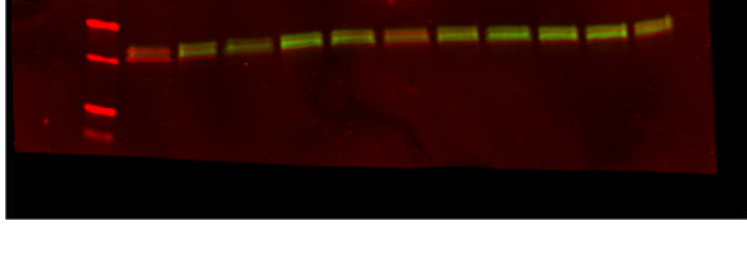
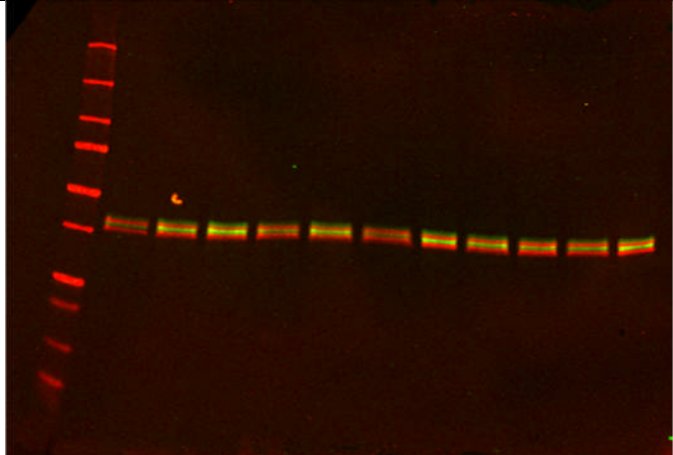


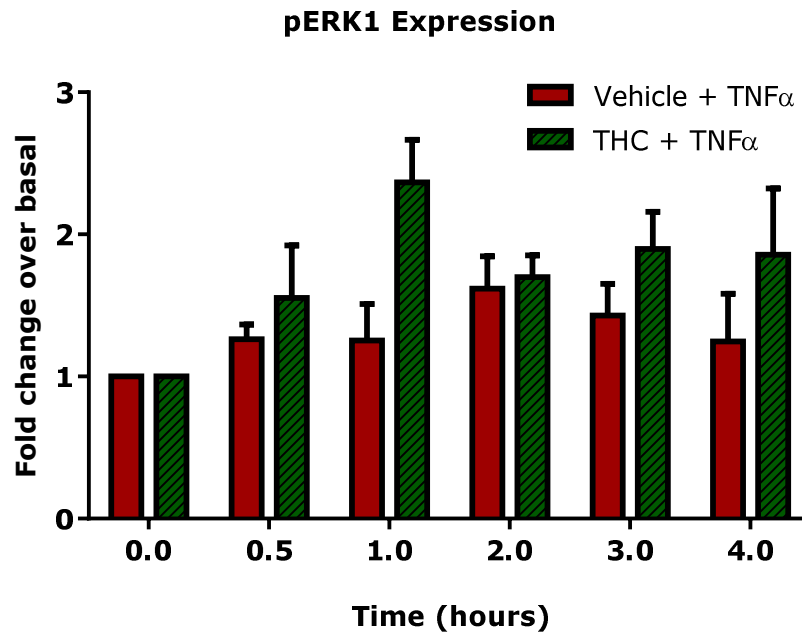
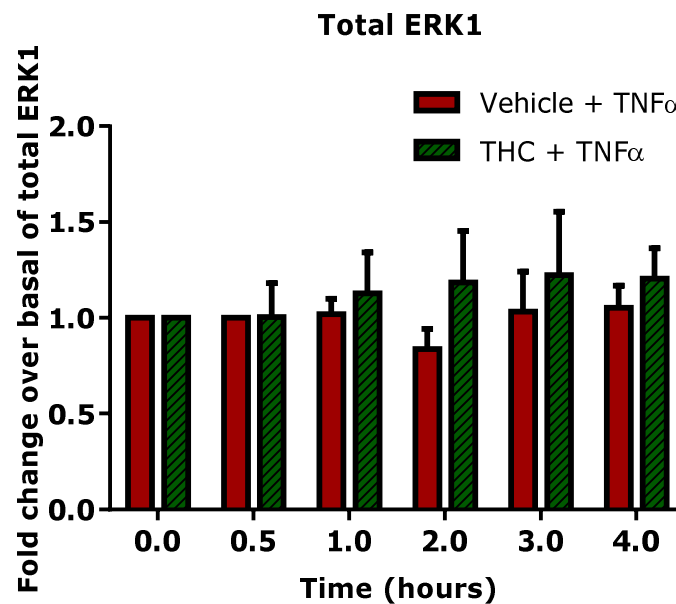
C	 <p>Labelled as image A except lane 1 –TNFα 10 ng/ml and lane 2- Molecular weight ladder</p>								
D	 <p>Labelled as image A except lane 2- TNFα and lane 3 -anandamide</p>								
E	 <p>Labelled as image A, except lane 3 – TNFα 10 ng/ml and lane 9-Anandamide for image F.</p>								
F	 <table border="1" data-bbox="371 1877 1407 2020"> <tr> <td>Lane 1</td><td>Molecular weight ladder</td></tr> <tr> <td>Lane 2</td><td>TNFα 10 ng/ml</td></tr> <tr> <td>Lane 3</td><td>Basal</td></tr> <tr> <td>Lane 4</td><td>Vehicle, 0.3% EtOH</td></tr> </table>	Lane 1	Molecular weight ladder	Lane 2	TNF α 10 ng/ml	Lane 3	Basal	Lane 4	Vehicle, 0.3% EtOH
Lane 1	Molecular weight ladder								
Lane 2	TNF α 10 ng/ml								
Lane 3	Basal								
Lane 4	Vehicle, 0.3% EtOH								

	Lane 5	Anandamide 30 μ M
	Lane 6	THC 30 μ M
	Lane 7	THC + TNF α
	Lane 8	Basal
	Lane 9	Vehicle, 0.3% EtOH
	Lane 10	Anandamide 30 μ M
	Lane 11	THC 30 μ M
	Lane 12	THC + TNF α
G		

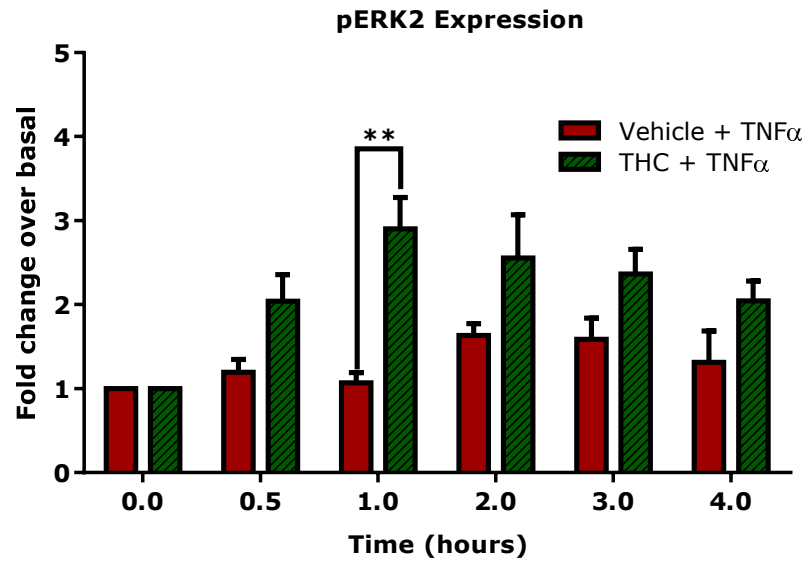
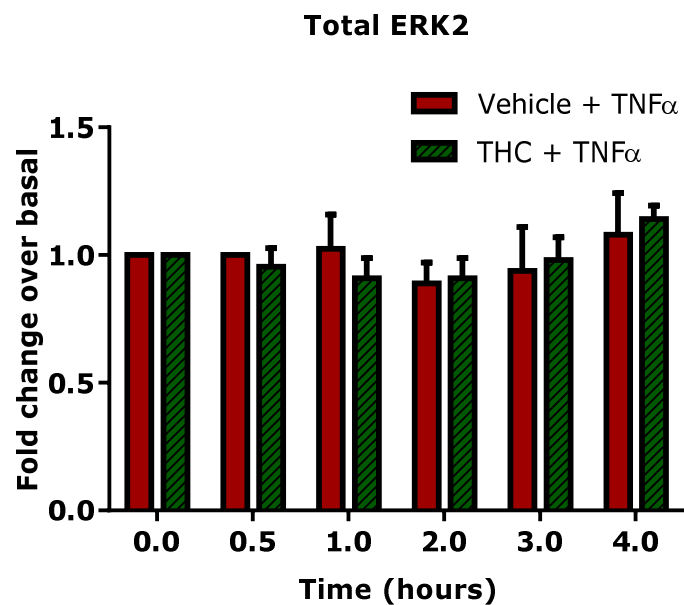
3. Original blot for *Figure 6-3*. Labelled as image A unless otherwise stated.
Red signals- total ERK1/2, Green signals-pERK

A		
	Lane 1	Molecular weight ladder
	Lane 2	Basal untreated cells
	Lane 3	TNF α 10 ng/ml 0.5 h
	Lane 4	TNF α 10 ng/ml 1 h
	Lane 5	TNF α 10 ng/ml 2 h
	Lane 6	TNF α 10 ng/ml 3 h
	Lane 7	TNF α 10 ng/ml 4 h
	Lane 8	THC 30 μ M + TNF α 0.5 h
	Lane 9	THC 30 μ M + TNF α 1 h
	Lane 10	THC 30 μ M + TNF α 2 h
	Lane 11	THC 30 μ M + TNF α 3 h
	Lane 12	THC 30 μ M + TNF α 4 h

B		
C		
D		

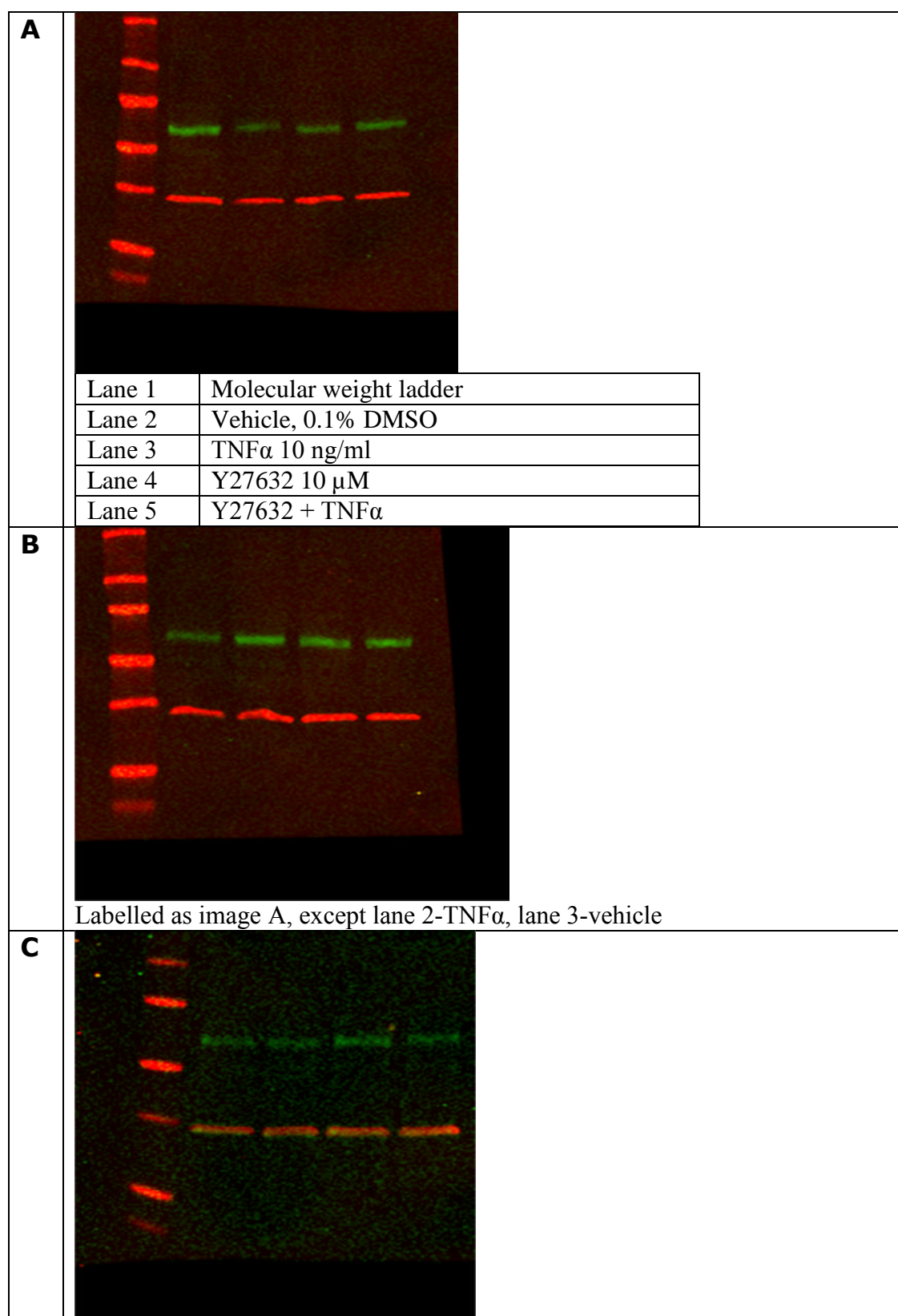
A**B**

A Semi-quantitative analysis of ERK1 expression level, which is normalised according to *B*. the total ERK1 expressed at various time points of up to 4 hours following TNFα exposure or combined THC+TNFα treatment. Data are presented as mean of fold change to protein expression over basal (untreated) cells ± SEM; n=4, no statistical significance is detected when analysed using paired Student's t-test, compared to TNFα (10 ng/ml).

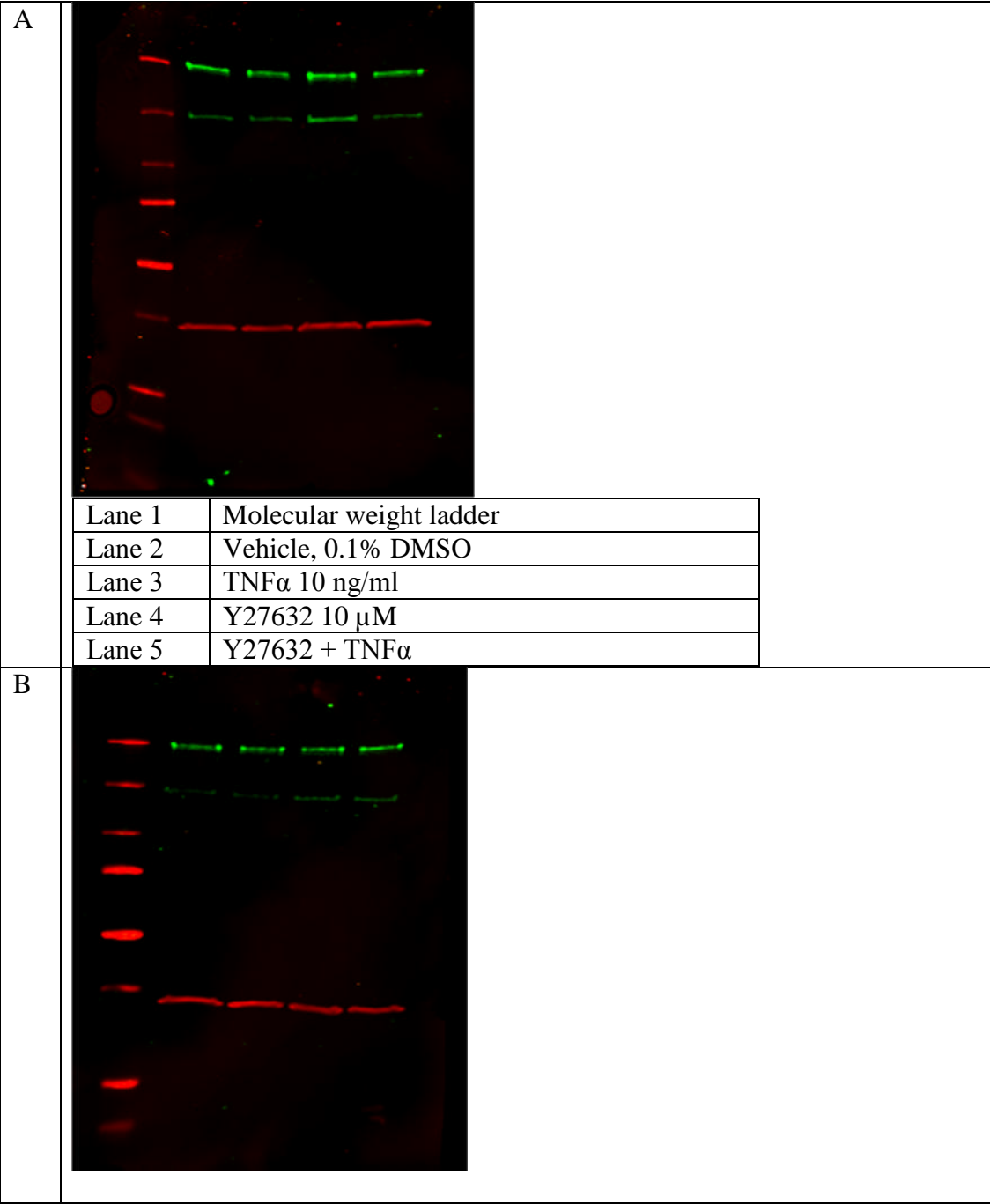
A**B**

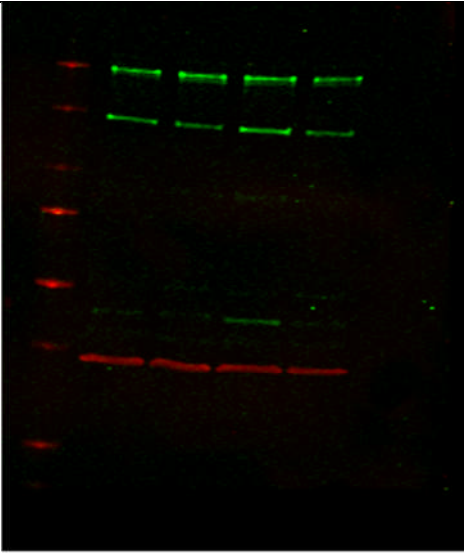
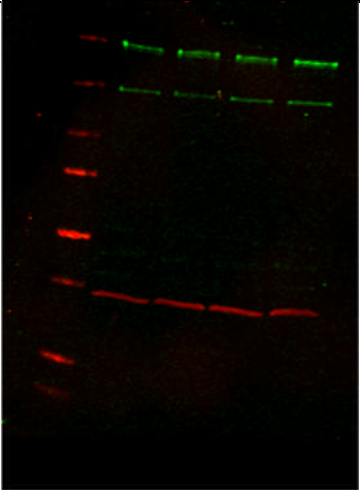
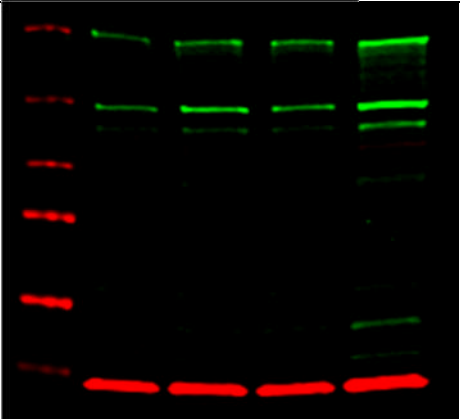
A Semi-quantitative analysis of ERK2 expression level, which is normalised according to *B*. the total ERK1 expressed at various time points of up to 4 hours following TNF α exposure or combined THC+TNF α treatment. Data are presented as mean of fold change to protein expression over basal (untreated) cells \pm SEM; $n=4$, ** $P<0.01$, paired Student's t -test, compared to TNF α (10 ng/ml) at 1 hour.

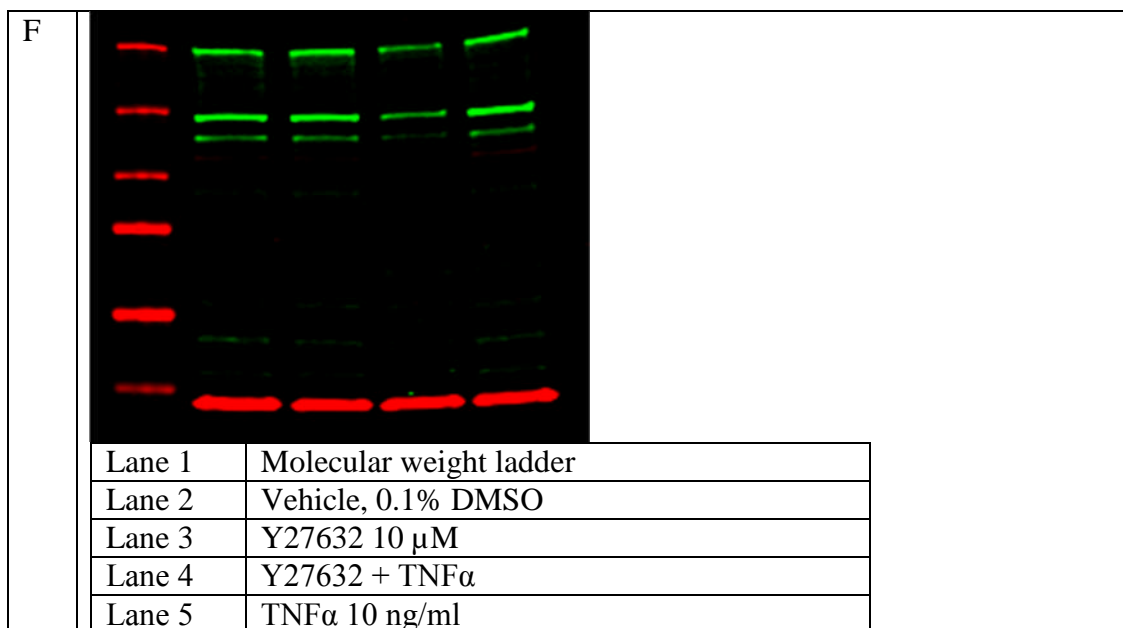
4. Original blot for *Figure 6-5*. Labelled as image A unless otherwise stated.



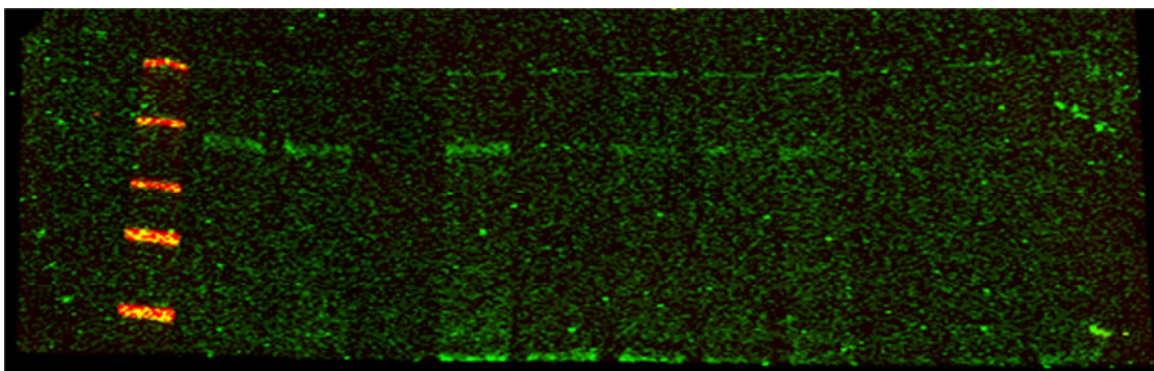
5. Original blot for *Figure 6-6*. Labelled as image A unless otherwise stated.



C	 <table border="1" data-bbox="256 739 1042 936"> <tr> <td>Lane 1</td><td>Molecular weight ladder</td></tr> <tr> <td>Lane 2</td><td>Vehicle, 0.1% DMSO</td></tr> <tr> <td>Lane 3</td><td>Y27632 10 μM</td></tr> <tr> <td>Lane 4</td><td>Y27632 + TNFα</td></tr> <tr> <td>Lane 5</td><td>TNFα 10 ng/ml</td></tr> </table>	Lane 1	Molecular weight ladder	Lane 2	Vehicle, 0.1% DMSO	Lane 3	Y27632 10 μ M	Lane 4	Y27632 + TNF α	Lane 5	TNF α 10 ng/ml
Lane 1	Molecular weight ladder										
Lane 2	Vehicle, 0.1% DMSO										
Lane 3	Y27632 10 μ M										
Lane 4	Y27632 + TNF α										
Lane 5	TNF α 10 ng/ml										
D											
E	 <table border="1" data-bbox="256 1841 1042 2033"> <tr> <td>Lane 1</td><td>Molecular weight ladder</td></tr> <tr> <td>Lane 2</td><td>TNFα 10 ng/ml</td></tr> <tr> <td>Lane 3</td><td>Vehicle, 0.1% DMSO</td></tr> <tr> <td>Lane 4</td><td>Y27632 10 μM</td></tr> <tr> <td>Lane 5</td><td>Y27632 + TNFα</td></tr> </table>	Lane 1	Molecular weight ladder	Lane 2	TNF α 10 ng/ml	Lane 3	Vehicle, 0.1% DMSO	Lane 4	Y27632 10 μ M	Lane 5	Y27632 + TNF α
Lane 1	Molecular weight ladder										
Lane 2	TNF α 10 ng/ml										
Lane 3	Vehicle, 0.1% DMSO										
Lane 4	Y27632 10 μ M										
Lane 5	Y27632 + TNF α										

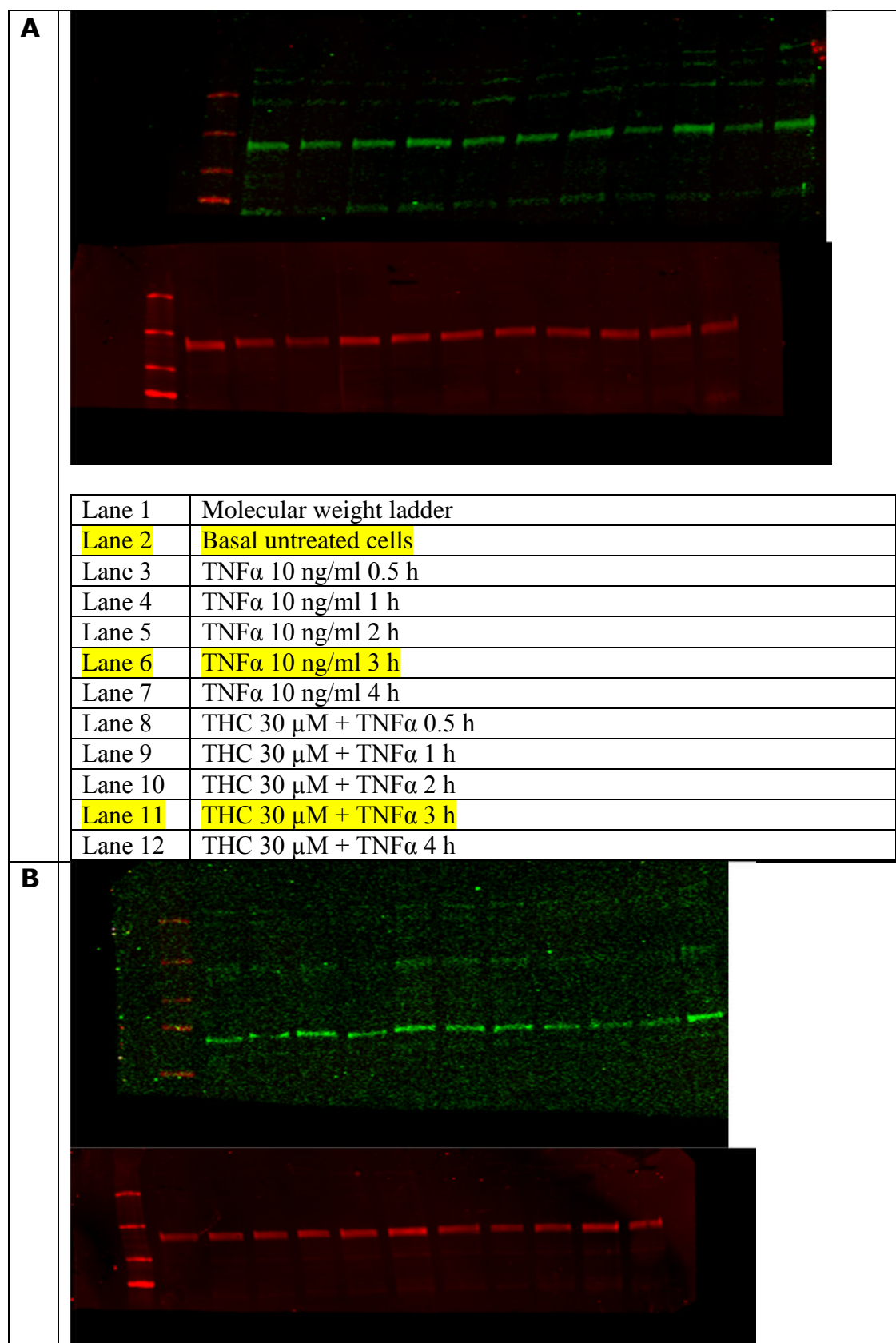


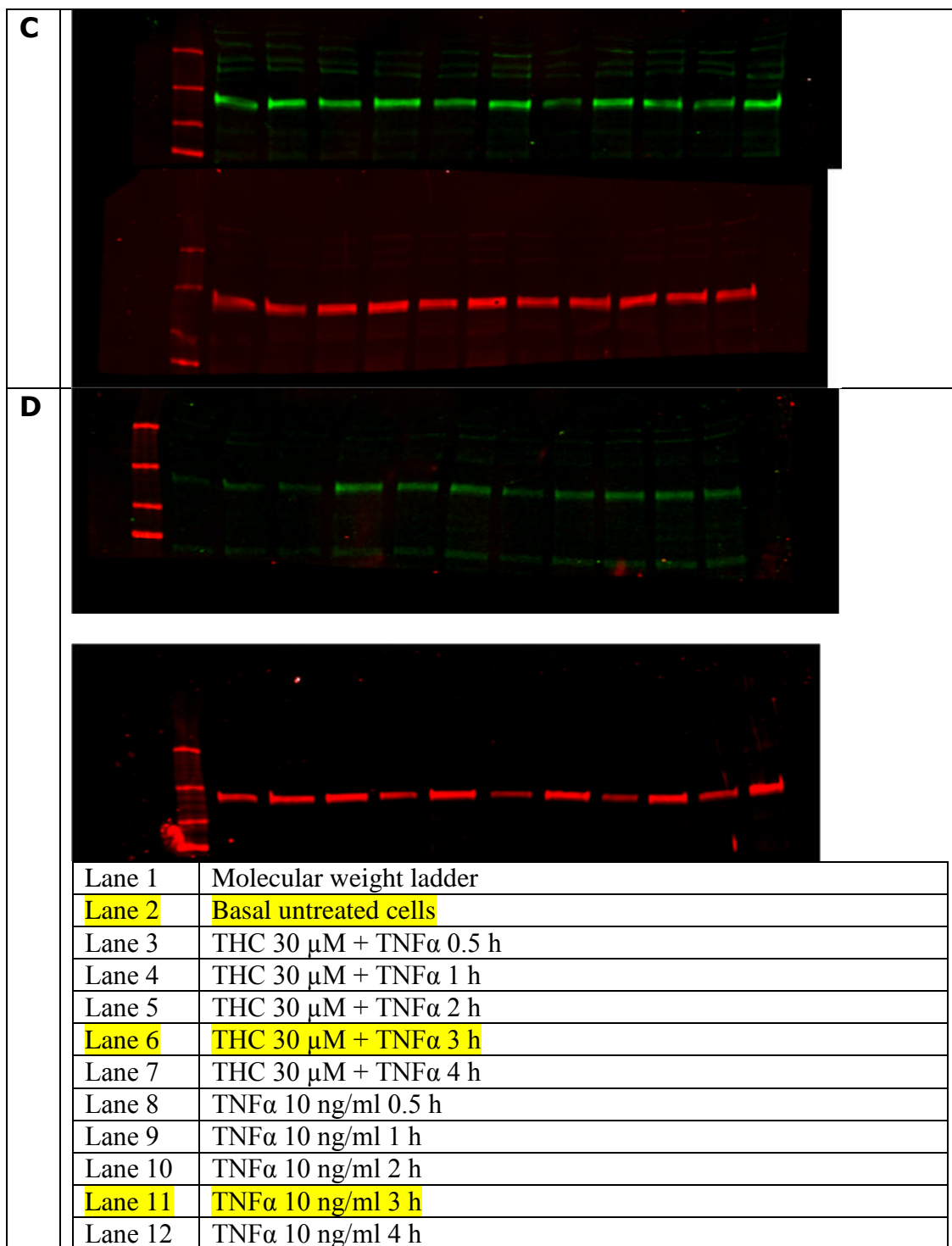
6. Original blot of pMYPT signalling up to 20 mins

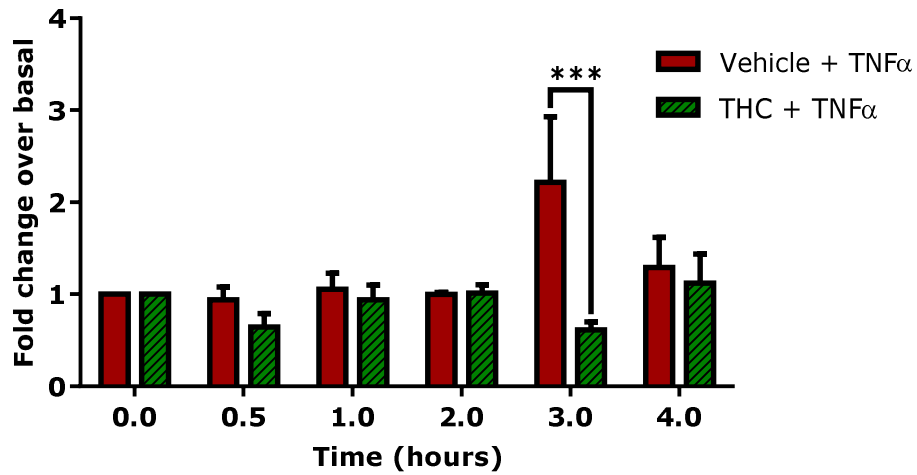


Typical immunoblot showing weak fluorescent signals for phospho-MYPT1 (Thr696) (top) expression following basolateral application of TNF α (10 ng/ml) alone or in the presence of THC (30 μ M) up to 20 minutes in serum-starved 21-day old Calu-3 cells, cultured in ALI.

7. Original blot for *Figure 6-7*. Labelled as image A unless otherwise stated.

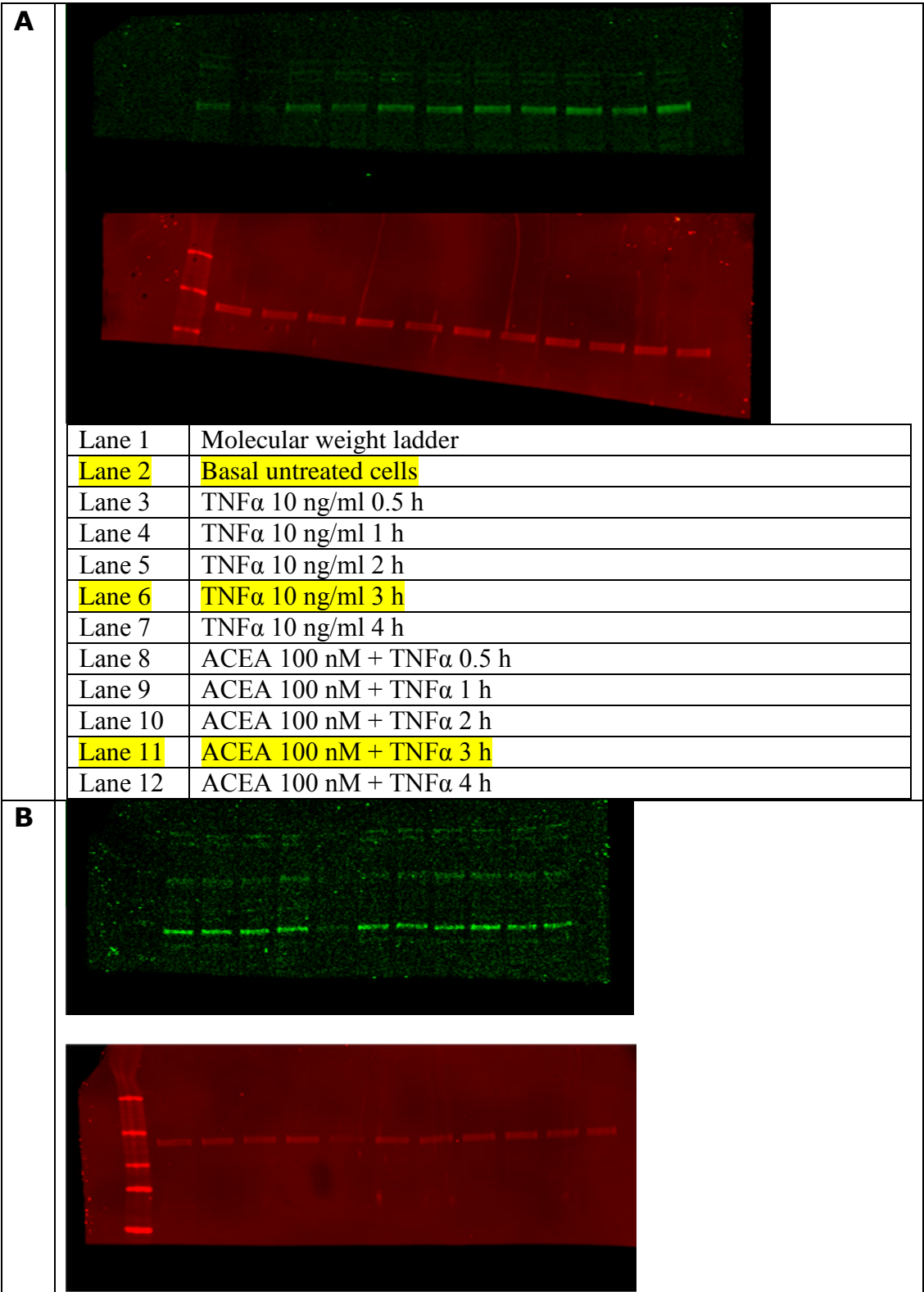




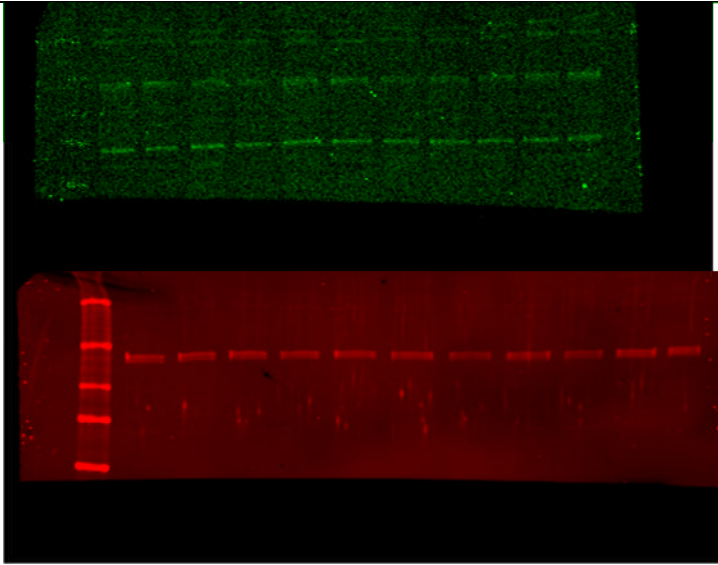


*A Semi-quantitative analysis of pMYPT Thr696 expression level, which is normalised according to **B.** the total MYPT1 expressed at various time points of up to 4 hours following TNF α or THC+TNF α exposure. Data are presented as mean of fold change to protein expression over basal (untreated) cells \pm SEM; $n=4$, $^{**}P<0.01$, paired Student's t -test, compared to TNF α (10 ng/ml) at 3 hours.*

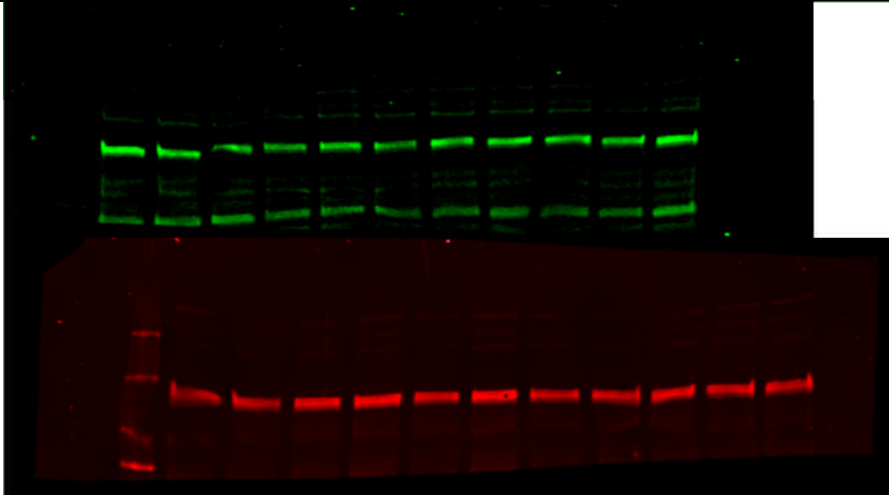
8. Original blot for *Figure 6-8*. Labelled as image A unless otherwise stated.

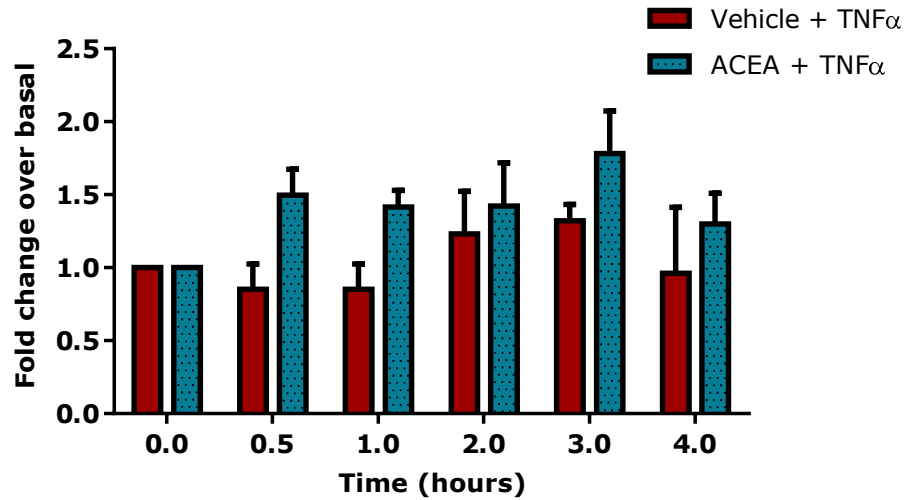


C



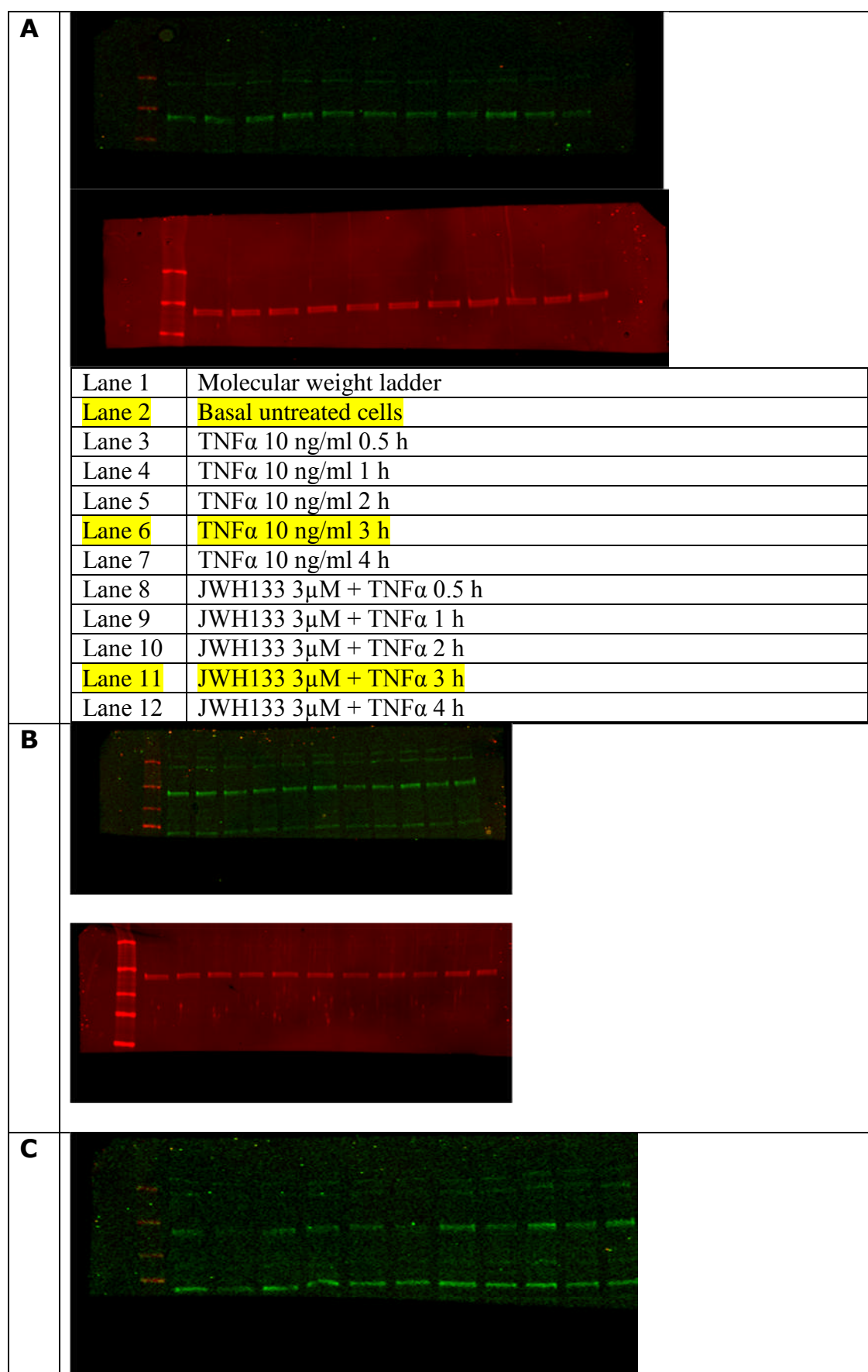
D

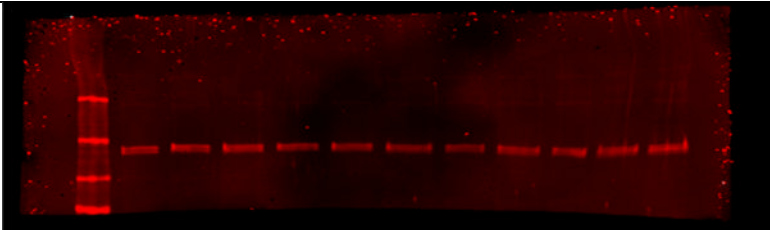
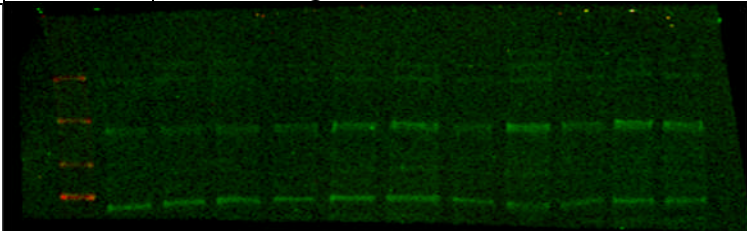
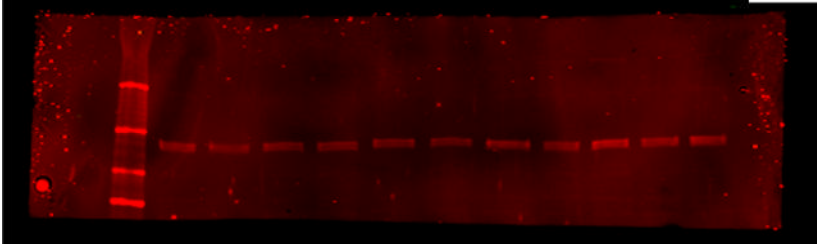


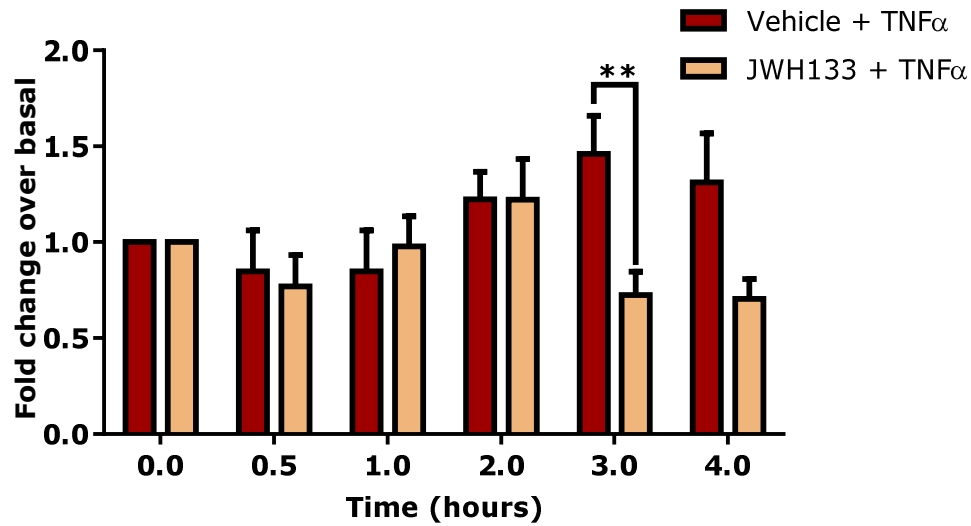


*A Semi-quantitative analysis of pMYPT Thr696 expression level, which is normalised according to **B.** the total MYPT1 expressed at various time points of up to 4 hours following TNF α exposure or ACEA+TNF α . Data are presented as mean of fold change to protein expression over basal (untreated) cells \pm SEM; $n=4$, $**P<0.01$, paired Student's t -test, compared to TNF α (10 ng/ml) at 3 hours.*

9. Original blot for *Figure 6-9*. Labelled as image A unless otherwise stated.



		
	Lane 1	Molecular weight ladder
	Lane 2	Basal untreated cells
	Lane 3	JWH133 3 μ M + TNF α 0.5 h
	Lane 4	JWH133 3 μ M + TNF α 1 h
	Lane 5	JWH133 3 μ M + TNF α 2 h
	Lane 6	JWH133 3 μ M + TNF α 3 h
	Lane 7	JWH133 3 μ M + TNF α 4 h
	Lane 8	TNF α 10 ng/ml 0.5 h
	Lane 9	TNF α 10 ng/ml 1 h
	Lane 10	TNF α 10 ng/ml 2 h
	Lane 11	TNF α 10 ng/ml 3 h
	Lane 12	TNF α 10 ng/ml 4 h
D		
		
	Lane 1	Molecular weight ladder
	Lane 2	Basal untreated cells
	Lane 3	JWH133 3 μ M + TNF α 0.5 h
	Lane 4	JWH133 3 μ M + TNF α 1 h
	Lane 5	JWH133 3 μ M + TNF α 2 h
	Lane 6	JWH133 3 μ M + TNF α 3 h
	Lane 7	JWH133 3 μ M + TNF α 4 h
	Lane 8	TNF α 10 ng/ml 0.5 h
	Lane 9	TNF α 10 ng/ml 1 h
	Lane 10	TNF α 10 ng/ml 2 h
	Lane 11	TNF α 10 ng/ml 3 h
	Lane 12	TNF α 10 ng/ml 4 h



*A Semi-quantitative analysis of pMYPT Thr696 expression level, which is normalised according to **B.** the total MYPT1 expressed at various time points of up to 4 hours following TNF α exposure or ACEA+TNF α . Data are presented as mean of fold change to protein expression over basal (untreated) cells \pm SEM; n=4, **P<0.01, paired Student's t-test, compared to TNF α (10 ng/ml) at 3 hours.*

References

- ABADJI, V., LIN, S. Y., TAHA, G., GRIFFIN, G., STEVENSON, L. A., PERTWEE, R. G. & MAKRIYANNIS, A. 1994. (R)-Methanandamide - A chiral novel anandamide possessing higher potency and metabolic stability *J Med Chem*, 37, 1889-1893.
- ABBOUD, R. T. & SANDERS, H. D. 1976. Effect of oral-administration of delta-9-Tetrahydrocannabinol on airway mechanics in normal and asthmatic subjects. *Chest*, 70, 480-485.
- ABDULLAH, L. H., WOLBER, C., KESIMER, M., SHEEHAN, J. K. & DAVIS, C. W. 2012. Studying mucin secretion from human bronchial epithelial cell primary cultures. In: MCGUCKIN, M. A. & THORNTON, D. J. (eds.) *Mucins: Methods and Protocols*.
- ADAMS, R. B., PLANCHON, S. M. & ROCHE, J. K. 1993. IFN-Gamma modulation of epithelial barrier function - time course, reversibility, and site of cytokine binding *J Immunol*, 150, 2356-2363.
- ADRIAENSEN, D., BROUNS, I., PINTELON, I., DE PROOST, I. & TIMMERMANS, J. P. 2006. Evidence for a role of neuroepithelial bodies as complex airway sensors: comparison with smooth muscle-associated airway receptors. *J Appl Physiol*, 101, 960-970.
- ADRIAENSEN, D., BROUNS, I., VAN GENECHTEN, J. & TIMMERMANS, J. P. 2003. Functional morphology of pulmonary neuroepithelial bodies: Extremely complex airway receptors. *Anat Rec*, 270A, 25-40.
- AHSAN, F., ARNOLD, J. J., YANG, T. Z., MEEZAN, E., SCHWIEBERT, E. M. & PILLION, D. J. 2003. Effects of the permeability enhancers, tetradecylmaltoside and dimethyl-beta-cyclodextrin, on insulin movement across human bronchial epithelial cells (16HBE14o(-)). *Eur J Pharm Sci*, 20, 27-34.
- AKBARI, O., FAUL, J. L., HOYTE, E. G., BERRY, G. J., WAHLSTROM, J., KRONENBERG, M., DEKRUYFF, R. H. & UMETSU, D. T. 2006. CD4+ invariant T-cell-receptor plus natural killer T cells in bronchial asthma. *N Engl J Med*, 354, 1117-1129.
- AL-SADI, R., YE, D., SAID, H. M. & MA, T. Y. 2010. IL-1 beta-induced increase in intestinal epithelial tight junction permeability is mediated by MEKK-1 activation of canonical NF-kappa B pathway. *Am J Pathol*, 177, 2310-2322.
- ALESSI, D. R., CUENDA, A., COHEN, P., DUDLEY, D. T. & SALTIEL, A. R. 1995. PD-098059 is a specific inhibitor of the activation of mitogen-activated protein-kinase kinase in-vitro and in-vivo *J Biol Chem*, 270, 27489-27494.
- ALHAMORUNI, A., LEE, A. C., WRIGHT, K. L., LARVIN, M. & O'SULLIVAN, S. E. 2010. Pharmacological effects of cannabinoids on the Caco-2 cell culture model of intestinal permeability. *J Pharmacol Exp Ther*, 335, 92-102.
- ALHAMORUNI, A., WRIGHT, K. L., LARVIN, M. & O'SULLIVAN, S. E. 2012. Cannabinoids mediate opposing effects on inflammation-induced intestinal permeability. *Br J Pharmacol*, 165, 2598-2610.
- ALMADA, M., PISCITELLI, F., FONSECA, B. M., DI MARZO, V., CORREIA-DASILVA, G. & TEIXEIRA, N. 2015. Anandamide and decidual remodelling: COX-2 oxidative metabolism as a key regulator. *Biochimica Et Biophysica Acta-Molecular and Cell Biology of Lipids*, 1851, 1473-1481.

- ANGGADIREDJA, K., NAKAMICHI, M., HIRANITA, T., TANAKA, H., SHOYAMA, Y., WATANABE, S. & YAMAMOTO, T. 2004. Endocannabinoid system modulates relapse to methamphetamine seeking: Possible mediation by the arachidonic acid cascade. *Neuropsychopharmacology*, 29, 1470-1478.
- BAKER, C. L. & MCDOUGALL, J. J. 2004. The cannabinomimetic arachidonyl-2-chloroethylamide (ACEA) acts on capsaicin-sensitive TRPV1 receptors but not cannabinoid receptors in rat joints. *Br J Pharmacol*, 142, 1361-1367.
- BALDA, M. S., WHITNEY, J. A., FLORES, C., GONZALEZ, S., CEREJIDO, M. & MATTER, K. 1996. Functional dissociation of paracellular permeability and transepithelial electrical resistance and disruption of the apical-basolateral intramembrane diffusion barrier by expression of a mutant tight junction membrane protein. *J Cell Biol*, 134, 1031-1049.
- BALENGA, N. A. B., AFLAKI, E., KARGL, J., PLATZER, W., SCHRODER, R., BLATTERMANN, S., KOSTENIS, E., BROWN, A. J., HEINEMANN, A. & WALDHOER, M. 2011. GPR55 regulates cannabinoid 2 receptor-mediated responses in human neutrophils. *Cell Res*, 21, 1452-1469.
- BALZAR, S., CHU, H. W., STRAND, M. & WENZEL, S. 2005. Relationship of small airway chymase-positive mast cells and lung function in severe asthma. *Am J Respir Crit Care Med*, 171, 431-439.
- BARKER, D., VAN DER VELDEN, J., BARCHAM, G., KOUMOUNDOUROS, E. & SNIBSON, K. 2013. Microarray analysis of the epithelium following allergen challenge in a sheep model of asthma. *Respirology*, 18, 38-38.
- BARNES, P. J., CHOWDHURY, B., KHARITONOV, S. A., MAGNUSSEN, H., PAGE, C. P., POSTMA, D. & SAETTA, M. 2006. Pulmonary biomarkers in chronic obstructive pulmonary disease. *Am J Respir Crit Care Med*, 174, 6-14.
- BARNES, P. J., PEDERSEN, S. & BUSSE, W. W. 1998. Efficacy and safety of inhaled corticosteroids - New developments. *Am J Respir Crit Care Med*, 157, S1-S53.
- BARTEMES, K. R. & KITA, H. 2012. Dynamic role of epithelium-derived cytokines in asthma. *Clin Immunol*, 143, 222-235.
- BATEMAN, E. D., HURD, S. S., BARNES, P. J., BOUSQUET, J., DRAZEN, J. M., FITZGERALD, M., GIBSON, P., OHTA, K., O'BYRNE, P., PEDERSEN, S. E., PIZZICHINI, E., SULLIVAN, S. D., WENZEL, S. E. & ZAR, H. J. 2008. Global strategy for asthma management and prevention: GINA executive summary. *Eur Respir J*, 31, 143-178.
- BAXTER, M., ELTOM, S., DEKKAK, B., YEW-BOOTH, L., DUBUIS, E. D., MAHER, S. A., BELVISI, M. G. & BIRRELL, M. A. 2014. Role of transient receptor potential and pannexin channels in cigarette smoke-triggered ATP release in the lung. *Thorax*, 69, 1080-1089.
- BEAVEN, M. A. 2009. Our perception of the mast cell from Paul Ehrlich to now. *Eur J Immunol*, 39, 11-25.
- BEN-SHABAT, S., FRIDE, E., SHESKIN, T., TAMIRI, T., RHEE, M. H., VOGEL, Z., BISOGNO, T., DE PETROCELLIS, L., DI MARZO, V. & MECHOULAM, R. 1998. An entourage effect: inactive endogenous fatty acid glycerol esters enhance 2-arachidonoyl-glycerol cannabinoid activity. *Eur J Pharmacol*, 353, 23-31.

- BENAYOUN, L., DRUILHE, A., DOMBRET, M. C., AUBIER, M. & PRETOLANI, M. 2003. Airway structural alterations selectively associated with severe asthma. *Am J Respir Crit Care Med*, 167, 1360-1368.
- BERGER, J. T., VOYNOW, J. A., PETERS, K. W. & ROSE, M. C. 1999. Respiratory carcinoma cell lines - MUC genes and glycoconjugates. *Am J Respir Cell Mol Biol*, 20, 500-510.
- BERRIDGE, M. V. & TAN, A. S. 1993. Characterization of the cellular reduction of 3-(4,5-dimethylthiazol-2-yl)-2,5-diphenyltetrazolium bromide (MTT) - Subcellular-localization, substrate dependence, and involvement of mitochondrial electron-transport in MTT reduction *Arch Biochem Biophys*, 303, 474-482.
- BERRY, M., MORGAN, A., SHAW, D. E., PARKER, D., GREEN, R., BRIGHTLING, C., BRADDING, P., WARDLAW, A. J. & PAVORD, I. D. 2007. Pathological features and inhaled corticosteroid response of eosinophilic and non-eosinophilic asthma. *Thorax*, 62, 1043-1049.
- BESSAC, B. F. & JORDT, S. E. 2008. Breathtaking TRP channels: TRPA1 and TRPV1 in airway chemosensation and reflex control. *Physiology*, 23, 360-370.
- BEZZERRI, V., BORGATTI, M., FINOTTI, A., TAMANINI, A., GAMBARI, R. & CABRINI, G. 2011. Mapping the Transcriptional Machinery of the IL-8 Gene in Human Bronchial Epithelial Cells. *J Immunol*, 187, 6069-6081.
- BIO-RAD. 2015. *Bio-Dot® and Bio-Dot SF Microfiltration Apparatus* [Online]. <http://www.bio-rad.com/en-uk/product/bio-dot-bio-dot-sf-microfiltration-apparatus>. [Accessed 04.05.2015].
- BISCHOFF, S. C. 2007. Role of mast cells in allergic and non-allergic immune responses: comparison of human and murine data. *Nature Reviews Immunology*, 7, 93-104.
- BLANKMAN, J. L. & CRAVATT, B. F. 2013. Chemical Probes of Endocannabinoid Metabolism. *Pharmacol Rev*, 65, 849-871.
- BOJESSEN, I. N. & HANSEN, H. S. 2003. Binding of anandamide to bovine serum albumin. *J Lipid Res*, 44, 1790-1794.
- BOOZ, G. W. 2011. Cannabidiol as an emergent therapeutic strategy for lessening the impact of inflammation on oxidative stress. *Free Radic Biol Med*, 51, 1054-1061.
- BOUSQUET, J., JEFFERY, P. K., BUSSE, W. W., JOHNSON, M. & VIGNOLA, A. M. 2000. Asthma - From bronchoconstriction to airways inflammation and remodeling. *Am J Respir Crit Care Med*, 161, 1720-1745.
- BOYLE, E. C., BROWN, N. F. & FINLAY, B. B. 2006. Salmonella enterica serovar Typhimurium effectors SopB, SopE, SopE2 and SipA disrupt tight junction structure and function. *Cell Microbiol*, 8, 1946-1957.
- BRIGGS, M. W. & SACKS, D. B. 2003. IQGAP1 as signal integrator: Ca²⁺, calmodulin, Cdc42 and the cytoskeleton. *FEBS Lett*, 542, 7-11.
- BROIDE, D. H., LOTZ, M., CUOMO, A. J., COBURN, D. A., FEDERMAN, E. C. & WASSERMAN, S. I. 1992. Cytokines in symptomatic asthma airways *J Allergy Clin Immunol*, 89, 958-967.
- BROWN, A. J. & WISE, A. 2001. *Identification of modulators of GPR55 activity* [Online]. Available: <http://www.wipo.int/pctdb/en/wo.jsp?wo=2001086305> [Accessed 06.06.2015].
- BRUEWER, M., HOPKINS, A. M., HOBERT, M. E., NUSRAT, A. & MADARA, J. L. 2004. RhoA, Rac1, and Cdc42 exert distinct effects on epithelial barrier

- via selective structural and biochemical modulation of junctional proteins and F-actin. *Am J Physiol Cell Physiol*, 287, C327-C335.
- BRYAN, S. A., O'CONNOR, B. J., MATTI, S., LECKIE, M. J., KANABAR, V., KHAN, J., WARRINGTON, S. J., RENZETTI, L., RAMES, A., BOCK, J. A., BOYCE, M. J., HANSEL, T. T., HOLGATE, S. T. & BARNES, P. J. 2000. Effects of recombinant human interleukin-12 on eosinophils, airway hyper-responsiveness, and the late asthmatic response. *Lancet*, 356, 2149-2153.
- BTS. 2014. *SIGN 141: British guideline on the management of asthma* [Online]. British Thoracic Society/Scottish Intercollegiate Guidelines Network. Available: <https://www.brit-thoracic.org.uk/document-library/clinical-information/asthma/btssign-asthma-guideline-2014/> [Accessed 13.10.2015].
- BUCCHIERI, F., PUDDICOMBE, S. M., LORDAN, J. L., RICHTER, A., BUCHANAN, D., WILSON, S. J., WARD, J., ZUMMO, G., HOWARTH, P. H., DJUKANOVIC, R., HOLGATE, S. T. & DAVIES, D. E. 2002. Asthmatic bronchial epithelium is more susceptible to oxidant-induced apoptosis. *Am J Respir Cell Mol Biol*, 27, 179-185.
- BUSSE, W. W., COFFMAN, R. L., GELFAND, E. W., KAY, A. B. & ROSENWASSER, L. J. 1995. Mechanisms of persistent airway inflammation in asthma - A role for T-cells and T-cells products. *Am J Respir Crit Care Med*, 152, 388-393.
- BUSSE, W. W., HOLGATE, S., KERWIN, E., CHON, Y., FENG, J. Y., LIN, J. & LIN, S. L. 2013. Randomized, Double-Blind, Placebo-controlled Study of Brodalumab, a Human Anti-IL-17 Receptor Monoclonal Antibody, in Moderate to Severe Asthma. *Am J Respir Crit Care Med*, 188, 1294-1302.
- BUTTON, B., PICHER, M. & BOUCHER, R. C. 2007. Differential effects of cyclic and constant stress on ATP release and mucociliary transport by human airway epithelia. *J Physiol London*, 580, 577-592.
- CALIGNANO, A., KATONA, I., DESARNAUD, F., GIUFFRIDA, A., LA RANA, G., MACKIE, K., FREUND, T. F. & PIOMELLI, D. 2000. Bidirectional control of airway responsiveness by endogenous cannabinoids. *Nature*, 408, 96-101.
- CANNING, B. J. 2003. Modeling asthma and COPD in animals: a pointless exercise? *Curr Opin Pharmacol*, 3, 244-250.
- CARAMORI, G., DI GREGORIO, C., CARLSTEDT, I., CASOLARI, P., GUZZINATI, I., ADCOCK, I. M., BARNES, P. J., CIACCIA, A., CAVALLESCO, G., CHUNG, K. F. & PAPI, A. 2004. Mucin expression in peripheral airways of patients with chronic obstructive pulmonary disease. *Histopathology*, 45, 477-484.
- CARROLL, N. G., MUTAVDZIC, S. & JAMES, A. L. 2002. Increased mast cells and neutrophils in submucosal mucous glands and mucus plugging in patients with asthma. *Thorax*, 57, 677-682.
- CASAR, B., PINTO, A. & CRESPO, P. 2008. Essential role of ERK dimers in the activation of cytoplasmic but not nuclear substrates by ERK-scaffold complexes. *Mol Cell*, 31, 708-721.
- CASTILLO, A., TOLON, M. R., FERNANDEZ-RUIZ, J., ROMERO, J. & MARTINEZ-ORGADO, J. 2010. The neuroprotective effect of cannabidiol in an in vitro model of newborn hypoxic-ischemic brain damage in mice is mediated by CB2 and adenosine receptors. *Neurobiol Dis*, 37, 434-440.

- CELL BIOLABS, I. 2015. Product information: Rho Kinase (ROCK) Activity Assay. In: [HTTP://WWW.CELLBIOLABS.COM/RHO-KINASE-ROCK-ASSAYS](http://www.cellbiolabs.com/rho-kinase-rock-assays) (ed.). Cell Biolabs Inc website.
- CEMBRZYNSKANOWAK, M., SZKLARZ, E., INGLLOT, A. D. & TEODORCZYKINJEYAN, J. A. 1993. Elevated release of tumor-necrosis-factor-alpha and interferon-gamma by bronchoalveolar leukocytes from patients with bronchial-asthma *Am Rev Respir Dis*, 147, 291-295.
- CHANG, K. C., LO, C. W., FAN, T. C., CHANG, M. D. T., SHU, C. W., CHANG, C. H., CHUNG, C. T., FANG, S. L., CHAO, C. C., TSAI, J. J. & LAI, Y. K. 2010. TNF-alpha mediates eosinophil cationic protein-induced apoptosis in BEAS-2B cells. *Bmc Cell Biology*, 11.
- CHEN, M. L., GE, Z. M., FOX, J. G. & SCHAUER, D. B. 2006. Disruption of tight junctions and induction of proinflammatory cytokine responses in colonic epithelial cells by *Campylobacter jejuni*. *Infect Immun*, 74, 6581-6589.
- CHEN, Y. H., LU, Q., SCHNEEBERGER, E. E. & GOODENOUGH, D. A. 2000. Restoration of tight junction structure and barrier function by down-regulation of the mitogen-activated protein kinase pathway in Ras-transformed Madin-Darby canine kidney cells. *Mol Biol Cell*, 11, 849-862.
- CHOI, I. W., SUN, K., KIM, Y. S., KO, H. M., IM, S. Y., KIM, J. H., YOU, H. J., LEE, Y. C., LEE, J. H., PARK, Y. M. & LEE, H. K. 2005. TNF-alpha induces the late-phase airway hyperresponsiveness and airway inflammation through cytosolic phospholipase A(2) activation. *J Allergy Clin Immunol*, 116, 537-543.
- CHOW, J. C., YOUNG, D. W., GOLENBOCK, D. T., CHRIST, W. J. & GUSOVSKY, F. 1999. Toll-like receptor-4 mediates lipopolysaccharide-induced signal transduction. *J Biol Chem*, 274, 10689-10692.
- CHURG, A., DAI, J., TAI, H., XIE, C. S. & WRIGHT, J. L. 2002. Tumor necrosis factor-alpha is central to acute cigarette smoke-induced inflammation and connective tissue breakdown. *Am J Respir Crit Care Med*, 166, 849-854.
- CLAYBURGH, D. R., BARRETT, T. A., TANG, Y. M., MEDDINGS, J. B., VAN ELDIK, L. J., WATTERSON, D. M., CLARKE, L. L., MRSNY, R. J. & TURNER, J. R. 2005. Epithelial myosin light chain kinase-dependent barrier dysfunction mediates T cell activation-induced diarrhea in vivo. *J Clin Invest*, 115, 2702-2715.
- COLGAN, S. P., PARKOS, C. A., DELP, C., ARNAOUT, M. A. & MADARA, J. L. 1993. Neutrophil migration across cultured intestinal epithelial monolayers is modulated by epithelial exposure to IFN-gamma in a highly polarised fashion *J Cell Biol*, 120, 785-798.
- CORTELING, R. L., LI, S., GIDDINGS, J., WESTWICK, J., POLL, C. & HALL, I. P. 2004. Expression of transient receptor potential C6 and related transient receptor potential family members in human airway smooth muscle and lung tissue. *Am J Respir Cell Mol Biol*, 30, 145-154.
- COSTA, B., GIAGNONI, G., FRANKE, C., TROVATO, A. E. & COLLEONI, M. 2004. Vanilloid TRPV1 receptor mediates the antihyperalgesic effect of the nonpsychoactive cannabinoid, cannabidiol, in a rat model of acute inflammation. *Br J Pharmacol*, 143, 247-250.
- COWBURN, A. S., SLADEK, K., SOJA, J., ADAMEK, L., NIZANKOWSKA, E., SZCZEKLIK, A., LAM, B. K., PENROSE, J. F., AUSTEN, K. F., HOLGATE, S. T. & SAMPSON, A. P. 1998. Overexpression of leukotriene

- C-4 synthase in bronchial biopsies from patients with aspirin-intolerant asthma. *J Clin Invest*, 101, 834-846.
- COYNE, C. B., VANHOOK, M. K., GAMBLING, T. M., CARSON, J. L., BOUCHER, R. C. & JOHNSON, L. G. 2002. Regulation of airway tight junctions by proinflammatory cytokines. *Mol Biol Cell*, 13, 3218-3234.
- CRAVATT, B. F., GIANG, D. K., MAYFIELD, S. P., BOGER, D. L., LERNER, R. A. & GILULA, N. B. 1996. Molecular characterization of an enzyme that degrades neuromodulatory fatty-acid amides. *Nature*, 384, 83-87.
- CROMWELL, O., HAMID, Q., CORRIGAN, C. J., BARKANS, J., MENG, Q., COLLINS, P. D. & KAY, A. B. 1992. Expression and generation of interleukin-8, IL-6 and granulocyte macrophage colony-stimulating factor by bronchial epithelia-cells and enhancement by IL-1 beta and tumor-necrosis factor-alpha *Immunology*, 77, 330-337.
- CULPITT, S. V., ROGERS, D. F., SHAH, P., DE MATOS, C., RUSSELL, R. E. K., DONNELLY, L. E. & BARNES, P. J. 2003. Impaired inhibition by dexamethasone of cytokine release by alveolar macrophages from patients with chronic obstructive pulmonary disease. *Am J Respir Crit Care Med*, 167, 24-31.
- CUNNINGHAM, K. E. & TURNER, J. R. 2012. *Myosin light chain kinase: pulling the strings of epithelial tight junction function*, Book Series: Annals of the New York Academy of Sciences.
- DAVIES, C. & TOURNIER, C. 2012. Exploring the function of the JNK (c-Jun N-terminal kinase) signalling pathway in physiological and pathological processes to design novel therapeutic strategies. *Biochem Soc Trans*, 40, 85-89.
- DAVIES, D. E., WICKS, J., POWELL, R. M., PUDDICOMBE, S. M. & HOLGATE, S. T. 2003. Airway remodeling in asthma: New insights. *J Allergy Clin Immunol*, 111, 215-225.
- DAVIES, S. P., REDDY, H., CAIVANO, M. & COHEN, P. 2000. Specificity and mechanism of action of some commonly used protein kinase inhibitors. *Biochem J*, 351, 95-105.
- DE FILLIPPIS, D., IUVONE, T., D'AMICO, A., ESPOSITO, G., STEARDO, L., HERMAN, A. G., PELCKMANS, P. A., DE WINTER, B. Y. & DE MAN, J. G. 2008. Effect of cannabidiol on sepsis-induced motility disturbances in mice: involvement of CB receptors and fatty acid amide hydrolase. *Neurogastroenterol Motil*, 919, 919-927.
- DE PETROCELLIS, L. & DI MARZO, V. 2010. Non-CB1, non-CB2 receptors for endocannabinoids, plant cannabinoids, and synthetic cannabimimetics: Focus on G-protein-coupled receptors and Transient Receptor Potential Channels. *Journal of Neuroimmune Pharmacology*, 5, 103-121.
- DE PETROCELLIS, L., LIGRESTI, A., MORIELLO, A. S., ALLARA, M., BISOGNO, T., PETROSINO, S., STOTT, C. G. & DI MARZO, V. 2011. Effects of cannabinoids and cannabinoid-enriched Cannabis extracts on TRP channels and endocannabinoid metabolic enzymes. *Br J Pharmacol*, 163, 1479-1494.
- DELI, M. A. 2009. Potential use of tight junction modulators to reversibly open membranous barriers and improve drug delivery. *Biochimica Et Biophysica Acta-Biomembranes*, 1788, 892-910.
- DEN BESTE, K. A., HODDESON, E. K., PARKOS, C. A., NUSRAT, A. & WISE, S. K. 2013. Epithelial permeability alterations in an in vitro air-liquid

- interface model of allergic fungal rhinosinusitis. *International Forum of Allergy & Rhinology*, 3, 19-25.
- DEVANE, W. A., DYSARZ, F. A., JOHNSON, M. R., MELVIN, L. S. & HOWLETT, A. C. 1988. Determination and characterization of a cannabinoid receptor in rat-brain. *Mol Pharmacol*, 34, 605-613.
- DEVANE, W. A., HANUS, L., BREUER, A., PERTWEE, R. G., STEVENSON, L. A., GRIFFIN, G., GIBSON, D., MANDELBAUM, A., ETINGER, A. & MECOULAM, R. 1992. Isolation and structure of a brain constituent that binds to the cannabinoid receptor. *Science*, 258, 1946-1949.
- DI MARZO, V., DE PETROCELLIS, L. & BISOGNO, T. 2005. The biosynthesis, fate and pharmacological properties of endocannabinoids. In: PERTWEE, R. G. (ed.) *Handbook of Experimental Pharmacology*. Springer-Verlag Berlin, Heidelberger Platz 3, D-14197 Berlin, Germany.
- DIAMANT, Z., MANTZOURANIS, E. & BJERMER, L. 2009. Montelukast in the treatment of asthma and beyond. *Expert Rev Clin Immunol*, 5, 639-658.
- DIONISI, M., MILLNS, P. J., SUN, Y., BENNETT, A. J. & ALEXANDER, S. P. H. 2007. Characterization of endogenous cannabinoid systems in three human cell lines [Online]. Available: <http://www.pa2online.org/abstract/abstract.jsp?abid=28899&author=dionisi&cat=-1&period=-1> [Accessed 03.06.2015].
- DIPAOLLO, B. C. & MARGULIES, S. S. 2012. Rho kinase signaling pathways during stretch in primary alveolar epithelia. *Am J Physiol Lung Cell Mol Physiol*, 302, L992-L1002.
- DOERFEL, M. J. & HUBER, O. 2012. Modulation of Tight Junction Structure and Function by Kinases and Phosphatases Targeting Occludin. *Journal of Biomedicine and Biotechnology*.
- DONALDSON, G. C., SEEMUNGAL, T. A., PATEL, I. S. B., A., WILKINSON, T. M., HURST, J. R., MACCALLUM, P. K. & WEDZICHA, J. A. 2005. Airway and systemic inflammation and decline in lung function in patients with COPD. *Chest*, 128, 1995-2004.
- DREW, B. A., BUROW, M. E. & BECKMAN, B. S. 2012. MEK5/ERK5 pathway: The first fifteen years. *Biochimica Et Biophysica Acta-Reviews on Cancer*, 1825, 37-48.
- DRMOTA, T., GREASLEY, P. & GROBLEWSKI, T. 2004. Screening assays for cannabinoid-ligands type modulators of GPR55 [Online]. Available: <http://www.wipo.int/pctdb/en/wo.jsp?wo=2004074844> [Accessed 06.06.2015].
- DUNCIA, J. V., SANTELLA, J. B., HIGLEY, C. A., PITTS, W. J., WITYAK, J., FRIETZE, W. E., RANKIN, F. W., SUN, J. H., EARL, R. A., TABAKA, A. C., TELEHA, C. A., BLOM, K. F., FAVATA, M. F., MANOS, E. J., DAULERIO, A. J., STRADLEY, D. A., HORIUCHI, K., COPELAND, R. A., SCHERLE, P. A., TRZASKOS, J. M., MAGOLDA, R. L., TRAINOR, G. L., WEXLER, R. R., HOBBS, F. W. & OLSON, R. E. 1998. MEK inhibitors: The chemistry and biological activity of U0126, its analogs, and cyclization products. *Bioorg Med Chem Lett*, 8, 2839-2844.
- EHRHARDT, C., COLLNOT, E. M., BALDES, C., BECKER, U., LAUE, M., KIM, K. J. & LEHR, C. M. 2006. Towards an in vitro model of cystic fibrosis small airway epithelium: characterisation of the human bronchial epithelial cell line CFBE41o. *Cell Tissue Res*, 323, 405-415.

- ELAMIN, E., MASCLÉE, A., DEKKER, J. & JONKERS, D. 2014. Ethanol disrupts intestinal epithelial tight junction integrity through intracellular calcium-mediated Rho/ROCK activation. *Am J Physiol Gastrointest Liver Physiol*, 306, G677-G685.
- EUTAMENE, H., THEODOROU, V., SCHMIDLIN, F., TONDEREAU, V., GARCIA-VILLAR, R., SALVADOR-CARTIER, C., CHOVET, M., BERTRAND, C. & BUENO, L. 2005. LPS-induced lung inflammation is linked to increased epithelial permeability: role of MLCK. *Eur Respir J*, 25, 789-796.
- EVANS, M. J., VAN WINKLE, L. S., FANUCCHI, M. V. & PLOPPER, C. G. 2001. Cellular and molecular characteristics of basal cells in airway epithelium. *Exp Lung Res*, 27, 401-415.
- FANNING, A. S., JAMESON, B. J., JESAITIS, L. A. & ANDERSON, J. M. 1998. The tight junction protein ZO-1 establishes a link between the transmembrane protein occludin and the actin cytoskeleton. *J Biol Chem*, 273, 29745-29753.
- FIELDS, R. D. & LANCASTER, M. V. 1993. Dual-attribute continuous monitoring of cell-proliferation cytotoxicity *Am Biotechnol Lab*, 11, 48-&.
- FIORENTINO, M., DING, H., BLANCHARD, T. G., CZINN, S. J., SZTEIN, M. B. & FASANO, A. 2013. Helicobacter pylori-induced disruption of monolayer permeability and proinflammatory cytokine secretion in polarized human gastric epithelial cells. *Infect Immun*, 81, 876-883.
- FISCHER, A., GLUTH, M., PAPE, U.-F., WIEDENMANN, B., THEURING, F. & BAUMGART, D. C. 2013. Adalimumab prevents barrier dysfunction and antagonizes distinct effects of TNF-alpha on tight junction proteins and signaling pathways in intestinal epithelial cells. *Am J Physiol Gastrointest Liver Physiol*, 304, G970-G979.
- FLEMING, I. N., ELLIOTT, C. M. & EXTON, J. H. 1996. Differential translocation of Rho family GTPases by lysophosphatidic acid, endothelin-1, and platelet-derived growth factor. *J Biol Chem*, 271, 33067-33073.
- FORBES, B. & EHRHARDT, C. 2005. Human respiratory epithelial cell culture for drug delivery applications. *Eur J Pharm Biopharm*, 60, 193-205.
- FU, X. W., NURSE, C. A., WONG, V. & CUTZ, E. 2002. Hypoxia-induced secretion of serotonin from intact pulmonary neuroepithelial bodies in neonatal rabbit. *J Physiol London*, 539, 503-510.
- FUKUNAGA, K., KOHLI, P., BONNANS, C., FREDENBURGH, L. E. & LEVY, B. D. 2005. Cyclooxygenase 2 plays a pivotal role in the resolution of acute lung injury. *J Immunol*, 174, 5033-5039.
- GAONI, Y. & MECHOULAM, R. 1964. Isolation, structure and partial synthesis of an active constituent in hashish *J Am Chem Soc*, 86, 1646-+.
- GARCIA, J. G. N., WANG, P. Y., SCHAPHORST, K. L., BECKER, P. M., BORBIEV, T., LIU, F., BIRUKOVA, A., JACOBS, K., BOGATCHEVA, N. & VERIN, A. D. 2002. Critical involvement of p38 MAP kinase in pertussis toxin-induced cytoskeletal reorganization and lung permeability. *FASEB J*, 16, 1064-1076.
- GATLEY, S. J., GIFFORD, A. N., VOLKOW, N. D., LAN, R. & MAKRIYANNIS, A. 1996. 123I-labelled AM251: a radioiodinated ligand which binds in vivo to mouse brain cannabinoid CB1 receptors. *Eur J Pharmacol*, 307, 331-338.
- GERSHENWALD, J. E., FONG, Y., FAHEY, T. J., CALVANO, S. E., CHIZZONITE, R., KILIAN, P. L., LOWRY, S. F. & MOLDAWER, L. L.

1990. Interleukin-1 receptor blockade attenuates the host inflammatory response *Proc Natl Acad Sci U S A*, 87, 4966-4970.
- GIANNINI, L., NISTRI, S., MASTROIANNI, R., CINCI, L., VANNACCI, A., MARIOTTINI, C., PASSANI, M. B., MANNAIONI, P. F., BANI, D. & MASINI, E. 2008. Activation of cannabinoid receptors prevents antigen-induced asthma-like reaction in guinea pigs. *J Cell Mol Med*, 12, 2381-2394.
- GINA. 2014. Global Strategy for Asthma Management and Prevention. Available: http://www.ginasthma.org/local/uploads/files/GINA_Report_2015_Aug11.pdf [Accessed 01.06.2015].
- GINA. 2015. Diagnosis of diseases of chronic airflow limitations: Asthma and COPD and Asthma-COPD overlapping syndrome (ACOS). Available: http://www.ginasthma.org/local/uploads/files/ACOS_2015.pdf [Accessed 01.08.2015].
- GONZALEZ-MARISCAL, L., TAPIA, R. & CHAMORRO, D. 2008. Crosstalk of tight junction components with signaling pathways. *Biochimica Et Biophysica Acta-Biomembranes*, 1778, 729-756.
- GONZALEZ, J. E., DIGERONIMO, R. J., ARTHUR, D. A. E. & KING, J. M. 2009. Remodeling of the tight junction during recovery from exposure to hydrogen peroxide in kidney epithelial cells. *Free Radic Biol Med*, 47, 1561-1569.
- GOPALAKRISHNAN, S., RAMAN, N., ATKINSON, S. J. & MARRS, J. A. 1998. Rho GTPase signaling regulates tight junction assembly and protects tight junctions during ATP depletion. *Am J Physiol Cell Physiol*, 275, C798-C809.
- GRACE, M. S., BAXTER, M., DUBUIS, E., BIRRELL, M. A. & BELVISI, M. G. 2014. Transient receptor potential (TRP) channels in the airway: role in airway disease. *Br J Pharmacol*, 171, 2593-2607.
- GRAINGE, C. L., LAU, L. C. K., WARD, J. A., DULAY, V., LAHIFF, G., WILSON, S., HOLGATE, S., DAVIES, D. E. & HOWARTH, P. H. 2011. Effect of Bronchoconstriction on Airway Remodeling in Asthma. *N Engl J Med*, 364, 2006-2015.
- GRAINGER, C. I., GREENWELL, L. L., LOCKLEY, D. J., MARTIN, G. P. & FORBES, B. 2006. Culture of Calu-3 cells at the air interface provides a representative model of the airway epithelial barrier. *Pharm Res*, 23, 1482-1490.
- GRASSIN-DELYLE, S., NALINE, E., BUENESTADO, A., FAISY, C., ALVAREZ, J. C., SALVATOR, H., ABRIAL, C., ADVENIER, C., ZEMOURA, L. & DEVILLIER, P. 2014. Cannabinoids inhibit cholinergic contraction in human airways through prejunctional CB1 receptors. *Br J Pharmacol*, 171, 2767-2777.
- GRAY, T., COAKLEY, R., HIRSH, A., THORNTON, D., KIRKHAM, S., KOO, J. S., BURCH, L., BOUCHER, R. & NETTESHEIM, P. 2004a. Regulation of MUC5AC mucin secretion and airway surface liquid metabolism by IL-1 beta in human bronchial epithelia. *Am J Physiol Lung Cell Mol Physiol*, 286, L320-L330.
- GRAY, T., NETTESHEIM, P., LOFTIN, C., KOO, J. S., BONNER, J., PEDDADA, S. & LANGENBACH, R. 2004b. Interleukin-1 beta-induced mucin production in human airway epithelium is mediated by cyclooxygenase-2, prostaglandin E-2 receptors, and cyclic AMP-protein kinase A signaling. *Mol Pharmacol*, 66, 337-346.
- GRIMSEY, N. L., GOODFELLOW, C. E., SCOTTER, E. L., DOWIE, M. J., GLASS, M. & GRAHAM, E. S. 2008. Specific detection of CB(1) receptors;

- cannabinoid CB(1) receptor antibodies are not all created equal! *J Neurosci Methods*, 171, 78-86.
- GRONEBERG, D. A., EYNOTT, P. R., LIM, S., OATES, T., WU, R., CARLSTEDT, I., ROBERTS, P., MCCANN, B., NICHOLSON, A. G., HARRISON, B. D. & CHUNG, K. F. 2002. Expression of respiratory mucins in fatal status asthmaticus and mild asthma. *Histopathology*, 40, 367-373.
- HACKETT, T.-L. & KNIGHT, D. A. 2007. The role of epithelial injury and repair in the origins of asthma. *Curr Opin Allergy Clin Immunol*, 7, 63-68.
- HAMPSON, A. J., GRIMALDI, M., AXELROD, J. & WINK, D. 1998. Cannabidiol and (-)-Delta(9)-tetrahydrocannabinol are neuroprotective antioxidants. *Proc Natl Acad Sci U S A*, 95, 8268-8273.
- HAMPSON, A. J., HILL, W. A. G., ZAN-PHILLIPS, M., MAKRIYANNIS, A., LEUNG, E., EGLEN, R. M. & BORNHEIM, L. M. 1995. Anandamide hydroxylation by brain lipoxygenase: metabolite structures and potencies at the cannabinoid receptor. *Biochemical and Biophysical Acta.*, 1259, 173-179.
- HARDYMAN, M. A., WILKINSON, E., MARTIN, E., JAYASEKERA, N. P., BLUME, C., SWINDLE, E. J., GOZZARD, N., HOLGATE, S. T., HOWARTH, P. H., DAVIES, D. E. & COLLINS, J. E. 2013. TNF-alpha-mediated bronchial barrier disruption and regulation by src-family kinase activation. *J Allergy Clin Immunol*, 132, 665-675.
- HARHAJ, N. S. & ANTONETTI, D. A. 2004. Regulation of tight junctions and loss of barrier function in pathophysiology. *Int J Biochem Cell Biol*, 36, 1206-1237.
- HASSAN, S., ELDEEB, K., MILLNS, P. J., BENNETT, A. J., ALEXANDER, S. P. H. & KENDALL, D. A. 2014. Cannabidiol enhances microglial phagocytosis via transient receptor potential (TRP) channel activation. *Br J Pharmacol*, 171, 2426-2439.
- HEIJINK, I. H., VAN OOSTERHOUT, A. & KAPUS, A. 2010. Epidermal growth factor receptor signalling contributes to house dust mite-induced epithelial barrier dysfunction. *Eur Respir J*, 36, 1016-1026.
- HENSTRIDGE, C. M. 2012. Off-Target Cannabinoid Effects Mediated by GPR55. *Pharmacology*, 89, 179-187.
- HIBINO, Y., MORISE, M., ITO, Y., MIZUTANI, T., MATSUNO, T., ITO, S., HASHIMOTO, N., SATO, M., KONDO, M., IMAIZUMI, K. & HASEGAWA, Y. 2011. Capsaicinoids Regulate Airway Anion Transporters through Rho Kinase- and Cyclic AMP-Dependent Mechanisms. *Am J Respir Cell Mol Biol*, 45, 684-691.
- HILLARD, C. J., MANNA, S., GREENBERG, M. J., DICAMELLI, R., ROSS, R. A., STEVENSON, L. A., MURPHY, V., PERTWEE, R. G. & CAMPBELL, W. B. 1999. Synthesis and characterization of potent and selective agonists of the neuronal cannabinoid receptor (CB1). *J Pharmacol Exp Ther*, 289, 1427-1433.
- HOLGATE, S. T. 2007. Epithelium dysfunction in asthma. *J Allergy Clin Immunol*, 120, 1233-1246.
- HOLGATE, S. T., NOONAN, M., CHANEZ, P., BUSSE, W., DUPONT, L., PAVORD, I., HAKULINEN, A., PAOLOZZI, L., WAJDULA, J., ZANG, C., NELSON, H. & RAIBLE, D. 2011. Efficacy and safety of etanercept in moderate-to-severe asthma: a randomised, controlled trial. *Eur Respir J*, 37, 1352-1359.

- HOLGATE, S. T. & POLOSA, R. 2006. The mechanisms, diagnosis, and management of severe asthma in adults. *Lancet*, 368, 780-793.
- HONDA, K., MARQUILLIES, P., CAPRON, M. & DOMBROWICZ, D. 2004. Peroxisome proliferator-activated receptor gamma is expressed in airways and inhibits features of airway remodeling in a mouse asthma model. *J Allergy Clin Immunol*, 113, 882-888.
- HONG, K. U., REYNOLDS, S. D., GIANGRECO, A., HURLEY, C. M. & STRIPP, B. R. 2001. Clara cell secretory protein-expressing cells of the airway neuroepithelial body microenvironment include a label-retaining subset and are critical for epithelial renewal after progenitor cell depletion. *Am J Respir Cell Mol Biol*, 24, 671-681.
- HONG, K. U., REYNOLDS, S. D., WATKINS, S., FUCHS, E. & STRIPP, B. R. 2004. In vivo differentiation potential of tracheal basal cells: evidence for multipotent and unipotent subpopulations. *Am J Physiol Lung Cell Mol Physiol*, 286, L643-L649.
- HOWE, K., GAULDIE, J. & MCKAY, D. M. 2002. TGF-beta effects on epithelial ion transport and barrier: reduced Cl⁻ secretion blocked by a p38 MAPK inhibitor. *Am J Physiol Cell Physiol*, 283, C1667-C1674.
- HOWE, K. L., REARDON, C., WANG, A., NAZLI, A. & MCKAY, D. M. 2005. Transforming growth factor-beta regulation of epithelial tight junction proteins enhances barrier function and blocks enterohemorrhagic Escherichia coli O157 : H7-induced increased permeability. *Am J Pathol*, 167, 1587-1597.
- HOWLETT, A. C. 2005. Cannabinoid receptor signaling. In: PERTWEE, R. G. (ed.) *Handbook of Experimental Pharmacology*. Springer-Verlag Berlin, Heidelberger Platz 3, D-14197 Berlin, Germany.
- HOZUMI, A., NISHIMURA, Y., NISHIUMA, T., KOTANI, Y. & YOKOYAMA, M. 2001. Induction of MMP-9 in normal human bronchial epithelial cells by TNF-alpha via NF-kappa B-mediated pathway. *Am J Physiol Lung Cell Mol Physiol*, 281, L1444-L1452.
- HUFFMAN, J. W., LIDDLE, J., YU, S., AUNG, M. M., ABOOD, M. E., WILEY, J. L. & MARTIN, B. R. 1999. 3-(1',1'-dimethylbutyl)-1-deoxy-Delta(8)-THC and related compounds: Synthesis of selective ligands for the CB2 receptor. *Bioorg Med Chem*, 7, 2905-2914.
- HUKKANEN, J., PELKONEN, A., HAKKOLA, J. & RAUNIO, H. 2002. Expression and regulation of xenobiotic-metabolizing cytochrome P450 (CYP) enzymes in human lung. *Crit Rev Toxicol*, 32, 391-411.
- HUMBERT, M., BUSSE, W., HANANIA, N. A., LOWE, P. J., CANVIN, J., ERPENBECK, V. J. & HOLGATE, S. 2014. Omalizumab in Asthma: An Update on Recent Developments. *Journal of Allergy and Clinical Immunology-in Practice*, 2, 525-+.
- ICHIMURA, A., HIRASAWA, A., HARA, T. & TSUJIMOTO, G. 2009. Free fatty acid receptors act as nutrient sensors to regulate energy homeostasis. *Prostaglandins Other Lipid Mediat*, 89, 82-88.
- IWAMOTO, H., GAO, J., KOSKELA, J., KINNULA, V., KOBAYASHI, H., LAITINEN, T. & MAZUR, W. 2014. Differences in plasma and sputum biomarkers between COPD and COPD-asthma overlap. *Eur Respir J*, 43, 421-429.
- IZZO, A. A., FEZZA, F., CAPASSO, R., BISOGNO, T., PINTO, L., IUVONE, T., ESPOSITO, G., MASCOLO, N., DI MARZO, V. & CAPASSO, F. 2001.

- Cannabinoid CB1-receptor mediated regulation of gastrointestinal motility in mice in a model of intestinal inflammation. *Br J Pharmacol*, 134, 563-570.
- JAIN, R., PAN, J. H., DRISCOLL, J. A., WISNER, J. W., HUANG, T., GUNSTEN, S. P., YOU, Y. J. & BRODY, S. L. 2010. Temporal Relationship between Primary and Motile Ciliogenesis in Airway Epithelial Cells. *Am J Respir Cell Mol Biol*, 43, 731-739.
- JAYAWICKREME, S. P., GRAY, T., NETTESHEIM, P. & ELING, T. 1999. Regulation of 15-lipoxygenase expression and mucus secretion by IL-4 in human bronchial epithelial cells. *Am J Physiol Lung Cell Mol Physiol*, 276, L596-L603.
- JEAN-GILLES, L., BRAITCH, M., LATIF, M. L., ARAM, J., FAHEY, A. J., EDWARDS, L. J., ROBINS, R. A., TANASESCU, R., TIGHE, P. J., GRAN, B., SHOWE, L. C., ALEXANDER, S. P., CHAPMAN, V., KENDALL, D. A. & CONSTANTINESCU, C. S. 2015. Effects of pro-inflammatory cytokines on cannabinoid CB1 and CB2 receptors in immune cells. *Acta Physiologica*, 214, 63-74.
- JIA, Y. L., MCLEOD, R. L., WANG, X., PARRA, L. E., EGAN, R. W. & HEY, J. A. 2002. Anandamide induces cough in conscious guinea-pigs through VR1 receptors. *Br J Pharmacol*, 137, 831-836.
- JOHN, M., LIM, S., SEYBOLD, J., JOSE, P., ROBICHAUD, A., O'CONNOR, B., BARNES, P. J. & CHUNG, K. F. 1998. Inhaled corticosteroids increase interleukin-10 but reduce macrophage inflammatory protein-1 alpha, granulocyte-macrophage colony-stimulating factor, and interferon-gamma release from alveolar macrophages in asthma. *Am J Respir Crit Care Med*, 157, 256-262.
- JOOS, G. F., GERMONPRE, P. R. & PAUWELS, R. A. 2000. Neural mechanisms in asthma. *Clin Exp Allergy*, 30, 60-65.
- JOU, T. S., SCHNEEBERGER, E. E. & NELSON, W. J. 1998. Structural and functional regulation of tight junctions by RhoA and Rac1 small GTPases. *J Cell Biol*, 142, 101-115.
- KAKIASHVILI, E., SPEIGHT, P., WAHEED, F., SETH, R., LODYGA, M., TANIMURA, S., KOHNO, M., ROTSTEIN, O. D., KAPUS, A. & SZASZI, K. 2009. GEF-H1 mediates tumour necrosis factor-alpha induced Rho activation and myosin phosphorylation: role in regulation of tubular paracellular permeability. *J Biol Chem*, 284, 11454-11466.
- KAWKITINARONG, K., LINZ-MCGILLEM, L., BIRUKOV, K. G. & GARCIA, J. G. N. 2004. Differential regulation of human lung epithelial and endothelial barrier function by thrombin. *Am J Respir Cell Mol Biol*, 31, 517-527.
- KEATINGS, V. M., COLLINS, P. D., SCOTT, D. M. & BARNES, P. J. 1996. Differences in interleukin-8 and tumor necrosis factor-alpha in induced sputum from patients with chronic obstructive pulmonary disease or asthma. *Am J Respir Crit Care Med*, 153, 530-534.
- KEMP, P. J., SEARLE, G. J., HARTNESS, M. E., LEWIS, A., MILLER, P., WILLIAMS, S., WOOTTON, P., ADRIAENSEN, D. & PEERS, C. 2003. Acute oxygen sensing in cellular models: Relevance to the physiology of pulmonary neuroepithelial and carotid bodies. *Anat Rec*, 270A, 41-50.
- KENT, B. D., MITCHELL, P. D. & MCNICHOLAS, W. T. 2011. Hypoxemia in patients with COPD: cause, effects, and disease progression. *International Journal of Chronic Obstructive Pulmonary Disease*, 6, 199-208.

- KIBANGOU, I. B., BUREAU, F., ALLOUCHE, S., ARHAN, P. & BOUGLE, D. 2008. Interactions between ethylenediaminetetraacetic acid (EDTA) and iron absorption pathways, in the Caco-2 model. *Food Chem Toxicol*, 46, 3414-3416.
- KIM, V. & CRINER, G. J. 2015. The chronic bronchitis phenotype in chronic obstructive pulmonary disease: features and implications. *Curr Opin Pulm Med*, 21, 133-141.
- KIRKHAM, S., SHEEHAN, J. K., KNIGHT, D., RICHARDSON, P. S. & THORNTON, D. J. 2002. Heterogeneity of airways mucus: variations in the amounts and glycoforms of the major oligomeric mucins MUC5AC and MUC5B. *Biochem J*, 361, 537-546.
- KLEIN, T. W., LANE, B., NEWTON, C. A. & FRIEDMAN, M. 2000. The cannabinoid system and cytokine network. *Proc Soc Exp Biol Med*, 225, 1-8.
- KNIGHT, D. A. & HOLGATE, S. T. 2003. The airway epithelium: Structural and functional properties in health and disease. *Respirology*, 8, 432-446.
- KOIZUMI, J.-I., KOJIMA, T., OGASAWARA, N., KAMEKURA, R., KUROSE, M., GO, M., HARIMAYA, A., MURATA, M., OSANAI, M., CHIBA, H., HIMI, T. & SAWADA, N. 2008. Protein kinase C enhances tight junction barrier function of human nasal epithelial cells in primary culture by transcriptional regulation. *Mol Pharmacol*, 74, 432-442.
- KOZAK, K. R., CREWS, B. C., MORROW, J. D., WANG, L. H., MA, Y. H., WEINANDER, R., JAKOBSSON, P. J. & MARNETT, L. J. 2002a. Metabolism of the endocannabinoids, 2-arachidonylglycerol and anandamide, into prostaglandin, thromboxane, and prostacyclin glycerol esters and ethanolamides. *J Biol Chem*, 277, 44877-44885.
- KOZAK, K. R., GUPTA, R. A., MOODY, J. S., JI, C., BOEGLIN, W. E., DUBOIS, R. N., BRASH, A. R. & MARNETT, L. J. 2002b. 15-lipoxygenase metabolism of 2-arachidonylglycerol - Generation of a peroxisome proliferator-activated receptor alpha agonist. *J Biol Chem*, 277, 23278-23286.
- KOZAK, K. R., ROWLINSON, S. W. & MARNETT, L. J. 2000. Oxygenation of the endocannabinoid, 2-arachidonylglycerol, to glyceryl prostaglandins by cyclooxygenase-2. *J Biol Chem*, 275, 33744-33749.
- KOZELA, E., PIETR, M., JUKNAT, A., RIMMERMAN, N., LEVY, R. & VOGEL, Z. 2010. Cannabinoids delta(9)-tetrahydrocannabinol and cannabidiol differentially inhibit the lipopolysaccharide-activated NF-kappa B and interferon-beta/STAT proinflammatory pathways in BV-2 microglial cells. *J Biol Chem*, 285, 1616-1626.
- KREFT, M. E., JERMAN, U. D., LASIC, E., HEVIR-KENE, N., RIZNER, T. L., PETERNEL, L. & KRISTAN, K. 2015. The characterization of the human cell line Calu-3 under different culture conditions and its use as an optimized in vitro model to investigate bronchial epithelial function. *Eur J Pharm Sci*, 69, 1-9.
- KUMAR, R. K. & FOSTER, P. S. 2002. Modeling allergic asthma in mice - Pitfalls and opportunities. *Am J Respir Cell Mol Biol*, 27, 267-272.
- KURIHARA, R., TOHYAMA, Y., MATSUSAKA, S., NARUSE, H., KINOSHITA, E., TSUJIOKA, T., KATSUMATA, Y. & YAMAMURA, H. 2006. Effects of peripheral cannabinoid receptor ligands on motility and polarization in neutrophil-like HL60 cells and human neutrophils. *J Biol Chem*, 281, 12908-12918.

- LAITINEN, L. A., HEINO, M., LAITINEN, A., KAVA, T. & HAAHTELA, T. 1985. Damage of the airway epithelium and bronchial reactivity in patients with asthma. *Am Rev Respir Dis*, 131, 599-606.
- LAMBRECHT, B. N. & HAMMAD, H. 2012. The airway epithelium in asthma. *Nat Med*, 18, 684-692.
- LANONE, S., ZHENG, T., ZHU, Z., LIU, W., LEE, C. G., MA, B., CHEN, Q. S., HOMER, R. J., WANG, J. M., RABACH, L. A., RABACH, M. E., SHIPLEY, J. M., SHAPIRO, S. D., SENIOR, R. M. & ELIAS, J. A. 2002. Overlapping and enzyme-specific contributions of matrix metalloproteinases-9 and-12 in IL-13-induced inflammation and remodeling. *J Clin Invest*, 110, 463-474.
- LECKIE, M. J., TEN BRINKE, A., KHAN, J., DIAMANT, Z., O'CONNOR, B. J., WALLS, C. M., MATHUR, A. K., COWLEY, H. C., CHUNG, K. F., DJUKANOVIC, R., HANSEL, T. T., HOLGATE, T., STERK, P. J. & BARNES, P. J. 2000. Effects of an interleukin-5 blocking monoclonal antibody on eosinophils, airway hyper-responsiveness, and the late asthmatic response. *Lancet*, 356, 2144-2148.
- LEVINE, S. J., LARIVÉE, P., LOGUN, C., ANGUS, C. W., OGNIBENE, F. P. & SHELHAMER, J. H. 1995. Tumor-necrosis-factor-alpha induces mucin hypersecretion and MUC-2 gene expression by human airway epithelial cells. *Am J Respir Cell Mol Biol*, 12, 196-204.
- LI, D. X. & MRSNY, R. J. 2000. Oncogenic Raf-1 disrupts epithelial tight junctions via downregulation of occludin. *J Cell Biol*, 148, 791-800.
- LIN, X. H., YUECE, B., LI, Y. Y., FENG, Y. J., FENG, J. Y., YU, L. Y., LI, K., LI, Y. N. & STORR, M. 2011. A novel CB receptor GPR55 and its ligands are involved in regulation of gut movement in rodents. *Neurogastroenterol Motil*, 23, 862-E342.
- LIPSCHUTZ, J. H., LI, S., ARISCO, A. & BALKOVETZ, D. F. 2005. Extracellular signal-regulated kinases 1/2 control claudin-2 expression in Madin-Darby canine kidney strain I and II cells. *J Biol Chem*, 280, 3780-3788.
- LIU, J., WANG, L., HARVEY-WHITE, J., HUANG, B. X., KIM, H.-Y., LUQUET, S., PALMITER, R. D., KRYSTAL, G., RAI, R., MAHADEVAN, A., RAZDAN, R. K. & KUNOS, G. 2008. Multiple pathways involved in the biosynthesis of anandamide. *Neuropharmacology*, 54, 1-7.
- LORENZO, I. M., LIEDTKE, W., SANDERSON, M. J. & VALVERDE, M. A. 2008. TRPV4 channel participates in receptor-operated calcium entry and ciliary beat frequency regulation in mouse airway epithelial cells. *Proc Natl Acad Sci U S A*, 105, 12611-12616.
- LOUIS, R., LAU, L. C. K., BRON, A. O., ROLDAAN, A. C., RADERMECKER, M. & DJUKANOVIC, R. 2000. The relationship between airways inflammation and asthma severity. *Am J Respir Crit Care Med*, 161, 9-16.
- LU, Q., PAREDES, M., ZHANG, J. M. & KOSIK, K. S. 1998. Basal extracellular signal-regulated kinase activity modulates cell-cell and cell-matrix interactions. *Mol Cell Biol*, 18, 3257-3265.
- LU, T. S., AVRAHAM, H. K., SENG, S., TACHADO, S. D., KOZIEL, H., MAKRIYANNIS, A. & AVRAHAM, S. 2008. Cannabinoids Inhibit HIV-1 Gp120-Mediated Insults in Brain Microvascular Endothelial Cells. *J Immunol*, 181, 6406-6416.

- LUKACS, N. W., STRIETER, R. M., CHENSUE, S. W., WIDMER, M. & KUNKEL, S. L. 1995. TNF-alpha mediates recruitment of neutrophils and eosinophils during airway inflammation. *J. Immunol.*, 154, 5411-5417.
- LUMSDEN, A. B., MCLEAN, A. & LAMB, D. 1984. Goblet and Clara cells of human distal airways - evidence for smoking induced changes in their numbers *Thorax*, 39, 844-849.
- LUNN, C. A., FINE, J. S., ROJAS-TRIANA, A., JACKSON, J. V., FAN, X. D., KUNG, T. T., GONSIOREK, W., SCHWARZ, M. A., LAVEY, B., KOZLOWSKI, J. A., NARULA, S. K., LUNDELL, D. J., HIPKIN, R. W. & BOBER, L. A. 2006. A novel cannabinoid peripheral cannabinoid receptor-selective inverse agonist blocks leukocyte recruitment in vivo. *J Pharmacol Exp Ther*, 316, 780-788.
- MA, T. Y., IWAMOTO, G. K., HOA, N. T., AKOTIA, V., PEDRAM, A., BOIVIN, M. A. & SAID, H. M. 2004. TNF-alpha-induced increase in intestinal epithelial tight junction permeability requires NF-kappa B activation. *Am J Physiol Gastrointest Liver Physiol*, 286, G367-G376.
- MACCARRONE, M., VAN DER STELT, M., ROSSI, A., VELDINK, G. A., VLIEGENTHART, J. F. G. & AGRIO, A. F. 1998. Anandamide hydrolysis by human cells in culture and brain. *J Biol Chem*, 273, 32332-32339.
- MAESTRELLI, P., BOSCHETTO, P., FABBRI, L. M. & MAPP, C. E. 2009. Mechanisms of occupational asthma. *J Allergy Clin Immunol*, 123, 531-542.
- MAI, P., TIAN, L., YANG, L., WANG, L., YANG, L. & LI, L. 2015. Cannabinoid receptor 1 but not 2 mediates macrophage phagocytosis by G((alpha)i/o)/RhoA/ROCK signaling pathway. *J Cell Physiol*, 230, 1640-1650.
- MAKWANA, R., VENKATASAMY, R., SPINA, D. & PAGE, C. 2015. The effect of phytocannabinoids on airway hyper-responsiveness, airway inflammation, and cough. *J Pharmacol Exp Ther*, 353, 169-180.
- MALLAT, A., TEIXEIRA-CLERC, F. & LOTERSZTAJN, S. 2013. Cannabinoid signaling and liver therapeutics. *J Hepatol*, 59, 891-896.
- MARINI, P., CASCIO, M.-G., KING, A., PERTWEE, R. G. & ROSS, R. A. 2013. Characterization of cannabinoid receptor ligands in tissues natively expressing cannabinoid CB2 receptors. *Br J Pharmacol*, 169, 887-899.
- MASSA, F., MARSICANO, G., HERMANN, H., CANNICH, A., MONORY, K., CRAVATT, B. F., FERRI, G. L., SIBAEV, A., STORR, M. & LUTZ, B. 2004. The endogenous cannabinoid system protects against colonic inflammation. *J Clin Invest*, 113, 1202-1209.
- MATSUDA, L. A., LOLAIT, S. J., BROWNSTEIN, M. J., YOUNG, A. C. & BONNER, T. I. 1990. Structure of a cannabinoid receptor and functional expression of the cloned cDNA *Nature*, 346, 561-564.
- MATSUSAKA, T., FUJIKAWA, K., NISHIO, Y., MUKAIDA, N., MATSUSHIMA, K., KISHIMOTO, T. & AKIRA, S. 1993. Transcription factors NF-IL6 and NF-Kappa-B synergistically activate transcription of the inflammatory cytokines, interleukin-6 and interleukin-8 *Proc Natl Acad Sci U S A*, 90, 10193-10197.
- MATTER, K. & BALDA, M. S. 2003. Signalling to and from tight junctions. *Nature Rev Mol Cell Biol*, 4, 225-236.
- MATTER, K. & BALDA, M. S. 2014. SnapShot: Epithelial Tight Junctions. *Cell*, 157.

- MATTOLI, S., MATTOSO, V. L., SOLOPERTO, M., ALLEGRA, L. & FASOLI, A. 1991. Cellular and biochemical characteristics of bronchoalveolar lavage fluid in symptomatic nonallergic asthma *J Allergy Clin Immunol*, 87, 794-802.
- MCGARVEY, L. P., BUTLER, C. A., STOKESBERRY, S., POLLEY, L., MCQUAID, S., ABDULLAH, H., ASHRAF, S., MCGAHON, M. K., CURTIS, T. M., ARRON, J., CHOY, D., WARKE, T. J., BRADDING, P., ENNIS, M., ZHOLOS, A., COSTELLO, R. W. & HEANEY, L. G. 2014. Increased expression of bronchial epithelial transient receptor potential vanilloid 1 channels in patients with severe asthma. *J Allergy Clin Immunol*, 133, 704-+.
- MCKAY, K. O. & HOGG, J. C. 2002. The contribution of airway structure to early childhood asthma. *Med J Aust*, 177, S45-S47.
- MCKEMY, D. D., NEUHAUSSER, W. M. & JULIUS, D. 2002. Identification of a cold receptor reveals a general role for TRP channels in thermosensation. *Nature*, 416, 52-58.
- MCKENZIE, J. A. G. & RIDLEY, A. J. 2007. Roles of Rho/ROCK and MLCK in TNF-alpha-induced changes in endothelial morphology and permeability. *J Cell Physiol*, 213, 221-228.
- MECHOULAM, R., BENSHABAT, S., HANUS, L., LIGUMSKY, M., KAMINSKI, N. E., SCHATZ, A. R., GOPHER, A., ALMOG, S., MARTIN, B. R., COMPTON, D. R., PERTWEE, R. G., GRIFFIN, G., BAYEWITCH, M., BARG, J. & VOGEL, Z. 1995. Identification of an endogenous 2-monoglyceride, present in canine gut, that binds to cannabinoid receptors. *Biochem Pharmacol*, 50, 83-90.
- MECHOULAM, R., HANUS, L. O., PERTWEE, R. & HOWLETT, A. C. 2014. Early phytocannabinoid chemistry to endocannabinoids and beyond. *Nature Reviews Neuroscience*, 15, 757-764.
- MECHOULAM, R. & SHVO, Y. 1963. Hashish. 1. Structure of cannabidiol *Tetrahedron*, 19, 2073-&.
- MERCK MILLIPORE, U. 2015. Rho-associated Kinase (ROCK) Activity Assay. Merck Millipore, UK.
- MICKLEBOROUGH, T. D., LINDLEY, M. R. & RAY, S. 2005. Dietary salt, airway inflammation, and diffusion capacity in exercise-induced asthma. *Med Sci Sports Exerc*, 37, 904-914.
- MIKURIYA, T. H. 1969. Marijuana in medicine - Past present and future *Calif Med*, 110, 34-40.
- MINSHALL, E. M., LEUNG, D. Y. M., MARTIN, R. J., SONG, Y. L., CAMERON, L., ERNST, P. & HAMID, Q. 1997. Eosinophil-associated TGF-beta(1) mRNA expression and airways fibrosis in bronchial asthma. *Am J Respir Cell Mol Biol*, 17, 326-333.
- MIRANDA, L., CARPENTIER, S., PLATEK, A., HUSSAIN, N., GUEUNING, M.-A., VERTOMMEN, D., OZKAN, Y., SID, B., HUE, L., COURTOY, P. J., RIDER, M. H. & HORMAN, S. 2010. AMP-activated protein kinase induces actin cytoskeleton reorganization in epithelial cells. *Biochem Biophys Res Commun*, 396, 656-661.
- MITCHELL, J. A. & WARNER, T. D. 1999. Cyclo-oxygenase-2: pharmacology, physiology, biochemistry and relevance to NSAID therapy. *Br J Pharmacol*, 128, 1121-1132.

- MOLLER, G. M., OVERBEEK, S. E., VANHELDENMEEUWSEN, C. G., VANHAARST, J. M. W., PRENS, E. P., MULDER, P. G., POSTMA, D. S. & HOOGSTEDEN, H. C. 1996. Increased numbers of dendritic cells in the bronchial mucosa of atopic asthmatic patients: Downregulation by inhaled corticosteroids. *Clin Exp Allergy*, 26, 517-524.
- MONFORTE-MUNOZ, H. & WALLS, R. L. 2004. Intrapulmonary airways visualized by staining and clearing of whole-lung sections: the transparent human lung. *Mod Pathol*, 17, 22-27.
- MONTEFORT, S., ROCHE, W. R. & HOLGATE, S. T. 1993. Bronchial epithelial shedding in asthmatics and non-asthmatics. *Respir Med*, 87, 9-11.
- MONTERO, C., CAMPILLO, N. E., GOYA, P. & PAEZ, J. A. 2005. Homology models of the cannabinoid CB1 and CB2 receptors. A docking analysis study. *Eu J Med Chem*, 40, 75-83.
- MORRISON, D., RAHMAN, I., LANNAN, S. & MACNEE, W. 1999. Epithelial permeability, inflammation, and oxidant stress in the air spaces of smokers. *Am J Respir Crit Care Med*, 159, 473-479.
- MOVAHED, P., JONSSON, B. A. G., BIRNIR, B., WINGSTRAND, J. A., JORGENSEN, T. D., ERMUND, A., STERNER, O., ZYGMUNT, P. M. & HOGESTATT, E. D. 2005. Endogenous unsaturated C18N-acylethanolamines are vanilloid receptor (TRPV1) agonists. *J Biol Chem*, 280, 38496-38504.
- MUCCIOLI, G. G., NASLAIN, D., BACKHED, F., REIGSTAD, C. S., LAMBERT, D. M., DELZENNE, N. M. & CANI, P. D. 2010. The endocannabinoid system links gut microbiota to adipogenesis. *Molecular Systems Biology*, 6.
- MULLIN, J. M., LAUGHLIN, K. V., MARANO, C. W., RUSSO, L. M. & SOLER, A. P. 1992. Modulation of tumor-necrosis factor -induced increased in renal (LLC-PK1) transepithelial permeability. *Am J Physiol*, 263, F915-F924.
- MUNRO, S., THOMAS, K. L. & ABUSHAAR, M. 1993. Molecular characterization of a peripheral receptor for cannabinoids *Nature*, 365, 61-65.
- NADEL, J. A. 2000. Role of neutrophil elastase in hypersecretion during COPD exacerbations, and proposed therapies. *Chest*, 117, 386S-389S.
- NANDAKARNI, A. K. 1976. India Materia Medica with Ayurvedic, Unani-Tibbi, Siddha, Allopathic, Homeopathic, Naturopathic and Home Remedies, Appendices and Indexes. 3rd ed.: Bombay Popular Prakashan Pvt. Ltd.
- NAVA, P., LOPEZ, S., ARIAS, C. F., ISLAS, S. & GONZALEZ-MARISCAL, L. 2004. The rotavirus surface protein VP8 modulates the gate and fence function of tight junctions in epithelial cells. *J Cell Sci*, 117, 5509-5519.
- NEWTON, R., HOLDEN, N. S., CATLEY, M. C., OYELUSI, W., LEIGH, R., PROUD, D. & BARNES, P. J. 2007. Repression of inflammatory gene expression in human pulmonary epithelial cells by small-molecule I kappa B kinase inhibitors. *J Pharmacol Exp Ther*, 321, 734-742.
- NITHIPATIKOM, K., GOMEZ-GRANADOS, A. D., TANG, A. T., PFEIFFER, A. W., WILLIAMS, C. L. & CAMPBELL, W. B. 2012. Cannabinoid receptor type 1 (CB1) activation inhibits small GTPase RhoA activity and regulates motility of prostate carcinoma cells. *Endocrinology*, 153, 29-41.
- NOMURA, D. K., HUDAK, C. S. S., WARD, A. M., BURSTON, J. J., ISSA, R. S., FISHER, K. J., ABOOD, M. E., WILEY, J. L., LICHTMAN, A. H. & CASIDA, J. E. 2008. Monoacylglycerol lipase regulates 2-arachidonoylglycerol action and arachidonic acid levels. *Bioorg Med Chem Lett*, 18, 5875-5878.

- NUIJSINK, M., HOP, W. C. J., STERK, P. J., DUIVERMAN, E. J., DE JORGSTE, J. C. & GRP, C. S. 2007. Long-term asthma treatment guided by airway hyperresponsiveness in children: a randomised controlled trial. *Eur Respir J*, 30, 457-466.
- NUSRAT, A., GIRY, M., TURNER, J. R., COLGAN, S. P., PARKOS, C. A., CARNES, D., LEMICHEZ, E., BOQUET, P. & MADARA, J. L. 1995. Rho-protein regulates tight junctions and perijunctional actin organisation in polarised epithelia *Proc Natl Acad Sci U S A*, 92, 10629-10633.
- NUSRAT, A., VON EICHEL-STREIBER, C., TURNER, J. R., VERKADE, P., MADARA, J. L. & PARKOS, C. A. 2001. Clostridium difficile toxins disrupt epithelial barrier function by altering membrane microdomain localization of tight junction proteins. *Infect Immun*, 69, 1329-1336.
- O'BRIEN, J. & POGNAN, F. 2001. Investigation of the Alamar blue (Resazurin) fluorescent dye for the assessment of mammalian cell cytotoxicity. *Toxicology*, 164, 132-132.
- O'SULLIVAN, S. E., KENDALL, D. A. & RANDALL, M. D. 2006. Further characterization of the time-dependent vascular effects of Delta(9)-tetrahydrocannabinol. *J Pharmacol Exp Ther*, 317, 428-438.
- OKA, S., IKEDA, S., KISHIMOTO, S., GOKOH, M., YANAGIMOTO, S., WAKU, K. & SUGIURA, T. 2004. 2-Arachidonoylglycerol, an endogenous cannabinoid receptor ligand, induces the migration of EoL-1 human eosinophilic leukemia cells and human peripheral blood eosinophils. *Journal of Leukocyte Biolog*, 76, 1002-1009.
- OKINE, B. N., NORRIS, L. M., WOODHAMS, S., BURSTON, J., PATEL, A., ALEXANDER, S. P. H., BARRETT, D. A., KENDALL, D. A., BENNETT, A. J. & CHAPMAN, V. 2012. Lack of effect of chronic pre-treatment with the FAAH inhibitor URB597 on inflammatory pain behaviour: evidence for plastic changes in the endocannabinoid system. *Br J Pharmacol*, 167, 627-640.
- OLSON, N., GREUL, A. K., HRISTOVA, M., BOVE, P. F., KASAHARA, D. I. & VAN DER VLIET, A. 2009. Nitric oxide and airway epithelial barrier function: Regulation of tight junction proteins and epithelial permeability. *Arch Biochem Biophys*, 484, 205-213.
- ORDONEZ, C. L., KHASHAYAR, R., WONG, H. H., FERRANDO, R., WU, R., HYDE, D. M., HOTCHKISS, J. A., ZHANG, Y., NOVIKOV, A., DOLGANOV, G. & FAHY, J. V. 2001. Mild and moderate asthma is associated with airway goblet cell hyperplasia and abnormalities in mucin gene expression. *Am J Respir Crit Care Med*, 163, 517-523.
- OSHIMA, T., MIWA, H. & JOH, T. 2008. Aspirin induces gastric epithelial barrier dysfunction by activating p38 MAPK via claudin-7. *Am J Physiol Cell Physiol*, 295, C800-C806.
- PACHER, P. & KUNOS, G. 2013. Modulating the endocannabinoid system in human health and disease successes and failures. *Febs Journal*, 280, 1918-1943.
- PATEL, K. D., DAVISON, J. S., PITTMAN, Q. J. & SHARKEY, K. A. 2010. Cannabinoid CB2 Receptors in Health and Disease. *Curr Med Chem*, 17, 1394-1410.
- PAVORD, I. D., KORN, S., HOWARTH, P., BLEECKER, E. R., BUHL, R., KEENE, O. N., ORTEGA, H. & CHANEZ, P. 2012. Mepolizumab for severe

- eosinophilic asthma (DREAM): a multicentre, double-blind, placebo-controlled trial. *Lancet*, 380, 651-659.
- PEAKE, J. L., REYNOLDS, S. D., STRIPP, B. R., STEPHENS, K. E. & PINKERTON, K. E. 2000. Alteration of pulmonary neuroendocrine cells during epithelial repair of naphthalene-induced airway injury. *Am J Pathol*, 156, 279-286.
- PEPE, C., FOLEY, S., SHANNON, J., LEMIERE, C., OLIVENSTEIN, R., ERNST, P., LUDWIG, M. S., MARTIN, J. G. & HAMID, Q. 2005. Differences in airway remodeling between subjects with severe and moderate asthma. *J Allergy Clin Immunol*, 116, 544-549.
- PERTWEE, R. 2010. Cannabinoid Receptor Ligands. *Tocris Bioscience Scientific Review Series* [Online]. Available: [http://www.tocris.com/pdfs/pdf_downloads/Cannabinoid Receptor Ligands Review.pdf](http://www.tocris.com/pdfs/pdf_downloads/Cannabinoid_Receptor_Ligands_Review.pdf) [Accessed 25.02.2015].
- PERTWEE, R. G. 2005. The therapeutic potential of drugs that target cannabinoid receptors or modulate the tissue levels or actions of endocannabinoids. *Aaps Journal*, 7, E625-E654.
- PERTWEE, R. G. 2006. The pharmacology of cannabinoid receptors and their ligands: an overview. *Int J Obes*, 30, S13-S18.
- PERTWEE, R. G. 2008. The diverse CB1 and CB2 receptor pharmacology of three plant cannabinoids: Delta(9)-tetrahydrocannabinol, cannabidiol and Delta(9)-tetrahydrocannabivarin. *Br J Pharmacol*, 153, 199-215.
- PERTWEE, R. G., HOWLETT, A. C., ABOOD, M. E., ALEXANDER, S. P. H., DI MARZO, V., ELPHICK, M. R., GREASLEY, P. J., HANSEN, H. S., KUNOS, G., MACKIE, K., MECHOULAM, R. & ROSS, R. A. 2010. International Union of Basic and Clinical Pharmacology. LXXIX. Cannabinoid receptors and their ligands: Beyond CB1 and CB2. *Pharmacol Rev*, 62, 588-631.
- PETECCHIA, L., SABATINI, F., USAI, C., CACI, E., VAREGIO, L. & ROSSI, G. A. 2012. Cytokines induce tight junction disassembly in airway cells via an EGFR-dependent MAPK/ERK1/2-pathway. *Lab Invest*, 92, 1140-1148.
- PETECCHIA, L., SABATINI, F., VAREGIO, L., CAMOIRANO, A., USAI, C., PEZZOLO, A. & ROSSI, G. A. 2009. Bronchial airway epithelial cell damage following exposure to cigarette smoke includes disassembly of tight junction components mediated by the Extracellular Signal-Regulated Kinase 1/2 pathway. *Chest*, 135, 1502-1512.
- PETECCHIA, L., USAI, C., SABATINI, F., VAREGIO, L., DE FLORA, S. & ROSSI, G. A. 2008. Map kinase interacts with tight junction (TJ) disruption in a human bronchial epithelial cell line (Beas-2B) by cigarette smoke (CS) exposure. *Cytometry Part A*, 73A, 100-101.
- PINI, A., MANNAIONI, G., PELLEGRINI-GIAMPIETRO, D., PASSANI, M. B., MASTROIANNI, R., BANI, D. & MASINI, E. 2012. The role of cannabinoids in inflammatory modulation of allergic respiratory disorders, inflammatory pain and ischemic stroke. *Current Drug Targets*, 13, 984-993.
- PIOMELLI, D., TARZIA, G., DURANTI, A., TONTINI, A., MOR, M., COMPTON, T. R., DASSE, O., MONAGHAN, E. P., PARROTT, J. A. & PUTMAN, D. 2006. Pharmacological profile of the selective FAAH inhibitor KDS-4103 (URB597). *Cns Drug Reviews*, 12, 21-38.

- PLOPPER, C. G., HILL, L. H. & MARIASSY, A. T. 1980. Ultrastructure of the non-ciliated bronchiolar epithelial (Clara) cell of mammalian lung. 3. A study of man with comparison of 15 mammalian-species *Exp Lung Res*, 1, 171-180.
- QUIROS, M. & NUSRAT, A. 2014. RhoGTPases, actomyosin signaling and regulation of the Epithelial Apical Junctional Complex. *Semin Cell Dev Biol*, 36, 194-203.
- RAHMAN, I., MORRISON, D., DONALDSON, K. & MACNEE, W. 1996. Systemic oxidative stress in asthma, COPD, and smokers. *Am J Respir Crit Care Med*, 154, 1055-1060.
- RAJESH, M., MUKHOPADHYAY, P., BATKAI, S., HASKO, G., LIAUDET, L., DREL, V. R., OBROSOVA, I. G. & PACHER, P. 2007a. Cannabidiol attenuates high glucose-induced endothelial cell inflammatory response and barrier disruption. *Am J Physiol Heart Circ Physiol*, 293, H610-H619.
- RAJESH, M., MUKHOPADHYAY, P., BATKAI, S., HASKO, G., LIAUDET, L., HUFFMAN, J. W., CSISZAR, A., UNGVARI, Z., MACKIE, K., CHATTERJEE, S. & PACHER, P. 2007b. CB2-receptor stimulation attenuates TNF-alpha-induced human endothelial cell activation, transendothelial migration of monocytes, and monocyte-endothelial adhesion. *Am J Physiol Heart Circ Physiol*, 293, H2210-H2218.
- RAJESH, M., MUKHOPADHYAY, P., HASKO, G., HUFFMAN, J. W., MACKIE, K. & PACHER, P. 2008. CB2 cannabinoid receptor agonists attenuate TNF-alpha-induced human vascular smooth muscle cell proliferation and migration. *Br J Pharmacol*, 153, 347-357.
- RAMADAS, R. A., LI, X., SHUBITOWSKI, D. M., SAMINENI, S., WILLS-KARP, M. & EWART, S. L. 2006. IL-1 receptor antagonist as a positional candidate gene in a murine model of allergic asthma. *Immunogenetics*, 58, 851-855.
- RAMAN, M., CHEN, W. & COBB, M. H. 2007. Differential regulation and properties of MAPKs. *Oncogene*, 26, 3100-3112.
- RAMSEY, I. S., DELLING, M. & CLAPHAM, D. E. 2006. An introduction to TRP channels. *Annu Rev Physiol*, 68, 619-647.
- RANDALL, M. D., KENDALL, D. A. & O'SULLIVAN, S. 2004. The complexities of the cardiovascular actions of cannabinoids. *Br J Pharmacol*, 142, 20-26.
- RANGE, S. P., PANG, L., HOLLAND, E. & KNOX, A. J. 2000. Selectivity of cyclo-oxygenase inhibitors in human pulmonary epithelial and smooth muscle cells. *Eur Respir J*, 15, 751-756.
- REYNOLDS, S. D., GIANGRECO, A., POWER, J. H. T. & STRIPP, B. R. 2000. Neuroepithelial bodies of pulmonary airways serve as a reservoir of progenitor cells capable of epithelial regeneration. *Am J Pathol*, 156, 269-278.
- RIBEIRO, R., WEN, J., LI, S. & ZHANG, Y. 2013. Involvement of ERK1/2, cPLA(2) and NF-kappa B in microglia suppression by cannabinoid receptor agonists and antagonists. *Prostaglandins Other Lipid Mediat*, 100, 1-14.
- RICHARDSON, D., PEARSON, R. G., KURIAN, N., LATIF, M. L., GARLE, M. J., BARRETT, D. A., KENDALL, D. A., SCAMMELL, B. E., REEVE, A. J. & CHAPMAN, V. 2008. Characterisation of the cannabinoid receptor system in synovial tissue and fluid in patients with osteoarthritis and rheumatoid arthritis. *Arthritis Research & Therapy*, 10.
- RINALDI-CARMONA, M., BARTH, F., MILLAN, J., DEROCQ, J., CASELLAS, P., CONGY, C., OUSTRIC, D., SARRAN, M., BOUABOULA, M.,

- CALANDRA, B., MARIELLE, P., SHIRE, D., BRELIERE, J. & LE FUR, G. 1998. SR144528, the first potent and selective antagonist of the CB2 cannabinoid receptor. *The Journal of Pharmacology*, 284, 644-650.
- RINCON-HEREDIA, R., FLORES-BENITEZ, D., FLORES-MALDONADO, C., BONILLA-DELGADO, J., GARCIA-HERNANDEZ, V., VERDEJO-TORRES, O., CASTILLO, A. M., LARRE, I., POOT-HERNANDEZ, A. C., FRANCO, M., GARIGLIO, P., REYES, J. L. & CONTRERAS, R. G. 2014. Ouabain induces endocytosis and degradation of tight junction proteins through ERK1/2-dependent pathways. *Exp Cell Res*, 320, 108-118.
- ROCK, J. R., ONAITIS, M. W., RAWLINS, E. L., LU, Y., CLARK, C. P., XUE, Y., RANDELL, S. H. & HOGAN, B. L. M. 2009. Basal cells as stem cells of the mouse trachea and human airway epithelium. *Proc Natl Acad Sci U S A*, 106, 12771-12775.
- ROGERS, D. F. 2004. Airway mucus hypersecretion in asthma: an undervalued pathology? *Curr Opin Pharmacol*, 4, 241-250.
- ROM, S. & PERSIDSKY, Y. 2013. Cannabinoid Receptor 2: Potential Role in Immunomodulation and Neuroinflammation. *Journal of Neuroimmune Pharmacology*, 8, 608-620.
- ROSENWASSER, L. J. 1998. Biologic activities of IL-1 and its role in human disease. *J Allergy Clin Immunol*, 102, 344-350.
- ROTH, H. M., WADSWORTH, S. J., KAHN, M. & KNIGHT, D. A. 2012. The airway epithelium in asthma: Developmental issues that scar the airways for life? *Pulm Pharmacol Ther*, 25, 420-426.
- ROUHANI, F. N., MEITIN, C. A., KALER, M., MISKINIS-HILLIGOSS, D., STYLIANOU, M. & LEVINE, S. J. 2005. Effect of tumor necrosis factor antagonism on allergen-mediated asthmatic airway inflammation. *Respir Med*, 99, 1175-1182.
- RUPAREL, N. B., PATWARDHAN, A. M., AKOPIAN, A. N. & HARGREAVES, K. M. 2011. Desensitization of Transient Receptor Potential Ankyrin 1 (TRPA1) by the TRP Vanilloid 1-selective cannabinoid arachidonoyl-2-chloroethanolamine. *Mol Pharmacol*, 80, 117-123.
- RUTGERS, S. R., TIMENS, W., KAUFMANN, H. F., VAN DER MARK, T. W., KOETER, G. H. & POSTMA, D. S. 2000. Comparison of induced sputum with bronchial wash, bronchoalveolar lavage and bronchial biopsies in COPD. *Eur Respir J*, 15, 109-115.
- RYAN, A., SMITH, A., MOORE, P., MCNALLY, S., CARRINGTON, S. D., REID, C. J. & CLYNE, M. 2015. Expression and Characterization of a Novel Recombinant Version of the Secreted Human Mucin MUC5AC in Airway Cell Lines. *Biochemistry (Mosc)*, 54, 1089-1099.
- RYBERG, E., LARSSON, N., SJOGREN, S., HJORTH, S., HERMANSSON, N. O., LEONOVA, J., ELEBRING, T., NILSSON, K., DRMOTA, T. & GEASLEY, P. J. 2007. The orphan receptor GPR55 is a novel cannabinoid receptor. *Br J Pharmacol*, 152, 1092-1101.
- SAATIAN, B., REZAEI, F., DESANDO, S., EMO, J., CHAPMAN, T., KNOWLDEN, S. & GEORAS, S. N. 2013. Interleukin-4 and interleukin-13 cause barrier dysfunction in human airway epithelial cells. *Tissue barriers*, 1, e24333-e24333.
- SAETTA, M., TURATO, G., BARALDO, S., ZANIN, A., BRACCIONI, F., MAPP, C. E., MAESTRELLI, P., CAVALLESCO, G., PAPI, A. & FABBRI, L. M. 2000. Goblet cell hyperplasia and epithelial inflammation in peripheral

- airways of smokers with both symptoms of chronic bronchitis and chronic airflow limitation. *Am J Respir Crit Care Med*, 161, 1016-1021.
- SAHA, S., DOE, C., MISTRY, V., SIDDIQUI, S., PARKER, D., SLEEMAN, M., COHEN, E. S. & BRIGHTLING, C. E. 2009. Granulocyte-macrophage colony-stimulating factor expression in induced sputum and bronchial mucosa in asthma and COPD. *Thorax*, 64, 671-676.
- SAMARIN, S. N., IVANOV, A. I., FLATAU, G., PARKOS, C. A. & NUSRAT, A. 2007. Rho/Rho-associated kinase-II signaling mediates disassembly of epithelial apical junctions. *Mol Biol Cell*, 18, 3429-3439.
- SAMSON, M. T., SMALL-HOWARD, A., SHIMODA, L. M. N., KOBLAN-HUBERSON, M., STOKES, A. J. & TURNER, H. 2003. Differential roles of CB1 and CB2 cannabinoid receptors in mast cells. *J Immunol*, 170, 4953-4962.
- SAPEY, E., BAYLEY, D., AHMAD, A., NEWBOLD, P., SNELL, N. & STOCKLEY, R. A. 2008. Inter-relationships between inflammatory markers in patients with stable COPD with bronchitis: intra-patient and inter-patient variability. *Thorax*, 63, 493-503.
- SCADDING, J. G. 1983. *Definition and clinical categories of asthma* London, Chapman and Hall.
- SCHAMBERGER, A. C., STAAB-WEIJNITZ, C. A., MISE-RACEK, N. & EICKELBERG, O. 2015. Cigarette smoke alters primary human bronchial epithelial cell differentiation at the air-liquid interface. *Scientific Reports*, 5.
- SCHMITZ, H., FROMM, M., BENTZEL, C. J., SCHOLZ, P., DETJEN, K., MANKERTZ, J., BODE, H., EPPLE, H. J., RIECKEN, E. O. & SCHULZKE, J. D. 1999. Tumor necrosis factor-alpha (TNF alpha) regulates the epithelial barrier in the human intestinal cell line HT-29/B6. *J Cell Sci*, 112, 137-146.
- SCHWARTZ, M. A. & SHATTIL, S. J. 2000. Signaling networks linking integrins and Rho family GTPases. *Trends Biochem Sci*, 25, 388-391.
- SEAGRAVE, J., DUNAWAY, S., MCDONALD, J. D., MAUDERLY, J. L., HAYDEN, P. & STIDLEY, C. 2007. Responses of differentiated primary human lung epithelial cells to exposure to diesel exhaust at an air-liquid interface. *Exp Lung Res*, 33, 27-51.
- SHANKARANARAYANAN, P. & NIGAM, S. 2003. IL-4 induces apoptosis in A549 lung adenocarcinoma cells: Evidence for the pivotal role of 15-hydroxyeicosatetraenoic acid binding to activated peroxisome proliferator-activated receptor gamma transcription factor. *J Immunol*, 170, 887-894.
- SHAO, M. X. G., NAKANAGA, T. & NADEL, J. A. 2004. Cigarette smoke induces MUC5AC mucin overproduction via tumor necrosis factor-alpha-converting enzyme in human airway epithelial (NCI-H292) cells. *Am J Physiol Lung Cell Mol Physiol*, 287, L420-L427.
- SHARIR, H. & ABOOD, M. E. 2010. Pharmacological characterization of GPR55, a putative cannabinoid receptor. *Pharmacol Ther*, 126, 301-313.
- SHEEHAN, J. K., KIRKHAM, S., HOWARD, M., WOODMAN, P., KUTAY, S., BRAZEAU, C., BUCKLEY, J. & THORNTON, D. J. 2004. Identification of molecular intermediates in the assembly pathway of the MUC5AC mucin. *J Biol Chem*, 279, 15698-15705.
- SHEN, L. 2012. Tight junctions on the move: molecular mechanisms for epithelial barrier regulation. In: FROMM, M. & SCHULZKE, J. D. (eds.) *Barriers and Channels Formed by Tight Junction Proteins II*.

- SIDHAYE, V. K., SCHWEITZER, K. S., CATERINA, M. J., SHIMODA, L. & KING, L. S. 2008. Shear stress regulates apuaporin-5 and airway epithelial barrier function. *Proc Natl Acad Sci U S A*, 105, 3345-3350.
- SIEGMUND, S. V., SEKI, E., OSAWA, Y., UCHINAMI, H., CRAVATT, B. F. & SCHWABE, R. F. 2006. Fatty acid amide hydrolase determines anandamide-induced cell death in the liver. *J Biol Chem*, 281, 10431-10438.
- SIEHLER, S. 2009. Regulation of RhoGEF proteins by G12/13-coupled receptors. *Br J Pharmacol*, 158, 41-49.
- SIMET, S. M., WYATT, T. A., DEVASURE, J., YANOV, D., ALLEN-GIPSON, D. & SISSON, J. H. 2012. Alcohol Increases the Permeability of Airway Epithelial Tight Junctions in Beas-2B and NHBE Cells. *Alcoholism-Clinical and Experimental Research*, 36, 432-442.
- SINGH, D., KOLSUM, U., BRIGHTLING, C. E., LOCANTORE, N., AGUSTI, A., TAL-SINGER, R. & INVESTIGATORS, E. 2014. Eosinophilic inflammation in COPD: prevalence and clinical characteristics. *Eur Respir J*, 44, 1697-1700.
- SONT, J. K., WILLEMS, L. N. A., BEL, E. H., VAN KRIEKEN, J., VANDENBROUCKE, J. P., STERK, P. J. & GRP, A. S. 1999. Clinical control and histopathologic outcome of asthma when using airway hyperresponsiveness as an additional guide to long-term treatment. *Am J Respir Crit Care Med*, 159, 1043-1051.
- SOONG, G., MARTIN, F. J., CHUN, J., COHEN, T. S., AHN, D. S. & PRINCE, A. 2011. Staphylococcus aureus Protein A mediates invasion across airway epithelial cells through activation of RhoA GTPase signaling and proteolytic activity. *J Biol Chem*, 286, 35891-35898.
- SOUSA, A. R., LANE, S. J., NAKHOSTEEN, J. A., LEE, T. H. & POSTON, R. N. 1996. Expression of interleukin-1 beta (IL-1 beta) and interleukin-1 receptor antagonist (IL-1ra) on asthmatic bronchial epithelium. *Am J Respir Crit Care Med*, 154, 1061-1066.
- SPINA, D. 1998. Epithelium smooth muscle regulation and interactions. *Am J Respir Crit Care Med*, 158, S141-S145.
- STEED, E., ELBEDIWY, A., VACCA, B., DUPASQUIER, S., HEMKEMEYER, S. A., SUDDASON, T., COSTA, A. C., BEAUDRY, J.-B., ZIHNI, C., GALLAGHER, E., PIERREUX, C. E., BALDA, M. S. & MATTER, K. 2014. MarvelD3 couples tight junctions to the MEKK1-JNK pathway to regulate cell behavior and survival. *J Cell Biol*, 204, 821-838.
- STEFFENS, M., ZENTNER, J., HONEGGER, J. & FEUERSTEIN, T. J. 2005. Binding affinity and agonist activity of putative endogenous cannabinoids at the human neocortical CB1 receptor. *Biochem Pharmacol*, 69, 169-178.
- STELLA, N. & PIOMELLI, D. 2001. Receptor-dependent formation of endogenous cannabinoids in cortical neurons. *Eur J Pharmacol*, 425, 189-196.
- STENGEL, P. W., COCKERHAM, S. L. & SILBAUGH, S. A. 2007. Inhaled anandamide reduces leukotriene D-4-induced airway obstruction in guinea pigs. *Eur J Pharmacol*, 557, 66-68.
- STEVENSON, D. D. & SZCZEKLIK, A. 2006. Clinical and pathologic perspectives on aspirin sensitivity and asthma. *J Allergy Clin Immunol*, 118, 773-786.
- STEWART, C. E., TORR, E. E., MOHD JAMILI, N. H., BOSQUILLON, C. & I, S. 2011. Evaluation of differentiated human bronchial epithelial cell culture systems for asthma research *J Allergy*, 2012, 1-11.

- STONE, K. D., PRUSSIN, C. & METCALFE, D. D. 2010. IgE, mast cells, basophils, and eosinophils. *J Allergy Clin Immunol*, 125, S73-S80.
- STUART, R. O., SUN, A., PANICHAS, M., HEBERT, S. C., BRENNER, B. M. & NIGAM, S. K. 1994. Critical role for intracellular calcium in tight junction biogenesis *J Cell Physiol*, 159, 423-433.
- SUAREZ, J., JAVIER BERMUDEZ-SILVA, F., MACKIE, K., LEDENT, C., ZIMMER, A., CRAVATT, B. F. & RODRIGUEZ DE FONSECA, F. 2008. Immunohistochemical description of the endogenous cannabinoid system in the rat cerebellum and functionally related nuclei. *J Comp Neurol*, 509, 400-421.
- SUGIHARA, K., ASANO, S., TANAKA, K., IWAMATSU, A., OKAWA, K. & OHTA, Y. 2002. The exocyst complex binds the small GTPase RAL1A to mediate filopodia formation. *Nat. Cell Biol.*, 4, 73-78.
- SUGIURA, T. 2007. 2-Arachidonoylglycerol: an endogenous cannabinoid receptor ligand. *Seikagaku*, 79, 655-668.
- SUN, G., STACEY, M. A., VITTORI, E., MARINI, M., BELLINI, A., KLEIMBERG, J. & MATTOLI, S. 1998. Cellular and molecular characteristics of inflammation in chronic bronchitis. *Eur J Clin Invest*, 28, 364-372.
- SUN, Y., WU, F., SUN, F. & HUANG, P. 2008. Adenosine promotes IL-6 release in airway epithelia. *J Immunol*, 180, 4173-4181.
- SZCZEKLIK, A. & STEVENSON, D. D. 2003. Aspirin-induced asthma: Advances in pathogenesis, diagnosis, and management. *J Allergy Clin Immunol*, 111, 913-921.
- SZCZUKA, A., WENNERBERG, M., PACKEU, A. & VAUQUELIN, G. 2009. Molecular mechanisms for the persistent bronchodilatory effect of the beta(2)-adrenoceptor agonist salmeterol. *Br J Pharmacol*, 158, 183-194.
- TAKAISHI, K., SASAKI, T., KOTANI, H., NISHIOKA, H. & TAKAI, Y. 1997. Regulation of cell-cell adhesion by Rac and Rho small G proteins in MDCK cells. *J Cell Biol*, 139, 1047-1059.
- TARRAN, R., BUTTON, B., PICHER, M., PARADISO, A. M., RIBEIRO, C. M., LAZAROWSKI, E. R., ZHANG, L. Q., COLLINS, P. L., PICKLES, R. J., FREDBERG, J. J. & BOUCHER, R. C. 2005. Normal and cystic fibrosis airway surface liquid homeostasis - The effects of phasic shear stress and viral infections. *J Biol Chem*, 280, 35751-35759.
- TASHKIN, D. P. 2013. Effects of marijuana smoking on the lung. *Annals of the American Thoracic Society*, 10, 239-47.
- TASHKIN, D. P., BALDWIN, G. C., SARAFIAN, T., DUBINETT, S. & ROTH, M. D. 2002. Respiratory and immunologic consequences of marijuana smoking. *J Clin Pharmacol*, 42, 71S-81S.
- TASHKIN, D. P., REISS, S., SHAPIRO, B. J., CALVARESE, B., OLSEN, J. L. & LODGE, J. W. 1977. Bronchial effects of aerosolized delta-9-tetrahydrocannabinol in healthy and asthmatic subjects *Am Rev Respir Dis*, 115, 57-65.
- TASHKIN, D. P., SHAPIRO, B. J. & FRANK, I. M. 1974. Acute effects of smoked Marijuana and oral delta9-tetrahydrocannabinol on specific airway conductance in asthmatic subjects *Am Rev Respir Dis*, 109, 420-428.
- TASKAPAN, O., KUTLU, A. & KARABUDAK, O. 2008. Evaluation of autologous serum skin test results in patients with chronic idiopathic urticaria,

- allergic/non-allergic asthma or rhinitis and healthy people. *Clin Exp Dermatol*, 33, 754-758.
- TAYLOR, D. R., DRAZEN, J. M., HERBISON, G. P., YANDAVA, C. N., HANCOX, R. J. & TOWN, G. I. 2000. Asthma exacerbations during long term beta agonist use: influence of beta(2) adrenoceptor polymorphism. *Thorax*, 55, 762-767.
- TAYLOR, L., CHRISTOU, I., KAPELLOS, T. S., BUCHAN, A., BRODERMANN, M. H., GIANELLA-BORRADORI, M., RUSSELL, A., IQBAL, A. J. & GREAVES, D. R. 2015. Primary Macrophage Chemotaxis Induced by Cannabinoid Receptor 2 Agonists Occurs Independently of the CB2 Receptor. *Scientific Reports*, 5.
- TEMELKOVSKI, J., HOGAN, S. P., SHEPHERD, D. P., FOSTER, P. S. & KUMAR, R. K. 1998. An improved murine model of asthma: selective airway inflammation, epithelial lesions and increased methacholine responsiveness following chronic exposure to aerosolised allergen. *Thorax*, 53, 849-856.
- TERRY, S., NIE, M., MATTER, K. & BALDA, M. S. 2010. Rho signaling and tight junction functions. *Physiology*, 25, 16-26.
- THORNTON, D. J., CARLSTEDT, I., HOWARD, M., DEVINE, P. L., PRICE, M. R. & SHEEHAN, J. K. 1996. Respiratory mucins: Identification of core proteins and glycoforms. *Biochem J*, 316, 967-975.
- THORNTON, D. J., ROUSSEAU, K. & MCGUCKIN, M. A. 2008. Structure and function of the polymeric mucins in airways mucus. *Annu Rev Physiol*.
- TILLIE-LEBLOND, I., PUGIN, J., MARQUETTE, C. H., LAMBLIN, C., SAULNIER, F., BRICHET, A., WALLAERT, B., TONNEL, A. B. & GOSSET, P. 1999. Balance between proinflammatory cytokines and their inhibitors in bronchial lavage from patients with status asthmaticus. *Am J Respir Crit Care Med*, 159, 487-494.
- TOMITA, M., HAYASHI, M. & AWAZU, S. 1996. Absorption-enhancing mechanism of EDTA, caprate, and decanoylcarnitine in Caco-2 cells. *J Pharm Sci*, 85, 608-611.
- TUCKER, R. C., KAGAYA, M., PAGE, C. P. & SPINA, D. 2001. The endogenous cannabinoid agonist, anandamide stimulates sensory nerves in guinea-pig airways. *Br J Pharmacol*, 132, 1127-1135.
- TURNER, J. R., ANGLE, J. M., BLACK, E. D., JOYAL, J. L., SACKS, D. B. & MADARA, J. L. 1999. PKC-dependent regulation of transepithelial resistance: roles of MLC and MLC kinase. *Am J Physiol Cell Physiol*, 277, C554-C562.
- TURNER, J. R., RILL, B. K., CARLSON, S. L., CARNES, D., KERNER, R., MRSNY, R. J. & MADARA, J. L. 1997. Physiological regulation of epithelial tight junctions is associated with myosin light-chain phosphorylation. *Am J Physiol*, 273, C1378-C1385.
- TWISS, M. A., HARMAN, E., CHESROWN, S. & HENDELES, L. 2002. Efficacy of calcium channel blockers as maintenance therapy for asthma. *Br J Clin Pharmacol*, 53, 243-249.
- UEDA, N., YAMAMOTO, K., YAMAMOTO, S., TOKUNAGA, T., SHIRAKAWA, E., SHINKAI, H., OGAWA, M., SATO, T., KUDO, I., INOUE, K., TAKIZAWA, H., NAGANO, T., HIROBE, M., MATSUKI, N. & SAITO, H. 1995. Lipoxygenase-catalysed oxygenation of

- arachidonylethanolamine, a cannabinoid receptor agonist *Biochimica Et Biophysica Acta-Lipids and Lipid Metabolism*, 1254, 127-134.
- ULLUWISHEWA, D., ANDERSON, R. C., MCNABB, W. C., MOUGHAN, P. J., WELL, J. M. & ROY, N. 2011. Regulation of tight junction permeability by intestinal bacteria and dietary components. *J Nutr*, 141, 769-776.
- UTECH, M., IVANOV, A. I., SAMARIN, S. N., BRUEWER, M., TURNER, J. R., MRSNY, R. J., PARKOS, C. A. & NUSRAT, A. 2005. Mechanism of IFN-gamma-induced endocytosis of tight junction proteins: Myosin II-dependent vacuolarization of the apical plasma membrane. *Mol Biol Cell*, 16, 5040-5052.
- VACHON, L., FITZGERA.MX, SOLLIDAY, N. H., GOULD, I. A. & GAENSLER, E. A. 1973. Single-dose effect of Marihuana smoke - Bronchial dynamics and respiratory-center sensitivity in normal subjects *N Engl J Med*, 288, 985-989.
- VAN DER STELT, M., VAN KUIK, J. A., BARI, M., VAN ZADELHOFF, G., LEEFLANG, B. R., VELDKINK, G. A., FINAZZI-AGRO, A., VLIEGENTHART, J. F. G. & MACCARRONE, M. 2002. Oxygenated metabolites of anandamide and 2-arachidonoylglycerol: Conformational analysis and interaction with cannabinoid receptors, membrane transporter, and fatty acid amide hydrolase. *J Med Chem*, 45, 3709-3720.
- VANHOUTTE, P. M. 2013. Airway epithelium-derived relaxing factor: myth, reality, or naivety? *Am J Physiol Cell Physiol*, 304, C813-C820.
- VASQUEZ-MARTINEZ, Y., OHRI, R. V., KENYON, V., HOLMAN, T. R. & SEPULVEDA-BOZA, S. 2007. Structure-activity relationship studies of flavonoids as potent inhibitors of human platelet 12-hLO, reticulocyte 15-hLO-1, and prostate epithelial 15-hLO-2. *Bioorg Med Chem*, 15, 7408-7425.
- VERMAELEN, K. & PAUWELS, R. 2003. Accelerated airway dendritic cell maturation, trafficking, and elimination in a mouse model of asthma. *Am J Respir Cell Mol Biol*, 29, 405-409.
- VIGNOLA, A. M., CHANEZ, P., CHIAPPARA, G., SIENA, L., MERENDINO, A., REINA, C., GAGLIARDO, R., PROFITA, M., BOUSQUET, J. & BONSIGNORE, G. 1999. Evaluation of apoptosis of eosinophils, macrophages, and T lymphocytes in mucosal biopsy specimens of patients with asthma and chronic bronchitis. *J Allergy Clin Immunol*, 103, 563-573.
- VIJAYANAND, P., SEUMOIS, G., PICKARD, C., POWELL, R. M., ANGCO, G., SAMMUT, D., GADOLA, S. D., FRIEDMANN, P. S. & DJUKANOVIC, R. 2007. Invariant natural killer T cells in asthma and chronic obstructive pulmonary disease. *N Engl J Med*, 356, 1410-1422.
- VINHAS, R., CORTES, L., CARDOSO, I., MENDES, V. M., MANADAS, B., TODO-BOM, A., PIRES, E. & VERISSIMO, P. 2011. Pollen proteases compromise the airway epithelial barrier through degradation of transmembrane adhesion proteins and lung bioactive peptides. *Allergy*, 66, 1088-1098.
- VLLASALIU, D., FOWLER, R., GARNETT, M., EATON, M. & STOLNIK, S. 2011. Barrier characteristics of epithelial cultures modelling the airway and intestinal mucosa: A comparison. *Biochem Biophys Res Commun*, 415, 579-585.
- VOYNOW, J. A., GENDLER, S. J. & ROSE, M. C. 2006. Regulation of mucin genes in chronic inflammatory airway diseases. *Am J Respir Cell Mol Biol*, 34, 661-665.

- VUOLO, F., PETRONILHO, F., SONAI, B., RITTER, C., HALLAK, J. E. C., ZUARDI, A. W., CRIPPA, J. A. & DAL-PIZZOL, F. 2015. Evaluation of serum cytokines levels and the role of cannabidiol treatment in animal model of asthma. *Mediators Inflamm.*
- WALDECK-WEIERMAIR, M., ZORATTI, C., OSIBOW, K., BALENGA, N., GOESSNITZER, E., WALDHOER, M., MALLI, R. & GRAIER, W. F. 2008. Integrin clustering enables anandamide-induced Ca(2+) signaling in endothelial cells via GPR55 by protection against CB1-receptor-triggered repression. *J Cell Sci*, 121, 1704-1717.
- WALTERS, M. S., GOMI, K., ASHBRIDGE, B., MOORE, M. A. S., ARBELAEZ, V., HELDRICH, J., DING, B. S., RAFII, S., STAUDT, M. R. & CRYSTAL, R. G. 2013. Generation of a human airway epithelium derived basal cell line with multipotent differentiation capacity. *Respiratory Research*, 14.
- WAN, H., WINTON, H. L., SOELLER, C., STEWART, G. A., THOMPSON, P. J., GRUENERT, D. C., CANNELL, M. B., GARROD, D. R. & ROBINSON, C. 2000. Tight junction properties of the immortalized human bronchial epithelial cell lines Calu-3 and 16HBE14o. *Eur Respir J*, 15, 1058-1068.
- WAN, H., WINTON, H. L., SOELLER, C., TOVEY, E. R., GRUENERT, D. C., THOMPSON, P. J., STEWART, G. A., TAYLOR, G. W., GARROD, D. R., CANNELL, M. B. & ROBINSON, C. 1999. Der p 1 facilitates transepithelial allergen delivery by disruption of tight junctions. *J Clin Invest*, 104, 123-133.
- WANG, A. C. C., DAI, X. H., LUU, B. & CONRAD, D. J. 2001. Peroxisome proliferator-activated receptor-gamma regulates airway epithelial cell activation. *Am J Respir Cell Mol Biol*, 24, 688-693.
- WANG, G. S., ZABNER, J., DEERING, C., LAUNSPACH, J., SHAO, J., BODNER, M., JOLLY, D. J., DAVIDSON, B. L. & MCCRAY, P. B. 2000. Increasing epithelial junction permeability enhances gene transfer to airway epithelia in vivo. *Am J Respir Cell Mol Biol*, 22, 129-138.
- WANG, Q., GUO, X.-L., WELLS-BYRUM, D., NOEL, G., PRITTS, T. A. & OGLE, C. K. 2008. Cytokine-induced epithelial permeability changes are regulated by the activation of the p38 mitogen-activated protein kinase pathway in cultured Caco-2 cells. *Shock*, 29, 531-537.
- WANG, X. S., WU, A. Y. Y., LEUNG, P. S. & LAU, H. Y. A. 2007. PGE(2) suppresses excessive anti-IgE induced cysteinyl leucotrienes production in mast cells of patients with aspirin exacerbated respiratory disease. *Allergy*, 62, 620-627.
- WANG, Y., ZHANG, J., YI, X. J. & YU, F. S. X. 2004. Activation of ERK1/2 MAP kinase pathway induces tight junction disruption in human corneal epithelial cells. *Exp Eye Res*, 78, 125-136.
- WASKEWICH, C., BLUMENTHAL, R. D., LI, H. L., STEIN, R., GOLDENBERG, D. M. & BURTON, J. 2002. Celecoxib exhibits the greatest potency amongst cyclooxygenase (COX) inhibitors for growth inhibition of COX-2-negative hematopoietic and epithelial cell lines. *Cancer Res*, 62, 2029-2033.
- WATANABE, H., VRIENS, J., PRENEN, J., DROOGMANS, G., VOETS, T. & NILIUS, B. 2003. Anandamide and arachidonic acid use epoxyeicosatrienoic acids to activate TRPV4 channels. *Nature*, 424, 434-438.
- WATZL, B., SCUDERI, P. & WATSON, R. R. 1991. Marijuana components stimulate human peripheral-blood mononuclear cells secretion of interferon-gamma and suppress interleukin-1-alpha invitro *Int J Immunopharmacol*, 13, 1091-1097.

- WHO. 2014. The top 10 causes of death. Available: <http://who.int/mediacentre/factsheets/fs310/en/> [Accessed 26/4/2015].
- WHO. 2015a. Asthma – Fact sheet #307. Available: <http://www.who.int/mediacentre/factsheets/fs307/en/index.html> [Accessed 2/4/2015].
- WHO. 2015b. Chronic respiratory diseases: Burden of COPD. Available: <http://www.who.int/respiratory/copd/burden/en/> [Accessed 2/4/2015].
- WILLIAMS, S. J., HARTLEY, J. P. R. & GRAHAM, J. D. P. 1976. Bronchodilator effect of delta1-tetrahydrocannabinol administered by aerosol to asthmatic-patient
Thorax, 31, 720-723.
- WOLLIN, L. & PIEPER, M. P. 2010. Tiotropium bromide exerts anti-inflammatory activity in a cigarette smoke mouse model of COPD. *Pulm Pharmacol Ther*, 23, 345-354.
- WOOD, L. G., BAINES, K. J., FU, J., SCOTT, H. A. & GIBSON, P. 2012. The neutrophilic inflammatory phenotype is associated with systemic inflammation in asthma. *Chest*, 142, 86-93.
- WRAY, S., BURDYGA, T. & NOBLE, K. 2005. Calcium signalling in smooth muscle. *Cell Calcium*, 38, 397-407.
- WRIGHT, K., ROONEY, N., FEENEY, M., TATE, J., ROBERTSON, D., WELHAM, M. & WARD, S. 2005. Differential expression of cannabinoid receptors in the human colon: Cannabinoids promote epithelial wound healing. *Gastroenterology*, 129, 437-453.
- WRIGHT, K. L., DUNCAN, M. & SHARKEY, K. A. 2008. Cannabinoid CB2 receptors in the gastrointestinal tract: a regulatory system in states of inflammation. *Br J Pharmacol*, 153, 263-270.
- WROBLEWSKI, L. E., SHEN, L., OGDEN, S., ROMERO-GALLO, J., LAPIERRE, L. A., ISRAEL, D. A., TURNER, J. R. & PEEK, R. M., JR. 2009. Helicobacter pylori dysregulation of gastric epithelial tight junctions by urease-mediated myosin II activation. *Gastroenterology*, 136, 236-246.
- WU, H.-L., GAO, X., JANG, Z.-D., DUAN, Z.-T., WANG, S.-K., HE, B.-S., ZHANG, Z.-Y. & XIE, H.-G. 2013. Attenuated expression of the tight junction proteins is involved in clopidogrel-induced gastric injury through p38 MAPK activation. *Toxicology*, 304, 41-48.
- XIAO, C., PUDDICOMBE, S. M., FIELD, S., HAYWOOD, J., BROUGHTON-HEAD, V., PUXEDDU, I., HAITCHI, H. M., VERNON-WILSON, E., SAMMUT, D., BEDKE, N., CREMIN, C., SONES, J., DJUKANOVIC, R., HOWARTH, P. H., COLLINS, J. E., HOLGATE, S. T., MONK, P. & DAVIES, D. E. 2011. Defective epithelial barrier function in asthma. *J Allergy Clin Immunol*, 128, 549-U177.
- YAMADA, T., DEITCH, E., SPECIAN, R. D., PERRY, M. A., SARTOR, R. B. & GRISHAM, M. B. 1993. Mechanisms of acute and chronic intestinal inflammation-induced by Indomethacin. *Inflammation*, 17, 641-662.
- YE, R. D. 2001. Regulation of nuclear factor kappa B activation by G-protein-coupled receptors. *J Leukoc Biol*, 70, 839-848.
- YOUMBA, S. B., BELMONTE, L., GALAS, L., BOUKHETTALA, N., BOLEFEYSOT, C., DECHELOTTE, P. & COEFFIER, M. 2012. Methotrexate Modulates Tight Junctions Through NF-kappa B, MEK, and JNK Pathways. *J Pediatr Gastroenterol Nutr*, 54, 463-470.

- YU, M., IVES, D. & RAMESHA, C. S. 1997. Synthesis of prostaglandin E-2 ethanolamide from anandamide by cyclooxygenase-2. *J Biol Chem*, 272, 21181-21186.
- ZABNER, J., WINTER, M., EXCOFFON, K., STOLTZ, D., RIES, D., SHASBY, S. & SHASBY, M. 2003. Histamine alters E-cadherin cell adhesion to increase human airway epithelial permeability. *J Appl Physiol*, 95, 394-401.
- ZHANG, K., ZHANG, H., XIANG, H., LIU, J., LIU, Y., ZHANG, X., WANG, J. & TANG, Y. 2013. TGF-beta 1 induces the dissolution of tight junctions in human renal proximal tubular cells: Role of the RhoA/ROCK signaling pathway. *Int J Mol Med*, 32, 464-468.
- ZHANG, W. K., WANG, D., DUAN, Y., LOY, M. M. T., CHAN, H. C. & HUANG, P. 2010. Mechanosensitive gating of CFTR. *Nat. Cell Biol.*, 12, 507-U214.
- ZHAO, J. M., MASKREY, B., BALZAR, S., CHIBANA, K., MUSTOVICH, A., HU, H. Z., TRUDEAU, J. B., O'DONNELL, V. & WENZEL, S. E. 2009. Interleukin-13-induced MUC5AC is regulated by 15-lipoxygenase 1 pathway in human bronchial epithelial cells. *Am J Respir Crit Care Med*, 179, 782-790.
- ZHU, Y., CHIDEKEL, A. & SHAFFER, T. H. 2010. Cultured human airway epithelial cells (calu-3): a model of human respiratory function, structure, and inflammatory responses. *Crit Care Res Pract*, 2010.
- ZIHNI, C., BALDA, M. S. & MATTER, K. 2014. Signalling at tight junctions during epithelial differentiation and microbial pathogenesis. *J Cell Sci*, 127, 3401-3413.
- ZOERNER, A. A., STICHTENOTH, D. O., ENGELI, S., BATKAI, S., WINKLER, C., SCHAUMANN, F., JANKE, J., HOLZ, O., KRUG, N., TSIKAS, D., JORDAN, J. & HOHLFELD, J. M. 2011. Allergen challenge increases anandamide in bronchoalveolar fluid of patients with allergic asthma. *Clin Pharmacol Ther*, 90, 388-391.